

Meereswissenschaftliche Berichte
MARINE SCIENCE REPORTS

No. 14

Ultraphytoplankton and protozoan communities and their
interactions in different marine pelagic ecosystems
(Arabian Sea and Baltic Sea)

by

Marcus Reckermann

Institut für Ostseeforschung
Warnemünde
1996

Die vorliegende Arbeit ist die inhaltlich unveränderte Fassung einer Dissertation, die am Institut für Ostseeforschung Warnemünde angefertigt und im Juni 1996 von der Mathematisch-Naturwissenschaftlichen Fakultät der Universität Rostock angenommen wurde.

Diese Arbeit wurde mit Mitteln des Bundesministeriums für Bildung, Wissenschaft, Forschung und Technologie (Projekt 03F0105B), sowie von der niederländischen Stiftung der Meereswissenschaften (SOZ) im Rahmen des NIOP-Programmes gefördert. Die Verantwortung für den Inhalt dieser Veröffentlichung liegt beim Autor.

Vice versa

Ein Hase sitzt auf einer Wiese,
des Glaubens, niemand sähe diese.

Doch, im Besitze eines Zeisses
betrachtet voll gehaltenen Fleisses

vom vis-à-vis gelegnen Berg
ein Mensch den kleinen Löffelzweg.

Ihn aber blickt hinwiederum
ein Gott von fern an, mild und stumm.

Christian Morgenstern

Table of Contents

Page

List of Abbreviations

Zusammenfassung

1.	Introduction	1
2.	Material and Methods	3
2.1.	Areas of investigation	3
2.1.1.	The Arabian Sea (Northwest Indian Ocean)	3
2.1.2.	The Gotland Sea (Baltic proper)	4
2.1.3.	The Pomeranian Bay	5
2.2.	Hydrography, nutrients and Chl.a	6
2.3.	Protozoan distribution	6
2.4.	Phytoplankton and carbon conversions	7
2.5.	Flow cytometry	8
2.5.1.	Theoretical background	8
2.5.2.	Shipboard instrumentation and operation	13
2.6.	Herbivory estimated in serial dilution experiments	14
2.6.1.	Theoretical background	14
2.6.2.	Experimental protocols	17
2.7.	Herbivory estimated in a light-dark experiment	17
2.8.	Bacterivory estimated by chemical inhibition	18
2.9.	List of activities	18
3.	Results	19
3.1.	The northwest Arabian Sea and adjacent areas during the SW monsoon 1992 (NIOP B1)	19
3.1.1.	Hydrography, nutrients and Chl.a	19
3.1.2.	Protozoan distributions	20
3.1.3.	Herbivory	25
3.1.4.	Bacterivory	27
3.2.	The northwest Arabian Sea and adjacent areas during the NE monsoon 1992/93 (NIOP B2)	29
3.2.1.	Hydrography, nutrients and Chl.a	29
3.2.2.	Protozoan distributions	30
3.2.3.	Herbivory	35
3.2.4.	Grazing on ultraphytoplankton analyzed by flow cytometry	36
3.2.5.	Grazer size differential grazing on ultraphytoplankton analyzed by flow cytometry	40
3.2.6.	Grazer size differential grazing on ultraphytoplankton in a light-dark experiment analyzed by flow cytometry	44
3.3.	The Gotland Sea (Baltic proper) during summer 1994	47
3.3.1.	Hydrography and nutrients	47
3.3.2.	Chl.a and ultraphytoplankton distributions analyzed by flow cytometry	48
3.3.3.	Protozoan distributions	54
3.3.4.	Grazer size differential grazing on ultraphytoplankton analyzed by flow cytometry	56

3.4.	The Pomeranian Bay during late summer 1993	60
3.4.1.	Drift 1: Hydrography, nutrients, Chl.a and protozoan distributions	60
3.4.2.	Drift 2: Hydrography, nutrients, Chl.a and protozoan distributions	65
3.4.3.	Herbivory	70
3.5.	The Pomeranian Bay during summer 1994	72
3.5.1.	Hydrography and nutrients	72
3.5.2.	Chl.a and ultraphytoplankton distibutions analyzed by flow cytometry	73
3.5.3.	Protozoan distributions	84
4.	Discussion	89
4.1.	Methodological considerations	89
4.1.1.	Terminology	89
4.1.2.	A critique of the serial dilution technique	90
4.1.3.	Alternative grazing methods used in this study	94
4.2.	Pelagic food web structure and trophic interactions in the Arabian Sea and the Baltic Sea	96
4.2.1.	Standing stocks and distributions of ultraphytoplankton	96
4.2.2.	Standing stocks and distributions of protozoa	104
4.2.3.	Ultraphytoplankton dynamics and grazing by microzooplankton	109
4.2.4.	Multiple trophic interactions within the microbial food web	112
4.3.	The concept of the microbial food web in pelagic ecosystems of different status	116
5.	Summary	122
6.	References	125
	Appendix	i - vi

Danksagung - Acknowledgments

List of general abbreviations

AvH	R.V. Alexander von Humboldt
Euks	Eukaryotes
FC	Flow Cytometry
HDIN	Heterotrophic Dinoflagellates
HNF	Heterotrophic Nanoflagellates
IOW	Institut für Ostseeforschung Warnemünde
NIOP	Netherland's Indian Ocean Programme
NIOZ	Nederlands Instituut voor Onderzoek der Zee
PAP	R.V. Professor Albrecht Penck
Syn	Synechococcus
SW	South West
NE	North East

List of abbreviations of principal stations in the Arabian Sea, the Gulf of Aden, and the southern Red Sea

BM	Bab-el-Mandeb
GA	Gulf of Aden
OFZ	Owen Fracture Zone
RS	Red Sea
SB	Somali Basin
SI	Socotra Island
US	Upwelling Somalia

Zusammenfassung

Die Zusammensetzung und Biomasse von Ultraphytoplankton- und Protozoen-Gemeinschaften, sowie deren trophische Wechselwirkungen wurden auf fünf Forschungsfahrten in verschiedenen Seegebieten unterschiedlichen Trophiegrades untersucht. Die nordwestliche Arabische See, der Golf von Aden und das südliche Rote Meer wurden während zwei verschiedener Monsun-Perioden beprobt (Südwest-Monsun im Sommer 1992 und Nordost-Monsun im Winter 1993). Zwei Untersuchungen fanden in der Pommerschen Bucht (südliche Ostsee) jeweils im Sommer 1993 und 1994 statt, und eine Expedition im Sommer 1994 führte in die Gotlandsee (mittlere Ostsee).

Die Zusammensetzung und Biomasse von Ultraphytoplankton-Gemeinschaften

Der Anteil des Ultraphytoplanktons an der gesamten Phytoplanktonbiomasse betrug etwa 60% während des meso- bis oligotrophen Nordost-Monsuns in der Arabischen See, aber nur 11% im zu dieser Zeit eutrophen südlichen Roten Meer. Mit Hilfe der Durchflußzytometrie konnten verschiedene Ultraphytoplankton-Gruppen unterschieden werden: die beiden prokaryotischen Genera *Prochlorococcus* und *Synechococcus*, sowie zwei weitere eukaryotische Ultraplankton-Gruppen. Die Eukaryoten und *Synechococcus* stellten den weitaus größten Anteil am Ultraphytoplankton-Bestand, wobei die Eukaryoten besonders an den eutrophen Stationen dominierten.

In der oligotrophen Gotlandsee betrug das Ultraphytoplankton etwa 35% der gesamten Phytoplanktonbiomasse. In diesem Seegebiet konnten *Synechococcus* und vier weitere eukaryotische Ultraphytoplankton-Gruppen mittels Durchflußzytometrie unterschieden werden. Auch hier stellten die Eukaryoten den größten Anteil an der Ultraphytoplanktonbiomasse.

In der meso- bis oligotrophen offenen Pommerschen Bucht betrug der Anteil des Ultraphytoplanktons an der gesamten Phytoplanktonbiomasse ca. 60%. Dieser Anteil verringerte sich in der eutrophen Ausstrom-Fahne der Oder auf etwa 45%. Hier konnten mittels Durchflußzytometrie und Epifluoreszenz-Mikroskopie 7 Gruppen unterschieden werden. Die Ultraphytoplankton-Gemeinschaft in der Pommerschen Bucht setzte sich neben *Synechococcus* aus drei unidentifizierten eukaryotischen Gruppen, sowie zwei Cryptophyceen zusammen. Im nährstoffarmen Wasser der offenen Bucht war *Synechococcus* die weitaus dominierende Art innerhalb der Ultraphytoplankton-Gemeinschaft, während in der Ausfluß-Fahne der Oder größere Eukaryoten und Cryptophyceen die höchsten Biomasse-Anteile hatten.

In der Ostsee wurden 1994 mittels Epifluoreszenz-Mikroskopie außergewöhnlich hohe Abundanzen von *Synechococcus* nachgewiesen (Gotlandsee: bis zu 812.000 cm^{-3} , Pommersche Bucht: bis zu $1.500.000 \text{ cm}^{-3}$). In der Arabischen See nahmen die Abundanzen an *Prochlorococcus* mit zunehmendem Trophiegrad ab. Aufgrund dieser Beobachtungen, und gestützt von Hinweisen in der Literatur wird spekuliert, daß *Prochlorococcus* ein perfekt auf regenerierte Systeme des offenen Ozeans angepaßter Organismus ist.

Die Zusammensetzung und Biomasse von Protozoen-Gemeinschaften

In der Arabischen See wurde die Protozoen-Gemeinschaft von heterotrophen Nanoflagellaten (HNF, Zellkonzentrationen: $304 - 1630 \text{ cm}^{-3}$, Kohlenstoff-Biomasse: $1 - 7 \mu\text{g dm}^{-3}$) und heterotrophen Dinoflagellaten (HDIN: $8 - 60 \text{ cm}^{-3}$ und $0,6 - 15 \mu\text{g dm}^{-3}$) dominiert. Ciliaten spielten an den meisten Stationen eine untergeordnete Rolle. Eine Ausnahme bildeten die eutrophen Stationen in einer Auftriebsblüte während des Südwest-Monsuns, im Golf von Aden und im südlichen Roten Meer während des Nordost-Monsuns. Dort stellten die Ciliaten den größten Anteil an der Protozoenbiomasse (bis zu 7.800 dm^{-3} und $17 \mu\text{g dm}^{-3}$). An diesen Stationen war die gesamte Protozoenbiomasse stark erhöht, teilweise aufgrund höherer

Zellkonzentrationen, aber auch aufgrund größerer Zellen. Die Flagellatengemeinschaft bestand bis zu 90% aus kleinen HNF ($<3\mu\text{m}$).

In der Ostsee war die Protozoenbiomasse generell höher als in der Arabischen See. In der Gotlandsee waren HNF (1.700 cm^{-3} und $12,6\ \mu\text{g dm}^{-3}$) weitaus bedeutender als Ciliaten (1.300 dm^{-3} und $2,4\ \mu\text{g dm}^{-3}$). In der Pommerschen Bucht wurden höchste Biomassenwerte in der Ausstrom-Fahne der Oder erreicht; dort stellten Ciliaten den größten Anteil der Protozoen (bis zu 176.000 dm^{-3} und $81\ \mu\text{g dm}^{-3}$). HNF erreichten bis zu 12.000 cm^{-3} und $58\ \mu\text{g dm}^{-3}$. Der heterotrophe Silicoflagellat *Ebria tripartita* erreichte nur vergleichsweise geringe Biomassen.

Die Beweidung von Ultraphytoplankton durch Mikrozooplankton

Die Durchführung von Verdünnungsexperimenten nach Landry und Hassett (1982) in Verbindung mit der Durchflußzytometrie erlaubte die Abschätzung von Freßraten von Mikrozooplankton ($<200\mu\text{m}$) auf verschiedene Ultraphytoplankton-Gruppen. In der Arabischen See während des Nordost-Monsuns unterlagen alle Gruppen einem hohen Fraßdruck. Indem etwa 100% (36 - 139%) der produzierten Biomasse täglich gefressen wurde, wurde ein Steady State - System in etwa aufrecht erhalten. Der Anteil des Ultraphytoplanktons an der insgesamt gefressenen Phytoplanktonbiomasse betrug in der Arabischen See etwa 100%. Die absoluten Kohlenstoff-Freßraten schwankten dort zwischen $4 - 28\ \mu\text{g dm}^{-3}\text{ d}^{-1}$. Dieser Anteil verringerte sich stark an den eutrophen Stationen im Golf von Aden und im südlichen Roten Meer, wo ein weitaus größerer Anteil an größeren Algen ($>5\mu\text{m}$) beweidet wurden ($71 - 146\ \mu\text{g dm}^{-3}\text{ d}^{-1}$).

Während des Südwest-Monsuns ergab sich ebenfalls ein zweigeteiltes Bild. An den durch ein Auftriebsereignis beeinflussten nördlichen Stationen waren die Kohlenstoff-Freßraten bedeutend höher als an einer oligotrophen südlichen Station. In der Auftriebsblüte betrug die Wegfraßrate $118\ \mu\text{g dm}^{-3}\text{ d}^{-1}$, während sie an den mesotrophen nördlichen Stationen mit $48 - 86\ \mu\text{g dm}^{-3}\text{ d}^{-1}$ etwas niedriger waren. An der südlichen Station, die nicht durch Auftriebsphänomene beeinflusst war, betrug die Wegfraßrate hingegen nur $20\ \mu\text{g dm}^{-3}\text{ d}^{-1}$. An dieser Station wurde ein Experiment zur Abschätzung des Fraßdrucks von Mikrozooplankton auf Bakterien durchgeführt. Es zeigte sich, daß dort Bakterien in etwa gleicher Höhe wie das Phytoplankton beweidet wurden ($25\ \mu\text{g dm}^{-3}\text{ d}^{-1}$).

Der Wegfraß des Phytoplanktons durch Mikrozooplankton in der Ostsee bewegte sich in derselben Größenordnung wie an den eutrophen Stationen in der Arabischen See. In der oligotrophen Gotlandsee betrug der Kohlenstoff-Wegfraß aller gemessenen Ultraphytoplankton-Gruppen zusammen $58 - 119\ \mu\text{g dm}^{-3}\text{ d}^{-1}$, während in der Pommerschen Bucht die Wegfraßrate des gesamten Phytoplanktons zwischen 83 und $140\ \mu\text{g dm}^{-3}\text{ d}^{-1}$ schwankte.

Eine 'trophische Kaskade' im mikrobiellen Nahrungsnetz

Verdünnungsexperimente, in denen verschiedene Größenklassen von Freßfeinden durch Größenfraktionierung vor Beginn der Inkubation entfernt worden waren, erlaubten die Identifizierung von mindestens zwei trophischen Ebenen innerhalb des Nanoplanktons ($<20\mu\text{m}$) in der Arabischen See zur Zeit des Nordost-Monsuns. Der Ausschluß von Freßfeinden größer als $10\mu\text{m}$ hatte eine erhebliche Steigerung des Fraßdrucks auf das autotrophe Ultraplankton zur Folge. Bis zu 83% der primären herbivoren Protozoen ($<10\mu\text{m}$) wurden durch größere Räuber ($10 - 200\mu\text{m}$) täglich gefressen. Dieser Effekt konnte in der Ostsee nicht nachgewiesen werden.

Schlußfolgerungen

Ultraphytoplankton ist ein allgegenwärtiger und meist dominanter Bestandteil des Nahrungsnetzes verschiedenster pelagischer Ökosysteme. Die Biomasse und Vielfalt eukaryotischer Algen innerhalb des Ultraplanktons nimmt im allgemeinen mit steigendem Trophiegrad zu. Das Gegenteil trifft auf *Prochlorococcus* zu: dieser phototrophe Prokaryot erreicht höchste Konzentrationen in oligotrophen ozeanischen Gebieten, und verliert mit steigendem Trophiegrad schnell an Bedeutung. *Prochlorococcus* scheint in besonderen Maße an evolutionsgeschichtlich alte regenerierte Systeme angepaßt zu sein.

In der Ostsee wurde *Prochlorococcus* bisher nicht gefunden.

Synechococcus andererseits kommt in der Ostsee etwa um eine Größenordnung zahlreicher vor als in ozeanischen Gebieten. Anders als *Prochlorococcus* erreicht *Synechococcus* auch in eutrophen Küstenregionen hohe Abundanzen, die jedoch meist überdeckt werden durch größere, blütenbildende Algen (Diatomeen, Dinoflagellaten, fädige Blaualgen). Es kann angenommen werden, daß der *Synechococcus*-Typ der Ostsee und anderer neritischer Regionen einer anderen Art angehört, als derjenige des offenen Ozeans. Die insgesamt höhere Biomasse aller am mikrobiellen Nahrungsnetz beteiligten Organismengruppen kann durch die hohe Zufuhr an Nährstoffen erklärt werden, die die räumlich relativ abgeschlossene Ostsee von Land erhält. Zusätzlich werden durch regelmäßige Blüten N_2 - fixierender Blaualgen und atmosphärische Einträge der euphotischen Zone "neuer" Stickstoff zugeführt. Diese Bedingungen führt dazu, daß die nährstoffverarmte euphotische Zone der mittleren Ostsee im Sommer weitaus höhere Biomassen tragen kann als ozeanische Gebiete unter oligotrophen Bedingungen. Bildlich gesprochen dreht sich die "Recycling-Maschine" des *Microbial Loop* in der Ostsee auf einem höheren Niveau als in ozeanischen oligotrophen Gebieten.

Kleine heterotrophe Nanoflagellaten sind von besonderer Bedeutung in oligotrophen Systemen. Sie scheinen die Voraussetzungen für Systeme regenerierter Produktion, nämlich hohe Wachstums-, Freß- und Remineralisierungsraten, in hohem Maße zu erfüllen. Die Bedeutung von Ciliaten hingegen nimmt mit steigendem Trophiegrad zu.

Die Beweidung des autotrophen Ultraplanktons ist in Systemen aller Trophiestufen sehr hoch. Ein täglicher Wegfraß von ca. 100% der täglichen Produktion führt generell zur Ausbildung eines statischen Systems ohne große Biomassenschwankungen der beteiligten Organismengruppen (steady state). Dieser relativ konstante Kohlenstofffluß durch das mikrobielle Nahrungsnetz wird allerdings in Anwesenheit großer Algen in Bedingungen neuer Produktion überdeckt.

In der Arabischen See während des Nordost-Monsuns wurde gezeigt, daß die Biomasse und Produktion des autotrophen Ultraplankton weitgehend durch Freßfeinde der Herbivoren kontrolliert wird ('top-down'- Kontrolle, trophische Kaskade).

Die Durchflußzytometrie ist ein sehr geeignetes Instrument zur Untersuchung pelagischer Ökosysteme. Phytoplankton bis hin zu den kleinsten Dimensionen kann schnell und präzise quantitativ und semi-qualitativ analysiert werden. Mit speziellen Methoden können auch heterotrophe Bakterien mittels Durchflußzytometrie quantifiziert werden. Spezifische Färbestoffe bieten hier ein weites Spektrum an Anwendungen.

1. Introduction

Our understanding of aquatic food webs has evolved dramatically within the past three decades. Due to methodological constraints, only the larger members of the pelagic community could be analyzed until the second half of the century. Although ciliates and heterotrophic flagellates had long been described by early investigators (CLAPARÈDE and LACHMANN 1858, LOHMANN 1908, GRIEBMANN 1913, FAURÉ-FREMIET 1924), the central role of small heterotrophic organisms for pelagic ecology such as bacteria and protozoa was not acknowledged until new experimental and descriptive methods were developed in the 60's and 70's (most notably the development of epifluorescence microscopy, FRANCISCO et al. 1973, HOBBIIE et al. 1977). Up to that time, the notion of a classical food chain predominated, basically consisting of three trophic steps: The phytoplankton (diatoms, dinoflagellates) as primary producers was consumed by the crustacean zooplankton, which was then eaten by predatory fish. This notion was shaken by STEELE (1974) and POMEROY (1974) in proposing a new paradigm that included a microbial food web, with heterotrophic bacteria and protozoa as principal protagonists, dominating material and energy fluxes in the pelagial. This new concept was further elaborated on grounds of more data some years later by WILLIAMS (1981) and AZAM et al. (1983), who coined the term *microbial loop*. It has become a central term in biological oceanography.

Another milestone in understanding the functioning of aquatic food webs was the establishment of the concept of *new* and *regenerated* production by DUGDALE and GOERING (1967). It has led to the realization of two qualitatively and quantitatively different nutrient regimes, responsible for the structure of the pelagic ecosystem under different environmental preconditions. The relative importance of the microbial food web and its main protagonists in these different ecosystems is largely a function of its trophic status. Eutrophic systems like upwelling areas, coastal zones and river drainage areas generally feature large organisms with few trophic steps and a high carbon transfer efficiency (new production systems, resembling more the classical food chain), whereas oligotrophic ones (e.g. the large oceanic gyres, tropical oceans or the stratified summer period in temperate waters) are characterized by small organisms, more trophic steps, a low carbon transfer efficiency (in contrast to rapid cycling), and an active microbial loop (systems of regenerated production).

The incorporation of very small phytoplankton (ultraplankton $<5\mu\text{m}$, and picoplankton $<2\mu\text{m}$) into the microbial food web, especially in regenerated systems was another important finding of the past two decades (LI et al. 1983). It is now well accepted that autotrophic picoplankton ($<2\mu\text{m}$), dominated by the prokaryote genera *Synechococcus* and *Prochlorococcus*, as well as eukaryotic cells of different taxonomic position, make up the bulk of primary production and phytoplankton biomass in large parts of the open oceans (FOGG 1995).

Especially the application of flow cytometry in marine oceanography in recent years has allowed the fast and precise quantification of ultra- and picoplankton and has largely contributed to our knowledge of their distributions (OLSON et al. 1985, WOOD et al. 1985, OLSON et al. 1988, VELDHUIS and KRAAY 1990, CAMPBELL and VAULOT 1993). Recently, it led to the discovery of oceanic prochlorophytes (*Prochlorococcus*), a minute ($0.6\mu\text{m}$) member of the autotrophic prokaryotic picoplankton (CHISHOLM et al. 1988, CHISHOLM et al. 1992) which had been overlooked before due to their small size and dim, fast fading autofluorescence (CAMPBELL et al. 1994). More recently, flow cytometry has been applied to growth and grazing experiments involving autotrophic pico- and ultraplancton in different environments (LANDRY et al. 1995b, VAULOT et al. 1995).

The importance of the microbial food web and the microbial loop in oligotrophic environments is well acknowledged while their function in more eutrophic systems is less well defined. Moreover,

the size structure and the way the different compartments interact in systems of different trophic status (i.e. oligotrophic vs. eutrophic) may be quite different. To assess the relative importance of the microbial food web in systems of different trophic status, standing stocks, size structure and trophic interactions of protozoa and autotrophic ultraplankton ($<5\mu\text{m}$) were analyzed by microscopy and flow cytometry in different environments of the Arabian Sea and the Baltic Sea. The application of flow cytometry allowed for the first time an estimation of grazing pressure on the autotrophic picoplankton in the Arabian Sea (including *Prochlorococcus*) and in the Baltic Sea by different grazer size classes, allowing also some insight into trophic interactions within the "black box" of the microzooplankton community.

Data were collected during two cruises to the Arabian Sea and three cruises to the Baltic Sea, specifically

- a. the northwestern part of the Arabian Sea off Somalia, the Gulf of Aden and the southernmost part of the Red Sea during the SW monsoon (Cruise B1: July-August 1992); here, oligotrophic and highly eutrophic upwelling stations were found in close vicinity,
- b. the same region during the NE monsoon (Cruise B2: January-February 1993); mostly oligo- to mesotrophic,
- c. the oligotrophic Gotland Sea (Baltic proper) during summer (July 1994),
- d. the Pomeranian Bay (Odra river drainage area, southern Baltic Sea), September / October 1993 during two drift experiments in the eutrophic river plume,
- e. the Pomeranian Bay in June / July 1994, featuring an eutrophic river plume, and a meso- to oligotrophic open bay.

The cruises to the Arabian Sea and its adjacent areas were conducted within the framework of project B of the Netherland's Indian Ocean Programme ("Monsoons and Pelagic Systems", BAARS 1994), the cruises to the Pomeranian Bay were part of the TRUMP project (Transport und Umsatzprozesse in der Pommerschen Bucht), a multidisciplinary, multinational research programme in the Pomeranian Bay, designed to quantify turnover and transport rates from the Odra estuary to the open Baltic Sea. The cruise to the Gotland Sea was part of the GOBEST project (Gotland-Becken-Stickstoff) of the IOW, attempting to characterize the nitrogen metabolism of the Gotland Sea ecosystem in summer.

Results are presented separately for each respective cruise, followed by a joint discussion of the respective components of the microbial food web and their interactions.

2. Material and Methods

2.1. Areas of investigation

2.1.1. The Arabian Sea (Northwest Indian Ocean)

The cruises to the northwest Arabian Sea were conducted within the framework of the "Netherlands Indian Ocean Programme 1992-93" (NIOP) on R.V. TYRO, as contributions to project B "Monsoons and Pelagic Systems" (BAARS 1994). The NIOP programme is a contribution to the multi-national, multi-disciplinary JGOFS programme (Joint Global Ocean Flux Study), designed to characterize and quantify carbon fluxes within the ocean, and exchange rates with the atmosphere. Cruise B1 (SW monsoon) started July 12, 1992 from Mombasa, Kenya, and ended August 8, 1992 in Djibouti; Cruise B2 (NE monsoon) started January 11, 1993 from Victoria, Mahé, The Seychelles, and terminated February 6, 1993 in Djibouti. Areas of investigation included the Somali Current, the western Arabian Basin, the Gulf of Aden, and the southernmost part of the Red Sea (Fig.1).

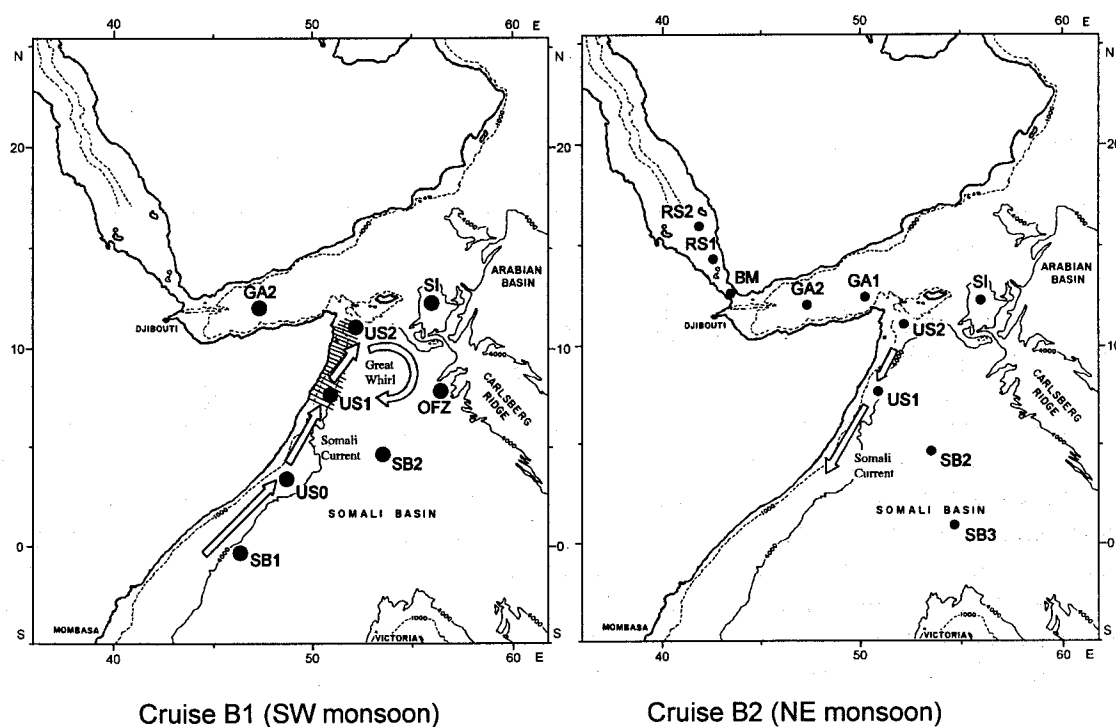


Fig.1 Principal stations in the Somali Basin, Gulf of Aden and the southern Red Sea during the two cruises on R.V.TYRO (NIOP programme 1992-93). Hatched area on the left panel (SW monsoon) symbolize upwelling of cold, nutrient-rich water. Note the reverse direction of the Somali current during the two seasons, and the "Great Whirl" during the SW monsoon.

Hydrography. The area is characterized by very dynamic seasonal changes in hydrography and biology, due to the opposite monsoon winds in the summer and winter. In summer, during the SW monsoon, a low pressure zone above the Arabian peninsula generates a strong and narrow tropospheric jet (the Findlater Jet), which causes high south-westerly windspeeds at sea level, thereby creating the Somali current (SHETYE et al. 1994). Ekman pumping generates upwelling events off the coasts of Somalia and Oman, resulting in an overall very high productivity and biomass in the region during the summer months. During this period, a pronounced anticyclonic mesoscale eddy develops at the Horn of Africa, known as the "Great Whirl" (SCHOTT et al. 1990). In winter, during the NE monsoon, a high pressure zone over the Arabian Peninsula establishes a

moderate northwesterly wind, which is strong enough to invert the Somali current. Cooler surface temperatures in the winter and strong winds also result in a deepened mixed layer due to increased thermal and wind convection (BANSE 1994a). The transition times in spring and autumn are characterized by calm winds and a strong stratification of the water column, with an oligotrophic mixed layer and a pronounced deep chlorophyll maximum.

Due to its seasonally changing monsoon winds and associated oscillating current systems, the Arabian Sea combines the most productive (in the upwelling areas during the SW monsoon in summer) with the most oligotrophic (the central Arabian Sea during the calm inter-monsoon periods) oceanic environments of the world's ocean in a relatively small ocean basin (BURKILL et al. 1993a). The biogeochemistry of the region is characterized by extensive low oxygen water masses at mid depth in the northern part of the basin (OWENS et al. 1993); these conditions favour vigorous denitrification rates and high N₂O (LAW and OWENS 1990, MANTOURA et al. 1993, NAQVI and SHAILAJA 1993, NAQVI 1994) and methane (OWENS et al. 1991) fluxes to the atmosphere, contributing significantly to global input of climate-relevant gases. However, it is not clear whether the Arabian Sea acts as a sink or a source for atmospheric CO₂ (SOMARSUNDAR et al. 1990, LAL 1994).

2.1.2. The Gotland Sea (Baltic proper)

Data were collected on July 14 - 26, 1994 during a drift study on board R.V. Alexander von Humboldt (AvH) east of the island of Gotland (Sweden) at approximately 57° 19' N and 20° 05' E (Fig.2).

Hydrography. The Baltic proper in summer is characterized by a highly stratified water column, which reflects seasonal changes in atmospheric forcing in its vertical structure. The most prominent feature is a permanent halocline at 60 - 80m, separating the high saline deep water, which originates from deep water intrusions from the North Sea, from the low saline Baltic Sea water.

The surface water in winter is characterized by deep mixing down to the halocline. Following the spring bloom, and with increasing solar energy and calm weather, a warm and nutrient depleted surface layer develops, often coinciding with the euphotic zone. A sharp thermocline at 20 to 30m separates this warm surface layer from the cold intermediate "winter" water, which originates from the thermal and wind-driven vertical convection in winter; this water conserves winter conditions of the mixed layer in terms of salinity, temperature, and nutrient chemistry.

Due to the long residence periods and permanent oxygen consumption in the stagnant deep water below the permanent halocline, these water masses can be subject to extensive sub- or anoxic conditions in the deep basins of the Baltic Sea, such as the Bornholm Basin or the Gotland Basin. These conditions persist until the stagnant water is displaced by fresh oxygenated North Sea water. The last intrusion of North Sea water to end anoxia in wide areas of the Baltic proper occurred in January 1993 (MATTHAEUS et al. 1993). The biogeochemical characteristics of the Baltic proper are strongly influenced by these anoxic deep water parcels, as their presence leads to an overall deficiency of oxidised nitrogen compounds in the water column through denitrification processes (GOCKE 1995). The low inorganic N/P ratio in the water column, well below the Redfield ratio of 6.6 (REDFIELD 1963), results in a nitrogen limitation of autotrophic growth, with phosphate and silicate still present in considerable amounts. These conditions, together with calm and warm weather, lead to extensive blooms of filamentous diazotrophic cyanobacteria (*Nodularia spumigena*, *Aphanizomemon flos-aquae*, *Anabaena sp.* and others) in summer (BURSA 1963, HOPPE 1981). This has consequences for the microbial food web in the oligotrophic surface layer of the Baltic proper in summer (see section 4.2.).

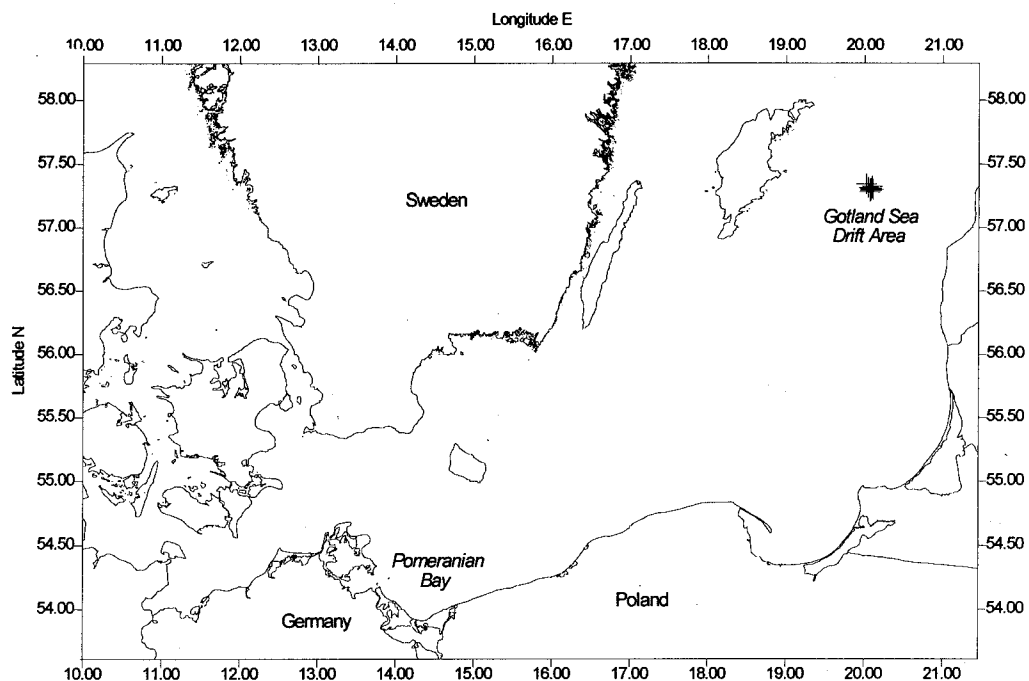


Fig.2 The research areas in the Baltic Sea: The Pomeranian Bay and the Gotland Sea. For detailed maps of the Pomeranian Bay see sections 3.4.1. (Fig.51) and 3.5.1. (Fig.67).

2.1.3. The Pomeranian Bay

Data from the Pomeranian Bay were collected during two cruises within the framework of the multi-disciplinary research project TRUMP (Transport und Umsätze in der Pommerschen Bucht, BMBF-Project 03F0105B), designed to investigate turnover rates of riverine dissolved and particulate material in the Pomeranian Bay and transport rates from the river mouths of the Odra river to the Bay and further to the open Baltic Sea. The first cruise (pilot study) was a drift study and was conducted from September 27 - October 7 1993 with R.V. Professor Albrecht Penck (PAP, Fig.51); during the second cruise with R.V. Alexander von Humboldt (AvH) from June 23 to July 8 1994, a fixed station grid was sampled (Fig.67).

Hydrography. The Pomeranian Bay (respectively the Szczecin lagoon as the primary drainage basin of the Odra river) is connected to the Odra river via three outlets: the peene river in the west (connected with the Greifswald Bodden) and the Dziwna river in the east, each contributing 15-20% to the total outflow, while the central Swine contributes to 60-70% (SIEGEL et al. 1996). Outflow is very dynamic as it largely depends on meteorological conditions. Often pulsewise freshwater injections from the lagoon occur, resulting in defined water parcels, which undergo subsequent mixing processes in the bay, depending on wind strength and direction. Southerly winds create a sea level depression in the southern bay, driving a net outflow of lagoon water into the bay. Conversely, northerly winds limit the outflow of lagoon water into the bay, or may even cause an inflow of bay water into the lagoon. A characteristic situation during constant westerly winds is the formation of a narrow band of lagoon water flowing along the polish coast to the Gdansk Bay, 300 nautical miles to the east. Under these conditions, coriolis-force driven Ekman transport forces the lagoon water along this narrow band along the coast line. Easterly winds result in a seaward component and broadening of this transport band, associated with upwelling and mixing with bay water (VON BODUNGEN et al. 1995). During the cruise in September / October 1993 with R.V. PAP, two distinct water parcels were followed along two drift trajectories (Fig.51), during which protozoan concentrations were determined and microzooplankton grazing was estimated. In June / July 1994, a fixed station grid was sampled for protozoan standing stocks and ultraphytoplankton analysis using flow cytometry (Fig.67).

2.2. Hydrography, nutrients and Chl.a

Discrete water samples for all analyses were obtained with a rosette water sampler, equipped with a Neill Brown (Arabian Sea B1), Seabird (Arabian Sea B2), or OM (Baltic Sea cruises) CTD. *Temperature* and *salinity* data were recorded on the uphaul by the respective CTD sensors. *Nutrient analyses* (nitrate, nitrite, ammonium, phosphate, and silicate) were carried out on board with an Autoanalyzer (Arabian Sea B1: H.A. van Koutrik, NIOZ; Arabian Sea B2: K.M.J. Bakker, NIOZ; Gotland Sea and Pomeranian Bay 1993: Dr. G. Nausch, IOW; Pomeranian Bay 1994: Dr. K. Nagel), following the protocols of GRASSHOFF (1976). Water samples (0.25 - 2L) for the determination of *Chlorophyll a* were filtered onto 25mm GF/F glass fibre filters and stored at -20°C until analysis. Filters were processed later on board (Arabian Sea cruises, G.W. Kraay, NIOZ), or in the laboratory (Baltic Sea cruises), and measured fluorometrically with a Turner Designs Fluorometer according to LORENZEN and JEFFREY (1978).

2.3. Protozoan distribution

Ciliates. Water was siphoned from the rosette sampling bottle directly into 250ml brown glass bottles by means of a submerged silicon tubing. The bottles had been pre-loaded with acid Lugol's Iodine (2% final concentration), as this had proven to be the best fixative for ciliates in various studies (e.g. LEAKEY 1989, OHMAN and SNYDER 1991). Samples were stored under dark and cool conditions until analysis in the laboratory. Ciliates were counted with an inverted microscope, using Utermöhl's settling technique (UTERMÖHL 1958). Settling volumes varied between 20 and 100 cm³, and a minimum of 50 cells were counted per sample. Linear dimensions of individual cells were measured with a calibrated micrometer eyepiece and converted to biovolumes using stereometric formulas (spherical, ellipsoid or conical shapes, EDLER 1979). Cell biovolumes were then converted to carbon biomass using a carbon conversion factor of 0.19 pg μm^{-3} (PUTT and STOECKER 1989).

Heterotrophic nanoflagellates (HNF) and *heterotrophic dinoflagellates (HDIN)*. Water samples were taken following the procedure described above, but using polyethylene (PE) bottles and 1% hexamine buffered Formaline as fixative. The fixed samples (10 - 60 cm³) were stained with DAPI (PORTER and FEIGG 1981, adjusted to 5 $\mu\text{g} / \text{cm}^3$ final concentration, Arabian Sea B2 and Baltic Sea cruises), or Proflavine (HAAS 1982, 5 $\mu\text{g} / \text{cm}^3$ final concentration, Arabian Sea B1 cruise), and filtered onto black stained (Sudan Black) 25mm 0.8 μm polycarbonate (PC) membrane filters, backed by 1.2 μm Cellulose Nitrate membrane filters after 3 - 5 minutes. The damp filter was transferred to a microscopic slide and allowed to dry until superficial dampness had evaporated. Then, a drop of non-fluorescent immersion oil was placed onto the center of the filter, and a cover slip placed on top. After the immersion oil had fully covered the filter, the prepare was frozen at -20°C until analysis in the laboratory.

Both DAPI (UV excitation) and Proflavine (blue excitation) allowed the discrimination between the red and orange autofluorescing phytoplankton cells, and the stained heterotrophic cells (PORTER and FEIGG 1981, HAAS 1982). HNF were identified by the absence of autofluorescence and the presence of one or more flagella; HDIN by the absence of autofluorescence and their characteristic shape. In addition to that, most HDIN showed a distinctive green autofluorescence under blue excitation (LESSARD and SWIFT 1986). A minimum of 50 cells per prepare was counted and measured. For the measurement of linear cell dimensions, a calibrated G12 New Porton Grid Eyepiece was used. Ellipsoid or spherical shapes were assumed for the calculation of biovolumes (EDLER 1979). Biovolumes were converted to carbon BØRSHEIM and BRATBAK (1987) for HNF (0.22 pg C μm^{-3}) and according to LESSARD (1991) for HDIN (0.14 pgC μm^{-3}).

2.4. Phytoplankton and carbon conversions

Ultraphytoplankton (<5 μm) was analyzed by flow cytometry (see below) on four cruises (in the Arabian Sea B2, courtesy Dr. M.Veldhuis, NIOZ; in the Gotland Sea, and in the Pomeranian Bay 1994). For the Arabian Sea cruises, large phytoplankton was examined only qualitatively in the ciliate samples. In the Baltic Sea (Gotland Sea, Pomeranian Bay) large phytoplankton was enumerated by Bettina Meyer-Harms (MEYER-HARMS 1996).

Carbon conversions. During cruise B2 in the Arabian Sea, individual cell carbon values were estimated as 175 fg / cell for *Synechococcus*, and 92 fg / cell for *Prochlorococcus* (M.Veldhuis, pers.comm.); values for small (925 - 2,500 fg / cell), and large pico-eukaryotic algae (5,090 fg / cell) were estimated using approximated cell diameters. *Synechococcus* was counted by epifluorescence microscopy during cruise Arabian Sea B1, in the Gotland Sea (Experiment 1) and in the Pomeranian Bay 1994. A minimum of 200 cells was counted per prepartate under blue or green excitation, using 1000x magnification. Carbon biomass was estimated using the above factor for the Arabian Sea, and by assuming an ESD of 1 μm for the Baltic Sea cruises (Tab.1). A C:Chl.a ratio (i.e. conversion factor) of 182 was estimated for both Arabian Sea cruises, by comparing Chl.a data with flow cytometrically determined cell abundances, applying the above cell carbon values (Veldhuis, pers.comm.). Only at station US2-230, a ratio of 50 was assumed, as large diatoms were blooming there. For the Gotland Sea and the open Pomeranian Bay, a C:Chl.a ratio of 50 was assumed, and of 32 in the Odra plume water (MEYER-HARMS 1996).

In the Gotland Sea, an approximate size determination of ultraphytoplankton cells was carried out by size fractionation. Water samples were passed through meshes or polycarbonate filters of different pore sizes (20 μm , 10 μm , 5 μm , 3 μm , 2 μm , 0.8 μm). The respective filtrates were then analyzed in the flow cytometer, allowing the assignment of a populations to a respective size range (Tab.1); the pore size retaining approximately 50% of a population was taken as its approximate equivalent spherical diameter (ESD). Cell number to carbon conversions were carried out according to Tab.1.

Tab.1 Assumed carbon factors for flow cytometrically measured phytoplankton groups in the Gotland Sea in summer 1994, as estimated by size fractionation. Volume specific carbon factors from VERITY et al. (1992). ESD = Equivalent Spherical Diameter.

	Size Range (μm)	ESD (μm)	Cell Vol. (μm^3)	C ($\text{pg} / \mu\text{m}^3$)	C (fg / cell)
Synechococcus	0.8-2	1	0.524	0.47	246
Pico-Euks	<2	2	4.189	0.36	1,508
Small Nano-Euks	3-5	3	14.137	0.36	5,089
Large Nano-Euks	5-10	5	65.450	0.36	23,562
PE1	5-10	5	65.450	0.36	23,562
SC1	5-10	5	65.450	0.36	23,562

2.5. Flow cytometry

Flow cytometry (FC) as a means of quantifying and characterizing ultraphytoplankton populations was used on four of the five cruises presented here. As this method is not widely used in marine ecology so far, I will first give a general introduction to the principles and applications of FC in biological oceanography, followed by a detailed description of the machines used on board and the problems that occurred during operation.

2.5.1. Theoretical background

Flow Cytometry is a tool for characterizing particles based on their optical properties. Individual particles are entrained in a fluid stream and pass through a spot of intense illumination (Mercury, or Xenon Arc lamp, or Laser). The resulting light scatter and fluorescence signals are collected by photomultipliers, processed by a computer, and depicted as one- or bivariate plots on screen, which then can be analyzed and interpreted. A description of the basic components of a simple flow cytometer is given in Fig.3. Originally designed for medical research (reviewed by DARZYNKIEWICZ and MELAMED 1993), flow cytometry has proven to be a valuable tool in aquatic ecology. Due to the unique chlorophyll autofluorescence of phytoplankton cells, FC is able to discriminate the phytoplankton from heterotrophic organisms or dead particles.

Basics of autofluorescence an photosynthetic pigments.

In the chloroplast, light energy is absorbed by the antenna pigments, and the excitation energy is transferred to the reaction centers. The central chlorophyll molecule of the photosystems (PSI and PSII) acts as final acceptor of excitation energy. There, the photosynthetic energy conversion is initiated, i.e. the creation of a proton gradient across the thylakoid membranes, and the subsequent production of ATP and NADH. When the excitation energy is sufficient, a delocalised π -electron of the conjugated double bond system of the tetrapyrrol ring structure of the chlorophyll molecule is promoted to an energy level that permits it to leave the molecule and reduce its redox partner plastoquinone (Q), starting a series of redox reactions. However, if Q is already in a reduced state ("closed"), the energy of the π -electron cannot be transferred, and it falls back to its initial energy level, thereby releasing the energy as heat or fluorescence light.

When light intensities exceed levels the photosystems can handle, a high percentage of absorbed light energy will be dissipated by fluorescence. However, this maximum fluorescence yield (when all reaction centers are "closed") only amounts to 3% of the absorbed light. When all reaction centers are "open", this fluorescence yield even decreases to 0.6%, demonstrating the high efficiency of the photosynthetic system. Most fluorescence is emitted by the chlorophyll *a* molecule of PSII. Due to their chemical structure (tetrapyrrol ring structures), phytoplankton autofluorescence is exclusively associated with the chlorophylls and the phycobilins, as only in these structures, the energy of an electron can be boosted to levels sufficient for the oxidation of the chlorophyll molecule.

Chlorophyll *a* emits fluorescence light in the far red (>630nm) end of the visible light spectrum, when excited by blue light (450-490nm). It is the principle photosynthetic pigment in all plants. Representing the only exception to date, the prochlorophytes, with the recently discovered oceanic *Prochlorococcus* (CHISHOLM et al. 1988), contain a chlorophyll *a* - derivate instead of the normal chlorophyll *a* (di-vinyl-chlorophyll *a*), showing a slightly red shifted absorption spectrum (GIESKES and KRAAY 1983, GOERICKE and REPETA 1992). Phycobilins (biliproteids) show autofluorescence in the yellow and orange (560-690nm) when excited by blue or green light (450-490nm, 515-530nm). The biliproteids are hydrophilic pigment-protein complexes, aggregated in phycobilisomes. Since these pigments are characteristic for cyanobacteria and cryptophyceae, the color of the emitted light can be used to differentiate these groups from the rest of the

phytoplankton. There are three major groups of phycobilins: phycocyanobilins (PCB), phycoerythrobilins (PEB), and phycourobilins (PUB), each group having its proper fluorescence characteristics. This allows to further discriminate between different subgroups within the morphologically uniform picocyanobacterium *Synechococcus* (WOOD et al 1985, OLSON et al. 1988, OLSON et al. 1990). Pigment concentrations per individual cell can be deduced indirectly by combining flow cytometric counts of respective fluorescence groups and fluorometrically (or HPLC) measured absolute pigment amounts (e.g. MOREL et al.1993, PARTENSKY et al. 1993, VELDHUIS and KRAAY 1993).

Light scatter characteristics. Intensities of scattered light can give information on relative size and optical properties like shape, granularity or transparency of the measured particle. Scattered light measured at low angles (forward scatter) are better suited to approximate size than large angle light scatter, but is still inferior to electronic methods ("coulter counter"), which are able to measure absolute volumes of (quasi-spherical) particles (PHINNEY and CUCCI 1989).

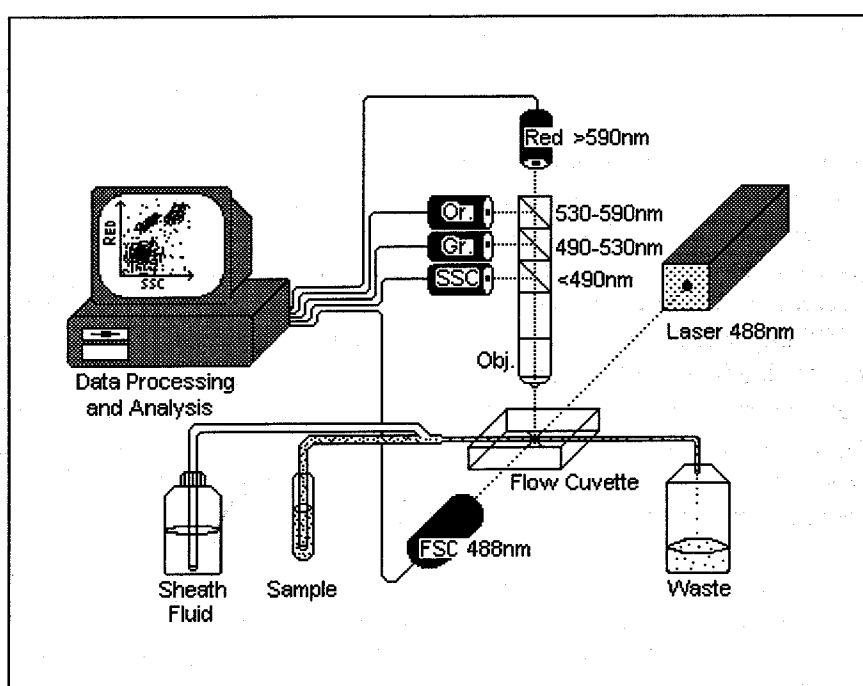


Fig.3 Sketch of a simple Flow Cytometer with its principal components. A water sample is pressed out of a sample tube into a Quartz glass cuvette by positive air pressure, where it is sheathed by particle free water (sheath fluid) and drawn out to a very thin thread of a few micrometers (hydrodynamic focussing). The particles entrained in this sample thread pass the laser beam, where they are excited to emit light of different wavelengths, depending on their pigment composition. Scattered laser light is collected by photomultipliers (PMTs) at two different angles (Forward Scatter FSC: 2 - 20°, Side Scatter SSC at 20 - 120°). Both parameters give relative information on size (FSC) or other optical properties like shape, granularity, transparency or surface properties (SSC). The passes through a system of light-collecting lenses (often a emitted light simple microscope objective), and is subsequently split into different wavelengths by appropriate optical filter combinations, and collected by PMTs. The PMT signals are then processed and spread across a logarithmic scale by a computer, and can be displayed on screen to be analyzed and interpreted by the investigator.

Basic design considerations for a flow cytometer suited for aquatic ecology. As almost all flow cytometers on the market have been basically designed for medical purposes, it is important to define the special requirements for analysing aquatic microorganisms. Most important is the ability to perform absolute cell counts to account for standing stocks and biomass which are basic variables in aquatic ecology. However, instruments equipped with this feature are the exception rather than the rule. Generally, it is assumed that the sample and sheath flow rates are stable enough to allow for the measurement of a fixed sample volume over a defined period of time. This can be checked by the use of a known concentration of fluorescence beads as an internal standard in the sample. The Partec PAS III, which was used in the Baltic Sea (sections 3.3. and 3.5.), is equipped with a system which allows the direct measurement of a defined sample volume: two electrodes are fixed at different levels in the sample reservoir; while the sample is pressed into the system, the upper electrode, when running dry, gives a signal to start the measurement. A second signal terminates the measurement when the sample surface reaches the lower electrode.

The wide range of concentrations and sizes of aquatic microorganisms also creates problems. Heterotrophic bacteria can have concentrations of several 10^6 per cm^3 in the sea, and autotrophic picoplankton can in some cases also exceed 10^6 per cm^3 (e.g. KUOSA 1991, this study), while large phytoplankton can be as scarce as a few cells per dm^3 . As size and concentration of a particle are generally inversely correlated in nature, the volume of water that must be measured to get a sufficiently precise measurement varies from a few litres for scarce large phytoplankton to less than 100 mm^3 for the abundant picoplankton. The sample flow rate must also be adjusted to these variables: small and abundant forms require slow flow rates (down to $1 \text{ mm}^3 / \text{min}$), while large and scarce forms require fast flow rates (some cm^3 / min). In most commercial instruments, the sample volume is limited to a few hundred mm^3 . Although the organisms under investigation span only up to 4 orders of magnitudes in diameter in the sea (ca. $0.5 - 500 \mu\text{m}$), their signal intensity (i.e. scatter and fluorescence light) may span a much wider range. However, the logarithmic span in commercial instruments is 4 decades at the most. A wider logarithmic span would be desirable to account for a wider range of signal intensities.

These considerations make the simultaneous measurement of all components of a given water sample impossible and call for different design types for oceanic ultraplankton and large coastal (often colonial and filamentous) phytoplankton. The requirements for small algae are in most cases sufficiently satisfied by commercial instruments (e.g. Becton Dickinson FacScan, FacSort, FacsCalibur, Coulter Epics XL, Ortho Cytoflow, Partec PAS III), although custom-built machines have also been successfully used (e.g. FRANKEL et al. 1990). A specially designed optical system (STEEN 1983, BioRad Bryte HS) proved to increase light scatter sensitivity even more, such that particles as small as $0.2 \mu\text{m}$, and with only $0.02 \mu\text{m}$ difference in diameter, can be resolved. Although up to date, this machine is available only with an arc lamp as excitation light source (possibly creating problems in exciting very small pigment or dye amounts), it seems to be an interesting alternative for microbiological purposes. Some commercial machines are equipped with a sorting module (e.g. Becton Dickinson FacSort, FacsCalibur, Partec PAS III).

Instruments for large phytoplankton are mostly custom built (e.g. HÜLLER et al. 1994). A joint effort to construct an optimized machine for large coastal phytoplankton found expression in the EurOPA machine (European Optical Plankton Analyzer, PEETERS et al. 1989, DUBELAAR et al. 1989). This instrument was designed with financial help from the EC (a MAST II joint project) to facilitate coastal monitoring (HOFSTRAAT et al. 1994), and it involved cooperation of various European workgroups, each contributing a specialized module. Outstanding features of the EurOPA are the unlimited sample volume, the large flow cell of $1,000 \times 1,000 \mu\text{m}$ (as compared to $250 \times 250 \mu\text{m}$ in commercial instruments), 4 additional forward scatter diffraction detectors and a pulse shape module (allowing to account for additional information of the shape of cells), an 8-decade logarithmic scale for all parameters, an "image-in-flow" module, capable of taking

digitised pictures of the cell while being measured, and the use of three lasers with different excitation wavelengths.

The question of sensitivity is of paramount importance for the measurement of picoplankton. While some older instruments have relied on massive laser power (up to 5 Watt) to obtain sufficient signal strengths, modern instruments use highly sensitive optical components, which allow low laser powers (generally a 15mW Argon laser). These small lasers can be run with wall current, thus relieving the scientist from the huge machinery of large water-cooled lasers. Some lasers are tuneable, i.e. the excitation wavelength is adjustable. This opens up more opportunities with respect to measuring specific phytoplankton fluorescence types (e.g. excitation of phycobilins by green light), as well as a wider range of choice of fluorescent probes for various applications. A high numerical aperture ($n > 1.2$) of the light collection optics is very important to achieve a low noise to signal ratio (ORMEROD 1990).

Signal analysis and interpretation: Defining regions for distinct phytoplankton clusters, and discrimination and quantification by gating. The fluorescence and scatter light signals of each individual particle are displayed by the computer in an x-y plot. Thus, every measured phytoplankton cell is defined in this x-y plane by its specific fluorescence or scatter light intensity. Cells of similar optical characteristics will form a cluster in the x-y plane. The number of cells in a cluster, and its specific fluorescence or scatter light intensities can be recorded by the computer, and written to a spreadsheet. For this purpose, a *region* is defined for a chosen cluster by drawing a line around it (R1, R2, R3 in Fig.4). This procedure is a purely subjective, and may raise problems when clusters overlap. However, the combination of different parameters in many x-y plots mostly helps to resolve the overlapping clusters.

Fig.4 demonstrates a basic procedure to analyze flow cytometric data obtained in the field. R1, R2 and R3 on panel A represent *regions* of clusters showing both red and orange fluorescence, i.e. phytoplankton containing phycobilins (causing orange fluorescence). Figure B displays the same measurement with red fluorescence plotted against Forward Light Scatter; all phytoplankton accessible by the machine is displayed in figure B, while only the orange-fluorescing cells appear in plot A.

In order to characterize and quantify clusters that overlap with phycobilin-containing groups in plot B, it is possible to subtract the regions defined in plot A from plot B. This procedure is called *Gating*. The cells of the clusters defined by R1, R2 and R3 in plot A will of course appear in plot B as well, possibly overlapping with other phytoplankton groups which show identical scatter and red fluorescence intensities, but lacking orange fluorescence. It is possible to let the computer *gate out* (i.e. subtract) R1, R2 and R3 from plot B. Consequently, there are no orange fluorescing cells left over in the resulting plot C. In this case, only few cells in figure B overlapped with R1, but R2 completely coincided with phytoplankton lacking orange fluorescence in plot B. In panel C, it is now possible to define new regions for the phytoplankton groups lacking phycobilins.

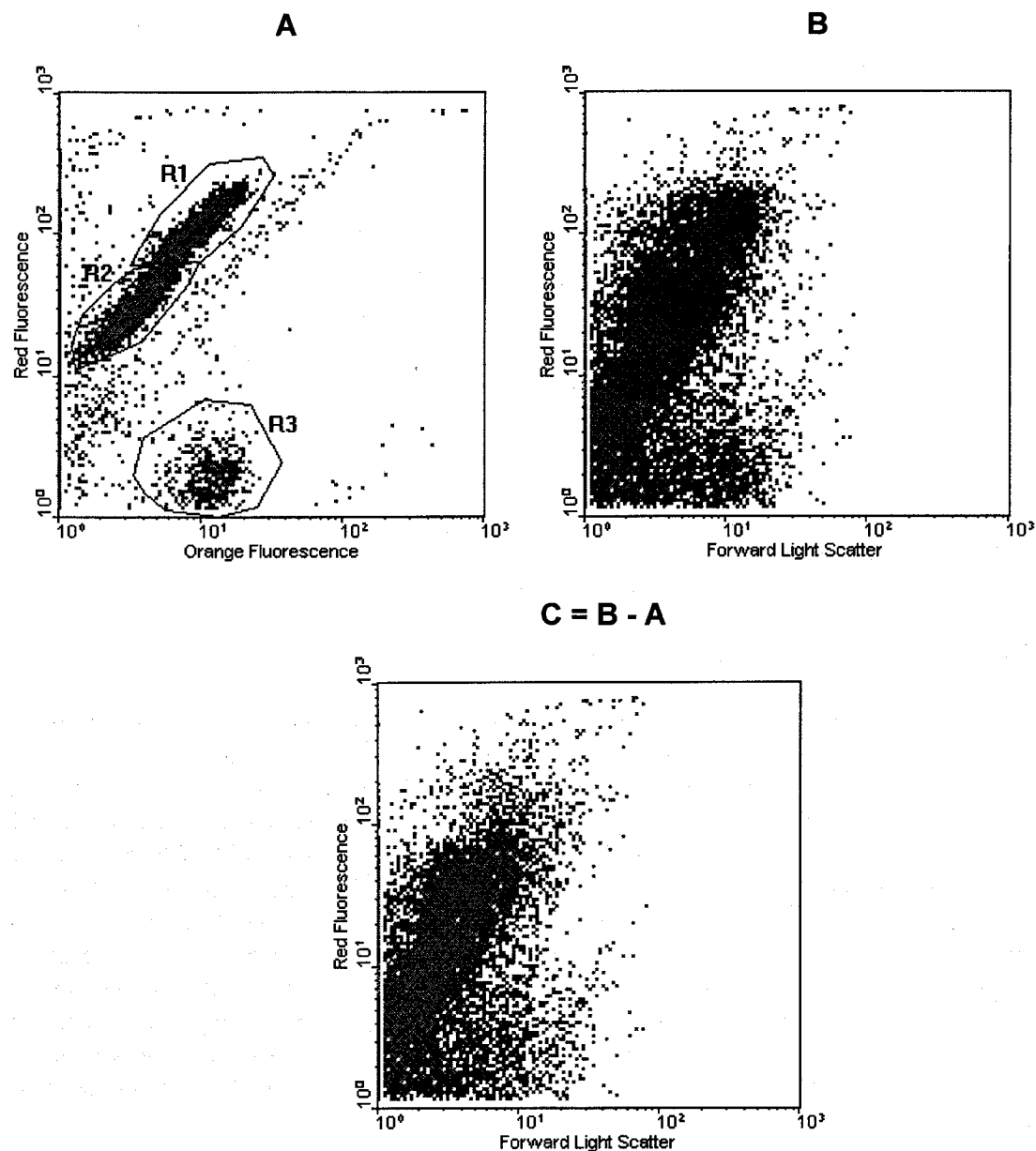


Fig.4 Flow cytometric plots, demonstrating the *gating* procedure. For explanation see text.

In contrast to HPLC pigment analyses, flow cytometry may provide almost real-time data on cell concentrations and fluorescence characteristics of *individual cells*. On the other hand, FC can only detect and discriminate the fluorescing porphyrin-derivates chlorophyll and the phycobilines, while HPLC data involve a set of accessory pigments, by which different phytoplankton classes can be specifically characterized (e.g. MANTOURA and LEWELLYN 1983). Thus, flow cytometric analysis of phytoplankton can only be ataxonomic. Different taxa with identical or overlapping optical features cannot be discriminated and will appear as a homogenous or overlapping cluster. This restriction makes FC best suitable in environments with a low diversity in small-sized algae, where microscopical analysis comes to its limits and the few phytoplankton taxa are well defined by their size and fluorescence characteristics. This generally applies to oligotrophic oceanic environments. In the late 1980s, an whole new class of prokaryotic phytoplankton (the oceanic prochlorophyte *Prochlorococcus*) was discovered by a combination of HPLC pigment analysis and flow cytometry (GIESKES and KRAAY 1983, CHISHOLM et al. 1988, see also section 4.2.1.). Tab.2 compares flow cytometry with other methods for the analysis of phytoplankton communities.

Tab.2 Different methods for analysing phytoplankton and their pros and cons.

		<i>Microscopy</i>	<i>Flow Cytometry</i>	<i>HPLC Pigment Analysis</i>	<i>Bulk Chl.a Analysis</i>
Taxonomic Information:	<i>Eutrophic Environment</i>	Species Level	Cyanobact./Crypt. Eukaryotes	Class Level	None
Taxonomic Information:	<i>Oligotrophic Environment</i>	Species Level*	Cyanobact./Crypt. Eukaryotes	Class Level	None
Biomass Information:		Most direct approach, abundance and biomass	On-line single cell analysis, abundance and biomass	Indirect biomass estimation	Indirect biomass estimation
Time Investment:		High	Low	Medium	Low
Money Investment:		Low	High	High	Low

* As picoplanktic forms dominate in much of oligotrophic environments, microscopical identification of these minute forms is often impossible.

2.5.2. Shipboard instrumentation and operation

Arabian Sea, cruise B2 (NE monsoon). During cruise B2, a Coulter ELITE CS cytometer, equipped with a water cooled, tuneable laser (max. power 5W) was used (Dr. Marcel Veldhuis, NIOZ). The fluid system and optics had been optimized for highest sensitivity *sensu* OLSON et al. (1990). The excitation wavelength was adjusted to 457nm. Although the laser output power at this wavelength was much lower than at 488nm, the increased fluorescence yield of both Chl.a and Chl.b at 457nm compensated for the loss of excitation energy (CAMPBELL and VAULOT 1993). Emission in the dark red (656 - 700nm) was used to measure chlorophyll fluorescence, and emission in the yellow-orange range (530 - 590nm) corresponded to phycoerythrin fluorescence. Forward and Sideward light scatter were detected at the proper laser wavelength, i.e. 457nm. All parameters were recorded on a four decade-logarithmic scale. Sensitivity was adjusted so that cells > ~3µm were off scale in the red channel. Up to 6 different phytoplankton groups could be discriminated and enumerated with this setting. Sample volume was 0.5ml. No problems occurred during the operation of the flow cytometer.

Baltic Proper and Pomeranian Bay. In the Gotland Sea and the Pomeranian Bay (AvH cruises), a PARTEC PAS III Flow Cytometer was used. It was equipped with a tuneable Argon laser (max. power 300mW), adjusted to 488nm. Emission light was detected as red (>630nm, chlorophyll fluorescence), yellow-orange (530-590nm, phycobilin autofluorescence), or turquoise (488nm, scatter signals) light. Signals were recorded a 3-decade logarithmic scale. The fixed sample volume was 0.7ml. The upper size limit of detectable cells was approximately 5µm.

During the operation on AvH, several problems occurred. Firstly, the sample flow speed could not be adjusted to sufficiently low flow rates to accurately count particles at very high concentrations. Secondly, the sensitivity of the optic system could not be optimized, so that the signals of the picocyanobacterial genus *Synechococcus* could not be separated from the axes (resp. the background noise). This, however, is a prerequisite for the separation from eukaryotic picoautotrophs and quantification in a bivariate plot (see Fig.3). Thirdly, the fluid system was very unstable, causing two effects: a vibrating sample flow due to engine generated low-frequent vibrations (only when the ship was steaming), a completely interrupted sample stream when the ship was tilting to one side, and an enormously widened sample stream while tilting to the other side. Thus, reliable measurements could only be made when the ship was drifting (engine off), and

when the sea was calm. Fortunately, these conditions were met during most of both cruises. However, the absolute counts of picocyanobacteria are probably underestimates.

2.6. Herbivory estimated in serial dilution experiments

2.6.1. Theoretical background

Estimating *in situ* grazing rates of microzooplankton is very difficult because of the size and fragility of these organisms. Protozoa and phytoplankton very much overlap in size, so that a separation by size fractionation or picking individuals, as can be done for larger crustacean grazers, is practically impossible. The serial dilution method, introduced to marine ecology by LANDRY and HASSETT (1982), overcomes this problem by artificially reducing the grazing pressure in a series of seawater dilutions. The basic idea behind the method is to simply reduce the predator-prey encounter rate by diluting the seawater, so that the prey in the diluted treatments experiences a lower grazing pressure as the prey in the undiluted bottles. The difference of prey abundance in the diluted samples after the incubation period (generally 24h) relative to the undiluted treatments allows the calculation of the grazing rate (= prey disappearance rate), as well as the prey growth rate. The method has been almost exclusively used to account for grazing on phytoplankton (*herbivory*), but could in principle also be applied to grazing on osmotrophic bacteria (*bacterivory*). Dilution experiments *sensu* LANDRY and HASSETT (1982) involve the exclusion of mesozooplankton (>200 μm) from the incubation vessels. This results in an estimate of grazing impact by the entire microzooplankton community (<200 μm).

The apparent growth rate k of the prey can be directly measured by concentration changes in the incubation over time and is calculated using the exponential model for phytoplankton growth:

$$k = (\ln N_t - \ln N_0) / t, \quad (1)$$

with N_0 representing the prey concentration at the beginning, N_t at the end of the experiment, and t the incubation duration. The apparent growth rate k integrates two processes: the specific growth rate of the individual prey cell, here termed μ , and the disappearance (= grazing) rate g of the prey. Assuming grazing to be the only loss factor for phytoplankton in an incubation experiment, the basic relationship is

$$k = \mu - g. \quad (2)$$

When expressed on a daily basis, prey doubling time can be derived from μ as:

$$\text{Doubling time (d)} = \ln 2 / \mu \quad (3)$$

The reciprocal of (3) yields the numbers of generations produced per day.

The prey concentration at the end of the experiment (N_t) can be described by the exponential equation

$$N_t = N_0 e^{(\mu-g)t}. \quad (4)$$

In order to account for separate values for μ and g , one of the two respective processes must be separately measurable in an experiment. The dilution technique fulfils this.

The method involves three basic assumptions. Firstly, the specific phytoplankton growth rate, i.e. the division rate of an individual cell, must be density independent (i.e. unaffected by dilution). Secondly, the grazer-prey encounter rate and the grazing pressure must be linearly related to the

dilution step, and thirdly, the exponential growth function for phytoplankton is assumed to hold (equations (1) and (4)). The validity and implications of these assumptions will be discussed in section 4.1.2.

With four dilution steps incubated (e.g. 100%, 75%, 50%, and 25% of original undiluted seawater), specific phytoplankton growth μ and grazing rates g can be calculated as

$$N_t = N_0 e^{(\mu-g*1)t} \quad \text{for the undiluted, original seawater sample,} \quad (5)$$

$$N_t = N_0 e^{(\mu-g*0.75)t} \quad \text{for the sample containing 75% undiluted, original seawater,} \quad (6)$$

$$N_t = N_0 e^{(\mu-g*0.5)t} \quad \text{for the sample containing 50% undiluted, original seawater} \quad (7)$$

$$N_t = N_0 e^{(\mu-g*0.25)t} \quad \text{for the sample containing 25% undiluted, original seawater.} \quad (8)$$

With N_0 and N_t measured directly, μ and g can be calculated for any combination of two dilution steps. In general, μ and g are determined graphically to check the linearity of the grazing pressure-dilution dependency. The apparent net growth rates $k (= \mu - g)$ in each bottle are calculated from (1) and plotted against the respective dilution factors (Fig.5). The y-axis intercept of the regression line represents the specific phytoplankton growth rate μ (in the hypothetical absence of grazers at 0% undiluted, original seawater), while the negative slope yields the phytoplankton disappearance rate attributed to grazing, hence the grazing rate g . For the related calculations, it is important to note that g is defined here as a positive number, although it is derived from a negative slope. For ecological interpretations, it is useful to convert the coefficients μ and g into relative or absolute values. The absolute amount of phytoplankton grazed per unit time can be inferred from the difference of the calculated potential standing stock at the end of the experiment (in the hypothetical absence of grazing),

$$N_t \text{ pot.} = N_0 e^{(\mu)t}, \quad (9)$$

and the actually measured standing stock at the end of the experiment

$$N_t \text{ act.} = N_0 e^{(\mu-g)t}. \quad (10)$$

The difference between the measured (10) and the hypothetically possible stock (9) allows the calculation of the amount of phytoplankton grazed per unit time:

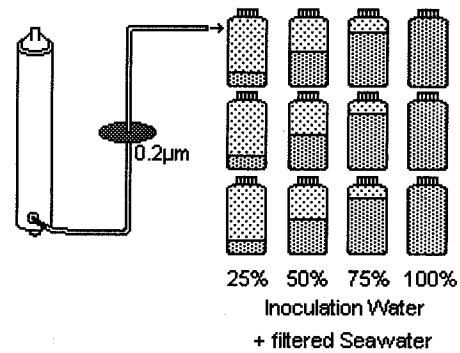
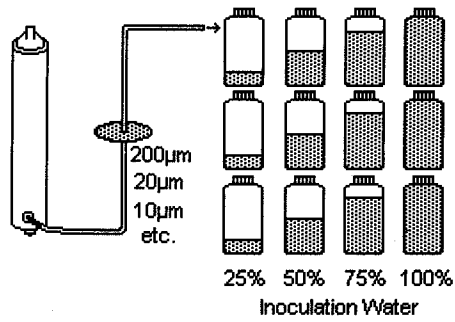
$$N_t \text{ graz.} = N_0 (1-e^{-gt}). \quad (9)-(10)$$

The term $(1-e^{-gt})$ represents the relative consumption per unit time (i.e. the portion of standing stock consumed per unit time). An estimation of the relative amount of gross production consumed per unit time is estimated by the ratio μ/g .

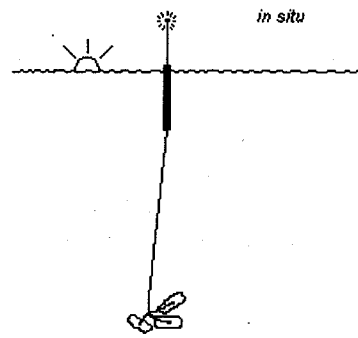
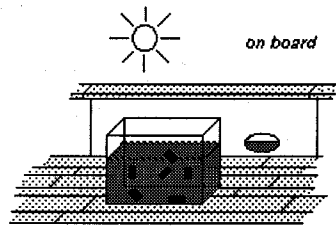
Although the majority of investigators have used Chl.a as a measure for phytoplankton biomass (e.g. PARANJAPPE 1987, BURKILL et al. 1993b), more specific methods like phytoplankton cell counts (REITMEIER 1994), HPLC pigment analysis (BURKILL et al. 1987, STROM and WELSCHMEYER 1991), or flow cytometry (LANDRY et al. 1995a, LANDRY et al. 1995b, this study) may provide additional information on feeding rates on specific phytoplankton groups. Fig.5 sketches the main procedures and the graphical analysis of a dilution experiment.

1. Drain appropriate volumes of inoculation water into prepared polycarbonate bottles, prescreen through desired nets / filters

2. Add 0.2µm filtered seawater from the same source, fill up to defined bottle volume



3. Take t_0 - subsamples at the start of incubation from each bottle and measure
 4. Incubate for 24h



5. Take t_{24} - sample and measure
 6. Plot k against the respective dilution factor for all bottles, calculate μ (y-intercept of the regression line), and g (negative slope of the regression line):

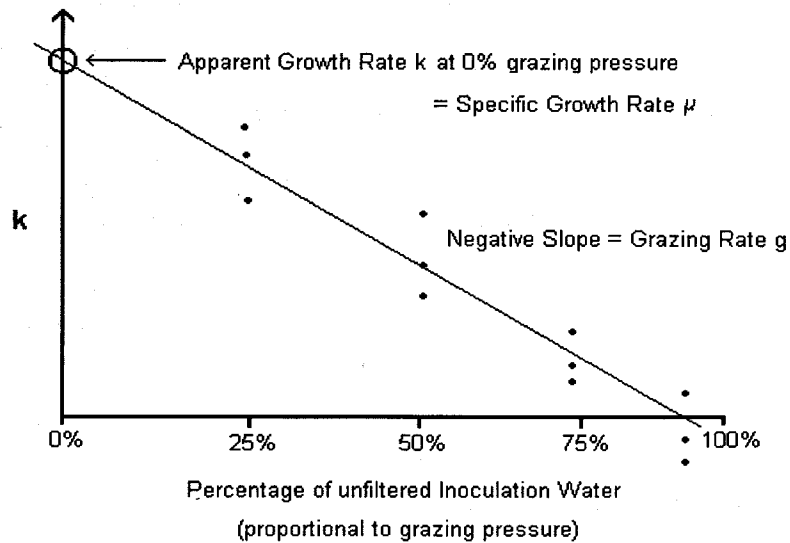


Fig.5 Basic procedures for the performance and analysis of a serial dilution experiment.

2.6.2. Experimental protocols

Phytoplankton concentrations were determined by bulk Chl.a measurements (Arabian Sea, Pomeranian Bay 1993) or flow cytometry (FC, Arabian Sea B2 and Gotland Sea). Water from different depths of the euphotic zone was taken from the rosette water bottles. The inoculation water was either siphoned into light-screened 20 dm³ polycarbonate (PC) carbuoys (Chl.a determinations Arabian Sea), light screened plastic beakers (FC determinations Arabian Sea B2), or directly into the incubation bottles (Baltic Sea) by means of a submerged silicon tubing. The filtration water was taken from the same depth and was also gently filled into PC-carbuoys. It was then filtered through 0.2µm membrane filters (Nalgene filter capsules) by means of positive air pressure (Chl.a determinations Arabian Sea), syringes (FC determinations Arabian Sea B2), or a peristaltic pump (Baltic Sea). This 0.2µm-filtered water was then combined with the unfiltered inoculation water (containing all the organisms) to give four dilution steps with three parallels (2 parallels per dilution during Arabian Sea B2 in size fractionation treatments). During the Arabian Sea cruises, 5 dm³ glass bottles were used for the dilution experiments based on Chl.a, while 60 cm³ polystyrene cell tissue culture bottles were used for the fractionated dilutions measured by flow cytometry. During the Baltic Sea cruises, 1 dm³ PC bottles were used for the Chl.a-dilutions, and 250 cm³ PC-bottles for the FC-measured dilutions. Any equipment that came into contact with the incubated water had been washed with 10% HCl and rinsed thoroughly with MilliQ water, or 0.2µm filtered seawater. For the experiments in the Gotland Sea, 0.2µm filtered nutrient-rich deep water was added to the incubation bottles (10% of the total bottle volume). Unspiked bottle were co-incubated to account for unmanipulated phytoplankton growth rates. During the Arabian Sea cruises and in the Gotland Sea, the bottles were incubated for 24h, freely floating in large plastic boxes equipped with running seawater cooling and light attenuation filters to simulate *in situ* mixed layer conditions. In the Pomeranian Bay 1993, bottles were attached to a floating rack, lowered to the appropriate depths, and incubated for 24h *in situ*.

2.7. Herbivory estimated in a light-dark experiment

At station RS2 of cruise B2 in the Arabian Sea, another approach was chosen to estimate specific growth and grazing mortality of phytoplankton. If cells do not divide in the dark, then the biomass development in a dark relative to a light treatment allows the calculation of a specific growth and grazing rate. Cell cycle analysis had shown that *Synechococcus* did not divide in the dark in the southern Red Sea (pers.comm. Dr. M.Veldhuis, NIOZ), which opened the opportunity to estimate growth and grazing simply by comparing *Synechococcus* growth in light and dark incubations (section 3.2.6.). The absence of cell division in the dark means that any disappearance during this period is due solely to grazing, provided lysis is negligible. In the light, grazing and growth are simultaneous processes. Thus the disappearance rate of *Synechococcus* in the dark represents the grazing rate. Prescreened water of each respective fraction was incubated in the light and in the dark (under simulated *in situ* conditions) in triplicate for 24h. The decrease in cell numbers in the dark bottles was used to calculate the negative apparent growth rate, which is assumed to be the specific grazing mortality rate g :

$$g = (\ln N_{t24} - \ln N_{t0})_{\text{dark}} \quad (11)$$

This, and the apparent growth rate k in the light bottles

$$k = (\ln N_{t24} - \ln N_{t0})_{\text{light}} \quad (12)$$

allows the calculation of μ , with $k = \mu - g$ (2):

$$\mu = (\ln N_{t24} - \ln N_{t0})_{\text{light}} + (\ln N_{t24} - \ln N_{t0})_{\text{dark}} \quad (13)$$

Time series measurements in the $<20\mu\text{m}$ fractions were used to correct for growth in the dark bottles at the beginning of the incubation time. Fractionations, incubations and flow cytometric measurements were performed as described above (section 2.6.2).

2.8. Bacterivory estimated by chemical inhibition

At station US0 of cruise B1 (Arabian Sea), a chemical inhibition experiment was carried out to estimate the grazing impact of two grazer size classes on heterotrophic bacteria, following the description by SHERR et al. (1986a). The method bases on the assumption that specific metabolic inhibitors may stop cell proliferation of either the predator or the prey in an incubation experiment. In either case, the equation $k = \mu - g$ can be completely resolved, as k can be directly measured, and either μ or g is set to zero by the specific inhibitors. Predators (and correspondingly predation) can be inhibited by specific eukaryotic inhibitors (e.g. cyclohexane). Specific prokaryote inhibitors can be used to set μ (defined as specific bacterial growth rate) to zero.

In this study, one set of incubation bottles was treated with a combination of Penicillin and Vanomycin to inhibit prokaryotic cell division. The disappearance of prokaryotes relative to an uninhibited control treatment allowed the calculation of a grazing rate. Cell disappearance due to processes other than grazing (i.e. autolysis) was corrected for in a third treatment containing both the prokaryote inhibitors and the eukaryote inhibitor cyclohexane (preventing growth of both the prokaryotic prey and the eukaryotic grazers). The observed disappearance of bacterial cells in the prokaryote inhibited samples was used to calculate the grazing rate g :

$$g = (\ln N_{t24} - \ln N_{t0})_{\text{inhib.}} \quad (14)$$

Using the apparent bacterial growth rate k in the non-inhibited control treatments

$$k = (\ln N_{t24} - \ln N_{t0})_{\text{non-inib.}} \quad (15)$$

the specific bacterial growth rate μ can be calculated from $k = \mu - g$ as

$$\mu = (\ln N_{t24} - \ln N_{t0})_{\text{non-inib.}} + (\ln N_{t24} - \ln N_{t0})_{\text{inhib.}} \quad (16)$$

2.9. List of activities

Tab.3 List of activities during the five cruises to the Arabian Sea and the Baltic Sea.

FC = Flow Cytometry; FC frakt. = fraktionated dilution experiments, measured by FC; Epifluor. = Epifluorescence microscopy. Parentheses indicate mixed layer values from the experimental bottles, no depth profiles.

	Arabian Sea		Baltic Sea		
	B1: SW monsoon	B2: NE monsoon	Gotland Sea	Pomeranian Bay 1993	Pomeranian Bay 1994
Experiments					
Dilution - Chl.a	+	+	-	+	-
Dilution - FC	-	+	+	-	-
Dilution - FC frakt.	-	+	+	-	-
Dilution Epifluor. (Syn.)	+	-	+	-	-
Light-Dark Difference	-	+	-	-	-
Chemical Inhibition	+	-	-	-	-
Stocks and Distribution					
Ultraplankton by FC	-	(+)	+	-	+
Protozoa	+	+	+	+	+

3. Results

3.1. The northwest Arabian Sea and adjacent areas during the SW monsoon 1992 (NIOP-B1)

3.1.1. Hydrography, nutrients and Chl.a

Hydrography. The hydrographical situation in July and August 1992 (cruise B1) in the investigation area was characterized by the northeasterly flow of the Somali Current and an intense upwelling plume off the coast of Somalia, which had been observed already at the beginning of June, with a northern ($\sim 11^\circ\text{N}$), and a southern upwelling core at $\sim 4^\circ\text{N}$ (Cruise B0, BAARS 1994). By the time of the B1 investigations, the SW monsoon had fully developed with wind speeds around 7 Bf. Temperature profiles indicated surfacing of cold water north of station US1 ($\sim 9^\circ\text{N}$), with low surface water temperatures ($<22^\circ\text{C}$) and no distinct thermocline (Fig.6). The southernmost stations SB1 and US0 (south of 4°N) showed surface temperatures above 26°C , and a distinct thermocline between 100 and 150m. Temperature profiles of the Somali Basin stations (OFZ, SB2 and SI, Fig.6) imply that the upwelling plume had been spread well across the Somali Basin by the easterly and southerly flow of the Great Whirl (see Fig.1). US2 was sampled twice, and it showed a distinct stratification at St. 257, as compared to St. 230 eight days earlier (Fig.6). The central Gulf of Aden (GA2) was well stratified with a very warm surface layer (30°C) and a sharp thermocline at 70m.

Nutrients. The nutrient distributions are generally mirrored in the temperature profiles (Fig.7). Surface concentrations of nitrate were highest at the upwelling station US2 ($12\mu\text{M}$) and in the Somali Basin ($9\mu\text{M}$), and low at the southern stations SB1 ($0.3\mu\text{M}$) and US0 ($0.5\mu\text{M}$). The central Gulf of Aden, however, was oligotrophic with surface nitrate being depleted. The other nutrients largely followed the vertical distributions of nitrate, with phosphate ($0.2 - 1.4\mu\text{M}$) and silicate ($2 - 10\mu\text{M}$) concentrations replete in the euphotic zone during the entire cruise.

Chlorophyll a and phytoplankton. Chlorophyll a concentrations were low ($<0.3\mu\text{g} / \text{dm}^{-3}$), with no distinct sub-surface maximum (Fig.8). Only at the upwelling station US2-230 (cast 23: $3\mu\text{g} / \text{dm}^{-3}$), and downstream the Great Whirl (station SI, $0.9\mu\text{g} / \text{dm}^{-3}$), concentrations were substantially higher (Fig.8). Chl.a concentrations at US2-257 had dropped by a factor of three as compared to US2-230 eight days earlier.

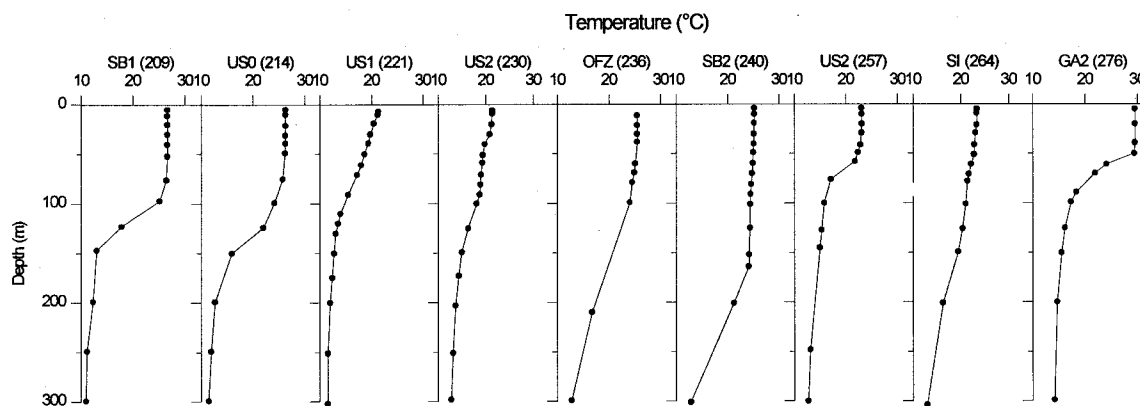


Fig. 6 Water column profiles of temperature during cruise B1 (SW monsoon).

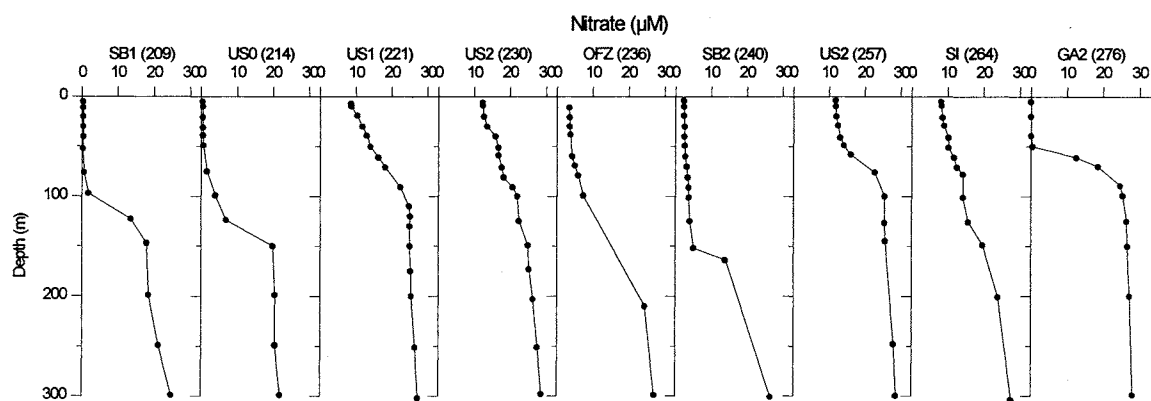


Fig.7 Water column profiles of nitrate during cruise B1 (SW monsoon).

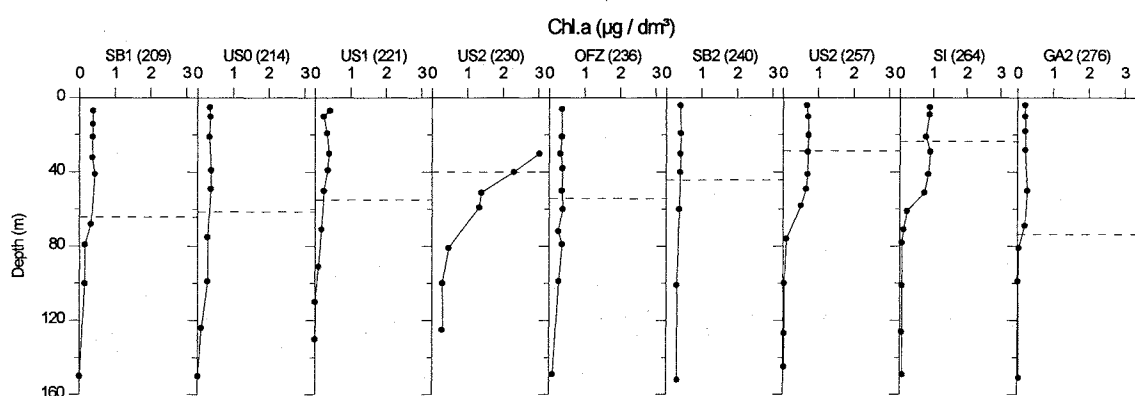


Fig.8 Water column profiles of Chl.a during cruise B1 (SW monsoon). Dashed lines indicate the depth of the euphotic zone (defined as 0.1% of surface irradiance).

The phytoplankton community at the non-upwelling stations was dominated by the picocyanobacterium *Synechococcus* and eukaryotic ultraphytoplankton, with minor contributions of the coccolithophorid *Emiliania huxleyi*. The picoautotrophic prokaryote *Prochlorococcus* was encountered only at the oligotrophic southern station US0 (VELDHUIS 1994).

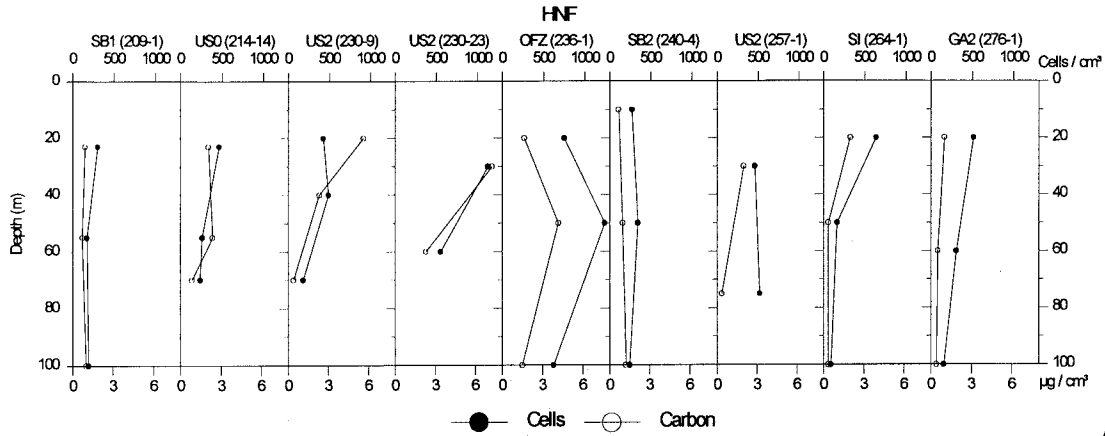
Large phytoplankton was found only in the upwelling plume at US2-230 / 23, where a variety of different diatom genera thrived (*Skeletonema*, *Chaetoceros*, *Nitzschia*, *Thalassiosira*, *Rhizosolenia*, *Biddulphia*, *Coscinodiscus*, *Asterionella*, *Navicula*, as well as the large chlorophyte *Scenedesmus* and *Phaeocystis*-type colonies). Fecal pellets of probably copepod origin (ca. 280 x 40 μm) were very abundant, pointing to intense grazing by crustaceans in the blooming water parcel. The other stations were poor in large phytoplankton. In the oligotrophic Gulf of Aden, small trichomes of the *Anabaena*-type (cyanobacteria) were frequently found.

3.1.2. Protozoan distributions

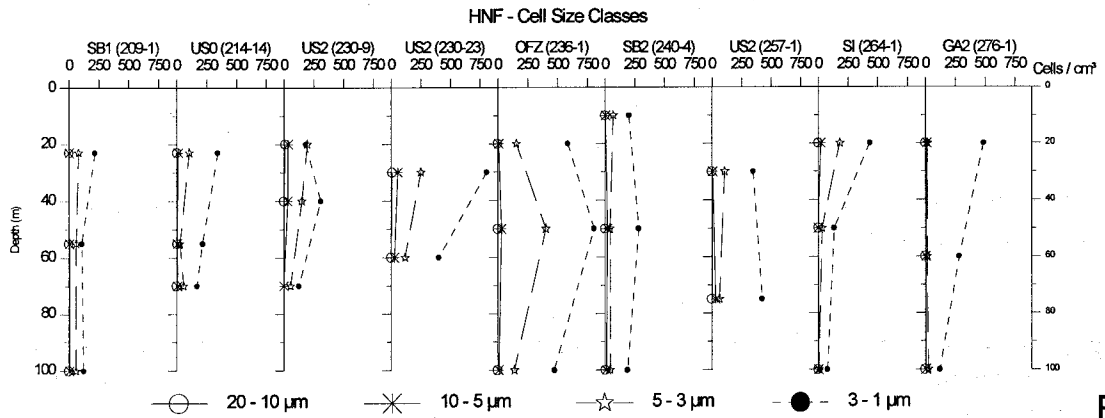
Heterotrophic nanoflagellate (HNF) cell concentrations in the euphotic zone (Fig.9A) were generally well below 1,000 cm⁻³ (304 - 640 cm⁻³), except for the upwelling station US2-230 and downstream at OFZ (1,128 and 1,243 cm⁻³, resp.). HNF carbon biomass (Fig.9A) ranged between 0.94 and 2.33 μg dm⁻³, and 7.25 μg dm⁻³ at US2. At all stations, the size fraction 3 - 1 μm was most abundant in terms of cell numbers (Fig.9B), followed by the next larger fractions. In terms of

carbon biomass, the fraction 3 - 5 μm was most important; only at US2 and GA2, the larger fractions 5 - 10 μm and 10 - 20 μm dominated (Fig.9C).

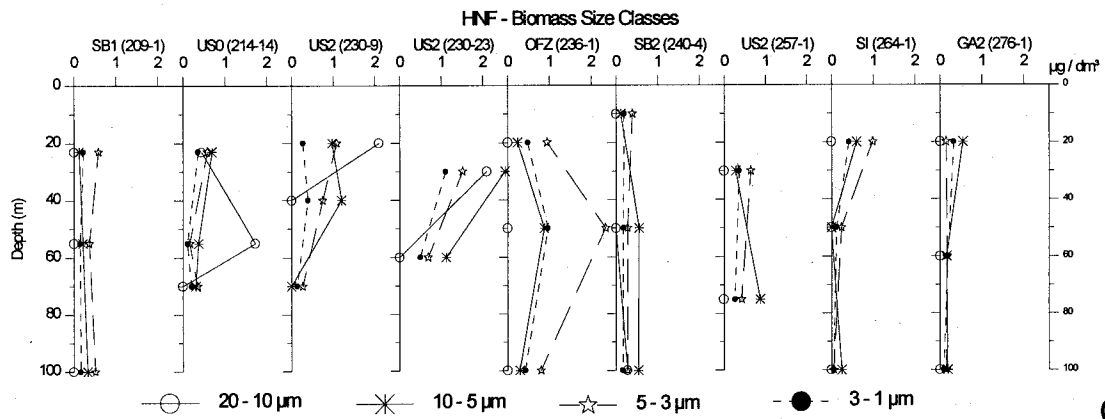
Cell concentrations of *heterotrophic dinoflagellates* ranged from 8 - 29 cm^{-3} , with carbon biomass ranging from 0.57 $\mu\text{g dm}^{-3}$ in the Somali Basin to 15.46 $\mu\text{g dm}^{-3}$ at the upwelling station. Small gymnodinoid forms (<20 μm) dominated throughout, with larger forms being present only at the upwelling station US2 (Fig.10).



A



B



C

Fig.9 Water column profiles of HNF during cruise B1 (SW monsoon). A: Total HNF numbers and carbon biomasses, B: Cell size classes, C: Carbon biomass size classes.

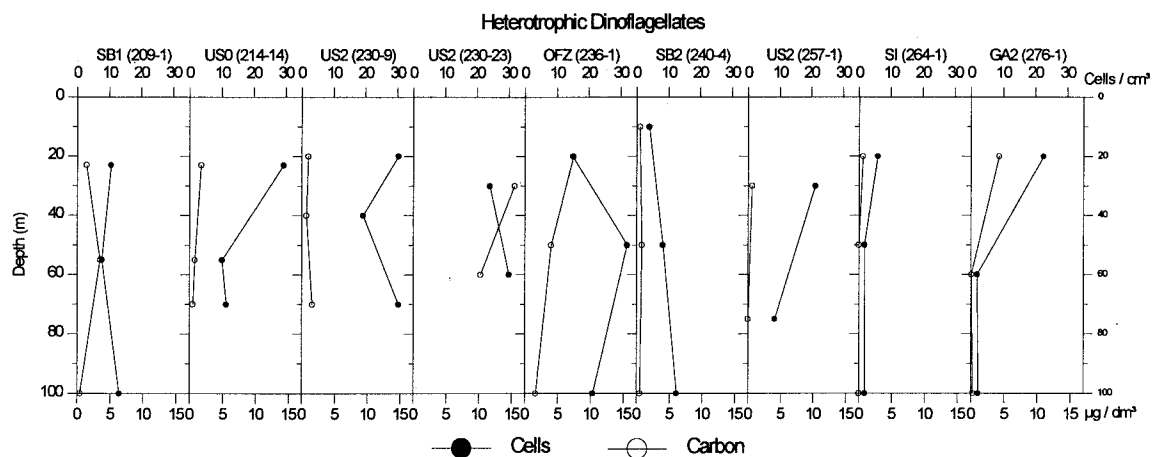


Fig.10 Water column profiles of heterotrophic dinoflagellate numbers and carbon biomasses during cruise B1 (SW monsoon).

Ciliate cell concentrations ranged from 657 dm^{-3} at station SI to $7,839 \text{ dm}^{-3}$ in the upwelling bloom at US2 (Fig.11). Ciliate carbon biomasses generally ranged around $1 \mu\text{g dm}^{-3}$ ($0.27 - 1.79 \mu\text{g dm}^{-3}$), with elevated values at GA2 ($6.11 \mu\text{g dm}^{-3}$) and US2 ($16.72 \mu\text{g dm}^{-3}$). Small oligotrich forms ($<20\mu\text{m}$) predominated at all stations, with larger individuals only at US2-230, but also in the oligotrophic Gulf of Aden at GA2.

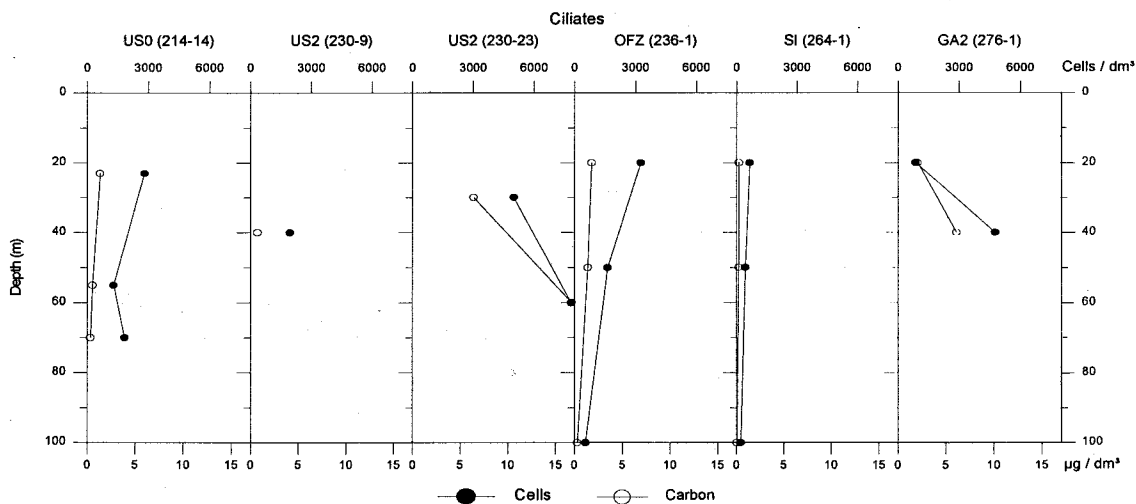
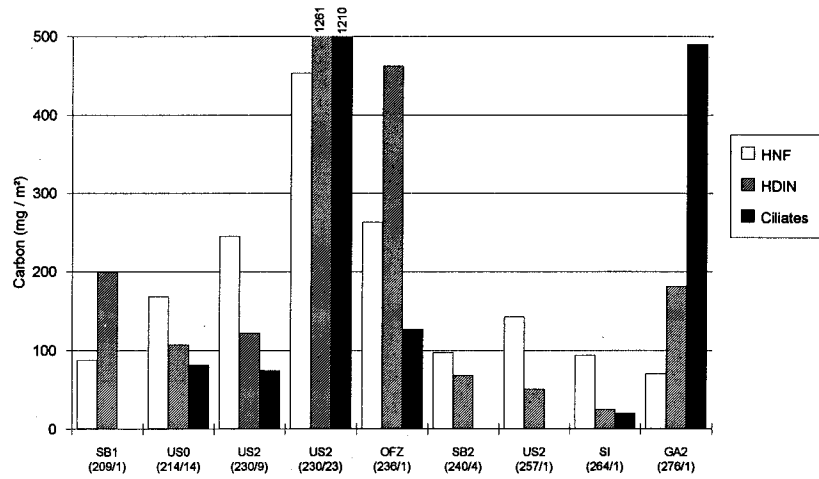
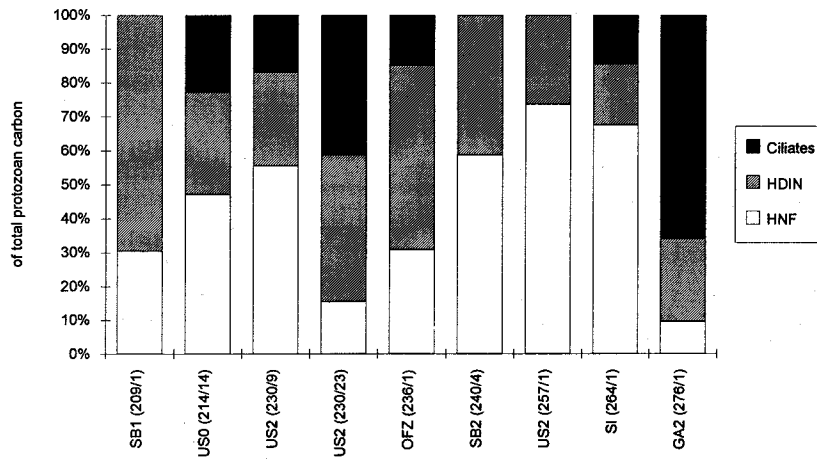


Fig.11 Water column profiles of abundance and carbon biomass of ciliates during cruise B1 (SW monsoon).

Fig.12 shows total carbon biomasses of protozoa, integrated over the upper 100m. Integrated HNF carbon biomass ranged from below 100 mg m^{-2} at the more oligotrophic stations to $4,500 \text{ mg m}^{-2}$ at US2-230. Integrated HDIN biomass ranged from 20 mg m^{-2} to over $1,200 \text{ mg m}^{-2}$ (US2-230), ciliate biomasses from 100 mg m^{-2} to $1,200 \text{ mg m}^{-2}$ (US2-230). Significantly elevated protozoan biomasses were found at the upwelling station US2-230, downstream at OFZ, and for HDIN and ciliates also in the oligotrophic Gulf of Aden at GA2. These high biomass values are primarily due to larger individuals at these stations, and only to a lesser extent to higher cell concentrations (Fig.14).



A



B

Fig.12 Protozoan carbon biomasses integrated over the upper 100m water column during cruise B1 (SW monsoon). A: Absolute values, B: as % of total protozoan carbon

While US2 (230-9) and US2 (257) did not significantly differ from the non-upwelling stations, US2 (230-23) showed dramatically increased protozoan concentrations and biomass (Fig.12A), complementing the observations of high Chl.a values (Fig.8) and large diatoms in this spatially confined blooming water parcel.

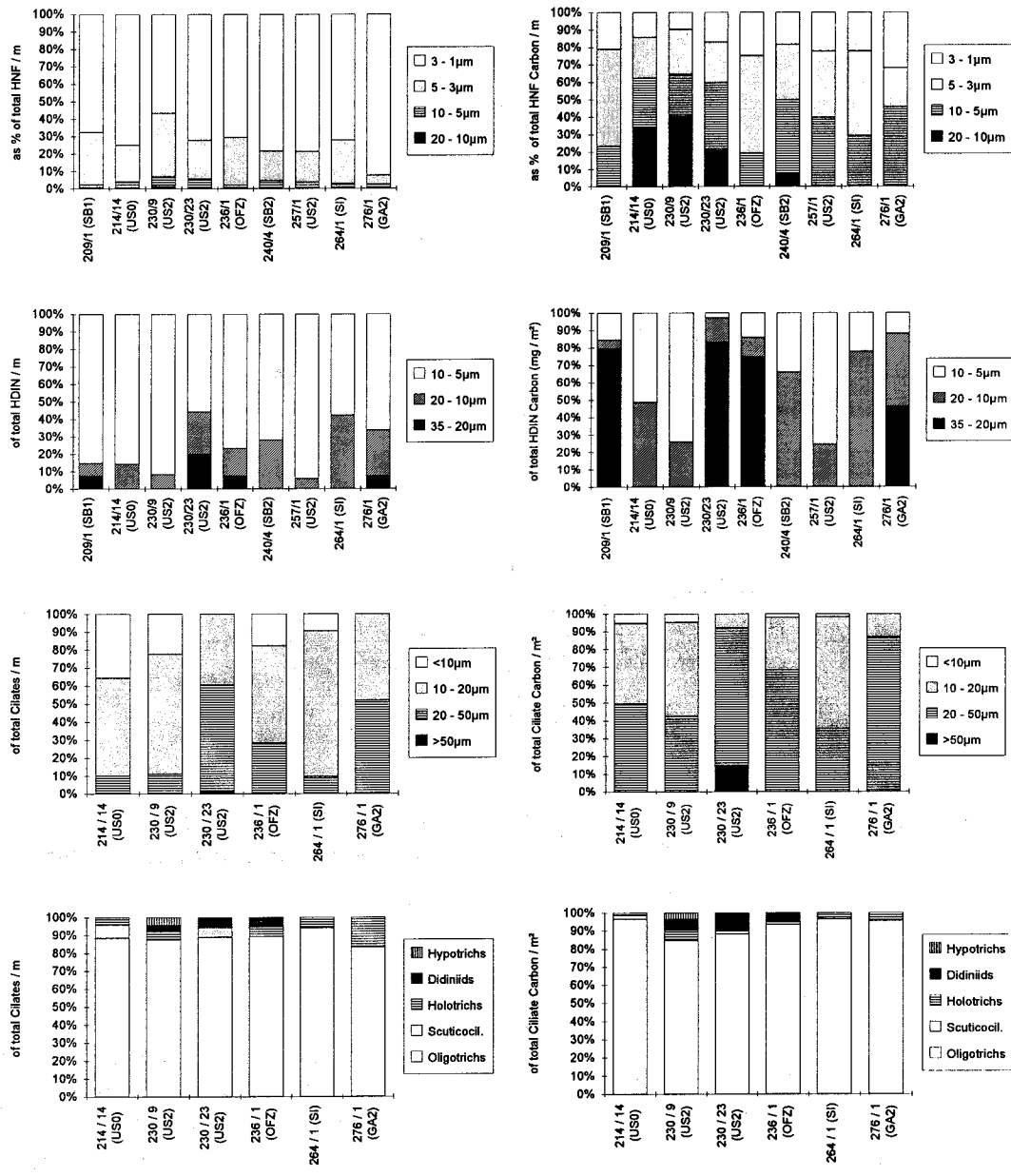


Fig. 13 Size class distributions of three protozoan groups during cruise B1 (SW monsoon). Left panel: as % of total cell numbers; right panel: as % of total carbon biomass.

A: heterotrophic nanoflagellates; B: heterotrophic dinoflagellates; C: ciliates. D: distribution of taxonomic ciliate groups

Fig. 13 shows relative integrated protozoan numbers and carbon biomass as a function of size class. Very small HNF cells ($<3\mu\text{m}$) were by far most abundant (55 - 90% of total cell counts); however, biomass was dominated by larger cells (3 - $5\mu\text{m}$ and 5 - $10\mu\text{m}$), with cells 20 - $10\mu\text{m}$ considerably contributing to HNF carbon biomass in the upwelling area (Fig. 13A).

Heterotrophic dinoflagellates (HDIN) were mostly smaller than $10\mu\text{m}$, with larger cells present in the upwelling area, but also at more oligotrophic sites, then clearly dominating biomass (Fig. 13B). Most ciliates were smaller than $20\mu\text{m}$, with larger individuals (20 - $50\mu\text{m}$) considerably contributing to ciliates biomass, especially in the upwelling bloom at US2 (230-23), where even larger specimen ($>50\mu\text{m}$) were found (Fig. 13C). Oligotrich ciliates clearly dominated both in terms of numbers and biomass, and the highest diversity was reached in the blooming upwelling plume (Fig. 13D).

Fig.14 demonstrates a considerable increase in individual protozoan body carbon (i.e. cell volume) in the upwelling area, and to a smaller extent also in the Gulf of Aden (for HDIN and ciliates).

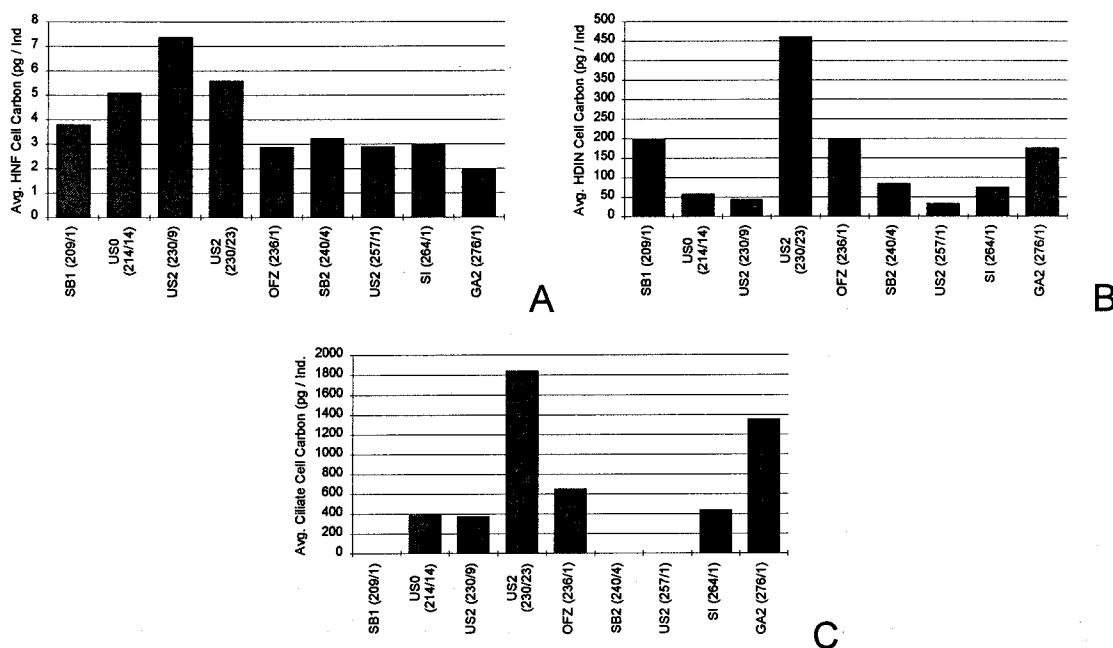


Fig.14 Average individual body carbon of three protozoan groups during cruise B1 (SW monsoon). A: heterotrophic nanoflagellates; B: heterotrophic dinoflagellates; C: ciliates.

3.1.3. Herbivory

During the SW monsoon, 5 dilution experiments based on Chl.a measurements were conducted. Herbivory varied between 14% and 48% of Chl.a stocks per day, and between 30% and 61% of Chl.a production per day, corresponding to an absolute Chl.a consumption of $0.11 - 2.36 \mu\text{g dm}^{-3} \text{d}^{-1}$. Again, the highest value was found at the upwelling station US2. Growth (μ) and grazing (g) coefficients varied between -0.096 to 1.062 and -0.605 to 0.649 , respectively (Tab.4). Phytoplankton consumption on a carbon basis was estimated applying an experimentally determined C:Chl.a ratio of 182 (Veldhuis, pers.comm.), except for the diatom bloom at US2, for which a ratio of 50 was taken. Based on these conversions, phytoplankton carbon consumption by microzooplankton ranged from 20 to $118 \mu\text{g dm}^{-3} \text{d}^{-1}$.

In four experiments, *Synechococcus* in the Chl.-bottles was counted by epifluorescence microscopy. Between 41% and 83% of *Synechococcus* standing stock (87% and 89% of production) was consumed by microzooplankton per day, corresponding to a carbon consumption of 3.4 and $8.4 \mu\text{g dm}^{-3} \text{d}^{-1}$, respectively (Tab.4). Dilution plots (apparent growth rate vs. dilution factor) are shown in Fig.15.

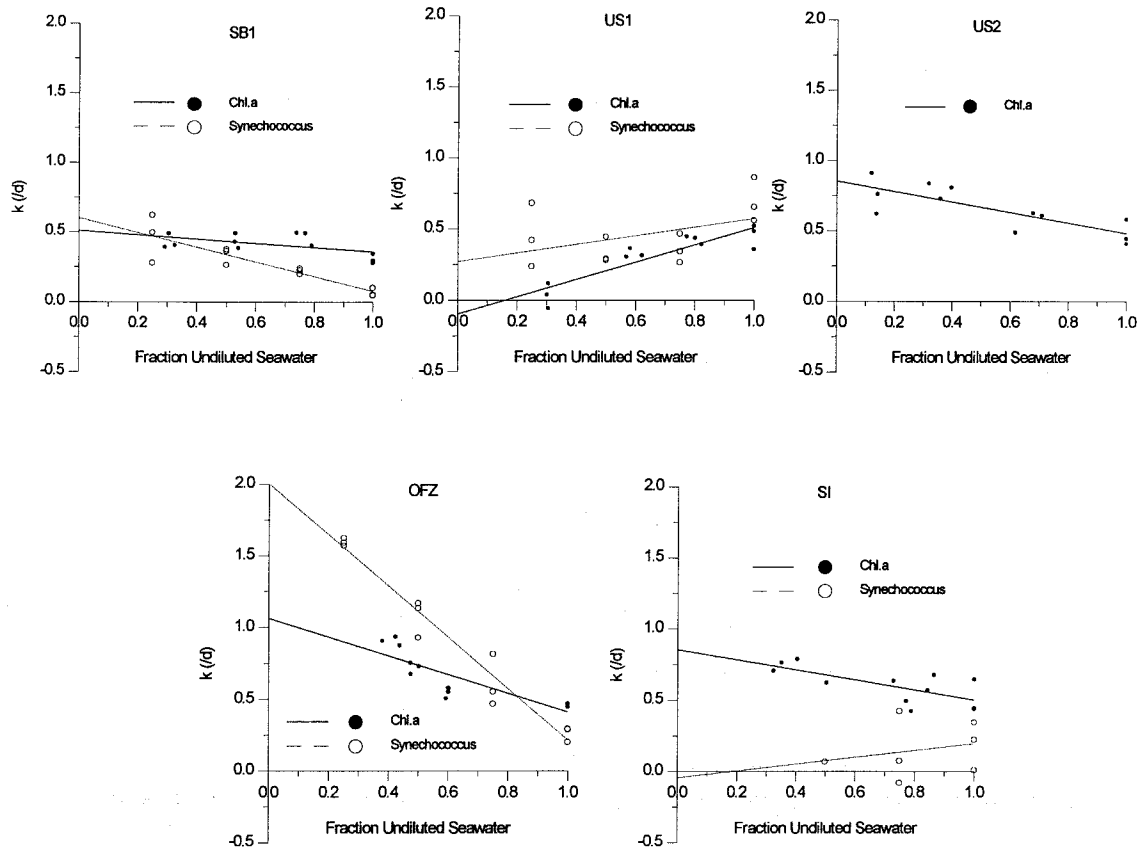


Fig.15 Regression plots of serial dilution experiments during cruise B1 (SW monsoon)

Tab.4 Results of serial dilution grazing experiments during cruise B1 (SW monsoon).

Chl.a									
Area	Station	Chl a Stock t0 mg / m ³	Grazing g (d)	Growth μ (d)	r	Stock grazed % / d	Prod.grazed % / d	Chl a grazed mg / m ³ * d	Phyto-C grazed mg / m ³ * d
SB1	209 / 1	0.77	0.152	0.510	0.539	14	30	0.11	19.81
US1	221 / 1	0.50	-0.605	-0.096	0.897	-	-	-	-
US2	230 / 9	7.62	0.372	0.854	0.798	31	44	2.36	118.21
OFZ	236 / 1	0.98	0.649	1.062	0.845	48	61	0.47	85.51
SI	264 / 1	0.88	0.352	0.855	0.710	30	41	0.26	47.79
Synechococcus									
Area	Station	Syn t0 # / ml	Grazing g (d)	Growth μ (d)	r	Stock grazed % / d	Prod.grazed % / d	Syn grazed # / cm ³ * d	Syn-C grazed mg / m ³ * d
SB1	209 / 1	47,330	0.525	0.602	0.885	41	87	19,318	3.38
US1	221 / 1	18,118	-0.301	0.271	0.448	-	-	-	-
OFZ	236 / 1	57,674	1.785	2.003	0.979	83	89	47,998	8.40
SI	264 / 1	26,289	-0.241	-0.043	0.247	-	-	-	-

Fig.16 shows that *Synechococcus* contributed to total phytoplankton consumption negligibly, not only in the upwelling plume or downstream, but also in the southern Somali Basin (SB1).

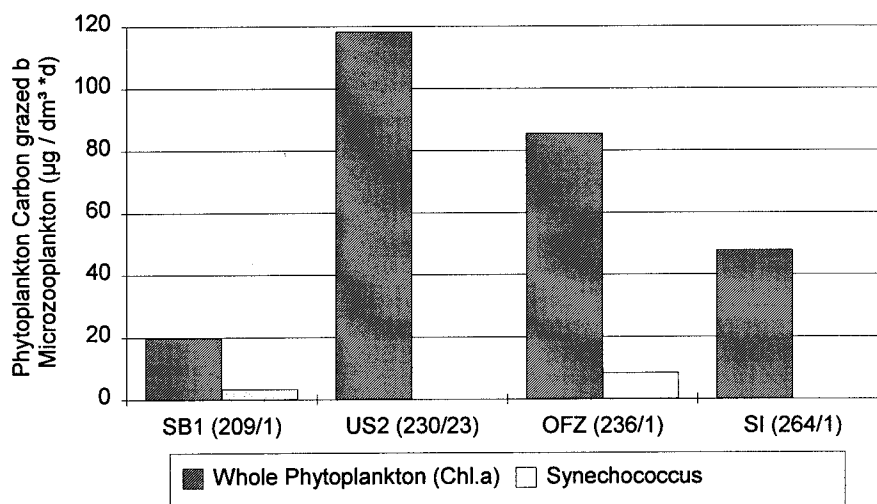


Fig.16 Carbon consumption rates of total phytoplankton (measured as Chl.a) and *Synechococcus* (measured by epifluorescence microscopy) by microzooplankton during cruise B1 (SW monsoon).

3.1.4. Bacterivory

At US0, the chemical inhibition method was used to estimate the grazing pressure of two microzooplankton size classes (<200µm and <15µm) on heterotrophic bacteria. Results are displayed as time series plots (Fig.17), and in Tab.5. Bacterial numbers decreased dramatically within the first 12h in all treatments, thereafter increasing in numbers until the experiment was stopped at 24h. The control treatment containing both pro- and eukaryote inhibitors changed only insignificantly. Although the absolute bacterial numbers had ceased also in the non-inhibited samples, the difference between the inhibited and the non-inhibited samples allowed the calculation of bacterial growth and grazing rates. After 12h, the cell numbers in the inhibited treatments increased again, indicating that the inhibition effect had weakened. Consequently, growth and grazing parameters were calculated over the first 12h (see section 2.7.).

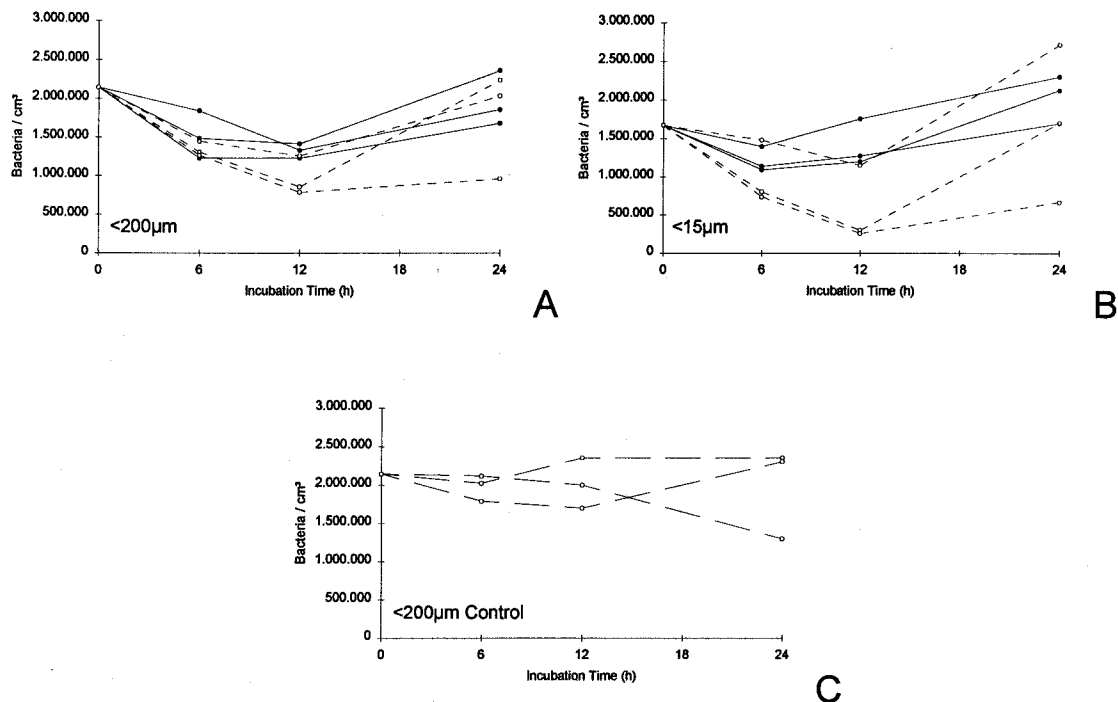


Fig. 17 Time series plots of the chemical inhibition experiment to estimate bacterivory at St. US0 of the B1 cruise (SW monsoon). A: Grazer size fraction <200µm; B: <15µm; C: <200µm control with both procaryotic and eukaryotic inhibitors. Black symbols and drawn out line = without manipulation; white symbols and dotted line = treated with inhibitors.

77% of bacterial biomass (233% of production) was removed by grazing daily in the <200µm fraction, 87% (resp. 112%) by the <15µm. Both growth and grazing coefficients were much higher in the smaller size fraction (Tab.5). Grazing exceeded growth in the experimental bottles (especially in the <200µm treatment), resulting in a net decrease of bacterial numbers.

Tab.5 Results of chemical inhibition experiment to estimate bacterivory at St. US0 of cruise B1 (SW monsoon).

Grazer Size Fract.	Bact. t0 # / cm³	Grazing g (d)	Growth µ (d)	Stock grazing % / d	Prod. grazing % / d	Bact. grazed # / cm³ * d	Bact.-C grazed mg / m³ * d
<200µm	2,144,493	1.473	0.631	77	233	1,652,729	24.92
<15µm	1,672,403	2.031	1.811	87	112	1,452,998	21.91

3.2. The Northwest Arabian Sea and adjacent areas during the NE monsoon 1992 / 1993 (NIOP B2)

3.2.1. Hydrography, nutrients and Chl.a

Hydrography. Strong northwesterly winds (4 - 7 Bft., average 5) characterized the NE monsoon in January and February 1993 (cruise B2). A sharp thermocline was detected only at the southernmost stations in the Somali Basin, and the mixed layer temperatures were generally below those measured during the summer (~ 26 °C). The Somali Current was now heading northeast, preventing upwelling of cool and nutrient rich water along the Somali coast (see Fig.1). Temperature profiles showed a gradual deepening of the less distinct thermocline towards the end of the cruise (Fig.18); however, observations at station SB2 indicated that this was due to high wind pressure in the entire area: as wind speeds increased from 4 to 7 Bft, the mixed layer deepened from 24 to 36m, and nitrate concentrations rose by a factor of 4 during the two days drift (BAARS et al. 1994). So the increasing mixed layer depth towards the end of the cruise is probably not an indicator for spatial heterogeneity, but a more or less simultaneous feature in the entire region due to wind convection.

Nutrients. Nitrate concentrations in the mixed layer (Fig.19) were low but not depleted at all stations (0.3 - 1.7 μM). Generally, a distinct nutricline coincided with the thermocline. Nitrite showed a sharp nitrification peak just below the nutricline at most stations. Meteorological conditions indicate a wind-induced entrainment of nutrient enriched water from deeper layers into the surface layer, both in the Somali Basin (elevated concentrations at US2 and SI), the Gulf of Aden (GA2) and the southern Red Sea (RS2). Mixed layer concentrations of phosphate (0.3 - 0.5 μM) and silicate (1.5 - 2.5 μM) were also low but not depleted.

Chlorophyll a and phytoplankton. Chlorophyll concentrations (Fig.20) were low in the Somali Basin and Gulf of Aden (<0.5 $\mu\text{g dm}^{-3}$); only in the southern Red Sea, Chl.a concentrations exceeded 1 $\mu\text{g dm}^{-3}$. Phytoplankton was dominated by picoplankton in the Somali Basin, with *Synechococcus*, *Prochlorococcus* and some unidentified eukaryotic pico- and nano-eukaryotes. HPLC pigment analysis indicated the presence of prymnesiophyceae, pelagophyceae, and *Micromonas*-type flagellates (VELDHUIS et al. 1994). Dinoflagellates were also abundant during the entire cruise (*Gymnodinium* and *Amphidinium* species), while cryptophytes were present only in low numbers.

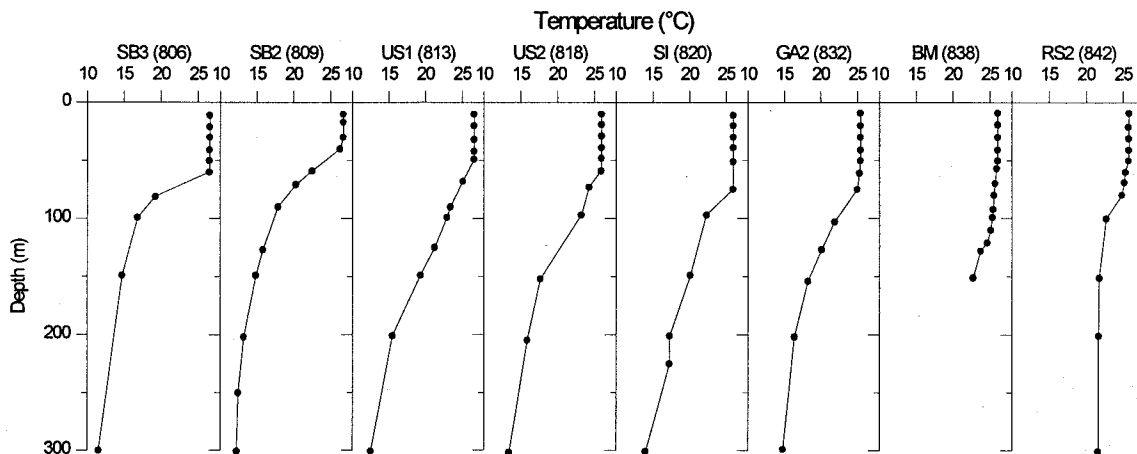


Fig.18 Water column profile of temperature during cruise B2 (NE monsoon).

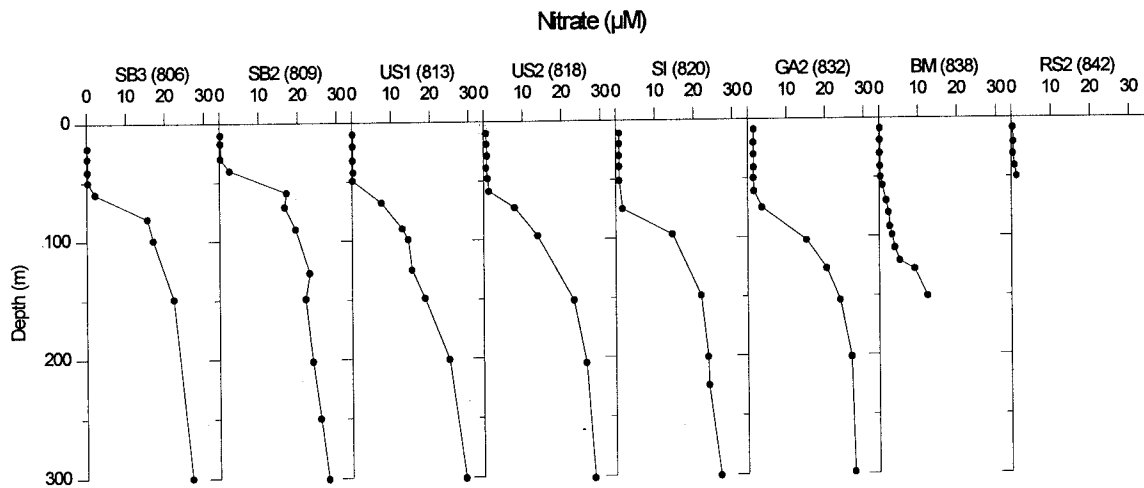


Fig.19 Water column profiles of nitrate during cruise B2 (NE monsoon).

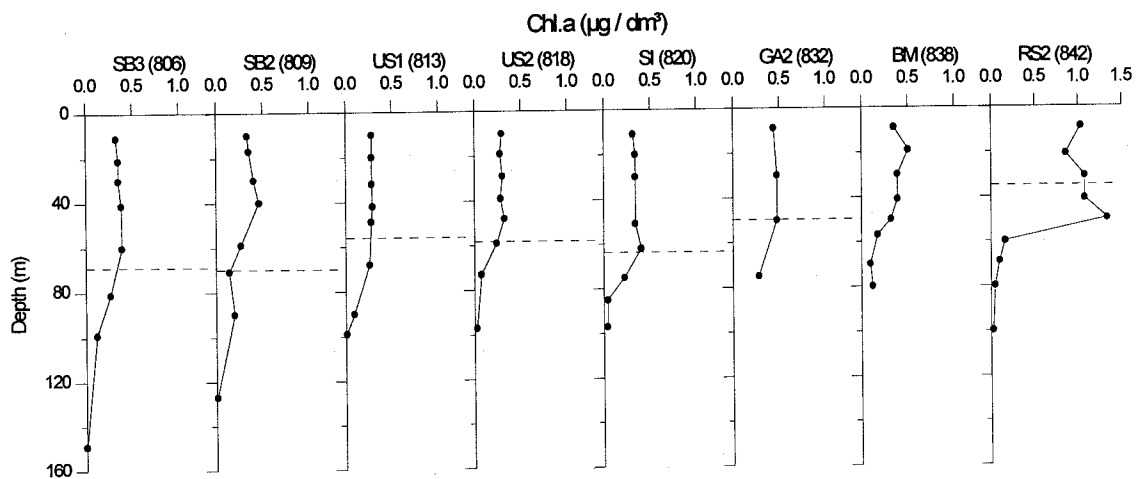


Fig.20 Water column profiles of Chl.a during cruise B2 (NE monsoon). Dashed lines indicate euphotic zone depth (0.1% of surface irradiance).

Although present in the Somali Basin, *Prochlorococcus* was virtually absent in the eutrophic inner Gulf of Aden and the southern Red Sea, while both types of *Synechococcus* were present in high abundances (up to $150,000 \text{ cm}^{-3}$). In the Gulf of Aden (GA2), the strait of Bab-el Mandab (BM), and the southern Red Sea (RS2), a highly diverse phytoplankton community was found, consisting of large diatoms (*Chaetoceros*, *Nitzschia*, *Coscinodiscus*, *Biddulphia*), dinoflagellates (*Gymnodinium* and *Amphidinium*), cryptophytes, as well as *Phaeocystis*-type colonies.

3.2.2. Protozoan distribution

Heterotrophic nanoflagellate (HNF) numbers and carbon biomasses were slightly higher than in the SW monsoon. Highest values were reached at SB3, (cells: $4,268 \text{ cm}^{-3}$, carbon: $6.28 \mu\text{g dm}^{-3}$, respectively), while concentrations elsewhere ranged from $1,630 \text{ cm}^{-3}$ and $2.12 \mu\text{g dm}^{-3}$ to 812 cm^{-3} and $1.79 \mu\text{g dm}^{-3}$. There was no pronounced gradient in depth down to 100m except for SB3, where surface values exceeded the depth values by a factor of 5. Flagellates 3 - $1 \mu\text{m}$ were most abundant at all stations, while biomass was dominated by the size fraction 5 - $3 \mu\text{m}$. Only at station SB3, where flagellates $<3 \mu\text{m}$ were extraordinarily abundant, they also accounted for the bulk of HNF biomass (Fig.21).

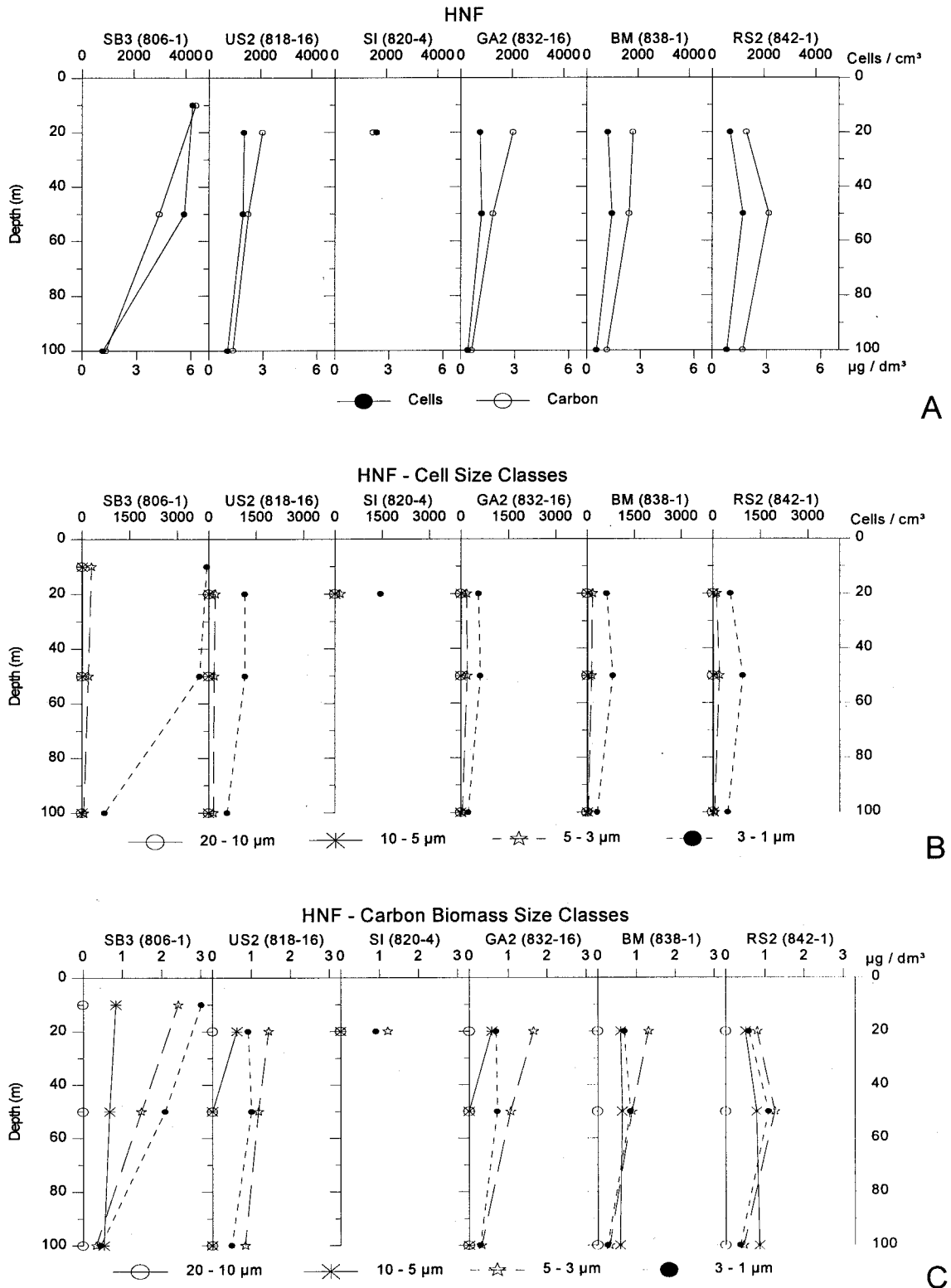


Fig.21 Water column profiles of HNF during cruise B2 (NE monsoon). A: Total HNF cell and carbon biomass concentrations, B: Cell size classes, C: Size classes of carbon biomass.

Heterotrophic dinoflagellate cell concentrations ranged from 13 - 60 cm^{-3} , and carbon biomasses from 1.07 - 6.74 $\mu\text{g dm}^{-3}$, respectively, slightly exceeding the values from the SW monsoon (Fig.22). Small gymnodinoid forms ($<20\mu\text{m}$) predominated.

Ciliate concentrations during the NE monsoon were significantly lower in the Somali Basin than during the SW monsoon (cells: 108 - 890 dm^{-3} , carbon: 0.17 - 0.87 $\mu\text{g dm}^{-3}$), but they increased dramatically in the southern Red Sea (BM: 4,860 dm^{-3} and 5.43 $\mu\text{g dm}^{-3}$; RS2: 8,748 dm^{-3} and 6.21 $\mu\text{g dm}^{-3}$). Small oligotrichs (<20 μm) predominated in the Somali Basin, while larger specimen (>20 μm) were more abundant at the Red Sea stations (Fig. 23).

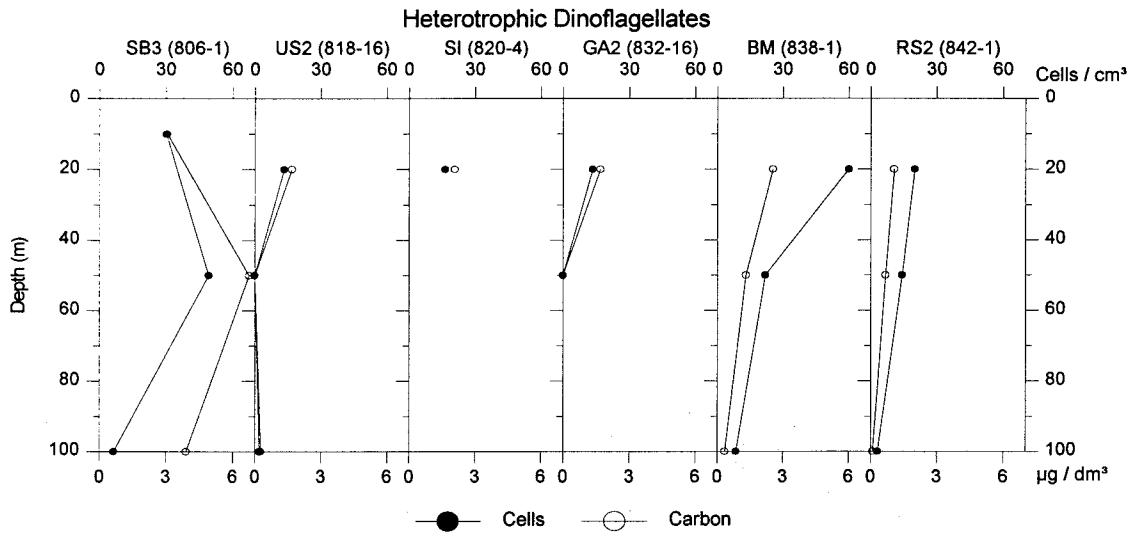


Fig.22 Water column profiles of abundance and carbon biomass of heterotrophic dinoflagellates during cruise B2 (NE monsoon).

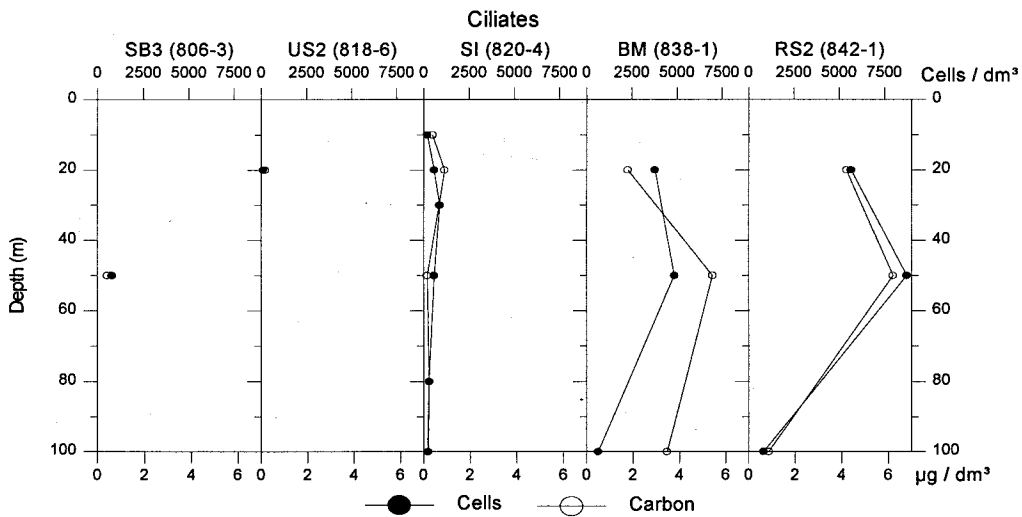


Fig.23 Water column profiles of abundance and carbon biomass of ciliates during cruise B2 (NE monsoon).

Protozoan carbon standing stocks integrated over the water column showed that HNF and HDIN clearly dominated biomass in the Somali Basin. Integrated HNF biomasses were relatively constant at 200 mg m^{-2} , except for SB3, where flagellate carbon biomass was about twice as high. Ciliate biomass in the Somali Basin was relatively low (~ 50 mg m^{-2}), but increased dramatically in the southern Red Sea (350 - 400 mg m^{-2} , Fig.24).

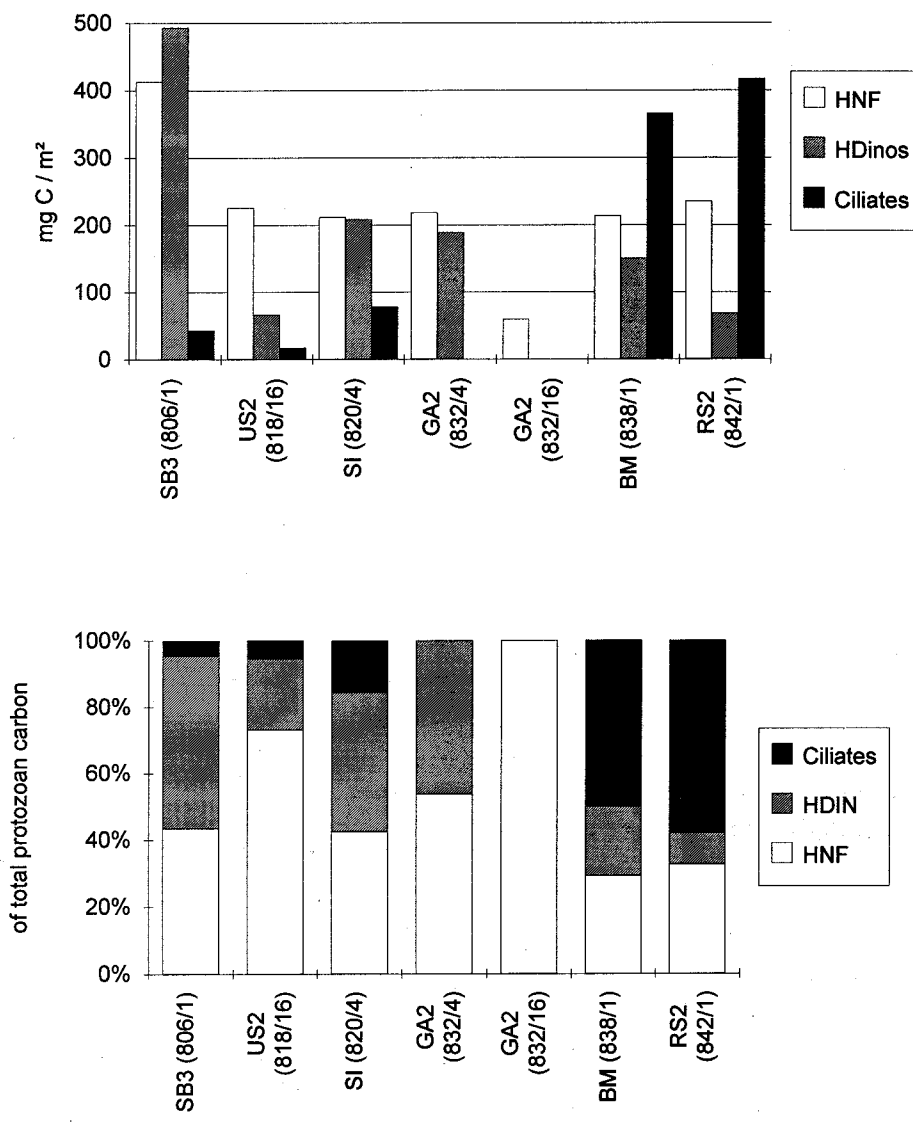


Fig.24 Protozoan carbon biomasses integrated over the upper 100m water column during cruise B2 (NE monsoon). A: Absolute values, B: as % of total protozoan carbon

The integrated size class plots (Fig.25) show that smaller HNF were present during the NE monsoon than during the SW monsoon. The portion of individuals $<10\mu\text{m}$ increased only slightly in the southern Red-Sea. In terms of biomass, flagellates $<5\mu\text{m}$ predominated (Fig.25A). Almost all HDIN were smaller than $20\mu\text{m}$, and a considerable portion even smaller $10\mu\text{m}$; these smaller forms were most abundant in the Red Sea (Fig.25B). Ciliates were likewise smaller than $20\mu\text{m}$, again clearly dominated by oligotrich forms, with minor contributions of other types (mostly holotrichs).

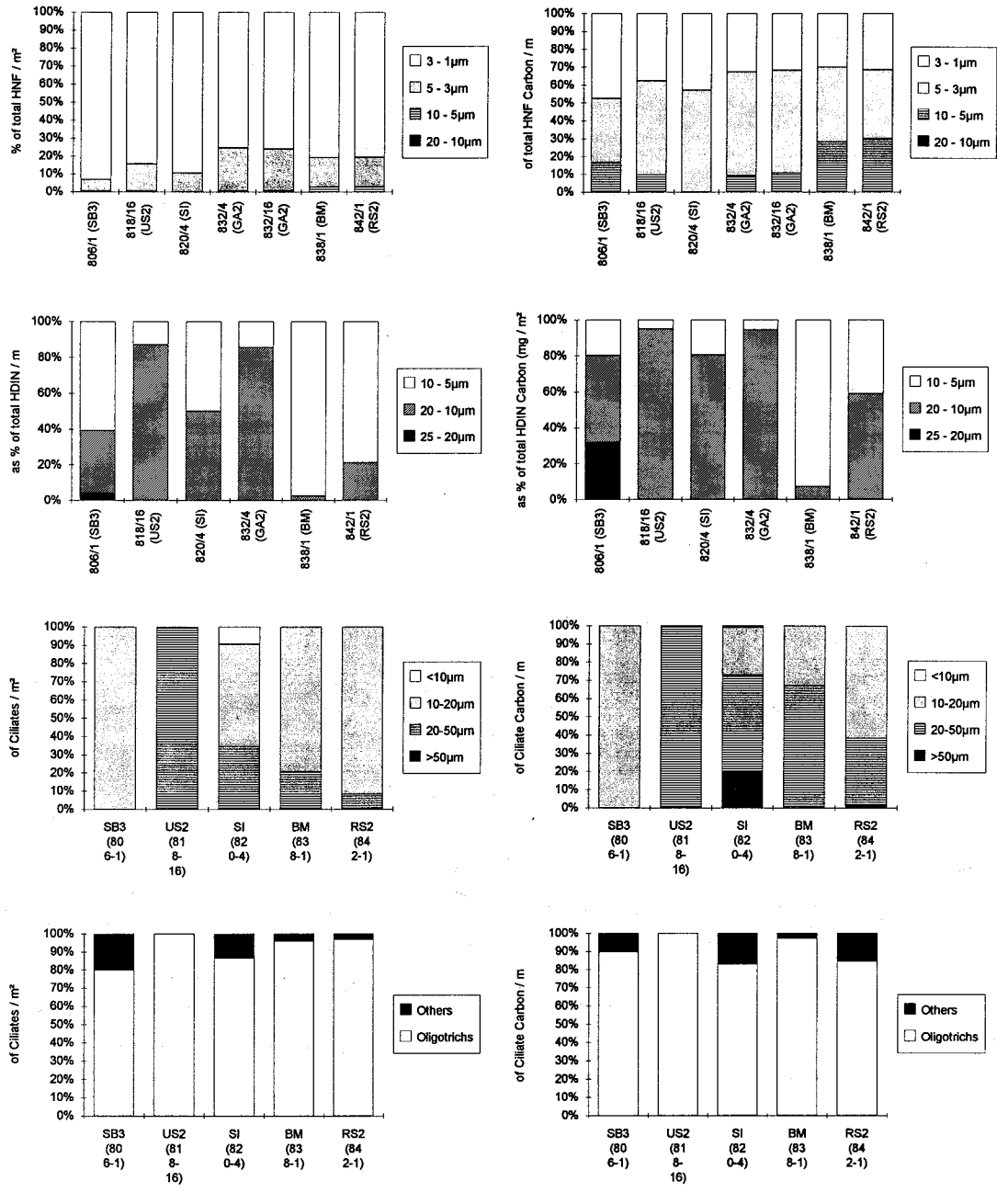


Fig.25 Size class distributions of three protozoan groups during cruise B2 (NE monsoon). Left panel: as % of total cell number; right panel: as % of total carbon biomass. A: heterotrophic nanoflagellates, B: heterotrophic dinoflagellates, C: ciliates. D: distribution of taxonomic ciliate groups.

Fig.26 shows average individual protozoan cell sizes, depicted as cell carbon values (corresponding to cell body volumes). HNF cell sizes apparently increased towards the Red Sea, while the opposite trend was observed for the dinoflagellates. Ciliate body sizes showed no clear tendency, but a substantial increase at US2.

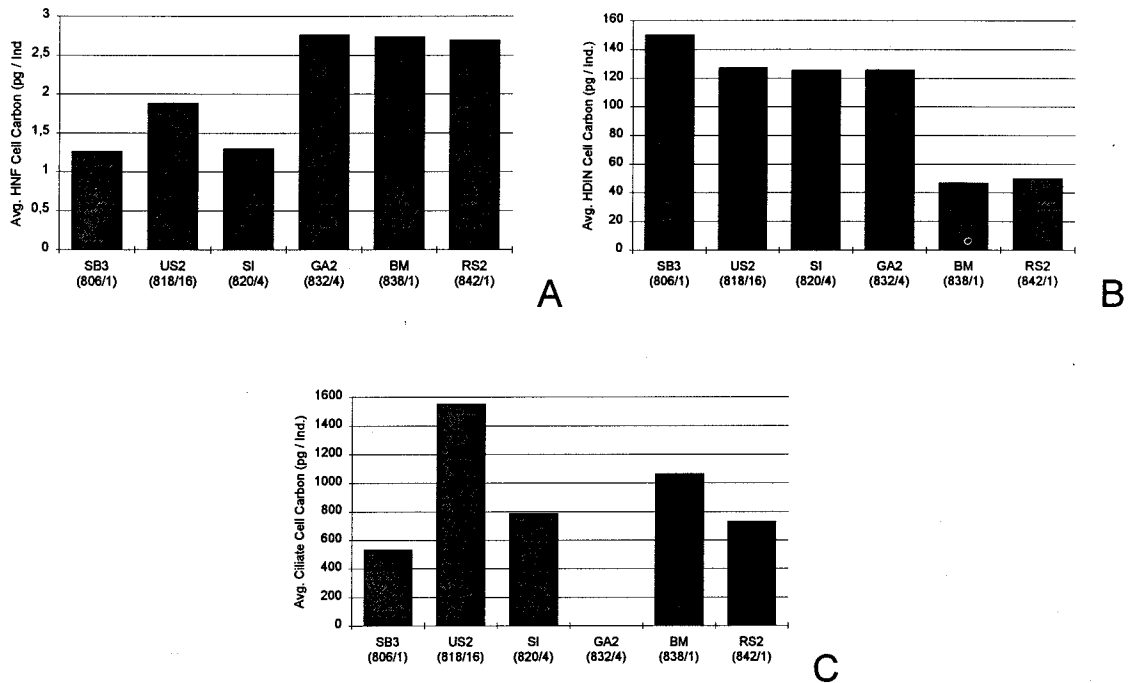
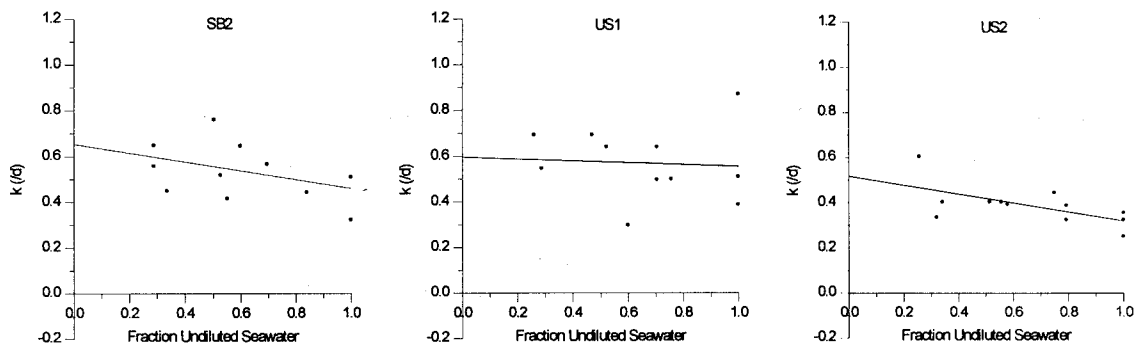


Fig.26 Individual average carbon contents per cell of three protozoan groups during cruise B2 (NE monsoon). A: heterotrophic nanoflagellates, B: heterotrophic dinoflagellates, C: ciliates.

3.2.3. Herbivory

During the NE monsoon, 8 Chl.a - based dilution experiments were carried out (Fig.27, Tab.6). Grazing ranged from 4% of stock per day at US1 to 69% at RS1, which corresponded to an absolute Chl.a consumption of $0.01 - 0.8 \mu\text{g dm}^{-3}$. Growth (μ) and grazing (g) coefficients ranged from 0.399 and 0.042 to 1.123 and 1.187, respectively; 7% (US1) - 106% (RS1) of daily phytoplankton production was consumed per day. Carbon consumption rates ranged from $2.31 \mu\text{g dm}^{-3}$ (US1) - $146 \mu\text{g dm}^{-3}$ at RS1.



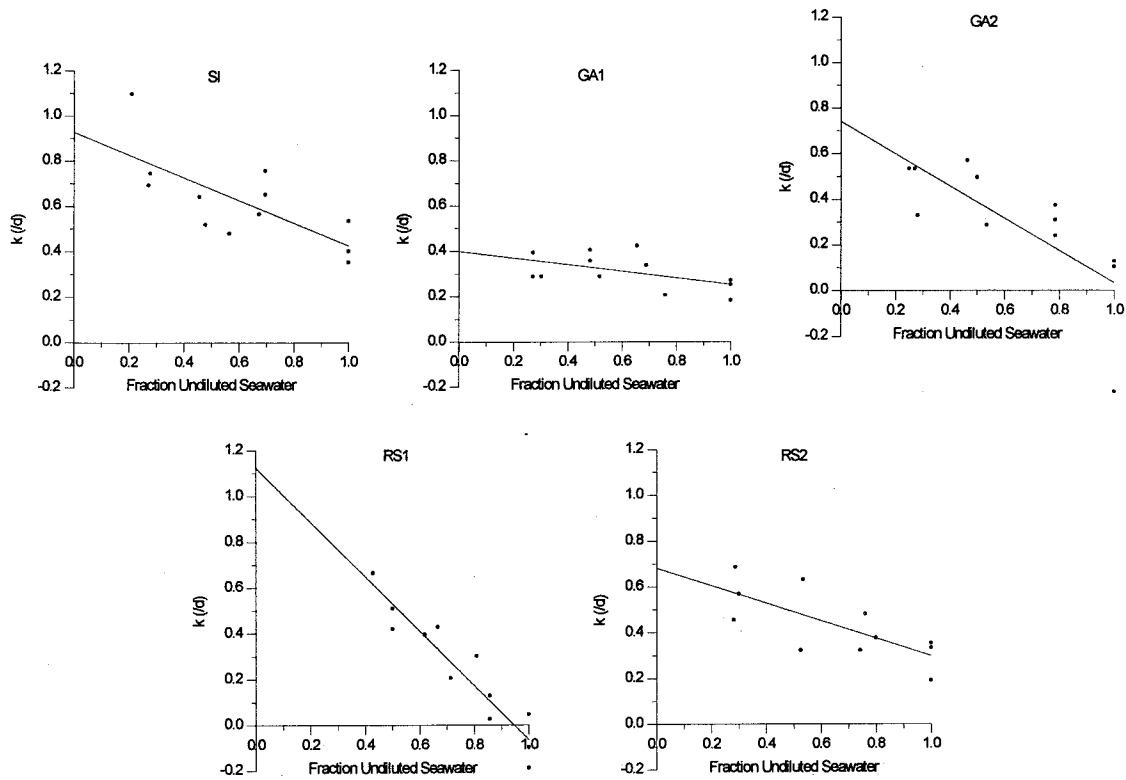


Fig.27 Serial dilution plots of Chl.a based experiments during cruise B2 (NE monsoon).

Tab.6 Results of serial dilution grazing experiments based on Chl.a determinations during cruise B2 (NE monsoon).

Area	Station	Chl a t0 mg / m ³	Grazing g (d)	Growth μ (d)	r	Stock grazed % / d	Prod. grazed % / d	Chl a grazed mg / m ³ * d	Phyto-C grazed mg / m ³ * d
SB2	809 / 4	0.34	0.192	0.653	0.442	17	29	0.06	10.67
US1	813 / 4	0.31	0.042	0.595	0.076	4	7	0.01	2.31
US2	818 / 8	0.38	0.201	0.520	0.630	18	39	0.07	12.46
SI	820 / 4	0.37	0.503	0.928	0.729	40	54	0.15	26.67
GA1	826 / 4	0.80	0.148	0.399	0.534	14	37	0.11	19.98
GA2	832 / 16	0.77	0.708	0.742	0.741	51	95	0.39	71.15
RS1	840 / 4	1.16	1.187	1.123	0.942	69	106	0.80	146.17
RS2	842 / 14	1.59	0.383	0.681	0.733	32	56	0.50	91.88

3.2.4. Grazing on ultraphytoplankton analyzed by flow cytometry

During cruise B2, the presence of a flow cytometer on board allowed the estimation of grazing on different autotrophic ultraplankton groups. These were the prokaryotic *Prochlorococcus* and *Synechococcus*, as well as two pico-eukaryotic groups (Tab.7). At some stations, subgroups of *Synechococcus* and *Prochlorococcus* ("dim" and "bright type") could be discriminated.

Fig.28 shows original flow cytometric plots with the main picoautotroph groups defined as clusters, Tab.7 gives an overview over the ultraphytoplankton cell concentrations in the incubation bottles at the start of the experiments (corresponding to average euphotic zone concentrations).

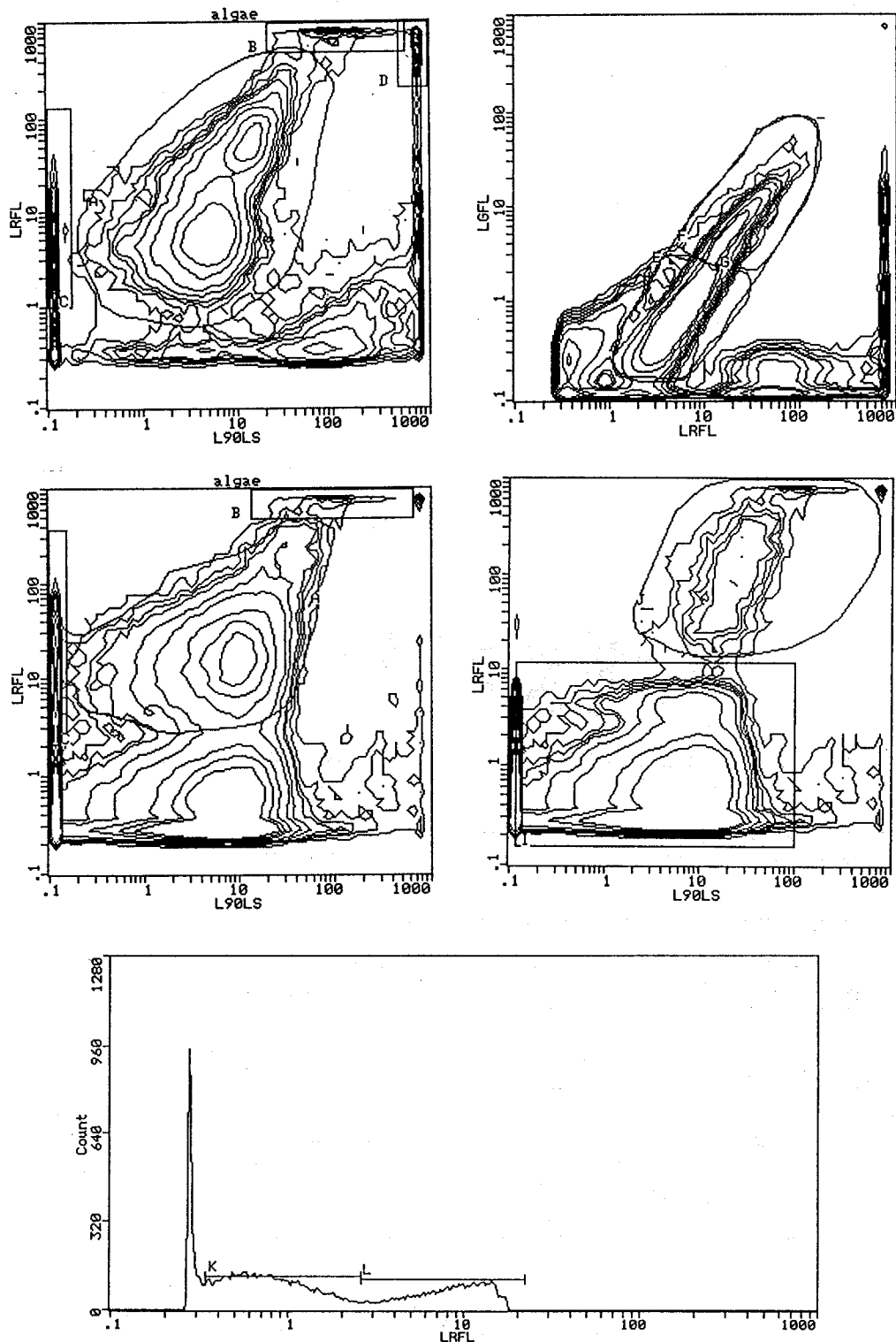


Fig.28 Flow cytometric contour plots at two stations during the NE monsoon. Upper left (RS2): Red Fluorescence (RFL) - Side Scatter ; upper right (RS2): RFL - Orange Fluorescence (ORF) with two subpopulations of *Synechococcus*; middle left (SI): RFL - SSC; middle right (SI): same as left panel, with *Synechococcus* subtracted and *Prochlorococcus* (lower cluster) and eukaryotes (upper cluster) well separated; lower panel (SI): two subpopulations of *Prochlorococcus*.

Tab.7 Cell concentrations of photosynthetic picoplankton in the size fractionated dilution incubations, as identified by Flow Cytometry. n.d. = not detected.

Location	<i>Prochlorococcus</i>	<i>Dim</i>	<i>Bright</i>	<i>Synechococcus</i>	<i>Dim</i>	<i>Bright</i>	Small Euks	Large Euks
SB2	-	-	-	67.183	n.d.	n.d.	6.420	n.d.
US1	-	-	-	51.145	n.d.	n.d.	7.686	n.d.
US2	50.239	26.777	23.462	43.685	n.d.	n.d.	5.396	n.d.
SI	66.253	40.772	25.481	53.583	n.d.	n.d.	7.172	812
GA2	13.198	n.d.	n.d.	142.225	92.784	50.504	18.342	1.601
RS2	n.d.	n.d.	n.d.	47.253	36.845	10.408	-	1.162

Fig.29 demonstrates the relative importance of the respective ultraplankton groups in terms of biomass (as percentage of total phytoplankton biomass, measured as Chl.a). Ultraphytoplankton contributed from less than 10% (Red Sea stations) to over 90% (Gulf of Aden) to phytoplankton biomass (Fi.29A). Within the ultraplankton, small eukaryotes, together with *Synechococcus* dominated biomass; towards the Gulf of Aden and the southern Red Sea, a large eukaryote increasingly contributed to autotrophic ultraplankton biomass. Small eukaryotes were not detected at RS2.

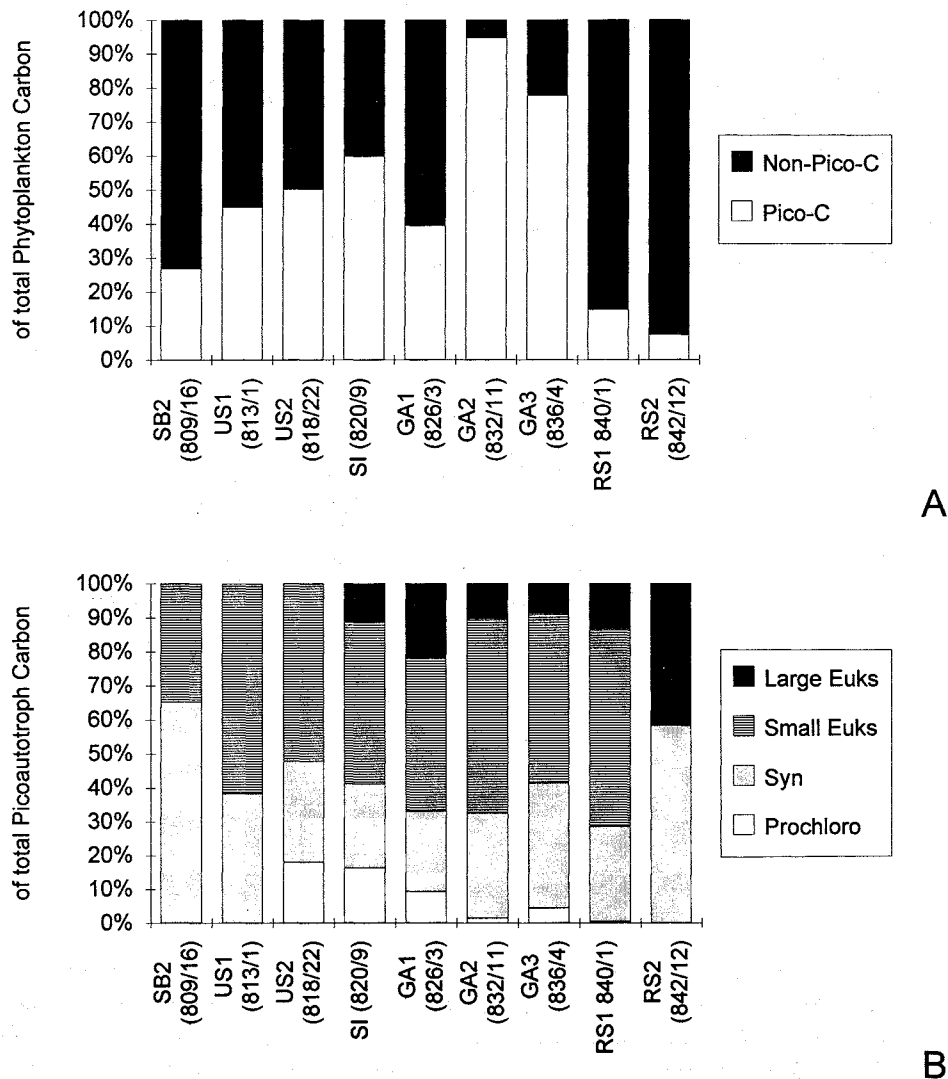
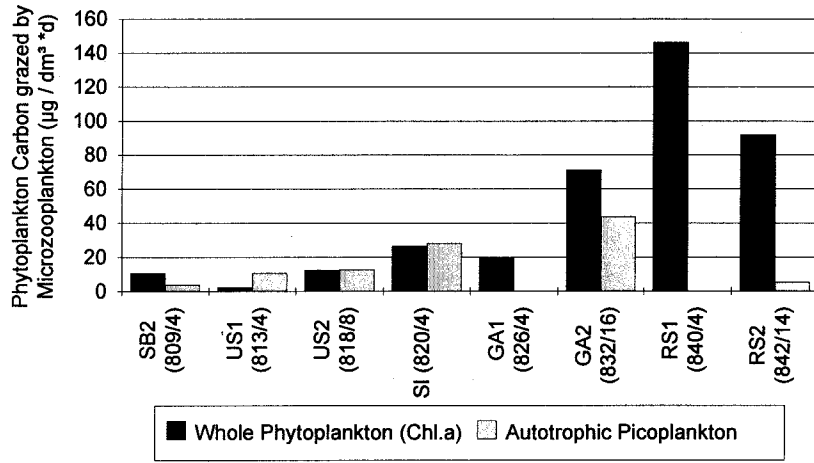
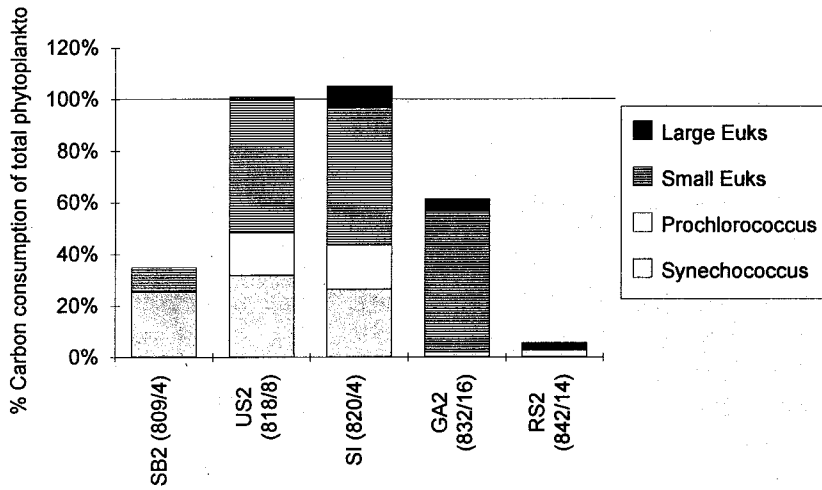


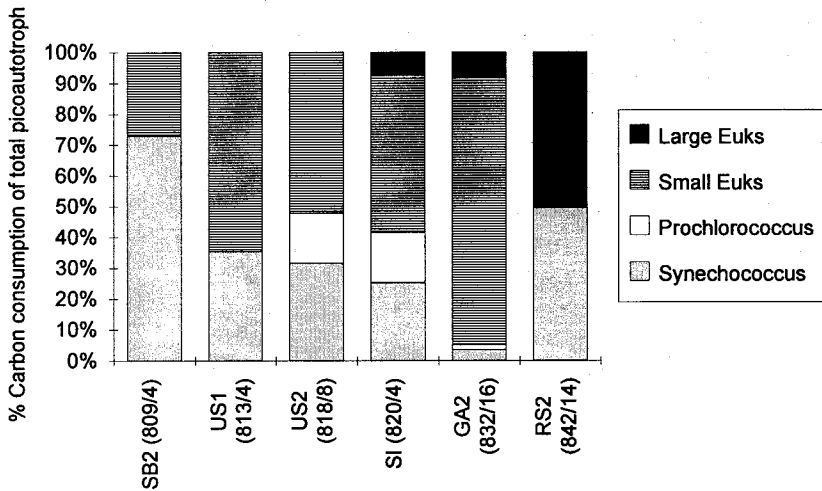
Fig.29 Autotrophic ultraplankton carbon biomass as percent of total phytoplankton biomass (A); respective groups as percent of total autotrophic ultraplankton carbon (B).



A



B



C

Fig.30 Carbon consumption rates of total phytoplankton (measured as Chl.a) and autotrophic ultraplankton (measured by flow cytometry) by microzooplankton during cruise B2 (NE monsoon). A: Absolute consumption rates of total phytoplankton carbon, and the sum of autotrophic ultraplankton carbon. B: Relative contribution of the respective ultraplankton groups to total phytoplankton consumption (US1 omitted). C: Relative contribution of the respective ultraplankton groups to total autotroph ultraplankton consumption.

A comparison of carbon consumption rates obtained by Chl.a and those for the specific picoplankton groups measured by flow cytometry reveals that in the Somali Basin, grazing on autotrophic ultraplankton roughly accounted for the total grazing on total phytoplankton (Fig.30). In the Gulf of Aden and the Red Sea, consumption rates on autotrophic ultraplankton did not rise proportionally to total phytoplankton consumption: here, ultraplankton carbon contributed only to a minor extent to total phytoplankton consumption (Fig.30A). The absolute importance of *Prochlorococcus* and *Synechococcus* as autotrophic prey organism decreased from the Somali Basin to the Gulf of Aden and Red Sea, while the importance of small eukaryotes remained high in the Gulf of Aden. The proportion of the large eukaryotes was rather low at all stations but increased towards the Red Sea (Fig.30B,C).

3.2.5. Grazer size differential grazing on ultraphytoplankton analyzed by flow cytometry

In addition to the "classical" dilution approach (exclusion of grazers $>200\mu\text{m}$ to estimate the impact of microzooplankton $<200\mu\text{m}$), several dilution experiments were performed with smaller grazer size classes which were excluded by prescreening with nets and polycarbonate filters ($20\mu\text{m}$, $10\mu\text{m}$, $3\mu\text{m}$, $2\mu\text{m}$ and $1\mu\text{m}$). The use of flow cytometry allowed an estimation of grazing by these grazer size classes on different ultraphytoplankton groups.

In all experiments, the smaller grazer size fractions ($<10\mu\text{m}$ and $<3\mu\text{m}$) showed higher rates as the larger fractions (<200 and $<20\mu\text{m}$). Fig.31 - 33 show absolute carbon consumption rates (panels A), the proportion of standing stock consumed per day (panels B), and apparent growth rates (representing net in- or decrease of a population, panels C), as a function of grazer size fractions for all prey groups at three stations (US2, SI and GA2). At all stations, absolute carbon consumption rates were highest for the eukaryotic ultraplankton (up to $38.1 \mu\text{g dm}^{-3}$), with *Synechococcus* (up to $8.1 \mu\text{g dm}^{-3}$) and *Prochlorococcus* (up to $5.19 \mu\text{g dm}^{-3}$) following in importance. As it is evident from the very similar relative consumption rates of all groups (% of stock consumed per day, panels B), the difference in the absolute consumption rates largely reflects the different standing stocks of the different prey groups, implying no real preference for a specific prey type. At US2, highest grazing pressure was exerted by the fraction $<10\mu\text{m}$, while smaller grazers ($<3\mu\text{m}$) apparently played only a minor role (Fig.31). At SI, high grazing was detected in the fractions $<10\mu\text{m}$ and $<3\mu\text{m}$, and also in the fractions $<2\mu\text{m}$, although this fraction was less important for the eukaryotes than for the prokaryotic ultraphytoplankton (Fig.32). At GA2, the fractions $<10\mu\text{m}$ and $<3\mu\text{m}$ showed the highest grazing impact on *Prochlorococcus* and *Synechococcus*, while the eukaryotes were mostly consumed by larger microzooplankton (Fig.33). However, the highest grazing pressure was found in the grazer fraction $<10\mu\text{m}$ at all stations, with up to 90% of the prey stock removed by grazing daily.

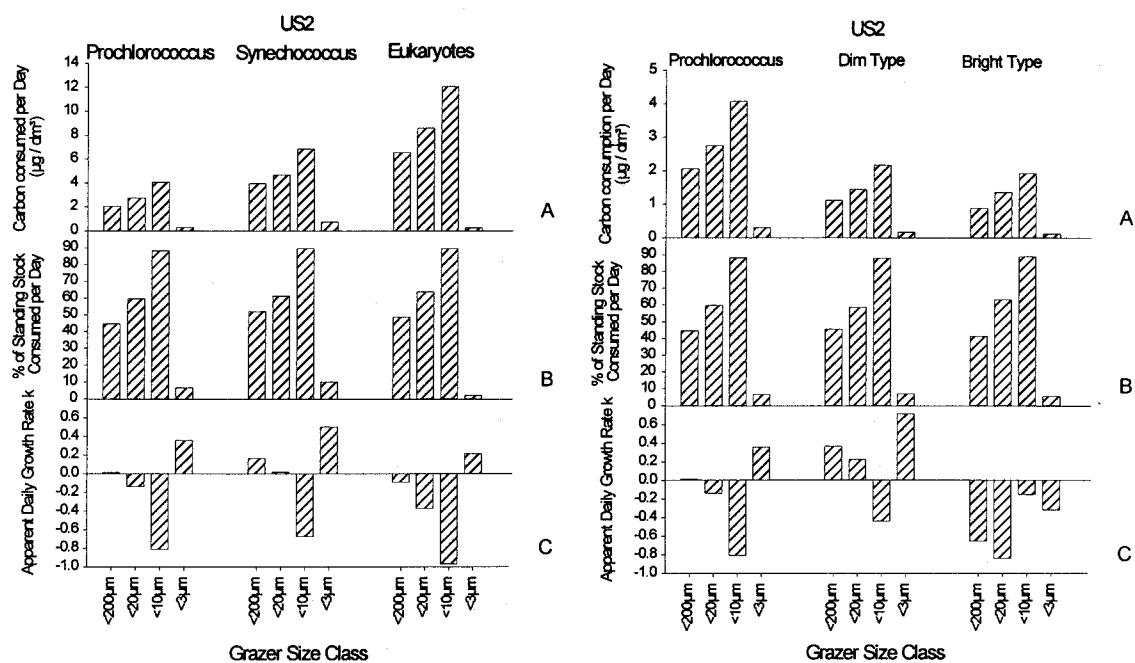


Fig.31 Size fractionated consumption rates of autotrophic ultraplankton estimated by serial dilution experiments at St.US2 during cruise B2 (NE monsoon). A: absolute carbon consumption rates, B: relative turnover rates as % of standing stock, C: apparent daily growth rates, corresponding to actual population increments.

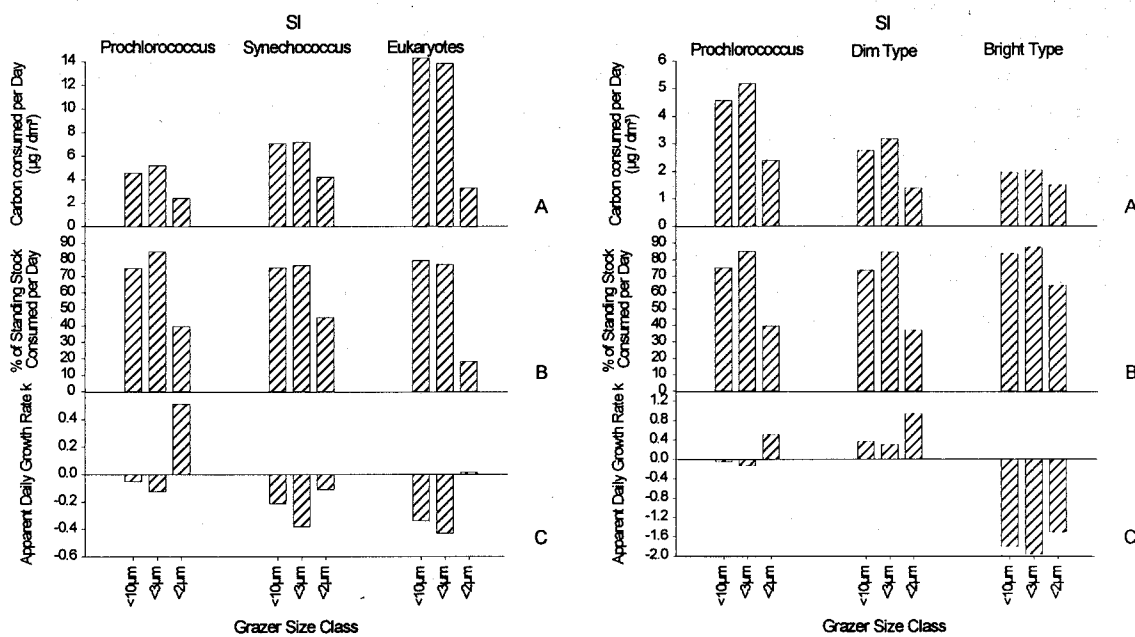


Fig.32 As for Fig.27, St. SI.

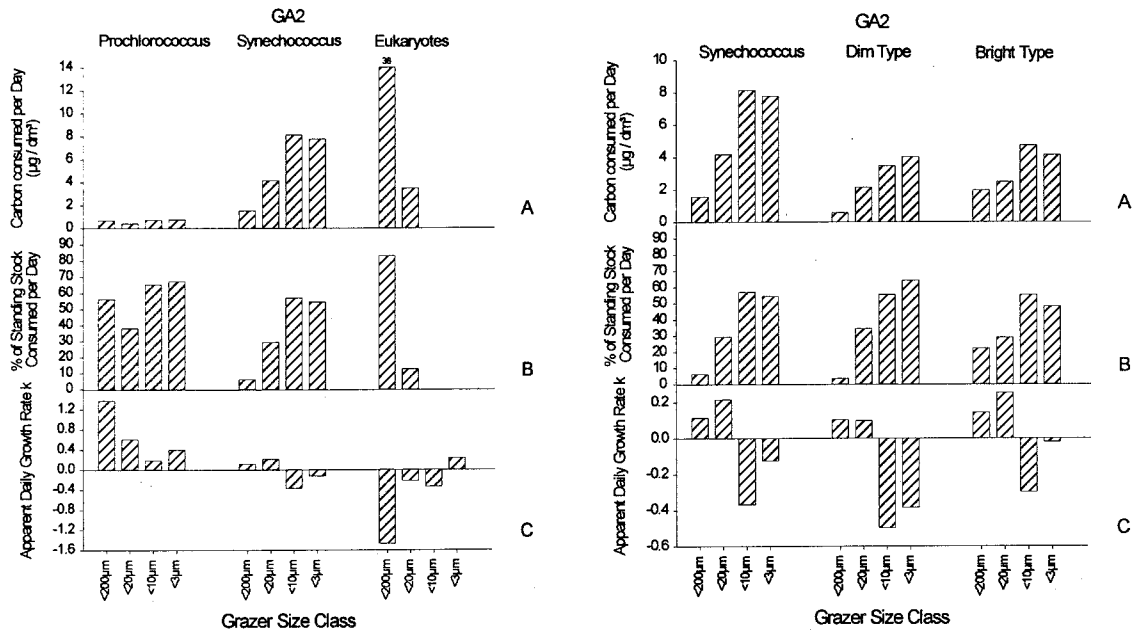


Fig.33 As for Fig.27, St. GA2.

At two stations in the Somali Basin (US2 and SI), two sub-populations of *Prochlorococcus* could be distinguished, based on their red fluorescence intensity ("dim" and "bright" type). While grazing rates on both types were remarkably similar, their growth rates differed dramatically (Fig.31 and 32, right panels). While the "dim type" thrived under the experimental conditions, the "bright type" experienced much lower specific growth rates. For the "bright type", this resulted in a population decrease. At GA2, the grazing impact on two distinct subpopulations of *Synechococcus* could be estimated (Fig.33, right panel). Grazing on both types increased dramatically in the smaller size fractions. Results of the size-fractionated grazing experiments are summarized in Table 8. Graphical plots of apparent growth rates vs. dilution factor for all size-fractionated dilution experiments are given in Appendix 1.

Tab.8 Results of size fractionated dilutions during cruise B2 (NE monsoon).

Station	Grazer Size Class	Grazing g / (d)	Growth μ / (d)	r	Stock grazed % / d	Prod. grazed % / d	Cells grazed # / cm ³ * d	Phyto-C grazed mg / m ³ * d
Prochlorococcus								
US2	<200 μ m	0.590	0.604	0.934	45	98	22,400	2.06
US2	<20 μ m	0.908	0.770	0.951	60	118	29,981	2.76
US2	<10 μ m	2.142	1.332	0.795	88	161	44,337	4.08
US2	<3 μ m	0.068	0.426	0.350	7	16	3,289	0.30
SI	<10 μ m	1.386	1.334	0.894	75	104	49,681	4.57
SI	<3 μ m	1.902	1.777	0.966	85	107	56,360	5.19
SI	<2 μ m	0.504	1.014	0.374	40	50	26,228	2.41
GA2	<200 μ m	0.824	2.200	0.682	56	37	7,411	0.68
GA2	<20 μ m	0.479	1.087	0.756	38	44	4,705	0.43
GA2	<10 μ m	1.062	1.251	0.937	65	85	8,082	0.74
GA2	<3 μ m	1.116	1.514	0.987	67	74	8,309	0.76
Dim Prochlorococcus								
US2	<200 μ m	0.608	0.977	0.935	46	62	12,198	1.12
US2	<20 μ m	0.879	1.108	0.961	59	79	15,665	1.44
US2	<10 μ m	2.121	1.683	0.789	88	126	23,566	2.17
US2	<3 μ m	0.071	0.787	0.357	7	9	1,838	0.17
SI	<10 μ m	1.327	1.698	0.877	73	78	29,957	2.76
SI	<3 μ m	1.874	2.176	0.961	85	86	34,513	3.18
SI	<2 μ m	0.464	1.402	0.349	37	33	15,126	1.39
Bright Prochlorococcus								
US2	<200 μ m	0.533	-0.120	0.913	41	-	9,691	0.89
US2	<20 μ m	0.999	0.159	0.917	63	629	14,823	1.36
US2	<10 μ m	2.207	0.678	0.814	89	325	20,880	1.92
US2	<3 μ m	0.057	-0.260	0.304	6	-	1,304	0.12
SI	<10 μ m	1.808	-0.004	0.958	84	-	21,300	1.96
SI	<3 μ m	2.083	0.119	0.971	88	1,743	22,305	2.05
SI	<2 μ m	1.030	-0.484	0.549	64	-	16,384	1.51
Synechococcus								
SB2	<200 μ m	0.264	0.262	0.927	23	101	15,571	2.72
US1	<200 μ m	0.508	0.380	0.902	40	134	20,362	3.56
US2	<200 μ m	0.733	0.897	0.945	52	82	22,697	3.97
US2	<20 μ m	0.949	0.966	0.937	61	98	26,767	4.68
US2	<10 μ m	2.290	1.619	0.794	90	141	39,262	6.87
US2	<3 μ m	0.105	0.608	0.587	10	17	4,344	0.76
SI	<10 μ m	1.404	1.191	0.903	75	118	40,418	7.07
SI	<3 μ m	1.457	1.075	0.982	77	136	41,097	7.19
SI	<2 μ m	0.599	0.489	0.433	45	122	24,147	4.23
GA2	<200 μ m	0.065	0.180	0.160	6	36	8,935	1.56
GA2	<20 μ m	0.347	0.563	0.588	29	62	23,912	4.18
GA2	<10 μ m	0.843	0.475	0.868	57	177	46,473	8.13
GA2	<3 μ m	0.788	0.663	0.983	55	119	44,499	7.79
RS2	<200 μ m	0.380	0.273	0.850	32	139	14,929	2.61
Dim Synechococcus								
GA2	<200 μ m	0.036	0.140	0.069	4	26	3,323	0.58
GA2	<20 μ m	0.420	0.519	0.596	34	81	12,238	2.14
GA2	<10 μ m	0.808	0.310	0.804	55	261	19,797	3.46
GA2	<3 μ m	1.025	0.640	0.979	64	160	22,896	4.01
RS2	<200 μ m	0.367	0.196	0.857	31	187	11,326	1.98
Bright Synechococcus								
GA2	<200 μ m	0.250	0.393	0.567	22	64	11,166	1.95
GA2	<20 μ m	0.341	0.593	0.620	29	57	14,166	2.48
GA2	<10 μ m	0.803	0.504	0.871	55	159	27,088	4.74
GA2	<3 μ m	0.656	0.636	0.970	48	103	23,593	4.13
RS2	<200 μ m	0.433	0.516	0.801	35	84	3,657	0.64

Station	Grazer Size Class	Grazing g (d)	Growth μ (d)	r	Stock grazed % / d	Prod. grazed % / d	Cells grazed # / cm ³ * d	Phyto-C grazed mg / m ³ * d
Small Eukaryotes								
SB2	<200 μ m	0.177	0.387	0.443	16	46	1,040	1.01
US1	<200 μ m	0.597	0.507	0.766	45	118	3,457	6.50
US2	<200 μ m	0.668	0.579	0.913	49	115	2,630	6.57
US2	<20 μ m	1.015	0.642	0.917	64	158	3,441	8.60
US2	<10 μ m	2.274	1.305	0.791	90	174	4,841	12.10
US2	<3 μ m	0.021	0.236	0.120	2	9	110	0.28
SI	<10 μ m	1.596	1.257	0.902	80	127	5,718	14.29
SI	<3 μ m	1.473	1.044	0.990	77	141	5,527	13.82
SI	<2 μ m	0.202	0.219	0.125	18	92	1,314	3.29
GA2	<200 μ m	1.777	0.307	0.748	83	578	15,239	38.10
GA2	<20 μ m	0.134	-0.085	0.289	13	-	1,391	3.48
GA2	<10 μ m	-0.066	-0.402	0.153	-	-	-	-
GA2	<3 μ m	-2.311	-2.078	0.860	-	-	-	-
Large Eukaryotes								
SI	<10 μ m	0.719	0.728	0.816	51	99	416	2.12
SI	<3 μ m	1.171	0.778	0.865	69	151	560	2.85
SI	<2 μ m	0.657	0.024	0.473	48	2,738	391	1.99
GA2	<200 μ m	0.553	0.421	0.783	42	131	680	3.46
GA2	<20 μ m	0.538	0.181	0.750	42	297	571	2.91
GA2	<10 μ m	0.430	0.135	0.627	35	320	480	2.44
GA2	<3 μ m	-1.039	-1.190	0.643	-	-	-	-
RS2	<200 μ m	0.599	0.923	0.853	45	65	524	2.67

3.2.6. Grazer size differential grazing on ultraphytoplankton in a light-dark experiment analyzed by flow cytometry

At station RS2, size fractionated grazing was estimated by prey concentration differences in incubations kept in the light and in the dark (see section 2.7.). Fig.34 shows time series plots for the fraction <20 μ m. For the first 6h, cell concentrations remained similar in all treatments; during the next 6h, cell concentrations decreased dramatically in the dark bottles. After nightfall (12h), cell numbers in the light bottles decreased at the same rate as in the dark bottles.

Fig.35 and Tab.9 show fractionated growth and grazing parameters at RS2, estimated by light-dark difference. Like in the dilution experiments, grazing was most intense in the fractions <10 μ m and <3 μ m, with up to 43% (*Synechococcus*), and 74% (eukaryotes) of standing stock consumed per day. Absolute carbon consumption rates amounted to 3.1 μ g dm⁻³ (*Synechococcus*), and 4.06 μ g dm⁻³ (eukaryotes).

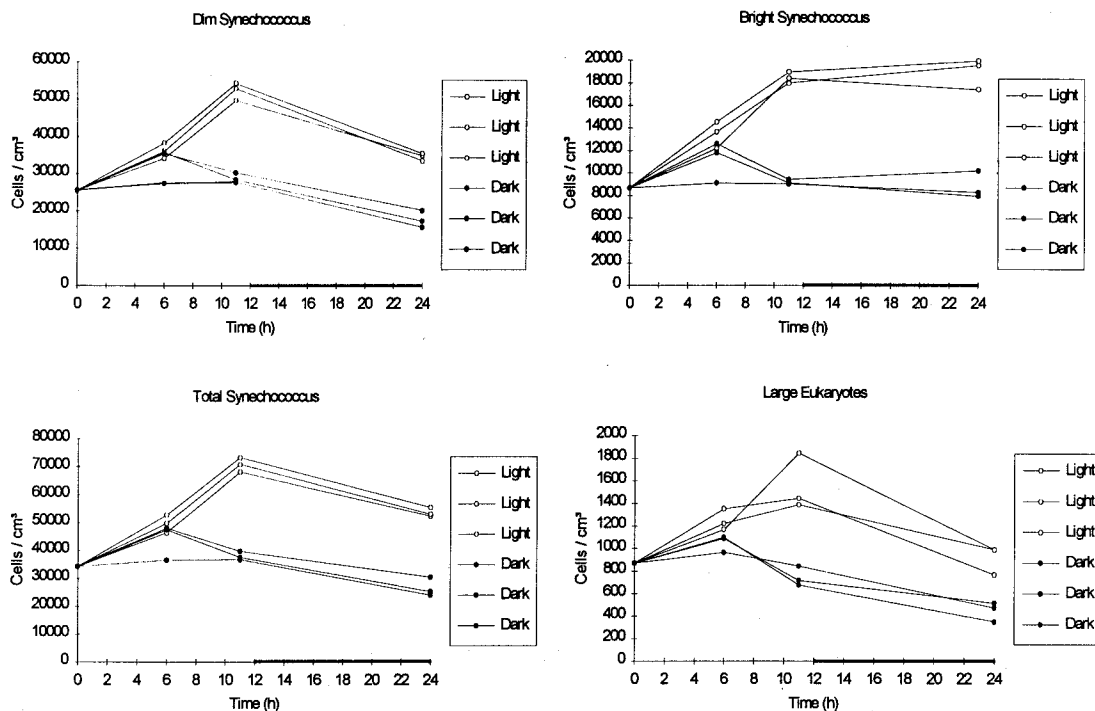


Fig.34 Time series of light and dark incubations at RS2 during cruise B2 (NE monsoon)

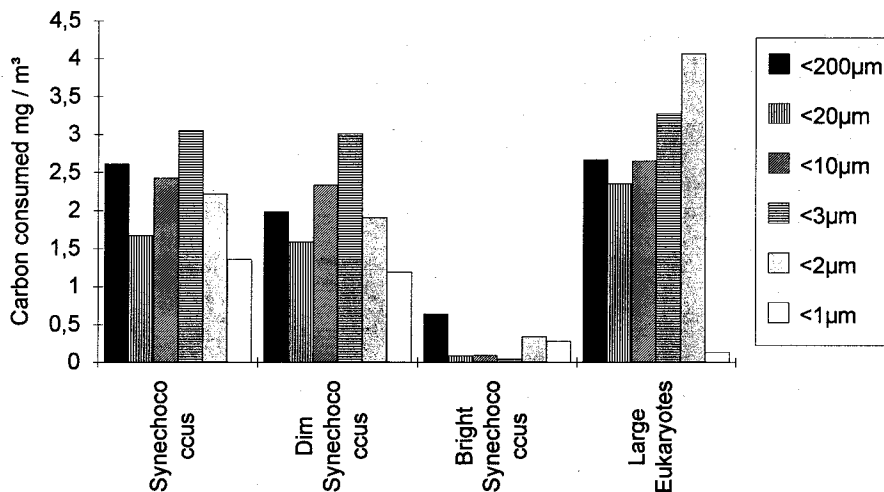


Fig.35 Carbon consumption rates of two subpopulations of *Synechococcus* and a pico-eukaryote ("large eukaryote") in light and dark incubations at St. RS2 during cruise B2 (NE monsoon). <200 values (black columns) are derived from a separate dilution experiment.

Tab.9 Results of size fractionated light-dark grazing experiments at St.RS2 of cruise B2 (NE monsoon). Values <200 μ m are derived from a separate dilution experiment.

Grazer Size Class	N t0	Grazing g (d)	Growth μ (d)	r	Stock grazed % / d	Prod. grazed % / d	Cells grazed # / cm ³ * d	Phyto-C grazed mg / m ³ * d
Synechococcus								
<200 μ m	47,253	0.380	0.273	0.850	32	139	14,929	2.61
<20 μ m	34,205	0.328	0.779	-	28	42	9,560	1.67
<10 μ m	38,244	0.450	0.570	-	36	79	13,858	2.43
<3 μ m	41,031	0.554	0.621	-	43	89	17,454	3.05
<2 μ m	40,386	0.377	0.838	-	31	45	12,676	2.22
<1 μ m	33,639	0.263	0.738	-	23	36	7,776	1.36
Dim Synechococcus								
<200 μ m	36,845	0.367	0.196	0.857	31	187	11,326	1.98
<20 μ m	25,544	0.438	0.744	-	35	59	9,062	1.59
<10 μ m	28,585	0.628	0.589	-	47	107	13,327	2.33
<3 μ m	30,912	0.812	0.775	-	56	105	17,183	3.01
<2 μ m	29,532	0.461	0.920	-	37	50	10,909	1.91
<1 μ m	25,725	0.307	0.733	-	26	42	6,800	1.19
Bright Synechococcus								
<200 μ m	10,408	0.433	0.516	0.801	35	84	3,657	0.64
<20 μ m	8,661	0.061	0.845	-	6	7	512	0.09
<10 μ m	9,659	0.057	0.535	-	6	11	539	0.09
<3 μ m	10,119	0.028	0.352	-	3	8	275	0.05
<2 μ m	10,853	0.200	0.664	-	18	30	1,963	0.34
<1 μ m	7,914	0.225	0.843	-	20	27	1,594	0.28
Large Eukaryotes								
<200 μ m	1,162	0.599	0.923	0.853	45	65	524	2.67
<20 μ m	871	0.756	0.800	-	53	95	462	2.35
<10 μ m	1,005	0.729	0.539	-	52	135	520	2.65
<3 μ m	978	1.070	0.597	-	66	179	642	3.27
<2 μ m	1,103	1.287	-0.103	-	72	-	798	4.06
<1 μ m	36	1.335	0.698	-	74	191	27	0.14

3.3. The Gotland Sea (Baltic proper) during summer 1994

3.3.1. Hydrography and nutrients

Temperature profiles (Fig.36) showed a very thin warm surface layer with temperatures of 18°C; below 10m, temperatures dropped to a minimum of 2°C at 50m. Further below, temperatures increased to 5°C at 100m, but decreased again below 100m. A *halocline* (Fig.37) was found between 75 and 100m, separating the low saline surface water ($S = 7 - 8$) from higher saline deep water ($S = 10 - 12$). All nutrients except for silicate (surface: $5\mu\text{M}$) were depleted in surface waters, and increased below the euphotic zone (25m). Nitrate concentrations gradually increased to 6 - 9 μM at 100m, and only slightly below this depth (Fig.38). Nitrite was below $0.1\mu\text{M}$ at the surface, but showed a distinct nitrification peak of up to $0.3\mu\text{M}$ at 75m. Below this depth, values dropped down to surface concentrations. Phosphate gradually increased to peak values of about $3\mu\text{M}$ at 100 - 120m; further below, it decreased to $2\mu\text{M}$. A similar profile with elevated concentrations at intermediate depths was found in the case of silicate: peak values of more than $40\mu\text{M}$ were found at 100 - 120m; below, it decreased to $30\mu\text{M}$.

A saltwater intrusion in January 1993 had ended a long stagnation period in the Baltic proper (MATTHAEUS et al. 1993). This is reflected in the water column structure: a remnant of the stagnant anoxic water parcel was found at intermediate depths between 80 and 150m, characterized by slightly higher temperatures, low oxygen concentrations (a minimum of $1 - 2 \text{ cm}^3 / \text{dm}^3$), and high phosphate and silicate concentrations. Nitrate concentrations in this layer were also high, as the present oxygen prevented denitrification. Beneath this water body, temperatures, as well as phosphate and silicate concentrations were lower, and oxygen concentrations were higher ($3 \text{ cm}^3 / \text{dm}^3$); this deep water probably originated from the 1993 event, having already undergone intense mixing with the intermediate stagnant water.

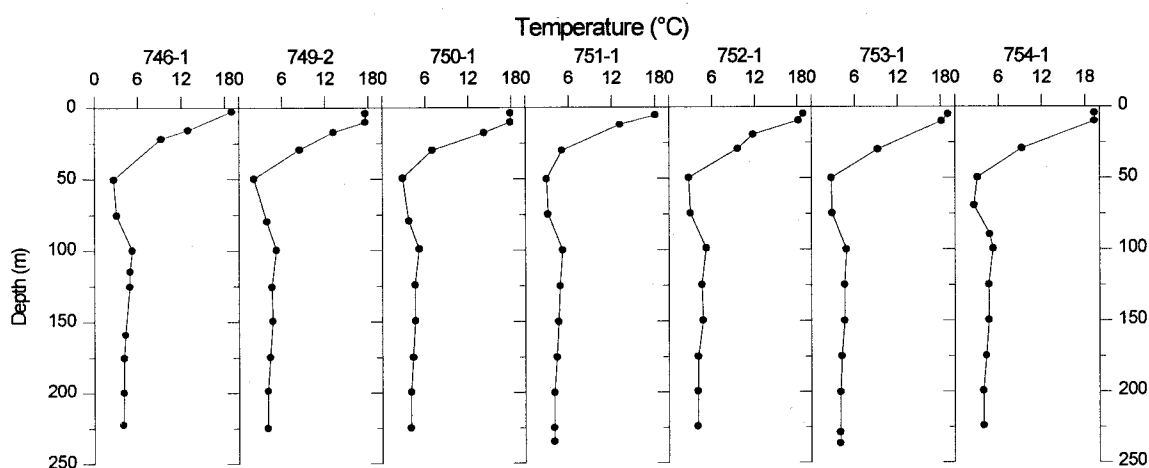


Fig.36 Water column profiles of temperature in the Gotland Basin in July 1994.

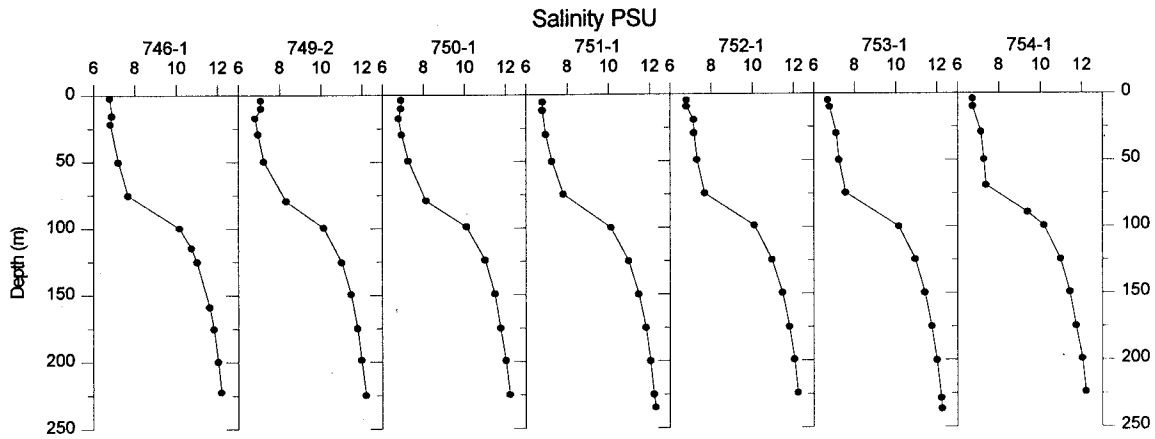


Fig.37 Water column profiles of salinity in the Gotland Basin in July 1994.

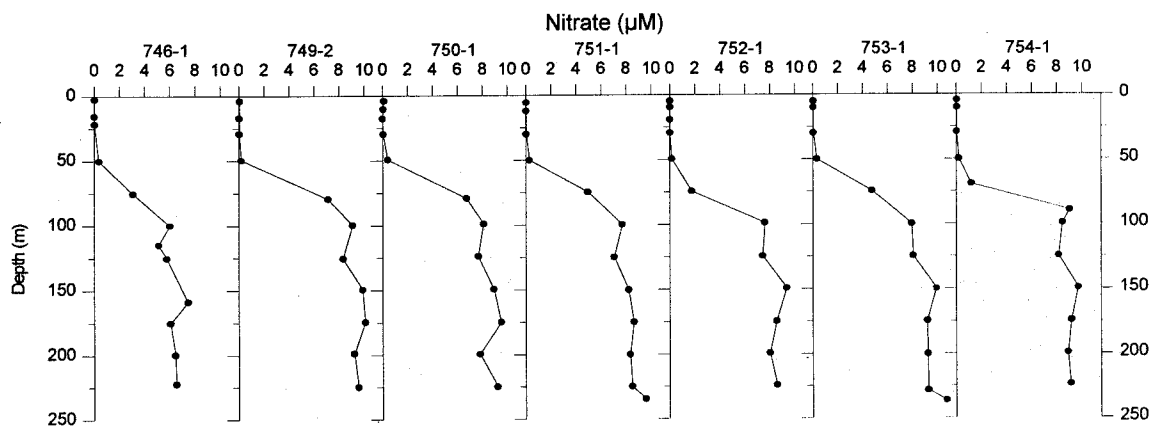


Fig.38 Water column profiles of nitrate in the Gotland Basin in July 1994.

3.3.2. Chl.a and ultraphytoplankton distributions analyzed by flow cytometry

Chl.a profiles measured by HPLC (MEYER-HARMS 1996) showed values of 1.5 - 2 $\mu\text{g dm}^{-3}$ at the surface, decreasing to zero at 20m (Fig.39). Phytoplankton $>5\mu\text{m}$ was dominated by filamentous cyanobacteria (*Aphanozomenon flos-aquae*, *Anabaena spp.*, *Nodularia spumigena*), and large dinoflagellates (*Dinophysis norvegica*).

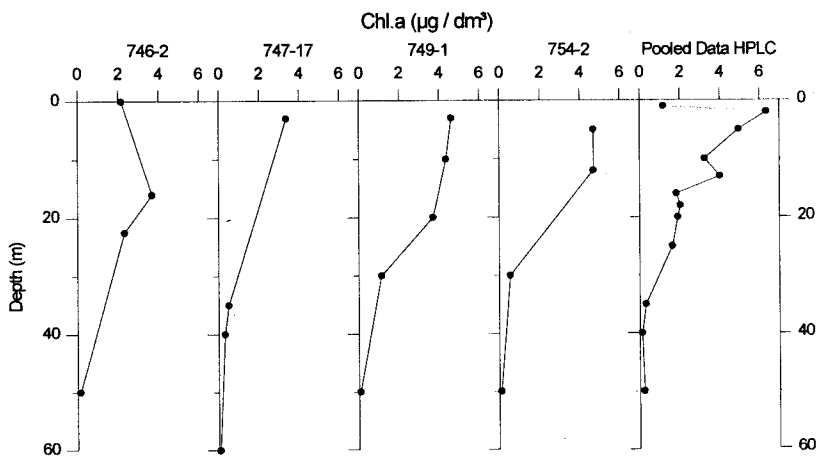


Fig.39 Water column profiles of Chl.a in the Gotland Basin in July 1994.

Ultraplankton ($<5\mu\text{m}$) was analysed by flow cytometry. The picocyanobacterium *Synechococcus* was characterized by the presence of orange fluorescence and low red fluorescence; three groups of eukaryotic ultraplankton were specified by the absence of orange fluorescence and different red fluorescence intensities (pico-eukaryotes, small nano-eukaryotes, and large nano-eukaryotes). These groups were present all through the cruise, while two additional groups appeared only at some stations. A group showing high red and orange fluorescence was named *PE1* (for phycoerythrin; presumably cyanobacteria or small cryptophytes), and a group showing a combination of weak red fluorescence signals (low chlorophyll content) and strong side scatter signals (large size), was labelled SC1 (for Scatter).

Fig.40 shows representative flow cytometric bivariate plots from St.753 (10m), with the designation of the different phytoplankton groups.

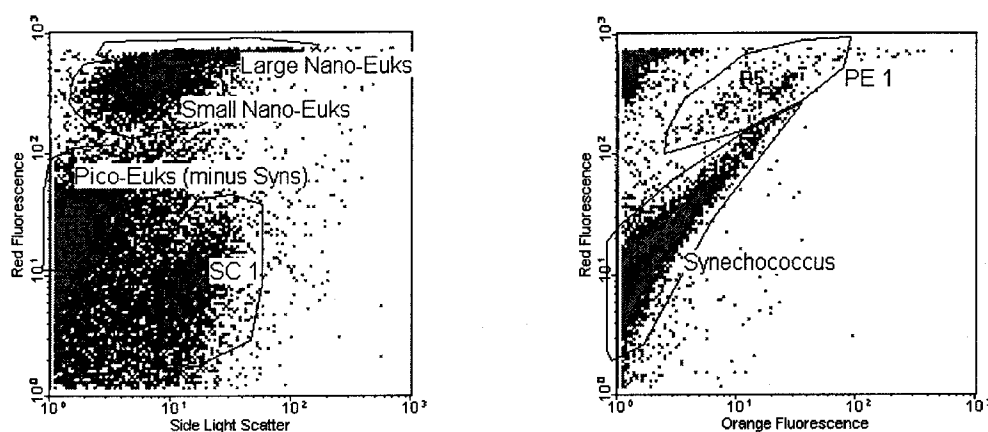


Fig.40 Representative flow cytometric plots from the Gotland Sea in July 1994 (St.753-6, 10m)

Size fractionation prior to measuring in the flow cytometer yielded an approximation for cell size of the respective ultraplankton groups (Fig.41). The orange fluorescing group PE1 and the large nano-eukaryotes obviously had an approximate cell diameter of $5\mu\text{m}$, as about half of the organisms of these groups passed this pore size. Likewise, it can be assumed that the small nano-eukaryotes had an average cell diameter of $3\mu\text{m}$, while the bulk of the pico-eukaryotes passed the $2\mu\text{m}$ membrane but did not pass the $0.8\mu\text{m}$ membrane. The majority of *Synechococcus* also passed the $2\mu\text{m}$ membrane, and 20% even passed the $0.8\mu\text{m}$ filter.

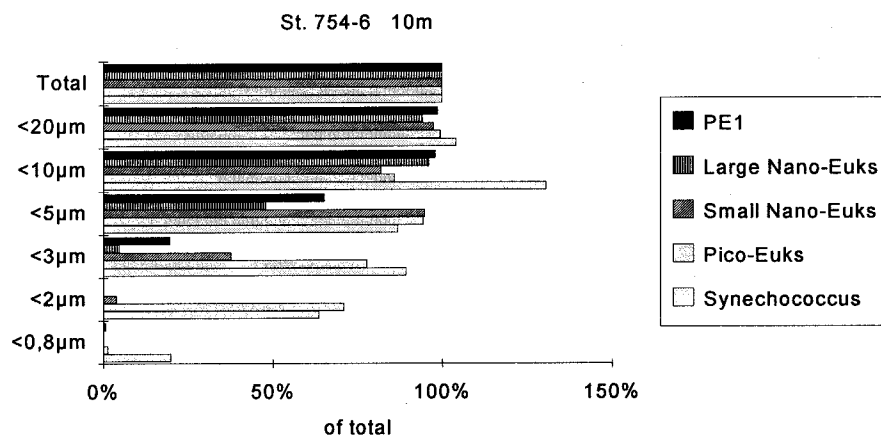
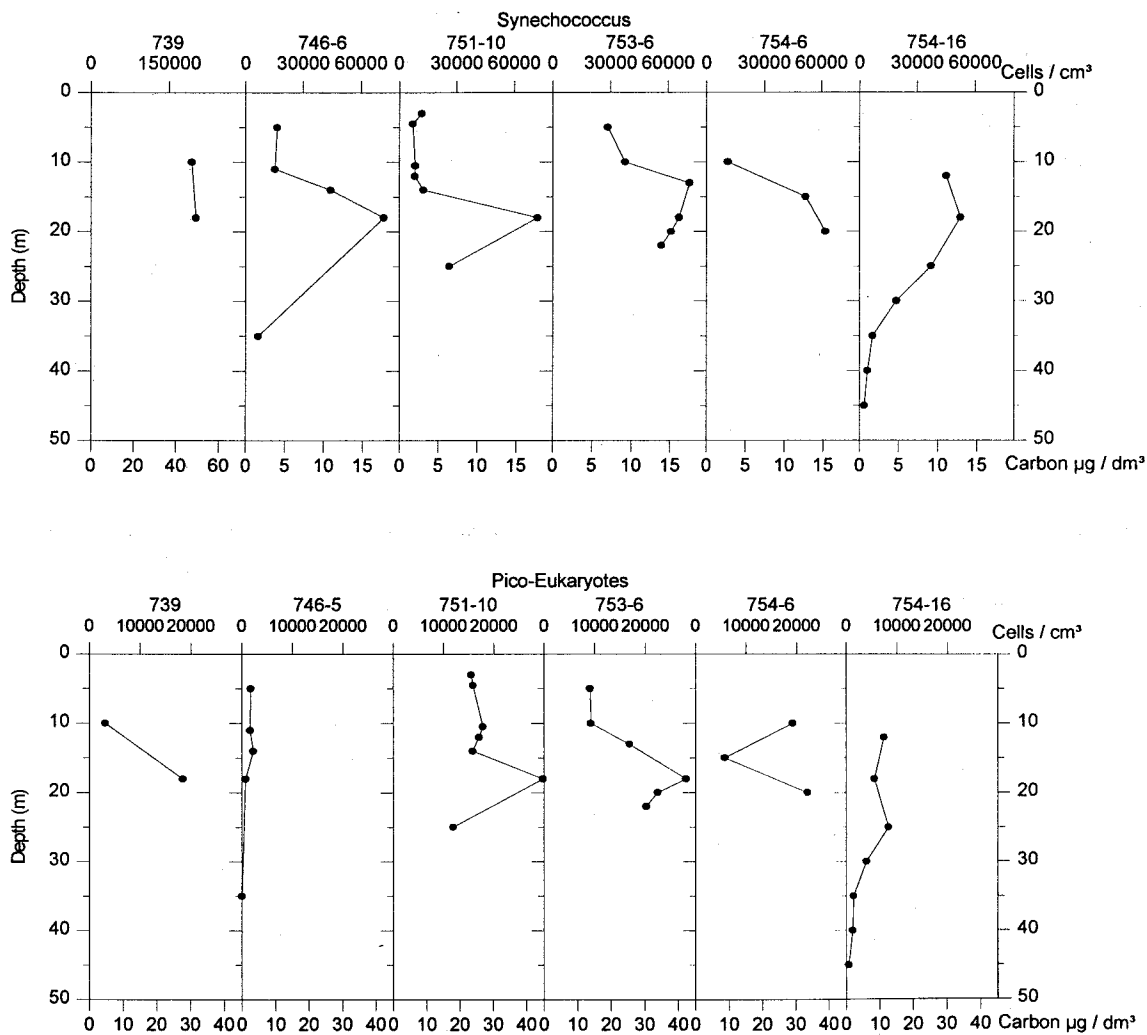


Fig.41 Size fractionated depth profiles of autotrophic ultraplankton as measured by flow cytometry in the Gotland Sea in July 1994 (St.754-6, 10m)

Fig.42 shows depth profiles of the phytoplankton groups analysed by the flow cytometer. Generally, abundances decreased with increasing cell size (*Synechococcus*: up to 200,800 cm⁻³ at the beginning of the drift, then decreasing to 60,000 - 70,000 cm⁻³), pico-eukaryotes: up to 29,700 cm⁻³; small nano-eukaryotes: up to 6,000 cm⁻³; large nano-eukaryotes: up to 2,400 cm⁻³; PE1: up to 660 cm⁻³; SC1: up to 4,600 cm⁻³). Highest abundances of *Synechococcus* were found deeper in the water column (15m to 20m) than for the other phytoplankton (generally 5m to 12m). Carbon biomasses were highest for the large nano-euks (up to 64.5 μg dm⁻³), except for the stations where SC1 were present (peak value of 108 μg dm⁻³); for the pico-euks, values peaked at 44.8 μg dm⁻³, and for the small nano-euks, up to 30.8 μg dm⁻³ were found. Only at the beginning of the drift, *Synechococcus* contributed considerably to phytoplankton biomass (up to 50 μg dm⁻³ at St.739). However, *Synechococcus* abundance and biomass was probably largely underestimated by the flow cytometer, as the concentrations in Experiment 1 (Tab.10) show, which were counted by epifluorescence microscopy. There, *Synechococcus* cells amounted to over 812,000 dm⁻³, corresponding to a carbon biomass of 200 μg dm⁻³ (Tab.10). In general, pico-autotrophs (pico-euks and *Synechococcus*) prevailed in the lower euphotic zone, while the larger nano-autotrophs dominated in shallower layers.



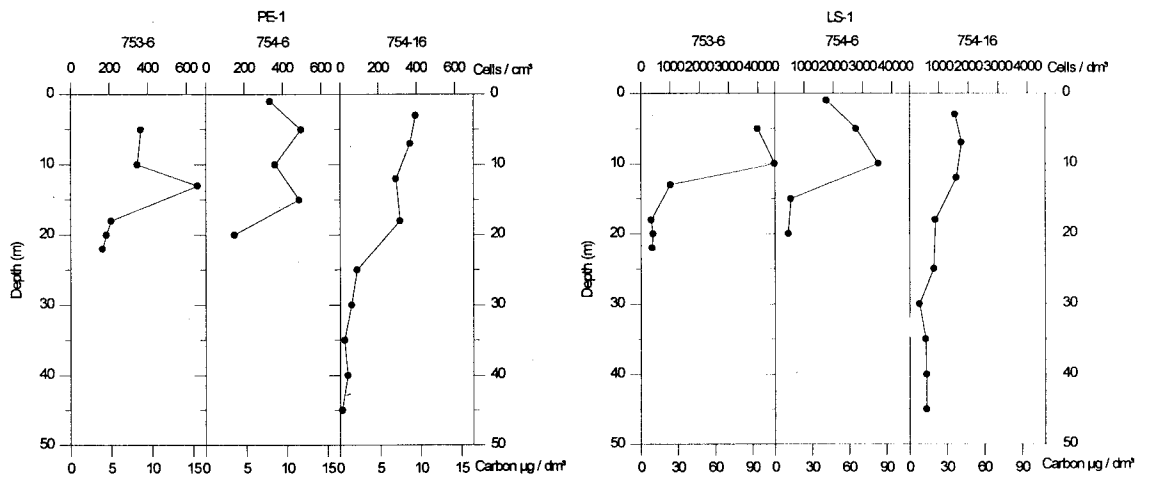
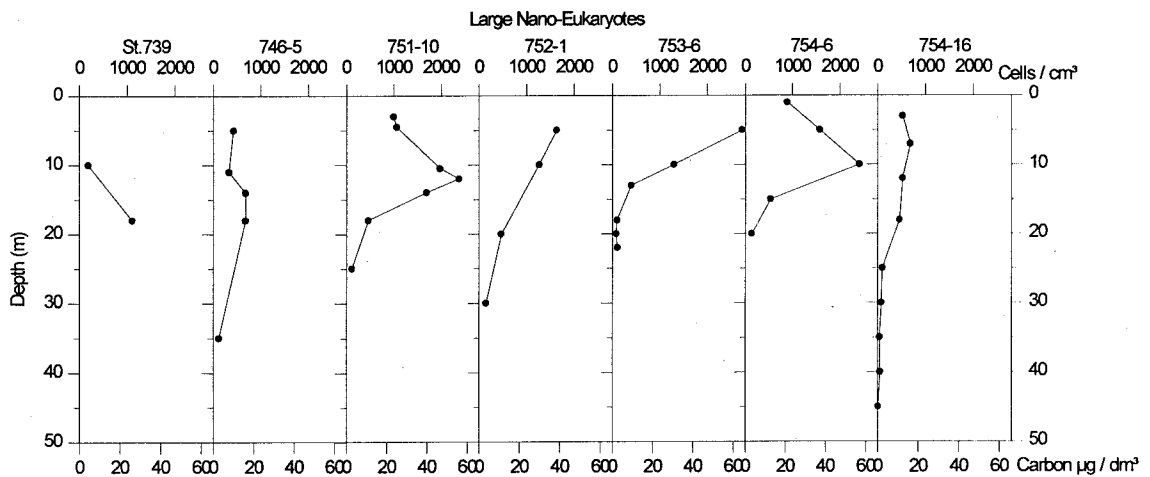
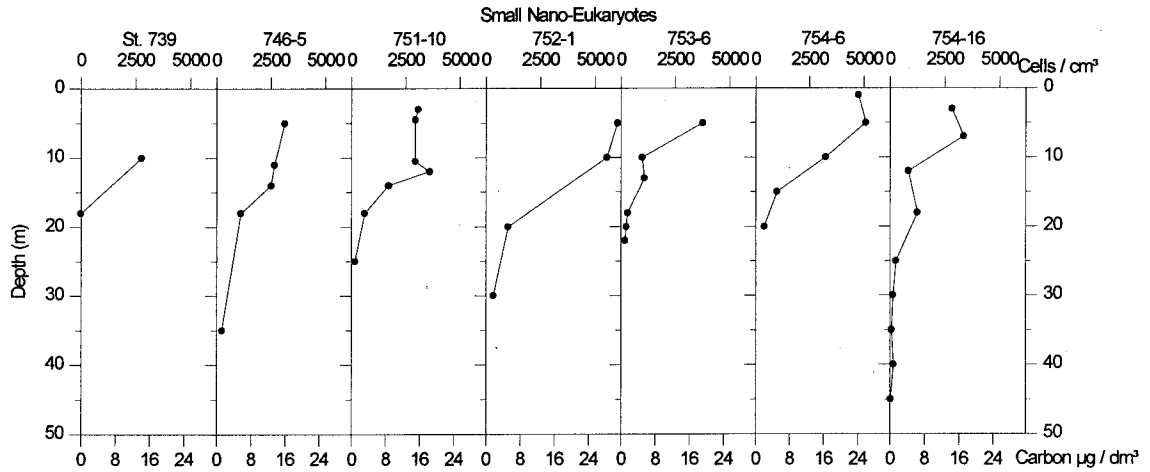


Fig.42 Depth profiles of ultraphytoplankton abundance and carbon biomass, as determined by flow cytometry in the Gotland Sea in July 1994.

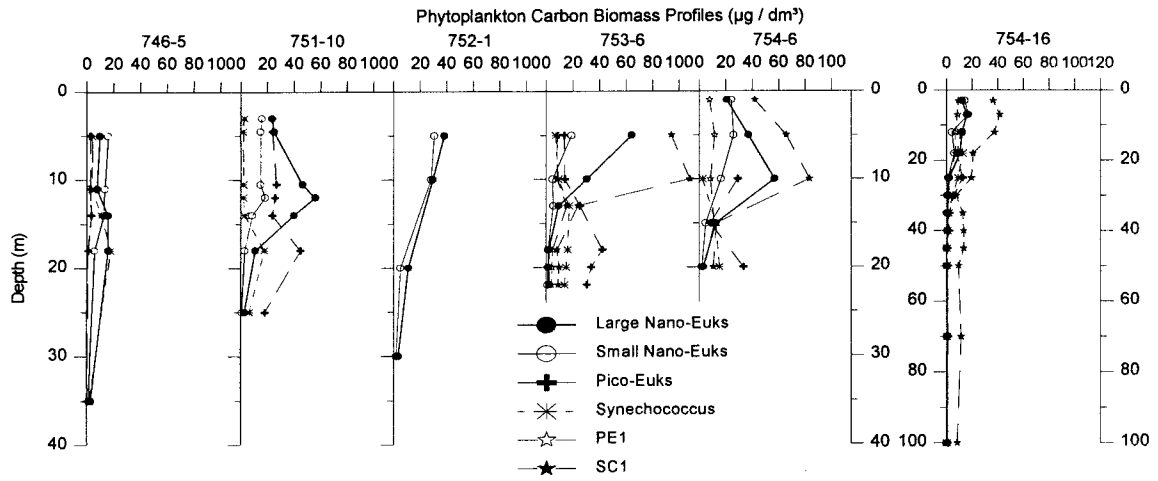


Fig.43 Depth profiles of ultraphytoplankton carbon biomass, as determined by flow cytometry in the Gotland Sea in July 1994. Cell concentrations were converted to carbon according to Tab.1.

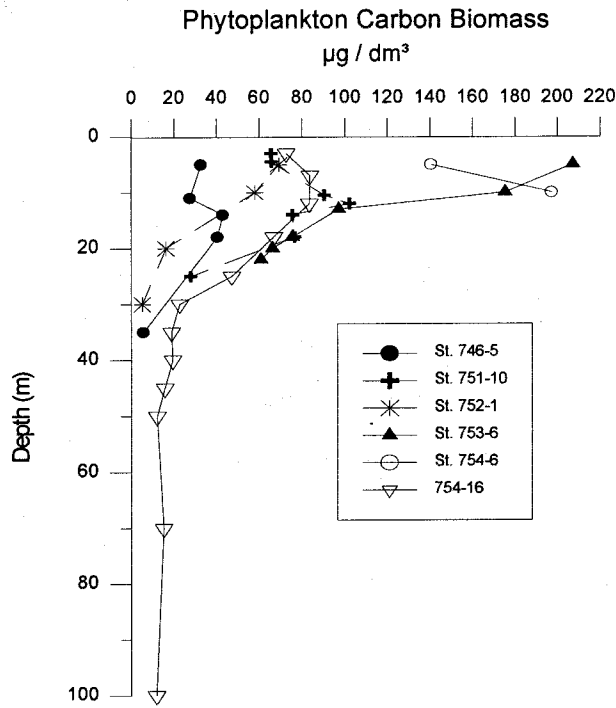


Fig.44 Depth profiles of ultraphytoplankton carbon biomass, as determined by flow cytometry in the Gotland Sea in July 1994. Cell concentrations were converted to carbon according to Tab.1.

Fig.45 demonstrates that pico-autotrophs (*Synechococcus* and pico-eukaryotes) were more important in the deeper water than at the surface, where the larger eukaryotes attained higher biomasses.

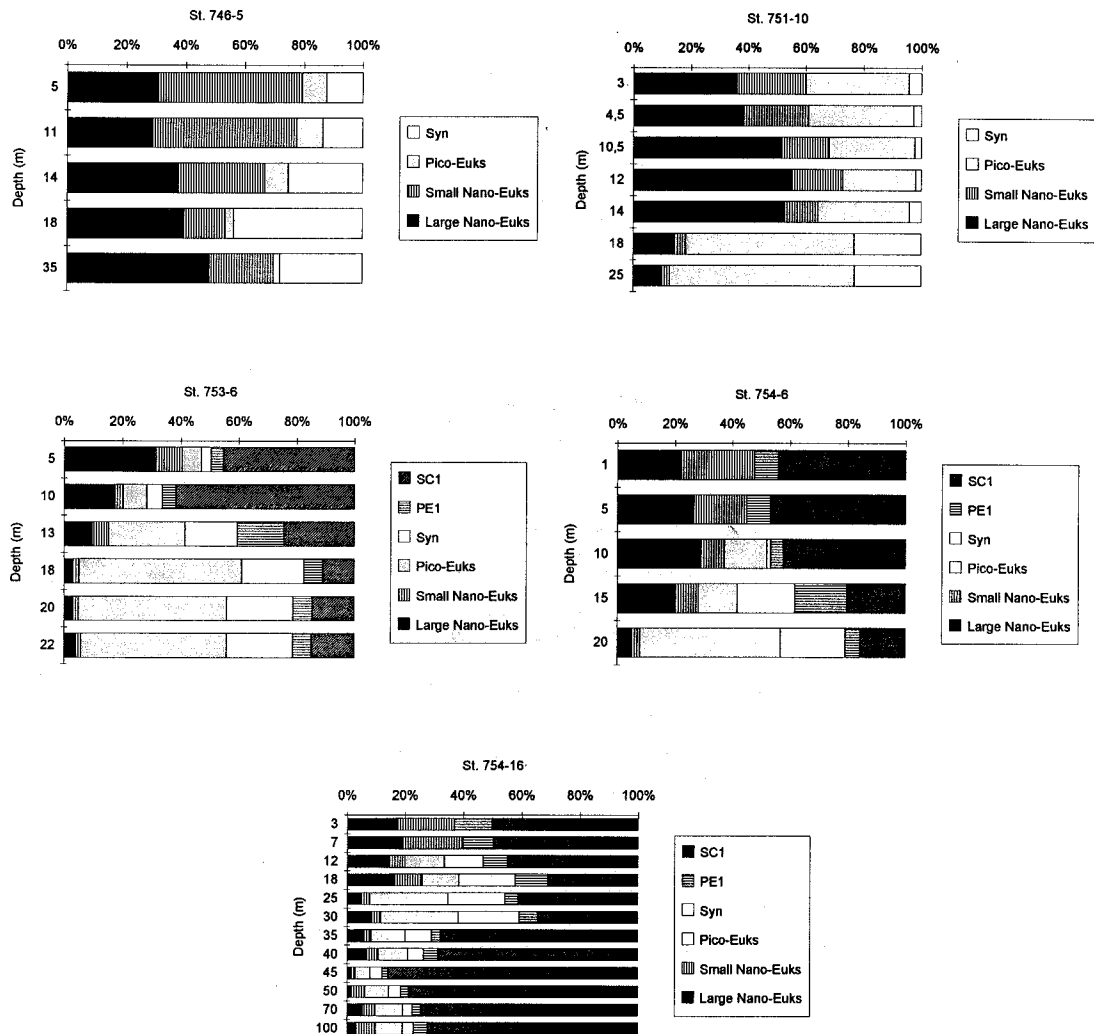


Fig.45 Relative carbon biomass contributions of the different ultraphytoplankton groups over the water column in the Gotland Sea in July 1994.

At three stations, the sum of the ultraphytoplankton carbon, as estimated by flow cytometry was compared to the bulk POC measurements (Maren Voss, IOW) at these stations (Fig.46). At two stations, phytoplankton carbon contributed to 17% - 39% to total POC; at St. 746-5, only 4 - 14% of POC was phytoplankton.

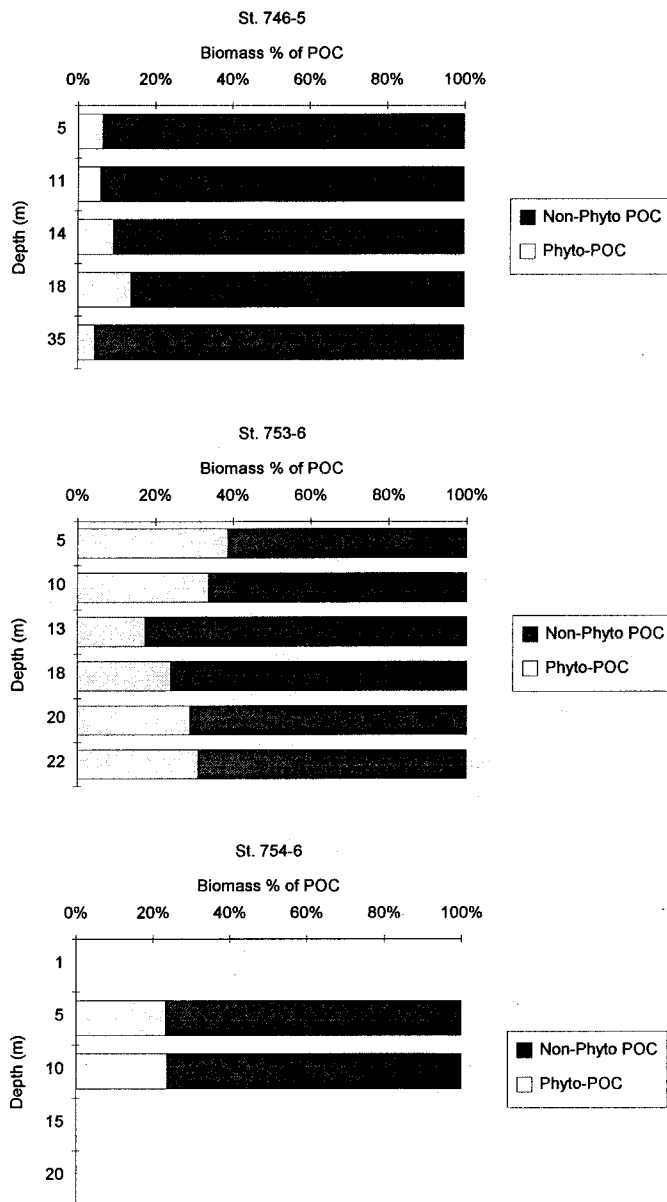


Fig.46 Depth profiles of autotrophic ultraplankton carbon as measured by flow cytometry as percentage of total POC in the Gotland Sea in July 1994.

3.3.3. Protozoan distributions

Protozoa were counted at two stations (Fig.47). At station 750-2, *HNF* numbers showed an peak abundance and biomass at 17m ($3,400 \text{ cm}^{-3}$ and $25.5 \mu\text{g dm}^{-3}$, respectively). Cells 3 - $5\mu\text{m}$ and 1 - $3\mu\text{m}$ were the most abundant, while biomasses were highest for the size fraction 3 - $5\mu\text{m}$ and 5 - $10\mu\text{m}$. *Ciliate* numbers at station 750-2 showed a peak at 12m ($2,800 \text{ dm}^{-3}$), with a carbon biomass of $4 \mu\text{g dm}^{-3}$ at 8m. At station 752-1, abundances were highest at 20m ($5,776 \text{ dm}^{-3}$), while biomasses were highest at 10m ($17 \mu\text{g dm}^{-3}$).

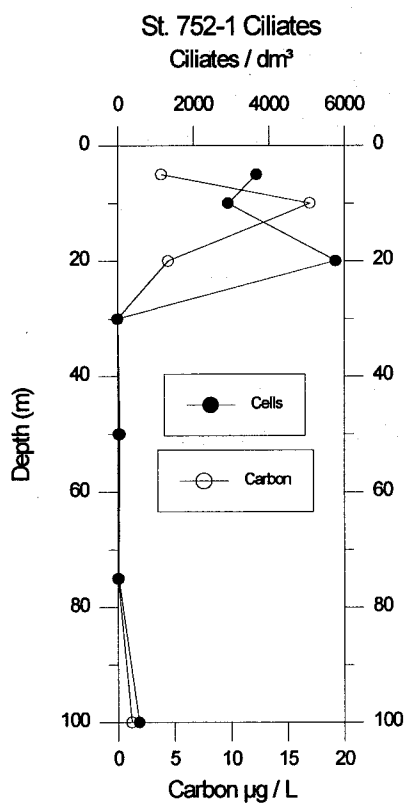
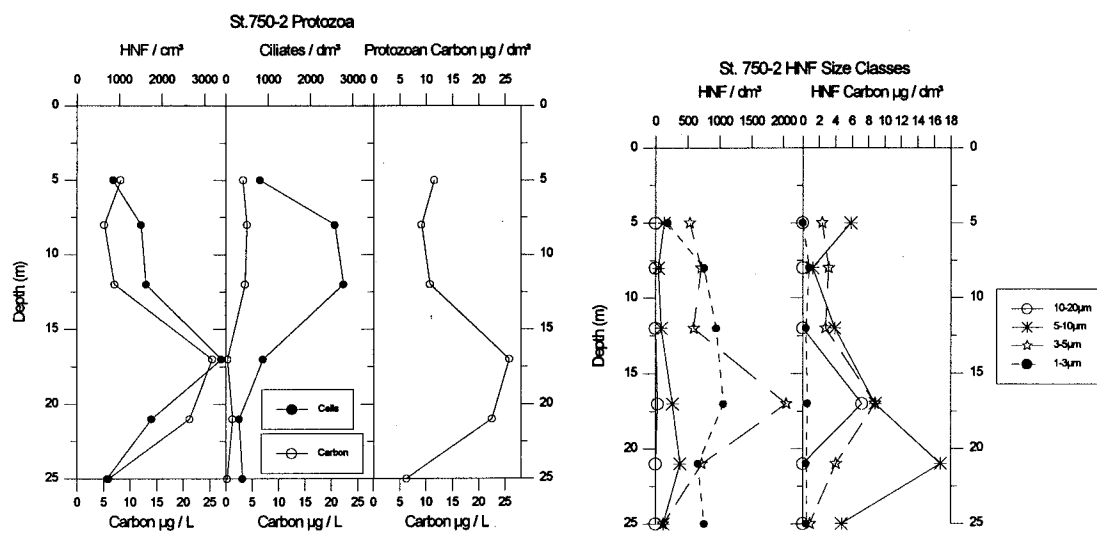


Fig.47 Water column profiles of protozoan abundance and carbon biomass at two stations in the Gotland Sea in July 1994. A: St.750, B: St.752.

3.3.4. Grazer size differential grazing on ultraphytoplankton analyzed by flow cytometry

Three size fractionated dilution experiments were carried out. Due to technical problems, the flow cytometer was used only in two experiments. In the first experiment, *Synechococcus* was enumerated by epifluorescence microscopy. Three grazer size fractions were taken: $<200\mu\text{m}$, $<20\mu\text{m}$, and $<5\mu\text{m}$. Results are summarized in Tab.10, dilution plots are shown in Fig.48 and 49. As nitrate and phosphate were depleted at the surface, incubations were spiked with 10% deep water from below the nutricline. This was to ensure that autotrophic growth was not limited by nutrients. An unspiked treatment was co-incubated to estimate the real, ambient growth rates. An unspiked treatment was co-incubated to estimate the real, ambient growth rates.

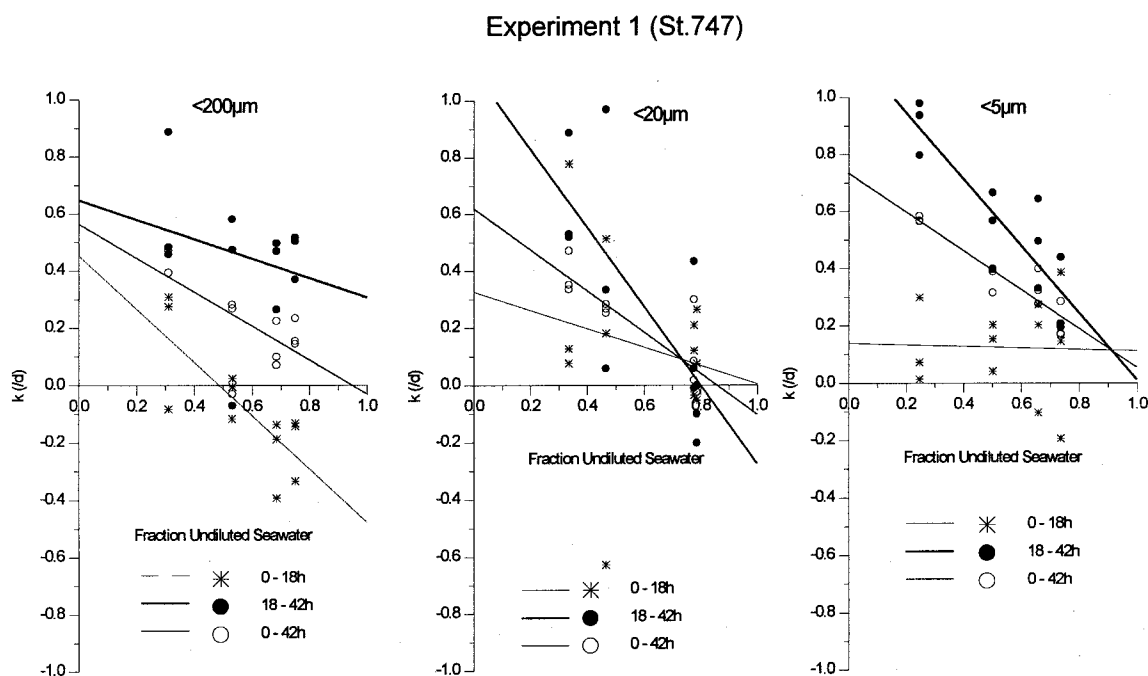


Fig.48 Serial dilution grazing plots for *Synechococcus* involving three grazer size classes ($<200\mu\text{m}$, $<20\mu\text{m}$, $<5\mu\text{m}$), and for three periods (0-18h: mostly dark, 18-42h: complete night-day period, and entire period 0-42h) carried out in the Gotland Sea in July 1994.

For Experiment 1 (Fig.48) sub-samples were taken after 18h and 42h, so that growth and grazing could be estimated for three periods : 0-18h, 18-42h, and over the entire period 0-42h. The experiment started in the afternoon (17:00h), so that only the period 18-42h covered a complete day-night rhythm. Calculations were made with results from the this period (Tab.10). During the first 18h (ca. 8h darkness), specific growth rates were lower as during the other periods, but grazing was highest during that period in the $<200\mu\text{m}$ fraction. During the full 24h period (18-42h), specific growth rates were highest, as were the grazing rates in the fractions $<20\mu\text{m}$ and $<5\mu\text{m}$. In these small fractions, both growth and grazing was lower during the first 18h; especially in the $<5\mu\text{m}$ fraction, growth and grazing on *Synechococcus* had ceased more or less, but increased dramatically during the next 24h.

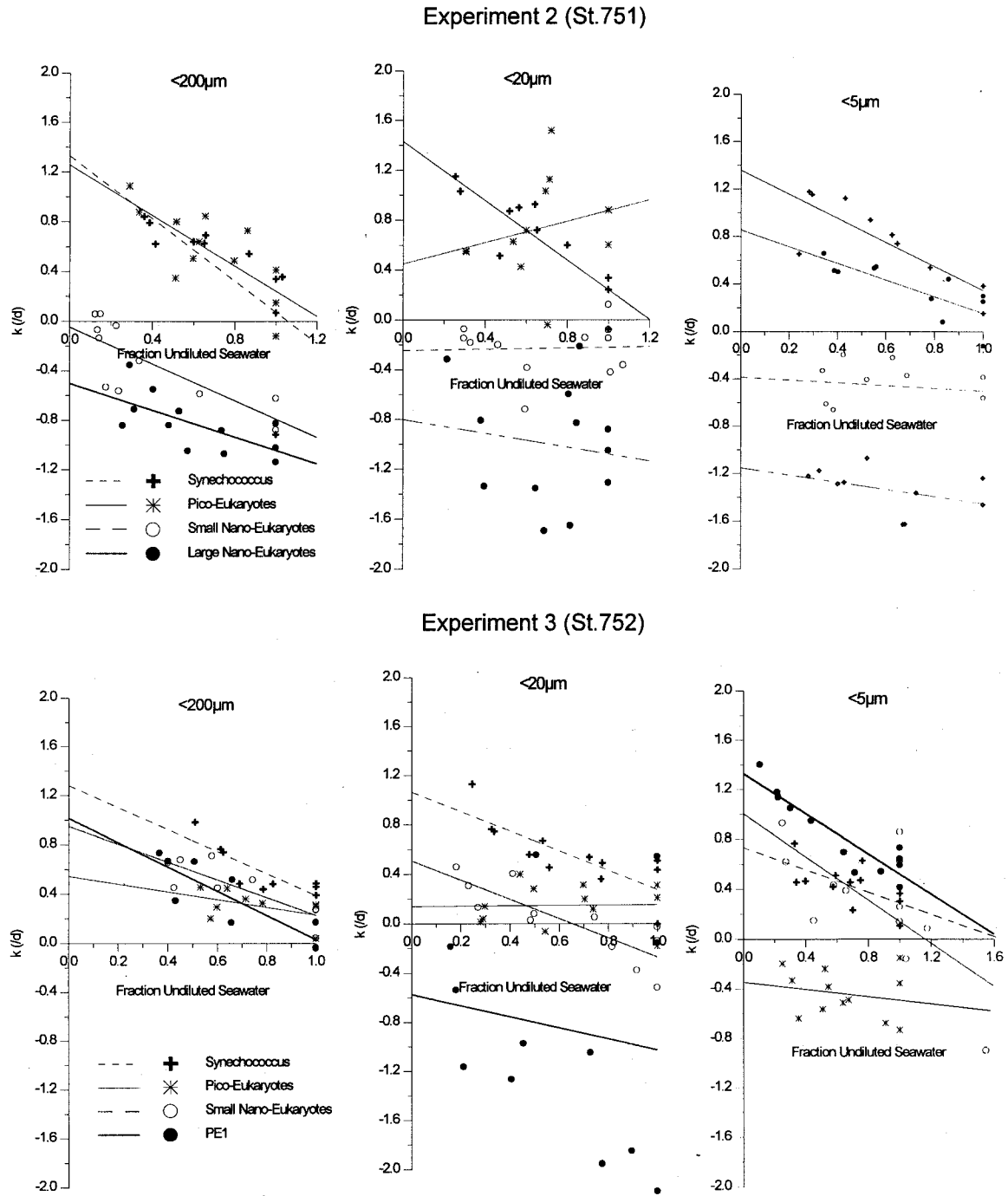
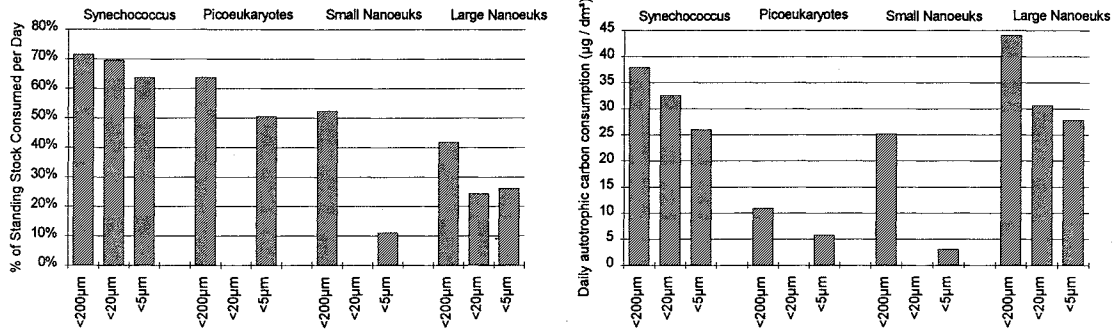


Fig.49 Serial dilution plots for three grazer size classes (<200 μm , <20 μm , <5 μm) in three experiments carried out in the Gotland Sea in July 1994.

Carbon consumption rates (Fig.50, Tab.10) by microzooplankton <200 μm on *Synechococcus* were high but decreased during the course of the drift (from 58 $\mu\text{g dm}^{-3} \text{d}^{-1}$ to 19.4 $\mu\text{g dm}^{-3} \text{d}^{-1}$, corresponding to 29 - 62 % of stock, and 133% - 81% of production grazed daily, respectively). Consumption rates of the other pico- and nano-autotrophs were slightly lower, and likewise decreased during the drift (pico-eukaryotes from 10.9 $\mu\text{g dm}^{-3} \text{d}^{-1}$ to 1.7 $\mu\text{g dm}^{-3} \text{d}^{-1}$ (64 - 27 % of stock, 87% - 49% of production consumed daily), and the small nano-eukaryotes from 25 $\mu\text{g dm}^{-3} \text{d}^{-1}$ - 20.5 $\mu\text{g dm}^{-3} \text{d}^{-1}$ (52.4 - 51.4 % of stock, and 66% of production consumed daily). The large nano-eukaryotes were found only in Exp.2 (44.8 $\mu\text{g dm}^{-3} \text{d}^{-1}$, 17 % of stock grazed daily), while the group PE1 (presumably cyanobacteria or cryptophytes) was found only in Exp.3 (17.4 $\mu\text{g dm}^{-3} \text{d}^{-1}$, 63 % of stock grazed daily). Consumption of the total ultraphytoplankton

community by microzooplankton ($<200\mu\text{m}$), as estimated serial dilution experiments analysed by flow cytometry amounted to 58.6 to $118\ \mu\text{g}\ \text{dm}^{-3}\ \text{d}^{-1}$.

Experiment 2 (St.751)



Experiment 3 (St.752)

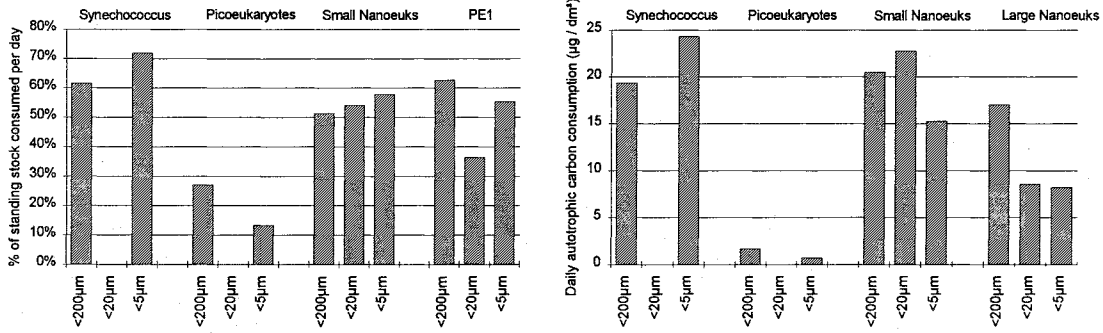


Fig.50 Absolute ultraphytoplankton carbon consumption rates (left) and percentages of ultraphytoplankton standing stock consumed per day (right) for two size fractionated serial dilution grazing experiments carried out in the Gotland Sea in July 1994, and analysed by flow cytometry.

With the exception of *Synechococcus* in Exp.1, there was no pronounced increase in grazing pressure in the small size fractions relative to the large ones, as was observed in the Arabian Sea (Fig.50). On the contrary, in Exp.2, grazing pressure on all prey types was highest in the fraction $<200\mu\text{m}$, encompassing the entire microzooplankton. In Exp.3, grazing on *Synechococcus* was only slightly higher in the $<5\mu\text{m}$ fraction relative to the $<200\mu\text{m}$ fraction ($\sim 10\%$, Fig.50), but for the other ultraphytoplankton, the opposite was the case.

Tab.10 Results of size fractionated dilution grazing experiments from the Gotland Sea in July 1994.

Exp.	Stat.	Grazer Size Class	N t0	Grazing g (d)	Growth μ (d)	r	Stock grazed % / d	Prod. grazed % / d	Cells grazed # / cm ³ * d	Phyto-C grazed mg / m ³ * d
Synechococcus										
1	747	<200 μ m	811,715	0.341	0.257	0.274	29	133	234,538	57.72
1	747	<20 μ m	660,464	1.205	1.588	0.675	70	76	462,528	113.82
1	747	<5 μ m	783,481	1.171	1.522	0.877	69	77	540,557	133.03
2	751	<200 μ m	215,838	1.256	0.873	0.675	72	144	154,369	37.99
2	751	<20 μ m	190,364	1.189	0.572	0.866	70	208	132,393	32.58
2	751	<5 μ m	165,760	1.014	0.899	0.827	64	113	105,628	25.99
3	752	<200 μ m	127,891	0.955	1.172	0.669	62	81	78,677	19.36
3	752	<20 μ m	151,888	-0.352	-0.290	0.529	-	-	-	-
3	752	<5 μ m	137,250	1.270	0.670	0.481	72	190	98,706	24.29
Pico-Eukaryotes										
2	751	<200 μ m	11,370	1.015	1.164	0.751	64	87	7,249	10.93
2	751	<20 μ m	8,270	-0.426	-0.282	0.260	-	-	-	-
2	751	<5 μ m	7,598	0.704	0.945	0.798	51	74	3,840	5.79
3	752	<200 μ m	4,179	0.315	0.647	0.485	27	49	1,129	1.70
3	752	<20 μ m	4,461	-0.014	0.038	0.023	-	-	-	-
3	752	<5 μ m	3,540	0.143	0.352	0.205	13	41	472	0.71
Small Nano-Eukaryotes										
2	751	<200 μ m	9,427	0.743	-0.134	0.781	52	-	4,943	25.16
2	751	<20 μ m	5,595	-0.025	-0.399	0.036	-	-	-	-
2	751	<5 μ m	5,389	0.118	-0.444	0.168	11	-	600	3.05
3	752	<200 μ m	7,828	0.722	1.091	0.829	51	66	4,025	20.49
3	752	<20 μ m	8,260	0.779	0.995	0.841	54	78	4,470	22.75
3	752	<5 μ m	5,185	0.864	0.718	0.683	58	120	3,000	15.27
Large Nano-Eukaryotes										
2	751	<200 μ m	4,471	0.542	-0.594	0.669	42	-	1,871	44.08
2	751	<20 μ m	5,329	0.280	-0.895	0.153	24	-	1,301	30.66
2	751	<5 μ m	4,515	0.303	-2.267	0.420	26	-	1,180	27.81
PE1										
3	752	<200 μ m	1,154	0.985	1.006	0.868	63	98	723	17.04
3	752	<20 μ m	1,000	0.452	0.996	0.163	36	45	364	8.57
3	752	<5 μ m	630	0.806	0.150	0.916	55	537	349	8.21

3.4. The Pomeranian Bay during late summer 1993

Within the framework of the TRUMP project (section 2.1.3.), a pilot drift study in the Pomeranian Bay was carried out in September and October 1993 on board R.V. Professor Albrecht Penck (PAP). Goal of the study was to characterize the transport and transformation of organic material derived from the Szczecin lagoon to the open Bay under different outflow conditions. The first drift trajectory followed a northwestern flow along the coast of the island of Usedom, while the second drift had a northeastern component into the open bay (Fig.51).

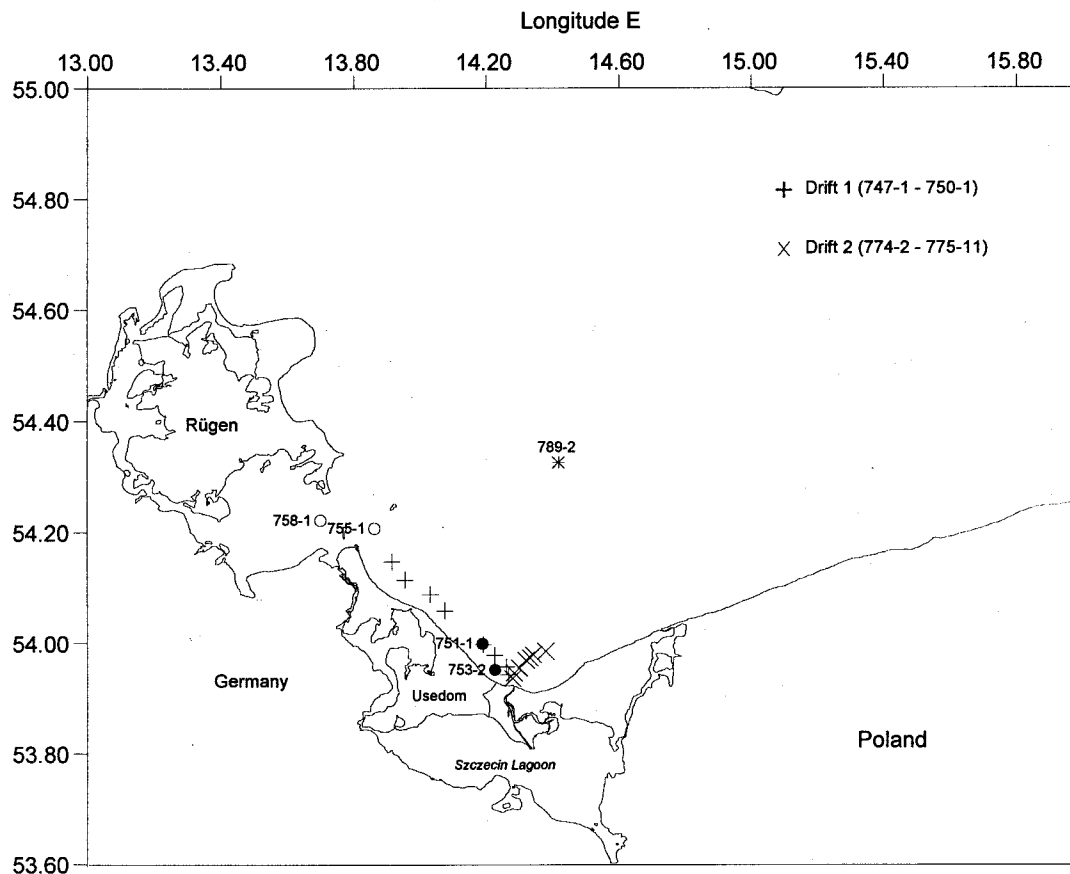


Fig.51 Drift (crosses) and anchor stations (dots) in the Pomerian Bay during a cruise on R.V. Professor Albrecht Penck in September / October 1993.

3.4.1. Drift 1: Hydrography, nutrients, Chl.a and protozoan distributions

During this 50h drift, a northwesterly trajectory along the coast of Usedom was followed. At the beginning of the drift, salinity data (Fig.52) showed a low saline water body at the surface ($S < 5$), separated from a high saline deep water body ($S > 7$). During the course of the drift, the upper water body was increasingly mixed with the higher saline bay water until the water column was well mixed to the bottom at the end of the drift.

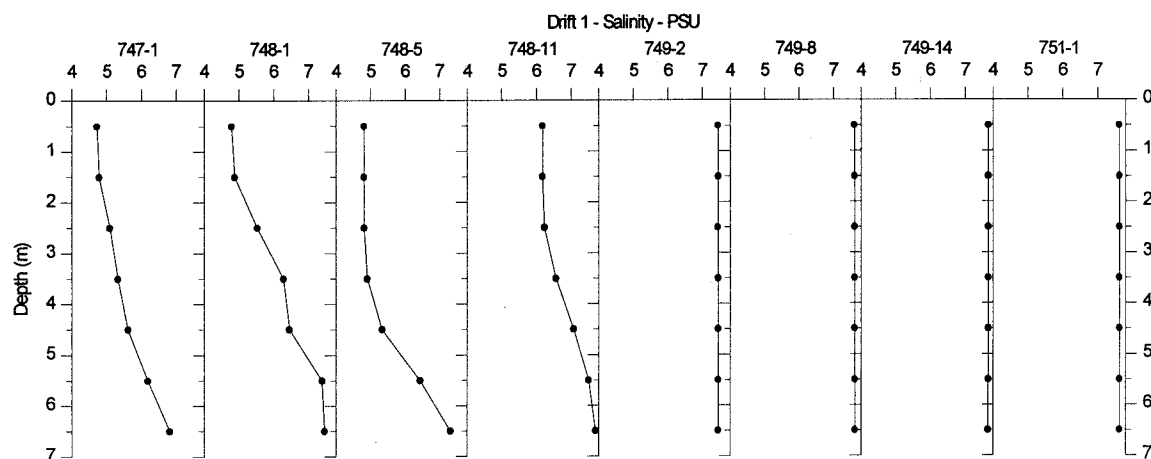


Fig.52 Water column profiles of salinity during Drift 1.

This was also seen in the nutrients (Fig.53): *nitrate* concentrations at the surface decreased from 9 μM to 3 μM , *nitrite* from 0.6 to 0.2 μM , *phosphate* from 3.8 to 1.2 μM , and *silicate* from 66 to 31 μM .

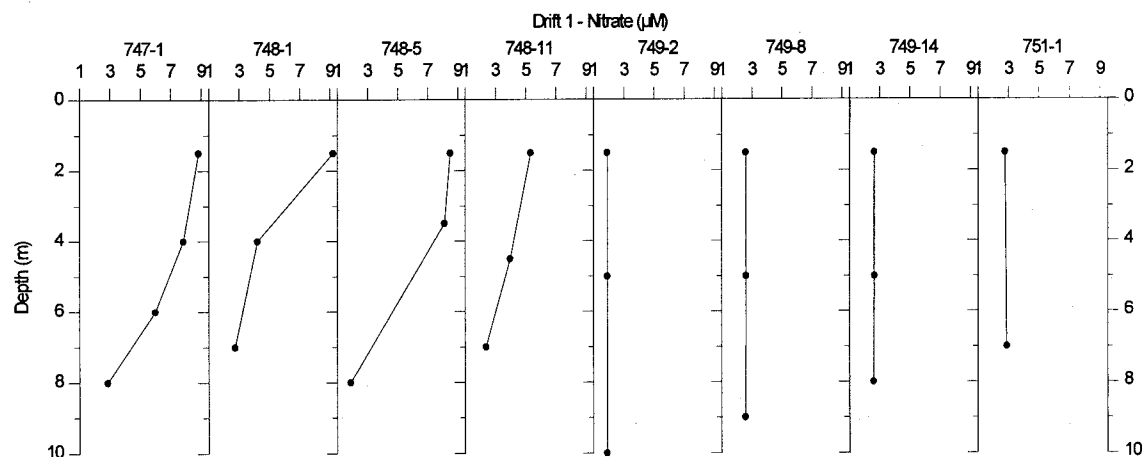


Fig.53 Water column profiles of nitrate during Drift 1.

Chl.a concentrations (Fig.54) at the surface decreased from 15 to 4 $\mu\text{g dm}^{-3}$. The *phytoplankton* was comprised of large filamentous and colonial forms of cyanophyceae and chlorophyceae; diatoms and cryptophyceae were present in smaller amounts. The different components of the phytoplankton community were diluted proportionally during the course of the drift, i.e. there was no distinct biomass increase of any particular phytoplankton groups during the drift (MEYER-HARMS 1996).

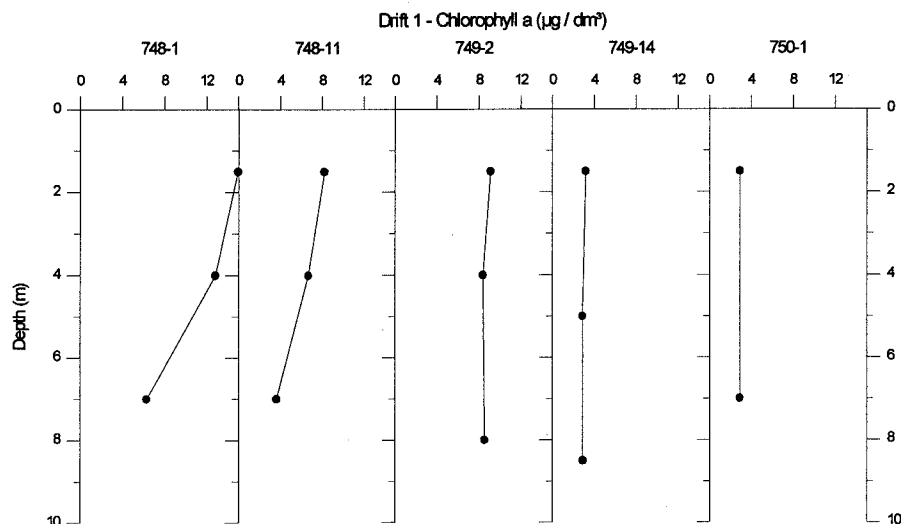


Fig.54 Water column profiles of Chl.a during Drift 1.

HNF cell concentrations (Fig.55A) at the surface decreased from $5,200 \text{ cm}^{-3}$ to $1,480 \text{ cm}^{-3}$ during the drift (respective carbon values from 137 to $18 \mu\text{g dm}^{-3}$). Cells $3 - 5 \mu\text{m}$ were most abundant in the whole water column, while the larger $5 - 10 \mu\text{m}$ flagellates dominated biomass, except at the first station at the surface, where few very large individuals $>10 \mu\text{m}$ made up the bulk of HNF biomass. HNF $<3 \mu\text{m}$ were of minor importance both in terms of numbers and biomass (Fig.55B, C, for integrated values see Fig.64A). Concentrations of the heterotrophic silicoflagellate *Ebria tripartita* (Fig.56A) also decreased during the course of the drift (from $4,900 \text{ dm}^{-3}$ (cells) and $9.6 \mu\text{g dm}^{-3}$ (carbon biomass) to 474 dm^{-3} and $0.9 \mu\text{g dm}^{-3}$, respectively). *Ciliate* numbers and biomasses (Fig.56B) were also high at the beginning (cells: $17,200 \text{ dm}^{-3}$, carbon biomass: $55 \mu\text{g dm}^{-3}$), and decreased gradually towards the end of the drift ($2,600 \text{ dm}^{-3}$ and $12.6 \mu\text{g dm}^{-3}$, respectively). Ciliates $20 - 50 \mu\text{m}$ made up the bulk of numbers and ciliate biomass (Fig.64B, integrated values), and oligotrichs clearly dominated the composition of the ciliate community (Fig.64C, integrated values). Total protozoan carbon biomass, expressed as the sum of the three respective protozoan groups, decreased from $163 \mu\text{g dm}^{-3}$ at the beginning, to $31 \mu\text{g dm}^{-3}$ at the end of the drift (Fig.57). HNF and ciliates together contributed to over 85% of protozoan biomass (Fig.65).

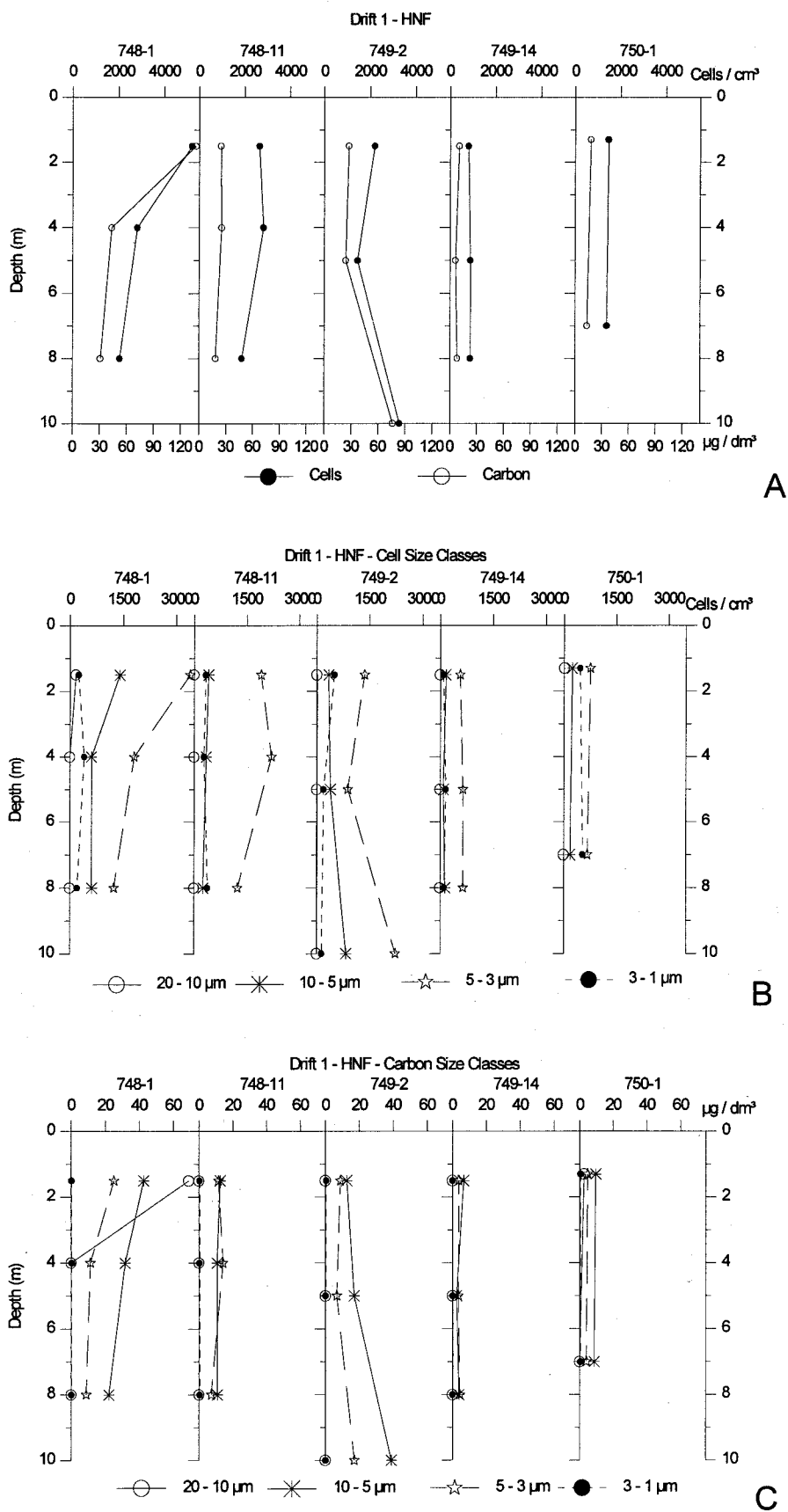


Fig.55 Water column profiles of HNF during Drift 1. A: Total HNF concentrations and carbon biomasses, B: Cell size classes, C: Carbon biomass size classes.

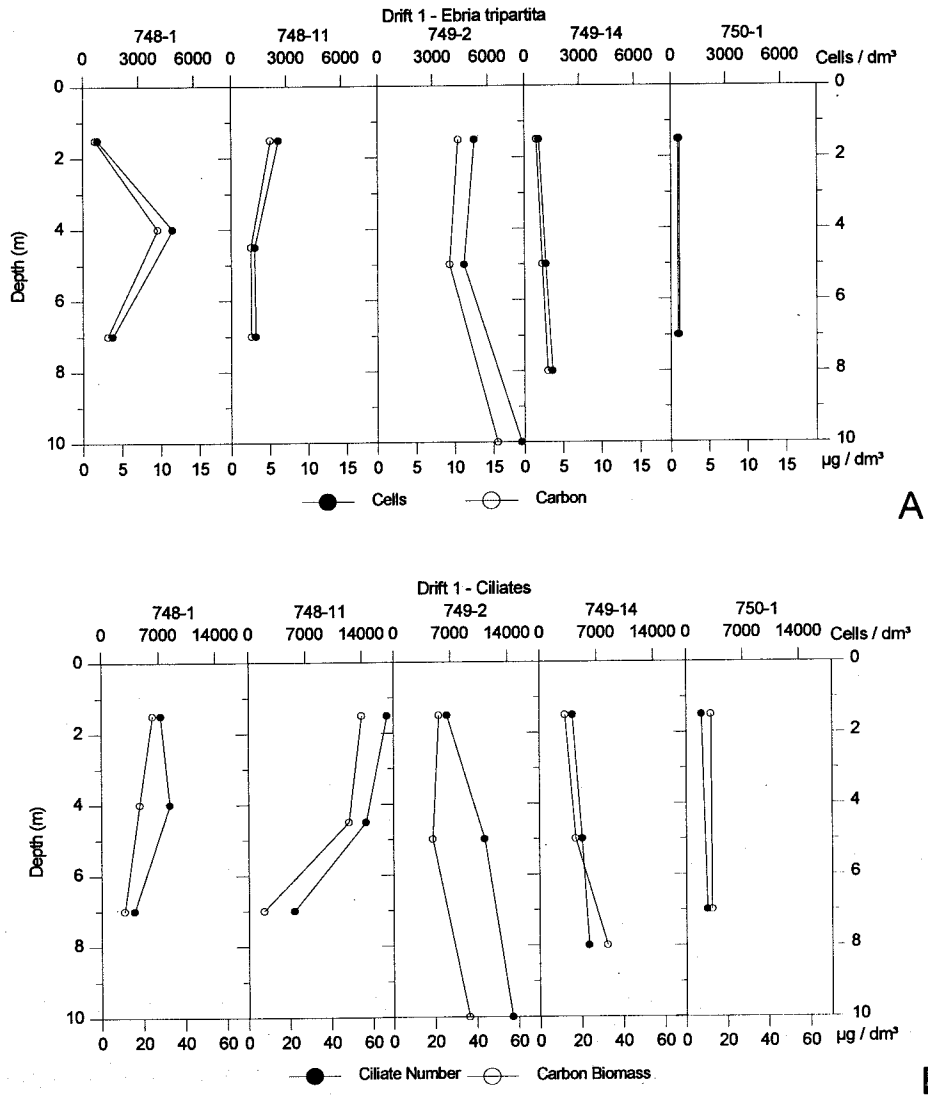


Fig.56 Water column profiles of *Ebria tripartita* (A) and ciliates (B).

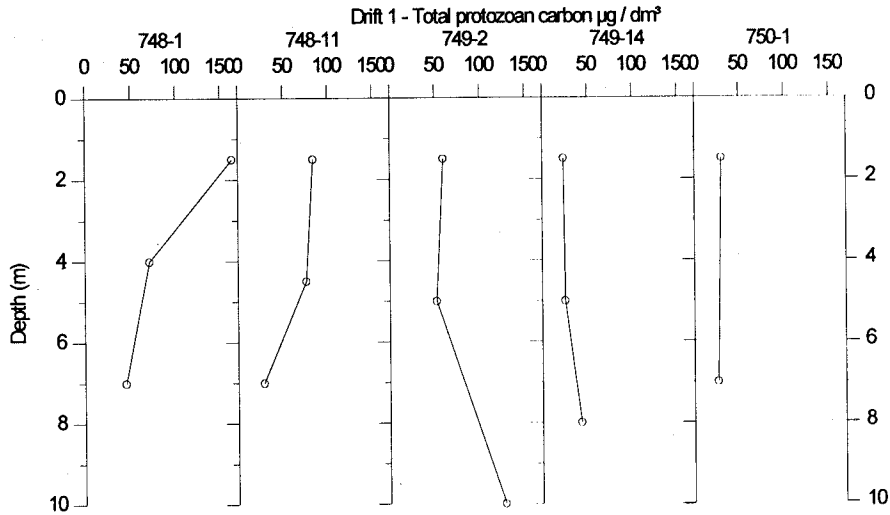


Fig.57 Water column profiles of total protozoan carbon biomass during Drift 1.

3.4.2. Drift 2: Hydrography, nutrients, Chl.a and protozoan distributions

The second drift (30h) was characterized by a northeasterly trajectory (Fig.51). The pronounced stratification between the low saline upper and the high saline bottom water body largely persisted, but weakened towards the end of the drift (surface salinity increased from 5.3 to 6); however, a well mixed water column did not develop during the second drift (Fig.58).

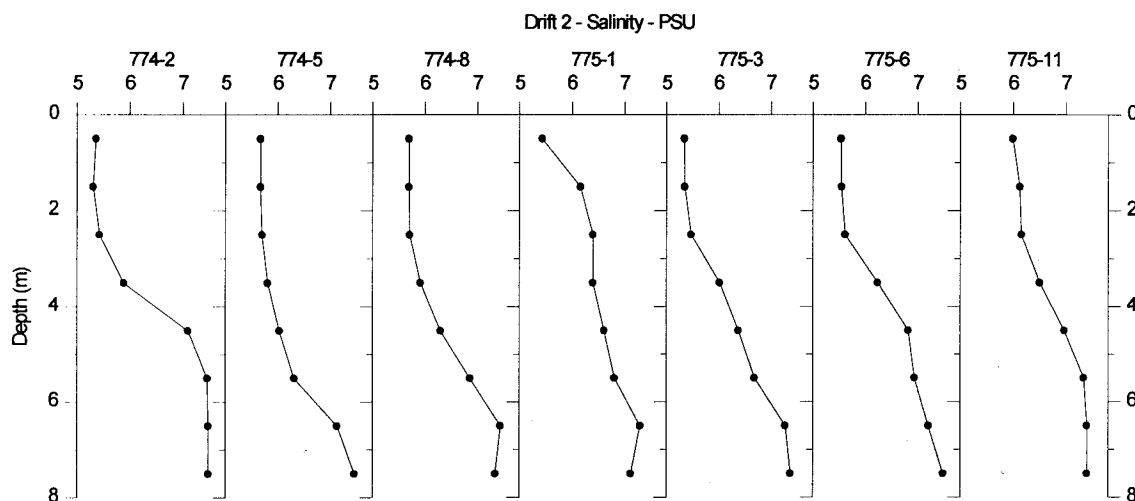


Fig.58 Water column profiles of Salinity during Drift 2.

Nutrient values at the surface remained high, and the gradient between the upper water body and the bottom water also persisted. *Nitrate* at the surface ranged from 10 - 12 μM , and from 1 - 3 μM at the bottom (Fig.59), *nitrite* 0.3 - 0.4 μM at the surface and around 0.1 μM at the bottom, *phosphate* around 2 μM at the surface and around 1 μM at the bottom, and *silicate* 50 - 60 μM at the surface and around 30 μM at the bottom.

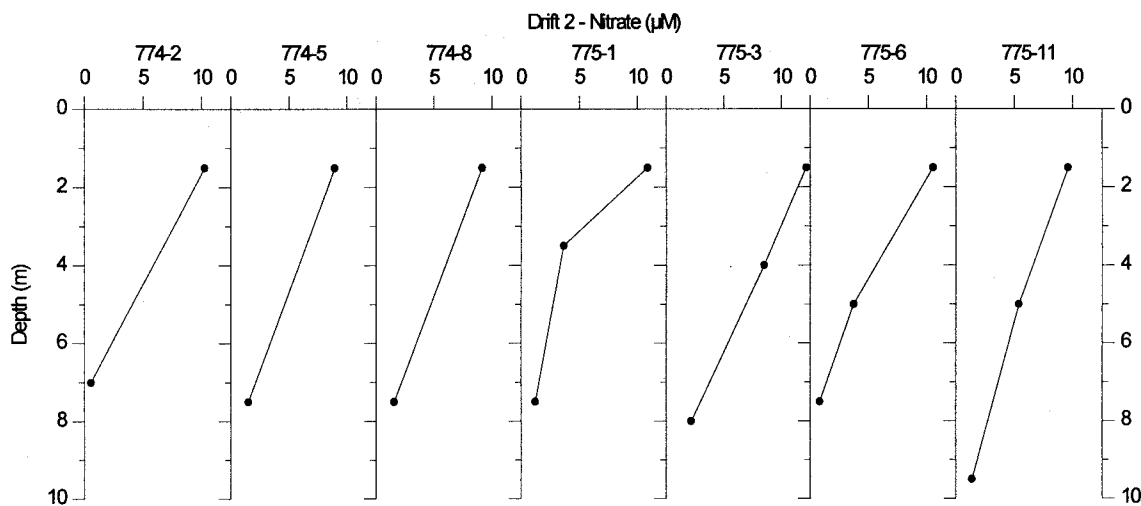


Fig.59 Water column profiles of nitrate during Drift 2.

Chl. a surface values ranged from 11 - 13 $\mu\text{g dm}^{-3}$, decreasing to bottom values of around 9 $\mu\text{g dm}^{-3}$. The *phytoplankton* composition largely resembled that of the first drift, but dilution was much less.

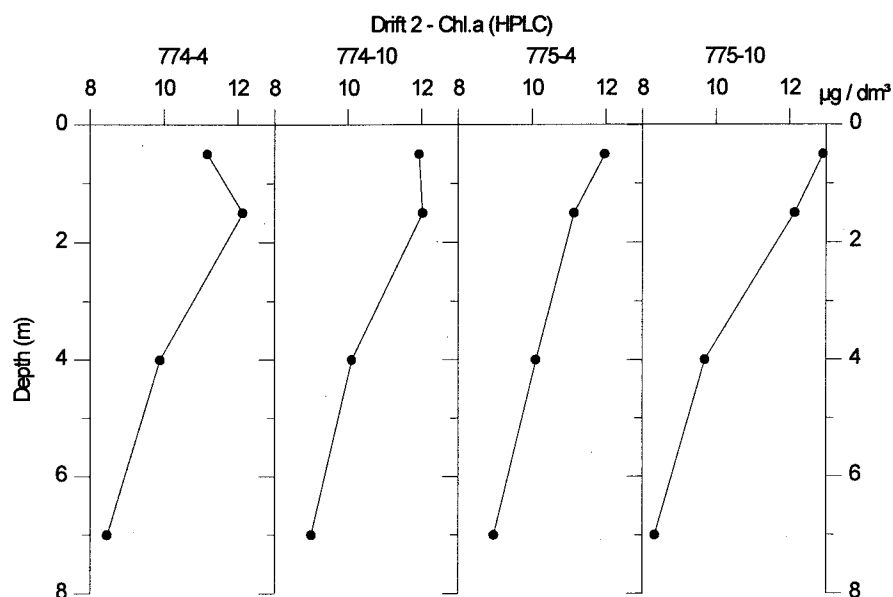
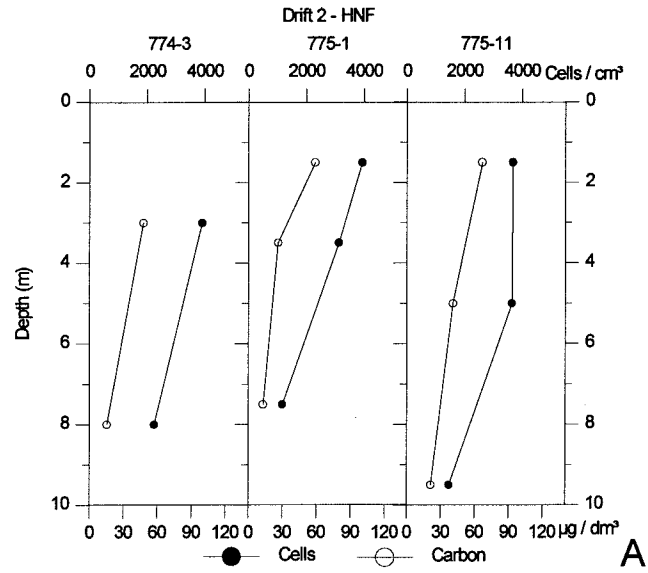
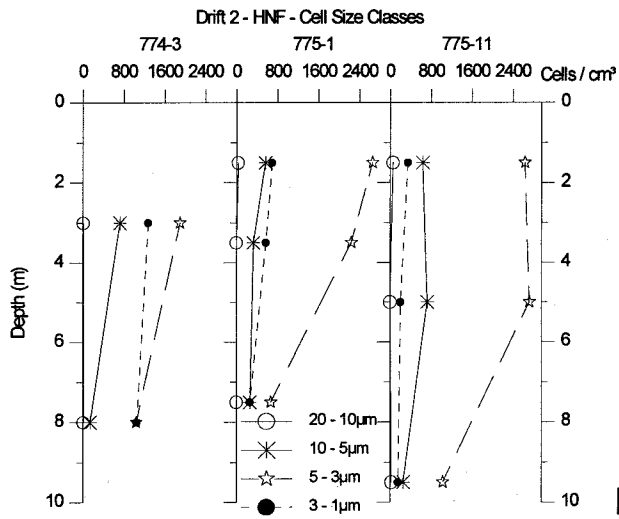


Fig.60 Water column profiles of Chl.a during Drift 2.

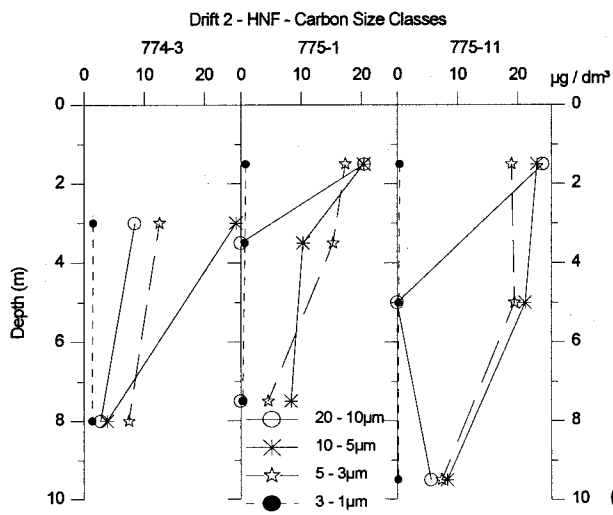
Protozoan concentrations were lower during the second drift as during the first drift, and remained relatively constant during the drift. *HNF* cell concentrations ranged from 3,950 cm^{-3} (start of the drift) to 3,630 cm^{-3} (end of the drift); respective carbon biomass values ranged from 48 $\mu\text{g dm}^{-3}$ to 76 $\mu\text{g dm}^{-3}$ (Fig.61A). Cells 3 - 5 μm were most important in terms of abundance (Fig.61B); in terms of carbon biomass, all size classes >3 μm were of similar importance (Fig.61C). *HNF* <3 μm were of minor importance, both in terms of numbers and biomass (Fig.61B, C, Fig.64A). Concentrations of the heterotrophic silicoflagellate *Ebria tripartita* (Fig.62A) ranged from 300 - 480 dm^{-3} (respective carbon biomass values: 0.6 - 1 $\mu\text{g dm}^{-3}$). Also, *ciliate* concentrations (Fig.62B) were much lower than during the first drift: cell numbers ranged from 1,330 to 3,500 dm^{-3} (carbon biomass values: 3.8 - 4.7 $\mu\text{g dm}^{-3}$). Cells 20 - 50 μm dominated the ciliate community, which mainly consisted of oligotrichs and didiniids (Fig.64). Total protozoan biomass ranged from 52 to 73 $\mu\text{g dm}^{-3}$ (Fig.63), and was clearly dominated by *HNF* (Fig.65).



A



B



C

Fig.61 Water column profiles of HNF during Drift 2. A: Total HNF, B: Cells size classes, C: Carbon biomass size classes

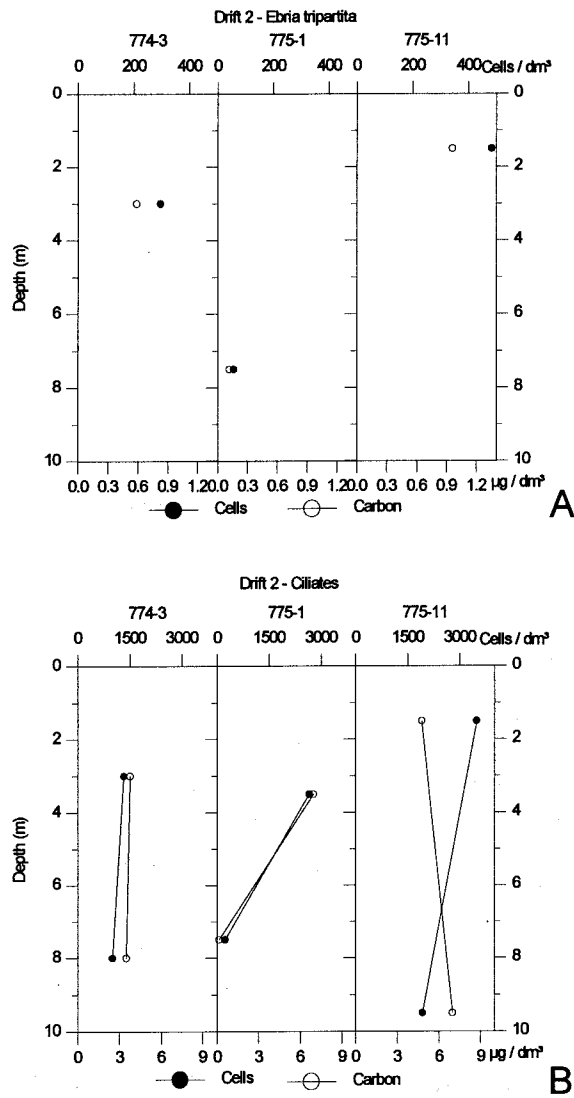


Fig.62 Water column profiles of *Ebria tripartita* (A) and ciliates (B) during Drift 2.

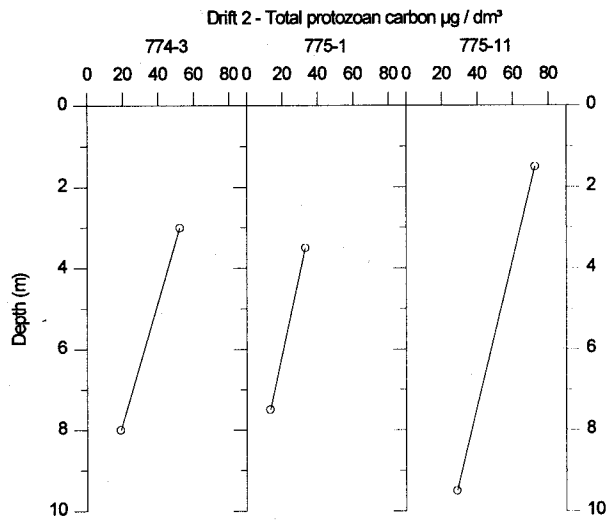


Fig.63 Water column profiles of total protozoan biomass during Drift 2.

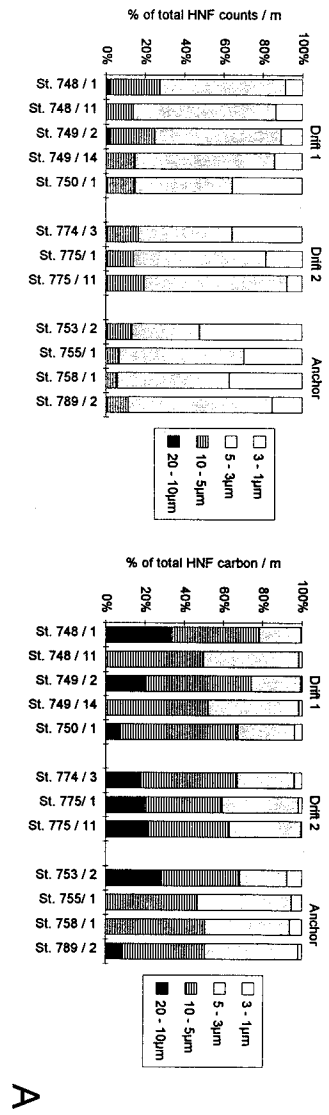


Fig.65 Protozoan carbon biomasses integrated over the water column during both drifts. Left panel: Absolute values; right panel: Relative contribution of the respective protozoan groups.

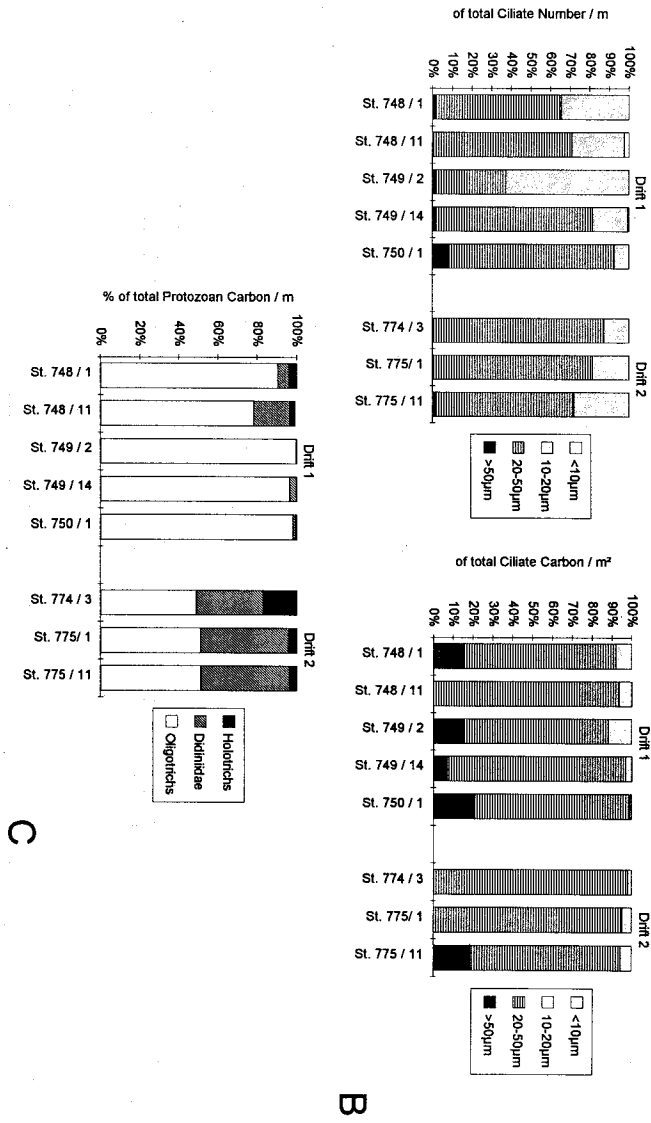


Fig.64 Size class distributions of protozoan abundances (left) and carbon biomasses (right), integrated over the water column during both drifts. A: HNF, B: Ciliates, C: Ciliate groups.

3.4.3. Herbivory

During the first drift, two dilution experiments were carried out based on bulk Chl.a measurements (Tab.11, Fig.66). At the beginning of the drift, no grazing was detected, and the specific growth rate of the phytoplankton was rather low ($\mu = 0.127$). The second experiment was performed towards the end of the drift, and showed high grazing and moderate growth rates. 38% of the phytoplankton standing stock, and 176% of production was grazed daily by microzooplankton, corresponding to a chlorophyll consumption of $1.88 \mu\text{g dm}^{-3} \text{d}^{-1}$ and a carbon consumption $94 \mu\text{g dm}^{-3} \text{d}^{-1}$. The third experiment was performed at an anchor station off the coast of Usedom (St. 751-1), located within the first drift trajectory in between the stations of the first and second experiment; but 54h after the first experiment. Growth and grazing were intermediate at this station, with 24% of phytoplankton grazed daily (51% of production), corresponding to $1.86 \mu\text{g dm}^{-3} \text{d}^{-1}$ Chl.a, or $93 \mu\text{g dm}^{-3} \text{d}^{-1}$ carbon consumed per day.

Tab.11 Results of serial dilution grazing experiments in the Pomeranian Bay in Sept./Oct.1993.

Location	Station	Depth m	Chl a t0 mg / m ³	Grazing g (d)	Growth μ (d)	r	Stock grazed % / d	Prod. grazed % / d	Chl a grazed mg / m ³ * d	Phyto-C grazed mg / m ³ * d
Drift 1	748 / 1	4	8.08	-0.050	0.127	0.134	-	-	-	-
Drift 1	749 / 8	4	4.97	0.476	0.271	0.880	38	176	1.88	94.12
Anchor	751 / 1	3	7.66	0.279	0.542	0.853	24	51	1.86	93.25
Drift 2	774 / 2	3	11.58	0.276	0.459	0.888	24	60	2.79	139.65
Odra Bank	789 / 2	3	2.41	-0.154	0.099	0.352	-	-	-	-

During the second drift, only one experiment was carried out, at the beginning of the drift. Here, growth and grazing rates were similar to the anchor station, with 24% of the phytoplankton, grazed daily (60% of production). However, absolute carbon consumption rates were higher ($140 \mu\text{g dm}^{-3} \text{d}^{-1}$), due to the higher ambient Chl.a concentrations.

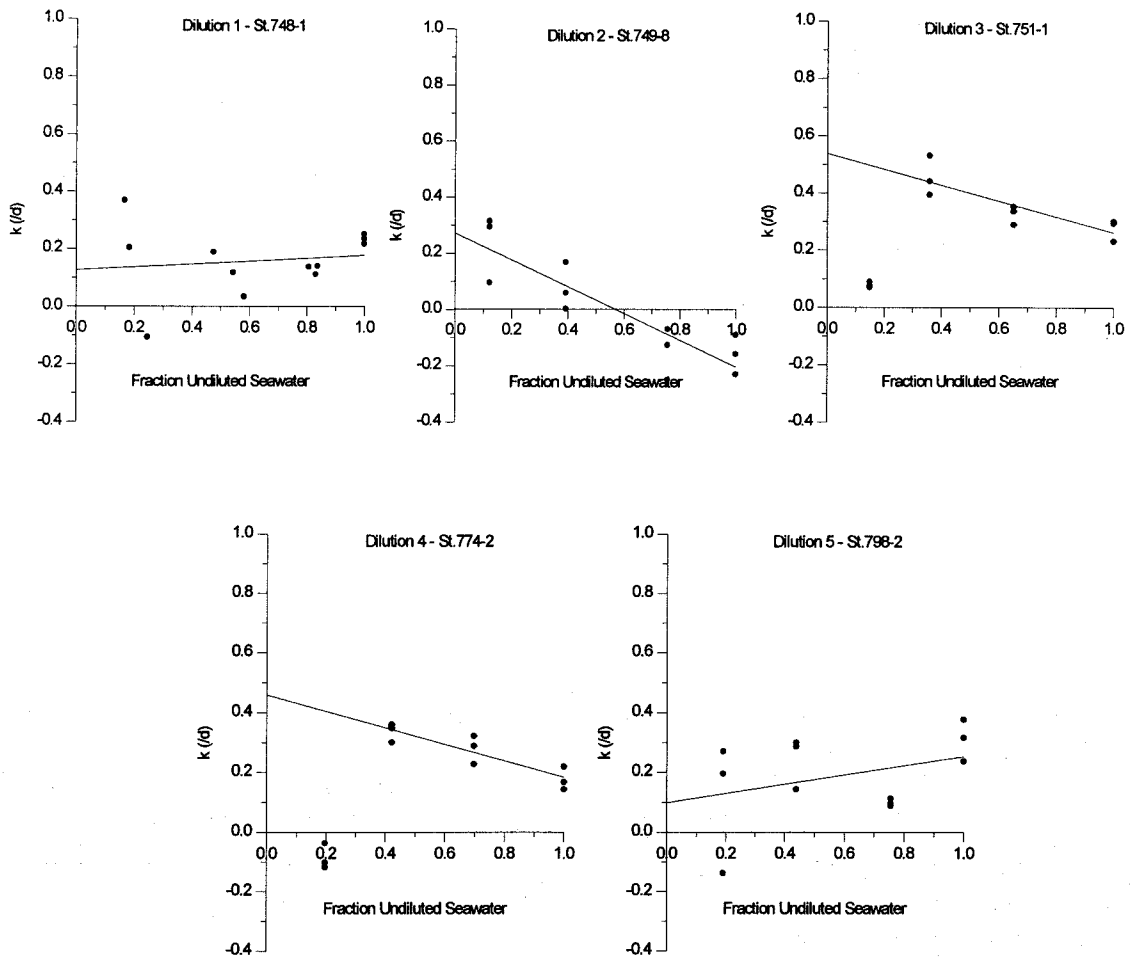


Fig.66 Dilution plots of serial dilution experiments carried out in the Pomeranian bay during Sept./Oct. 1993.

3.5. The Pomeranian Bay during summer 1994

A second cruise to the Pomeranian Bay was conducted on board R.V. AvH from June 23 to July 8, 1994. During this survey, a grid of fixed stations was sampled (Fig.67). The grid was re-sampled four days after commencing the first cycle, omitting the outer stations (St. 51 - 70). During this cruise, emphasis lay on the analysis of ultraphytoplankton by flow cytometry and the determination protozoan stocks by microscopy.

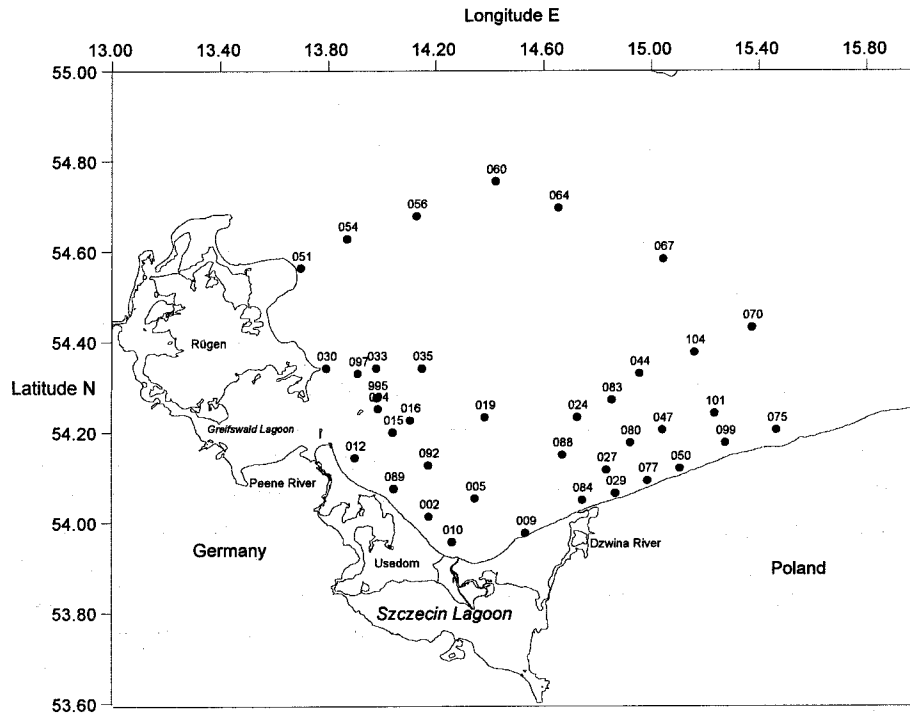


Fig.67 Sampling grid in the Pomeranian bay, sampled during a cruise on board R.V. Alexander von Humboldt in June / July 1994.

3.5.1. Hydrography and nutrients

A strong westerly wind, that had been prevailing for several weeks, forced a narrow band of low saline lagoon water along the polish coast during the first grid. Another band of low saline water came from the Greifswald Lagoon and Peene mouth, flowing southeast along the Usedom coast. Four days later (second grid), the wind had changed to easterly directions, which resulted in an expansion of the low saline transport belt towards the north and increased mixing with bay water (Fig.68).

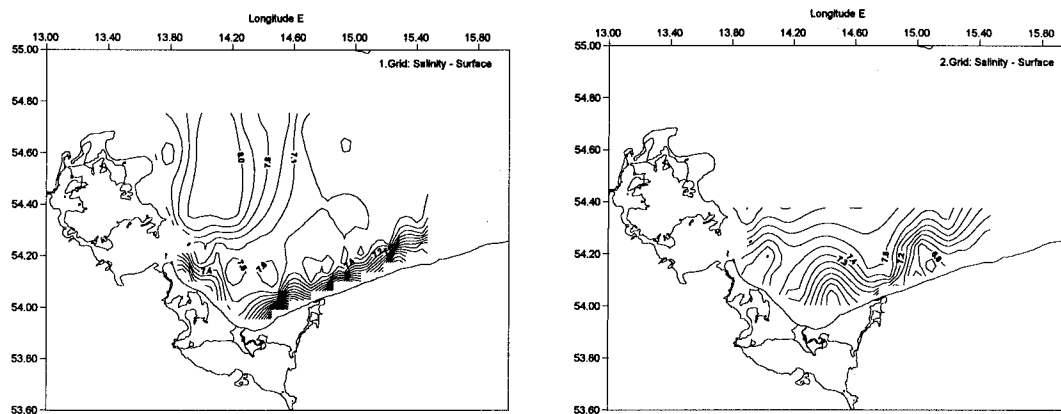


Fig.68 Surface salinity distributions in the Pomeranian Bay during the first (left panel) and the second grid (right panel) in June / July 1994.

Distributions of *nitrate* largely followed the discharge pattern of the low saline lagoon water (Fig.69). A narrow band of high concentrations ($>1 - 15\mu\text{M}$) was detected along the polish coast, with slightly elevated concentrations also along the Usedom coast, originating from the Greifswald lagoon and Peene mouth. In the open bay, concentrations were below $0.1\mu\text{M}$. *Phosphate* was at or below detection level in the southern bay, with elevated concentrations ($>0.1\mu\text{M}$) only in the deep water column in the northeast corner of the bay, corresponding to the southwest fringe of the Bornholm Basin. *Ammonium* was low in the open bay ($<0.5\mu\text{M}$), with elevated concentrations only near the mouth of the Dzwina (eastern outlet of the Szczecin lagoon, $2 - 3\mu\text{M}$), downstream along the coast ($0.5 - 3\mu\text{M}$), and in the deep water of the southwest Bornholm Basin. *Silicate* concentrations were relatively low in the northern bay ($<6\mu\text{M}$), but increased towards the south, with highest concentrations along the coast (up to $15\mu\text{M}$). Again, high concentrations were found at the northeast edge of the investigation area in the deep water column (up to $30\mu\text{M}$).

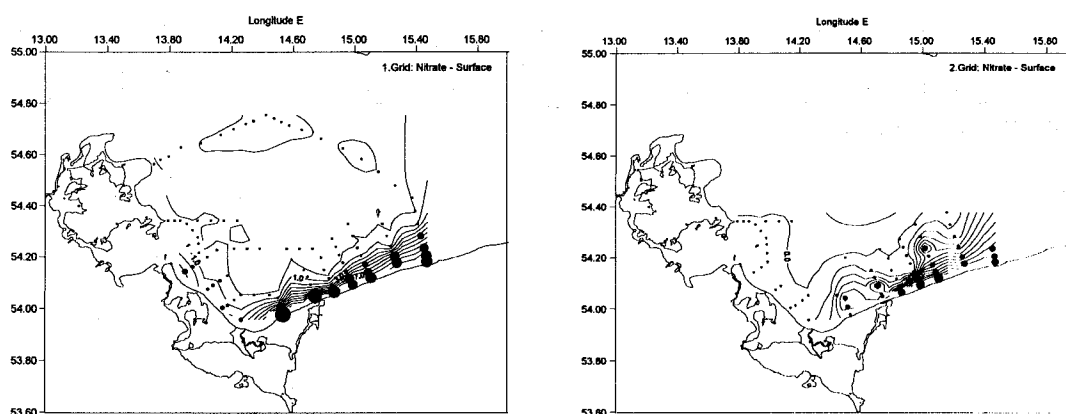


Fig.69 Surface salinity distributions in the Pomeranian Bay during the first (left panel) and the second grid (right panel) in June / July 1994.

3.5.2. Chl.a and phytoplankton distributions analyzed by flow cytometry

Fig.71 shows bay-scale distributions of *Chl.a*. Surface *Chl.a* distributions during the first grid largely correlated with the salinity and nitrate distributions. Highest concentrations were found in a narrow belt along the polish coast (up to $13\mu\text{g dm}^{-3}$) and off Usedom near the Peene mouth ($12.5\mu\text{g dm}^{-3}$), decreasing along the Usedom coast southeast towards the Swine mouth ($4.2\mu\text{g dm}^{-3}$). Open bay concentrations were much lower (around $1\mu\text{g dm}^{-3}$). *Chl.a* distributions at the bottom more or less followed the surface pattern, but values were about half of those at the

surface. Surface concentrations during the second grid very much reflected the different meteorological and hydrographical conditions. Concentrations along the Polish coast and off the Peene mouth had more than halved ($4.9 \mu\text{g dm}^{-3}$ and $4 \mu\text{g dm}^{-3}$, respectively) and were spread towards the open bay; in front of the Swine mouth, the concentration had increased almost by a factor of 5 ($18.8 \mu\text{g dm}^{-3}$). Distribution patterns and concentrations below the surface resembled those of the first grid, indicating that the change of wind direction had only affected the very surface layer at that point.

Flow cytometric analysis allowed the discrimination of six groups, characterised by their respective clusters in the bivariate flow cytometric plots (Fig.70). *Synechococcus* was counted by epifluorescence microscopy, because the flow cytometer was not adjusted appropriately in order to account for this picoplankton group.

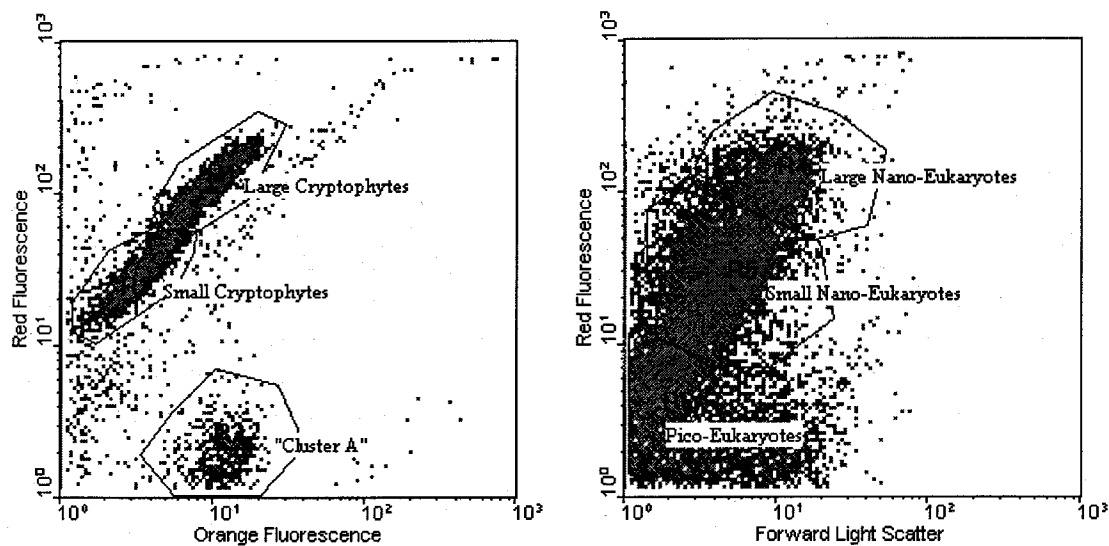


Fig.70 Flow cytometric bivariate plots of phytoplankton in the Pomeranian Bay in June / July 1994 (St.691 (50), 1m, off the Polish coast).

As stated earlier (section 2.5.1.), the clusters defined by identical optical characteristics do not necessarily represent identical taxonomic groups. In fact, a taxonomical classification was not possible for most groups, with three exceptions: two distinct groups of cryptophytes could be identified due to their characteristic orange fluorescence (confirmed by epifluorescence microscopy), and the abundant coccoid cyanobacterium *Synechococcus*, which was counted by epifluorescence microscopy. Four additional phytoplankton clusters were discriminated by the flow cytometer on the base of their red fluorescence and scatter light intensities (see Tab.12). Size fractionation allowed the approximation of cell sizes.

Tab.12 Phytoplankton groups measured by flow cytometry and their approximate cell diameters as estimated by differential size fractionation during June / July 1994 in the Pomeranian Bay.

Phytoplankton Group / Taxon	Approximate Cell Diameter
<i>Synechococcus</i> (counted by epifluorescence microscopy)	1-2 μ m
Pico-Eukaryotes	1-2 μ m
Small Nano-Eukaryotes	2-5 μ m
Large Nano-Eukaryotes	5-10 μ m
Small Cryptophytes	~5 μ m
Large Cryptophytes	5-10 μ m
"Cluster A"	5-10 μ m

Synechococcus showed high concentrations throughout the entire bay during both grids (Fig.72), with highest numbers (up to 1,500,000 cm⁻³) in the central parts of the bay. *Synechococcus* numbers were inversely correlated with the narrow band high chlorophyll concentrations. The *pico-eukaryotes* (Fig.73) showed high concentrations north of Usedom (up to 11,023 cm⁻³), decreasing towards the southeast. This pattern prevailed all through the water column (1st grid). Concentrations during the 2nd grid were much lower (up to 3,557 cm⁻³), with slightly higher values along the polish coast. The *small nano-eukaryotes* (Fig.74) showed high concentrations along the entire coastline during the 1st grid (up to 2,533 cm⁻³), with highest surface values in the east, and depth values in the west. However, during the 2nd grid, concentrations near the coast had increased, especially at the Swine mouth (3,751 cm⁻³) and at the south eastern part of the grid (up to 4,611 cm⁻³). Concentrations of the *large nano-eukaryotes* (Fig.75) were generally low and concentrated along the coast during the 1st grid (up to 2,092 cm⁻³). Bottom water values, however, were more evenly distributed. Values were still lower during the 2nd grid, with one exception: surface values in front of the Swine outlet were about an order of magnitude higher than the values elsewhere (11,641 cm⁻³). The *small cryptophytes* (Fig.76) showed highest concentrations along the coast (up to 2,055 cm⁻³), with a preponderance at the polish coast (1st grid). Concentrations there remained high below the surface, but shifted away from the coast slightly. Surface concentrations during the 2nd grid prevailed at the polish coast, but were more or less evenly distributed along the entire coastline below the surface. The *large cryptophytes* (Fig.77) were also concentrated along the coast, with highest concentrations at the western side (off Usedom) during the 1st grid (up to 4,197 cm⁻³), and less but more evenly distributed below the surface. During the 2nd grid, concentrations had further decreased all through the water column (up to 1,173 cm⁻³). The unidentified *Cluster A* (Fig.78) was characterized by a combination of strong orange and weak red fluorescence. Highest numbers were found along the Usedom coast during the first grid (up to 1,451 cm⁻³), with concentrations decreasing dramatically towards the open bay. During the second drift, overall concentrations were much lower, with elevated numbers along the polish coast (293 cm⁻³). For all phytoplankton groups except for *Synechococcus*, open bay concentrations (i.e. north of about 54° 30') were one to two orders of magnitude lower than those close to the coast.

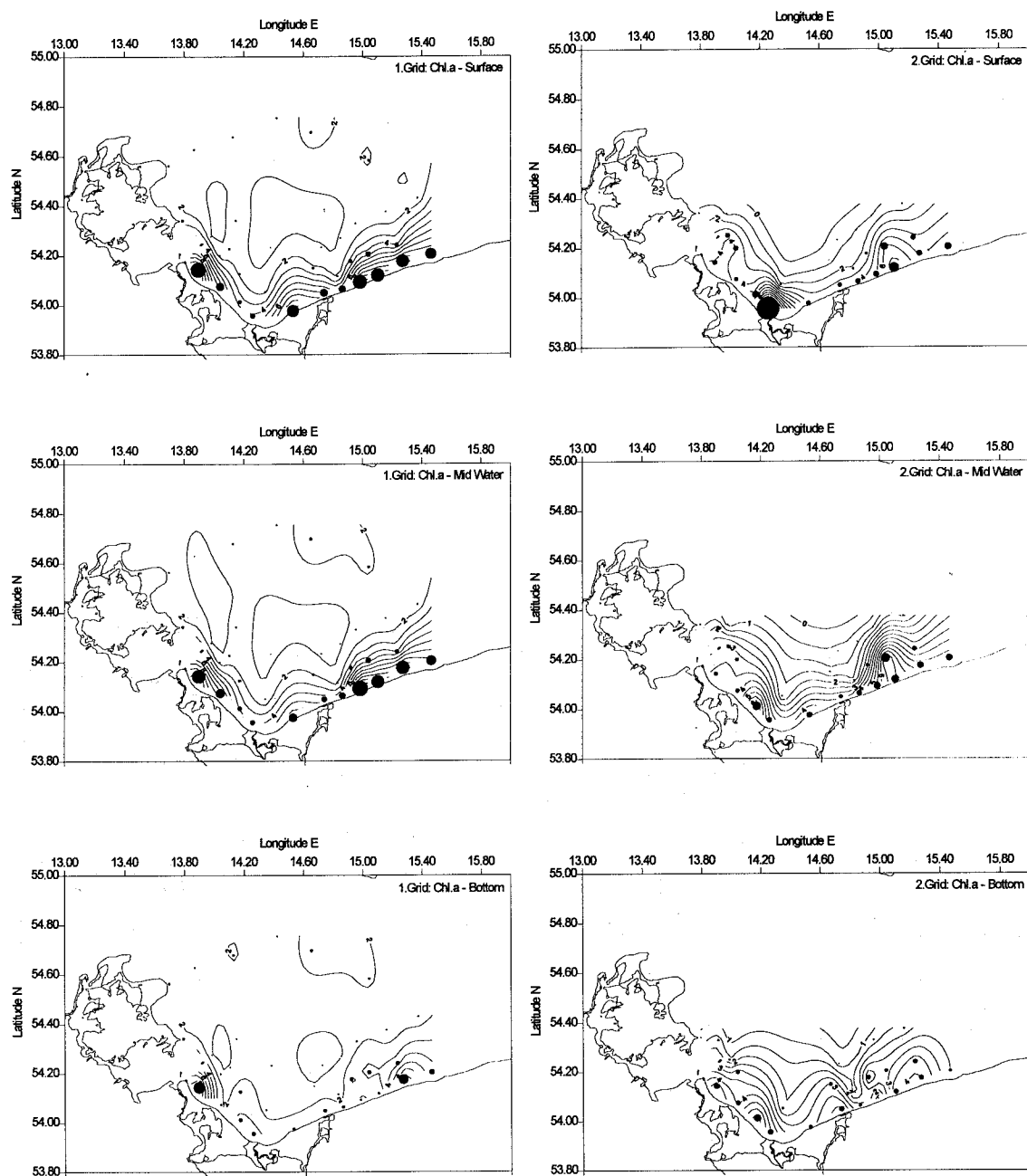


Fig.71 Distribution of Chl.a in the Pomeranian Bay during June / July 1994.
 Left panels: first grid, right panels: second grid. Upper, middle and lower figures refer to surface, mid water, and bottom values, respectively.

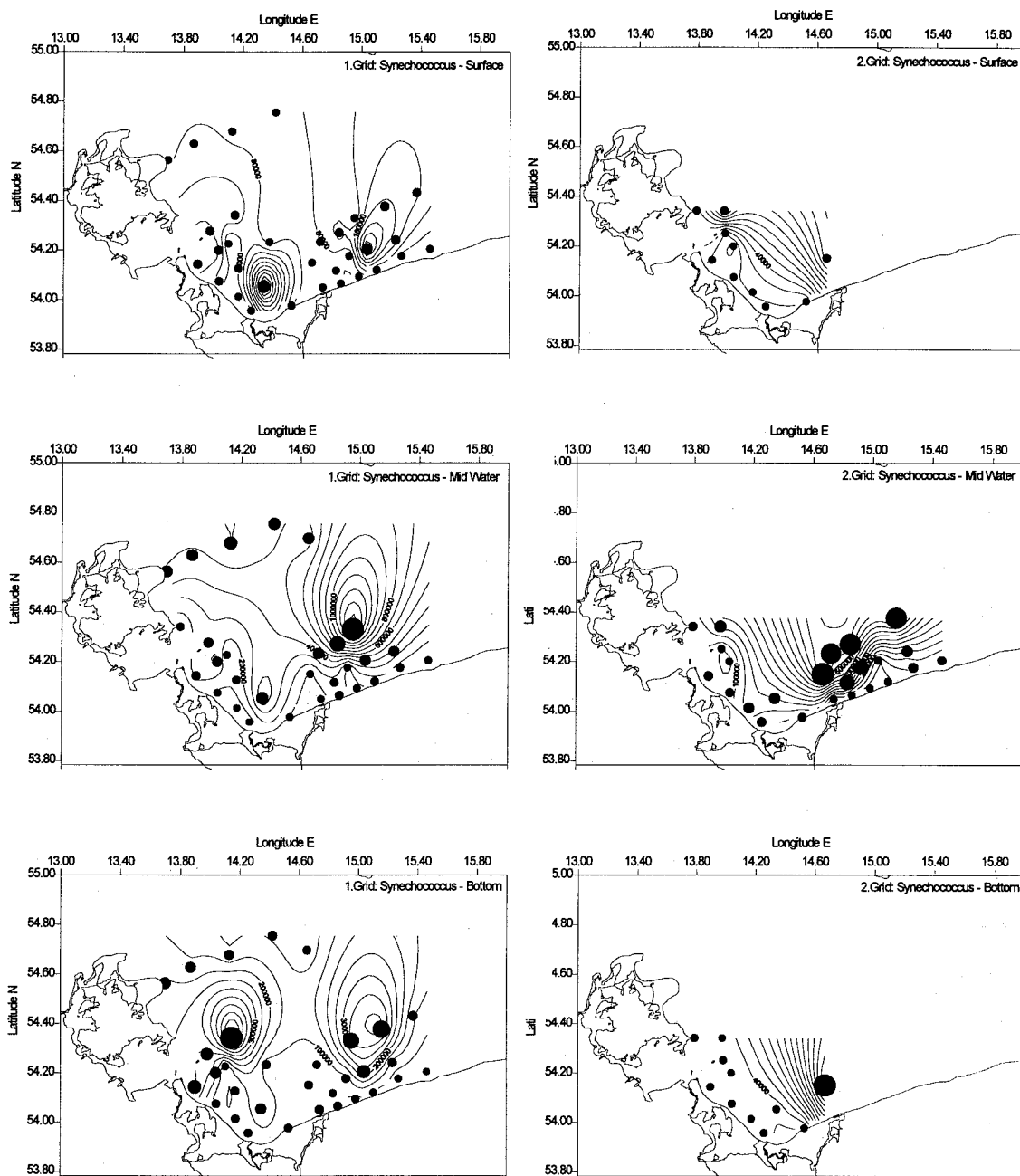


Fig.72 Distribution of *Synechococcus* in the Pomeranian Bay during June / July 1994. Left panels: first grid, right panels: second grid. Upper, middle and lower figures refer to surface, mid water, and bottom values, respectively.

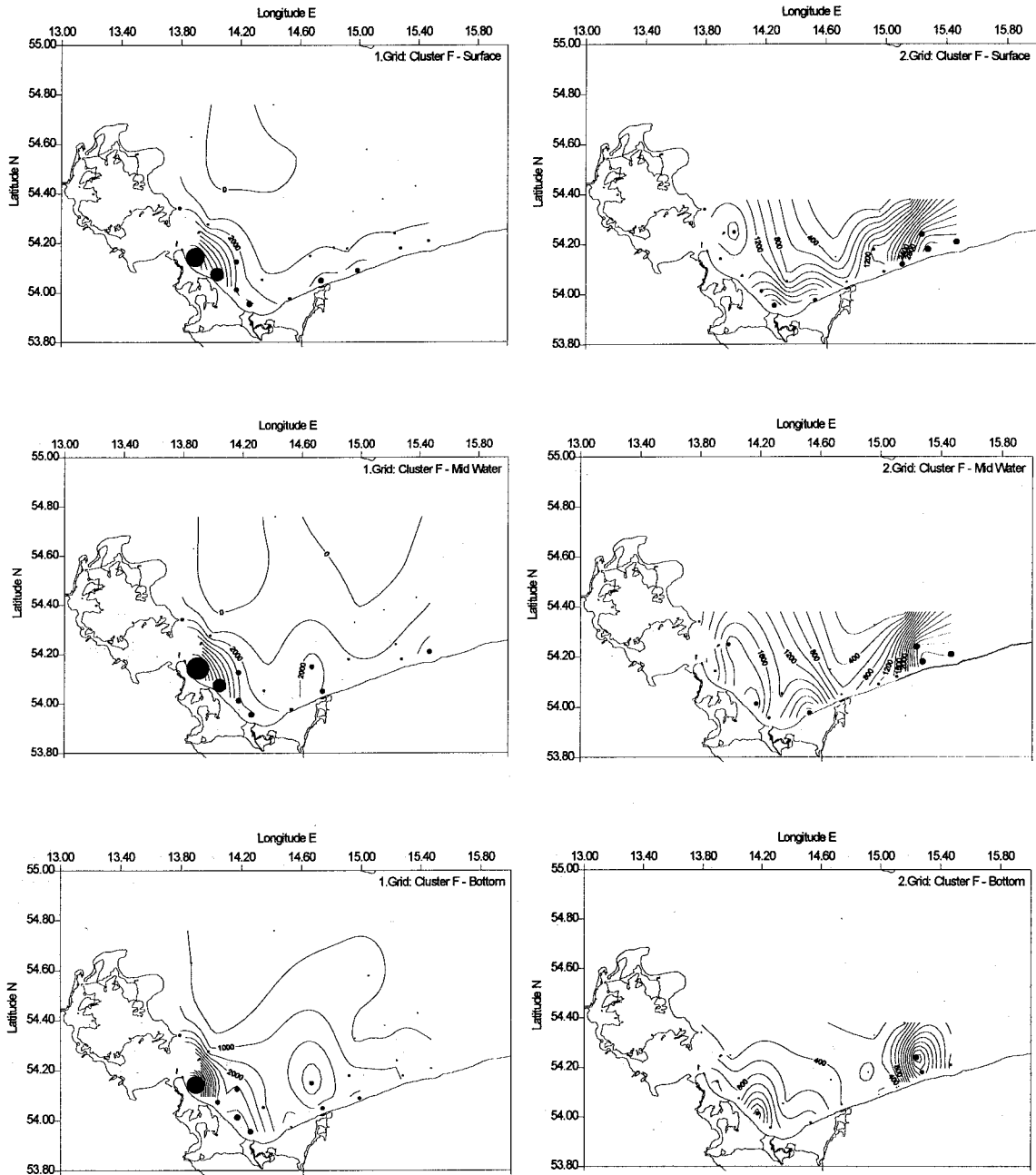


Fig.73 Distribution of pico-eukaryotes in the Pomeranian Bay during June / July 1994. Left panels: first grid, right panels: second grid. Upper, middle and lower figures refer to surface, mid water, and bottom values, respectively.

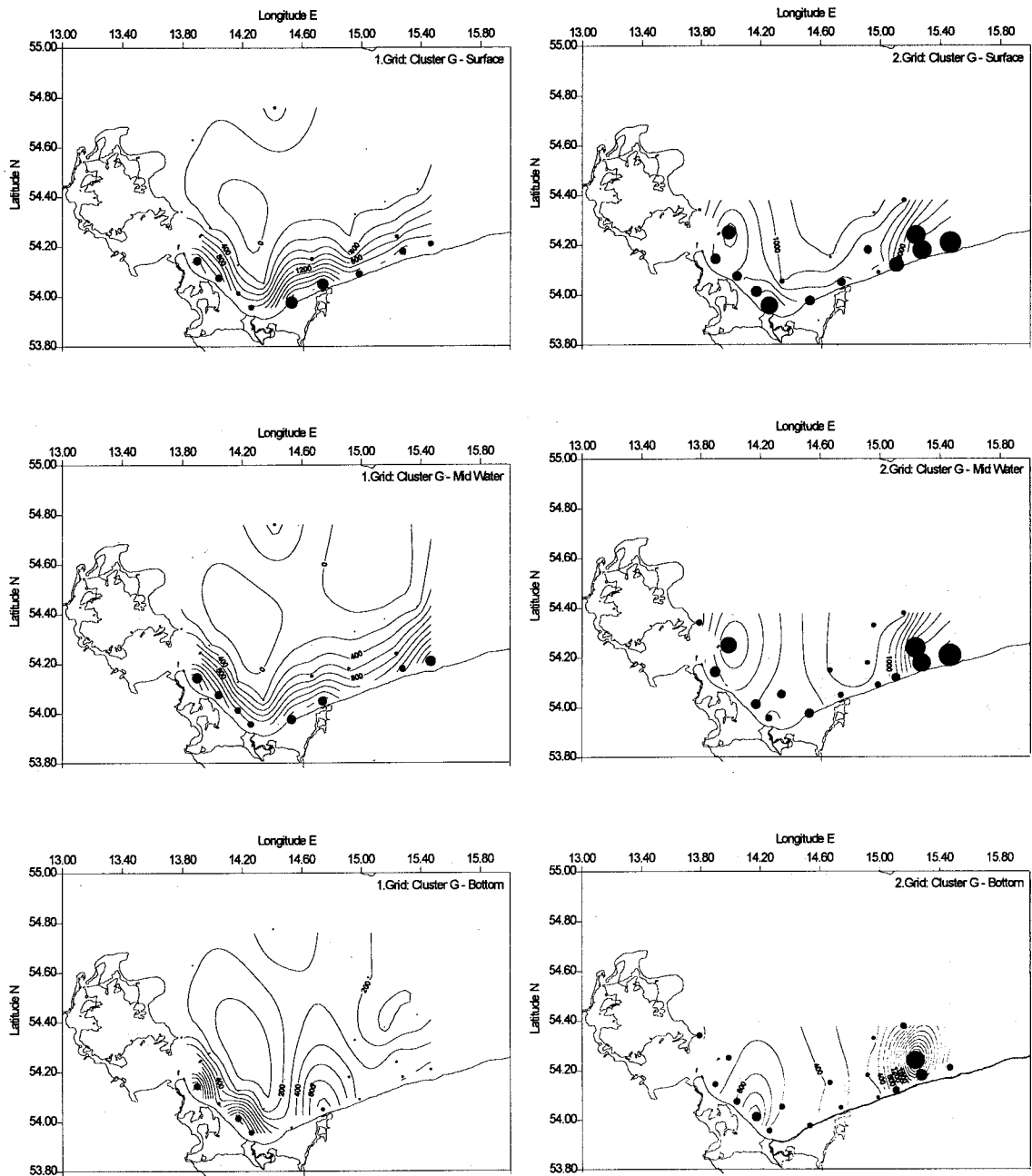


Fig.74 Distribution of small nano-eukaryotes in the Pomeranian Bay during June / July 1994. Left panels: first grid, right panels: second grid. Upper, middle and lower figures refer to surface, mid water, and bottom values, respectively.

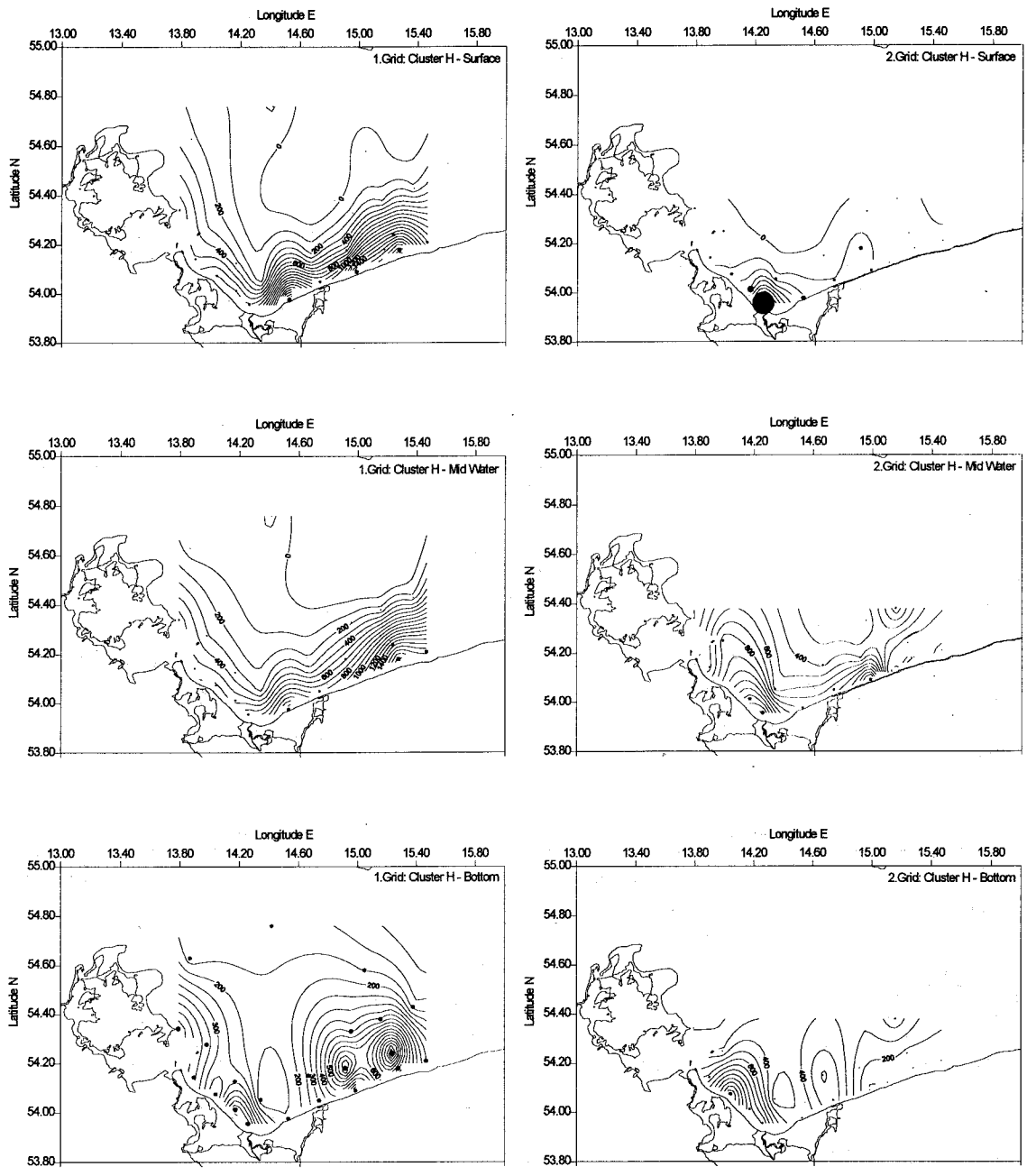


Fig.75 Distribution of large nano-eukaryotes in the Pomeranian Bay during June / July 1994. Left panels: first grid, right panels: second grid. Upper, middle and lower figures refer to surface, mid water, and bottom values, respectively.

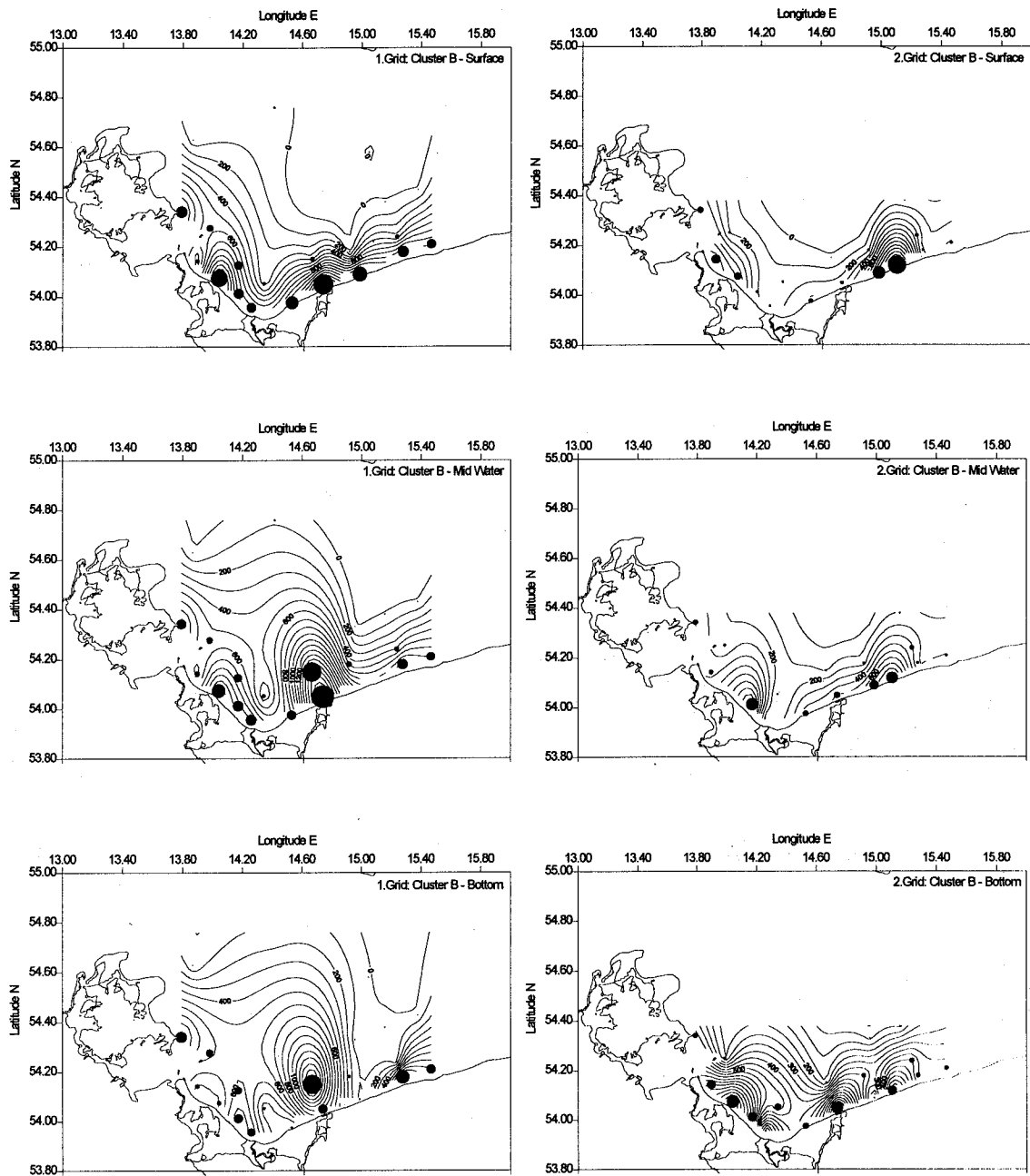


Fig.76 Distribution of small cryptophytes in the Pomeranian Bay during June / July 1994. Left panels: first grid, right panels: second grid. Upper, middle and lower figures refer to surface, mid water, and bottom values, respectively.

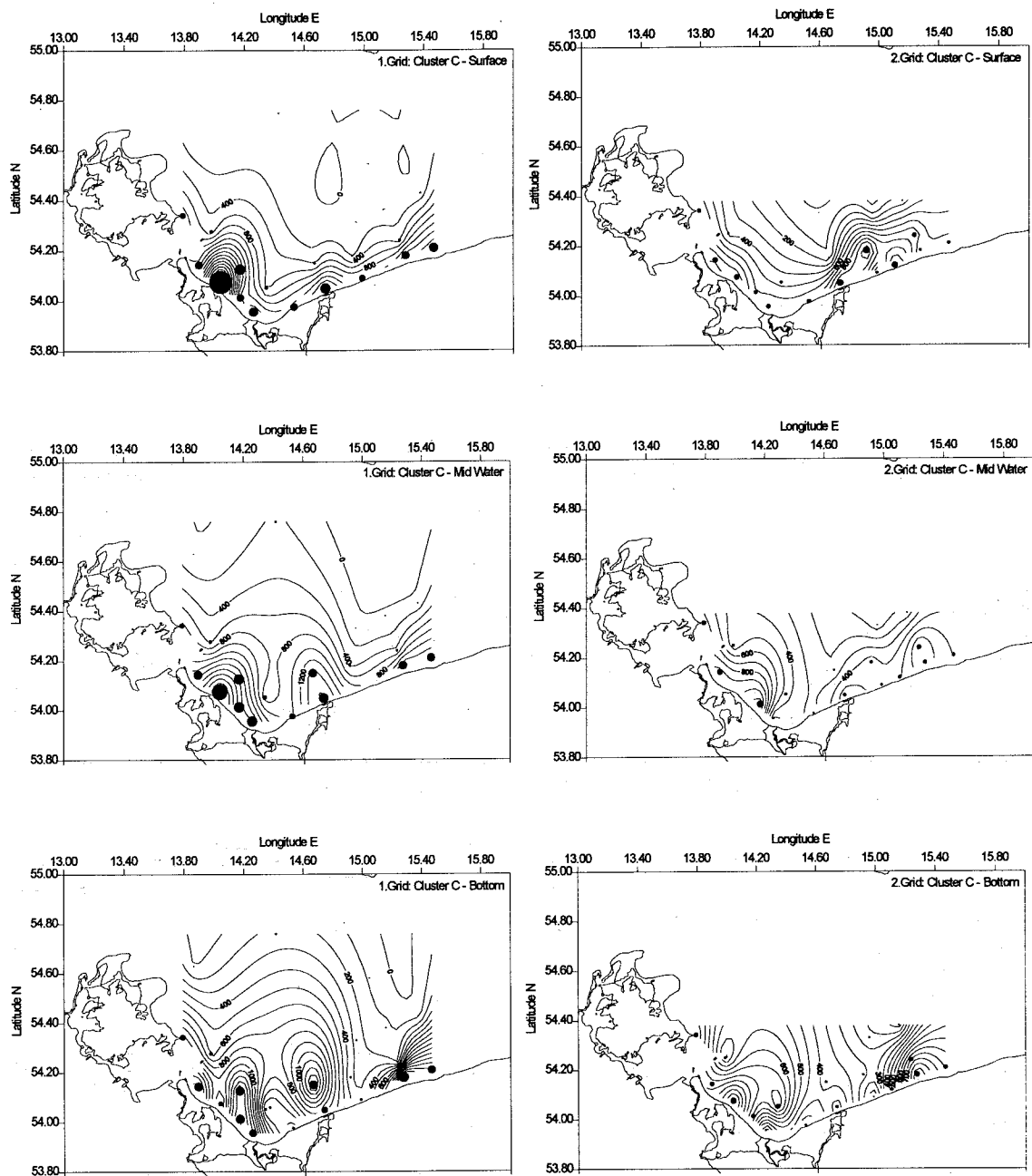


Fig.77 Distribution of large cryptophytes in the Pomeranian Bay during June / July 1994. Left panels: first grid, right panels: second grid. Upper, middle and lower figures refer to surface, mid water, and bottom values, respectively.

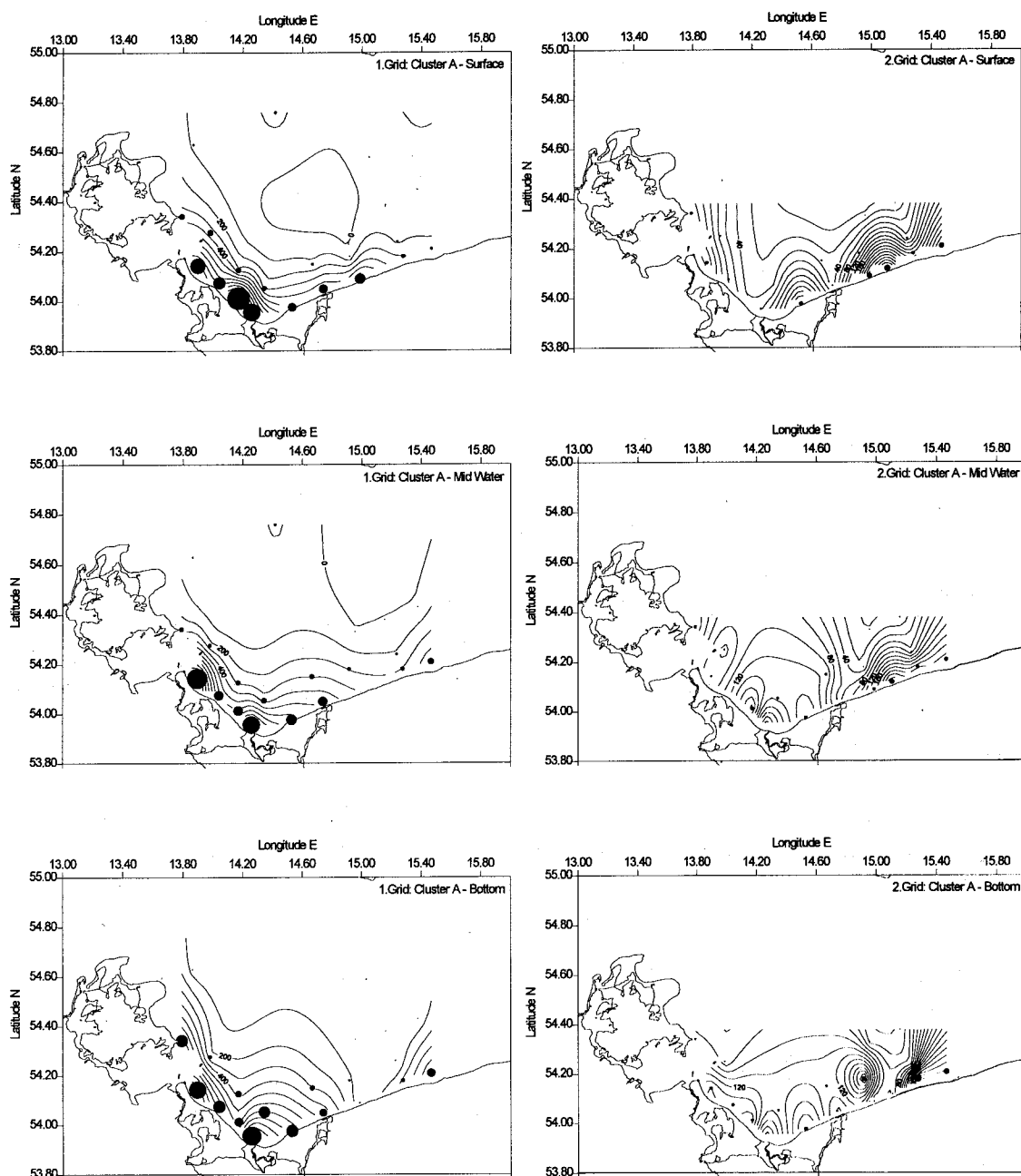


Fig.78 Distribution of "Cluster A" in the Pomeranian Bay during June / July 1994. Left panels: first grid, right panels: second grid. Upper, middle and lower figures refer to surface, mid water, and bottom values, respectively.

3.5.3. Protozoan distributions

Protozoa were counted only during the first grid at 5m. Fig.79 - 81 show spatial distributions of protozoan numbers and carbon biomasses. Five ciliate taxa were distinguished (*Didinium sp.*, *Mesodinium rubrum*, *Lohmaniella sp.*, unspecified strombiid ciliates and holotrichs), as well as the heterotroph silicoflagellate *Ebria tripartita* and heterotrophic nanoflagellates (Fig.79 - 81). Highest numbers and biomasses were again found close to the coastline, but as for the phytoplankton, different groups were distributed differently. *E. tripartita* (Fig.80) showed highest numbers ($10,872 \text{ dm}^{-3}$) and carbon biomasses ($17.5 \mu\text{g dm}^{-3}$) northeast of Usedom, close to the Greifswald Lagoon and the Peene outlet. Abundances and biomass of strombiid ciliates (Fig.80) were about evenly distributed between the eastern and western coast (up to $39,707 \text{ dm}^{-3}$, or $35.62 \mu\text{g dm}^{-3}$). *Lohmaniella sp.* (Fig.80), as the strombiids a member of the oligotrich ciliates, was primarily found at the eastern coast (up to $26,944 \text{ dm}^{-3}$, or $29.97 \mu\text{g dm}^{-3}$), as was *Didinium sp.* (Fig.81, up to $49,630 \text{ dm}^{-3}$, or $12.52 \mu\text{g dm}^{-3}$). Holotrich ciliates (Fig.81) were also most concentrated in the eastern half of the bay (up to $11,581 \text{ dm}^{-3}$, or $12.3 \mu\text{g dm}^{-3}$), but not so closely bound to the coast as the other groups. Abundance and biomass of the obligate autotroph ciliate *Mesodinium rubrum* (Fig.81) was highest at the northeast end of the bay ($8,863 \text{ dm}^{-3}$, or $4.3 \mu\text{g dm}^{-3}$), close to the Bornholm Basin. Coastal abundances were generally much lower ($<1,000 \text{ dm}^{-3}$), except for elevated values off Rügen and Usedom.

Total ciliate numbers and biomasses (Fig.79) concentrated along the polish coast (up to $175,841 \text{ dm}^{-3}$, or $80.82 \mu\text{g dm}^{-3}$), and, to a lesser degree, at the Usedom coast (up to $89,834 \text{ dm}^{-3}$, or $37 \mu\text{g dm}^{-3}$). HNF numbers and biomasses (Fig.79) were highest in the southeast part of the Bay (up to $11,909 \text{ cm}^{-3}$, or $58.52 \mu\text{g dm}^{-3}$). Total protozoan carbon (as the sum of ciliate, *Ebria* and HNF carbon, Fig.79) ranged from $7.69 \mu\text{g dm}^{-3}$ at the northernmost station to $121.73 \mu\text{g dm}^{-3}$ off the polish coast.

Size distributions of HNF and ciliates are shown in Fig.82. HNF $<5\mu\text{m}$ make up the bulk of the HNF numbers, with larger individuals being important only in terms of biomass. Ciliates $<20\mu\text{m}$ were most abundant throughout the bay.

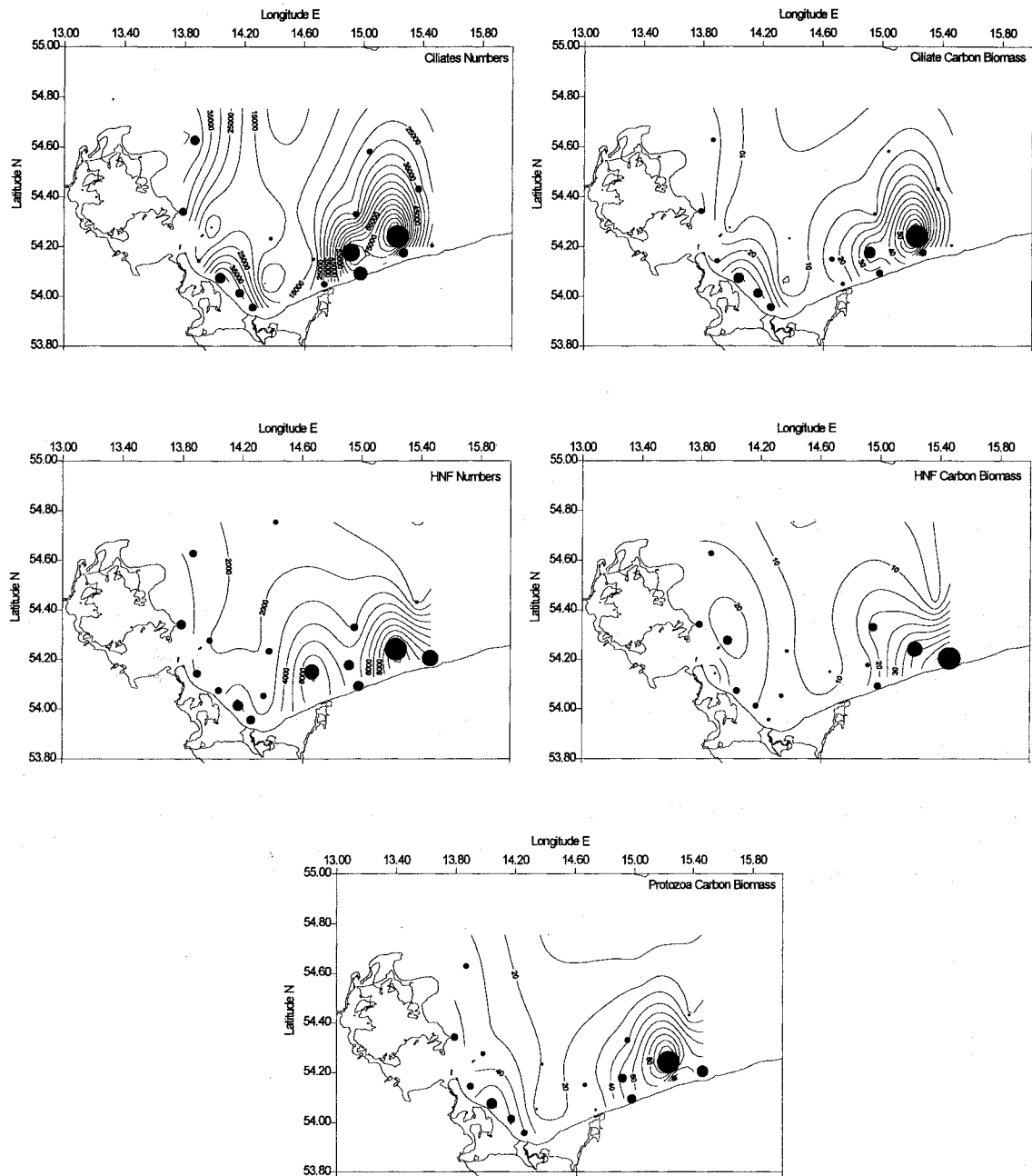


Fig.79 Distribution of protozoa in the Pomeranian Bay during June / July 1994.
 Left panels: cell concentrations, right panels: carbon biomasses. Upper panels: Ciliates;
 middle panels: HNF; lower panel: total protozoan carbon biomass.

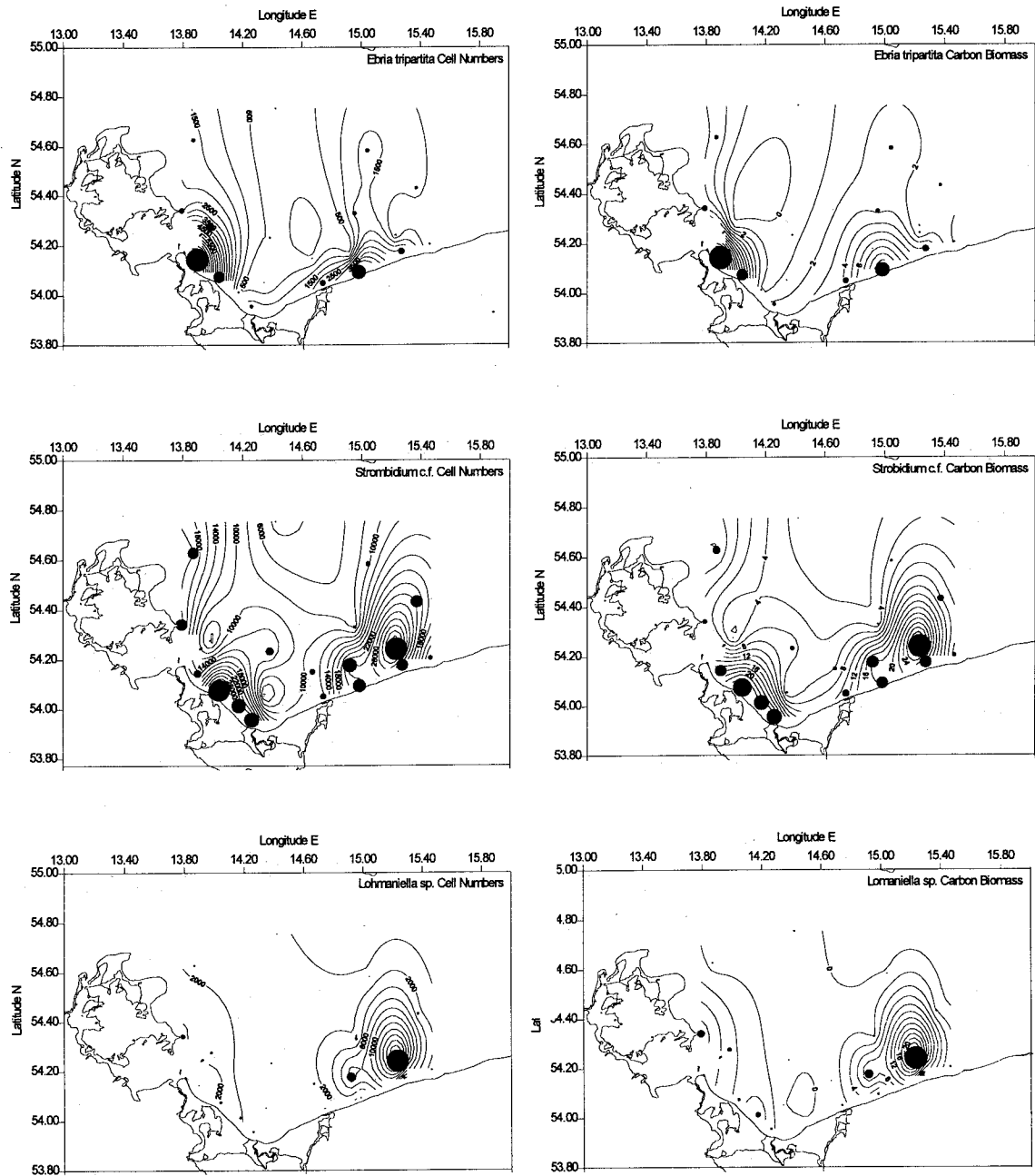


Fig.80 Distribution of protozoa in the Pomeranian Bay during June / July 1994.
 Left panels: cell concentrations, right panels: carbon biomasses. Upper panels: *Ebria tripartita*; middle panels: *Strombidium sp. c.f.*; lower panels: *Lohmaniella sp. c.f.*.

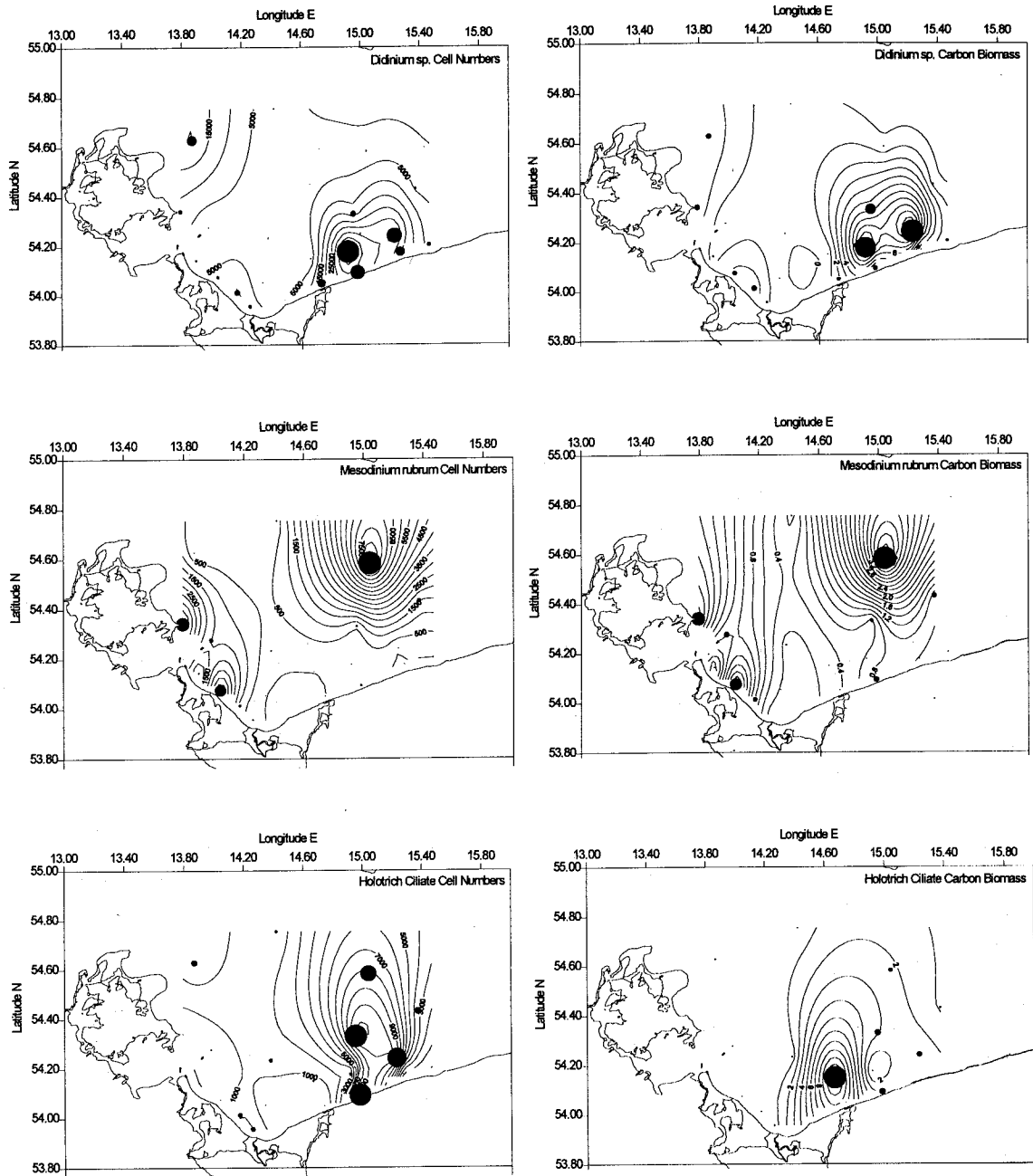


Fig.81 Distribution of protozoa in the Pomeranian Bay during June / July 1994.
 Left panels: cell concentrations, right panels: carbon biomasses. Upper panels:
Didinium sp. c.f.; middle panels: *Mesodinium rubrum*; lower panels: holotrich ciliates.

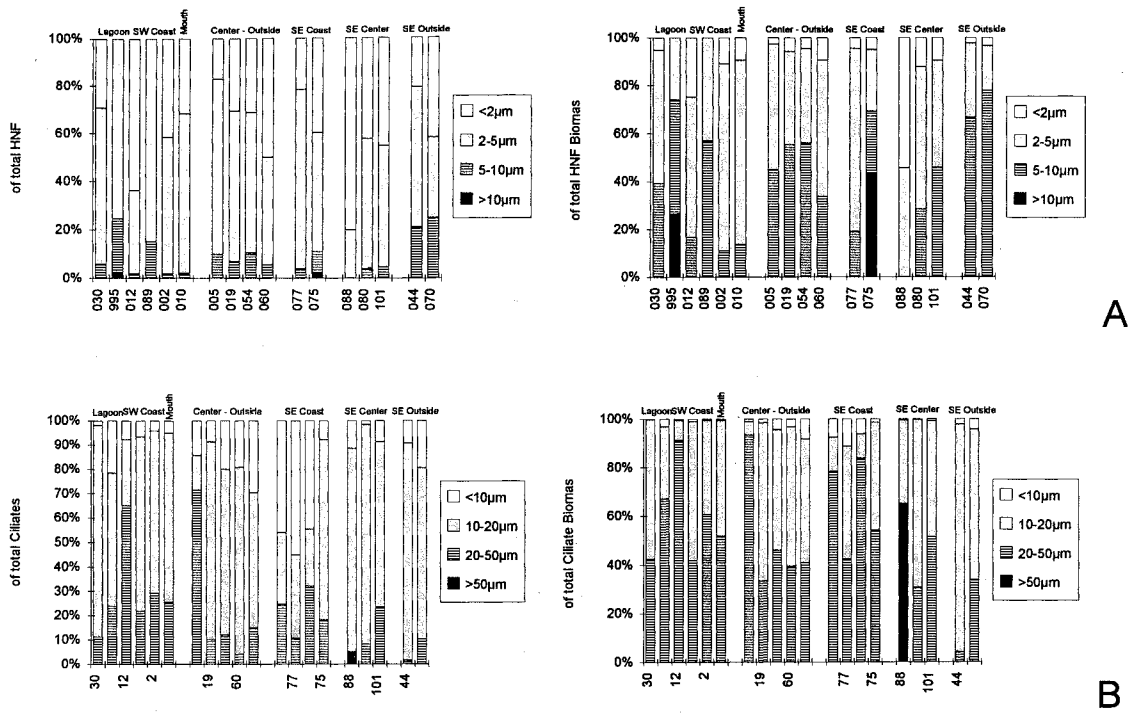


Fig.82 Size class distributions of protozoan cells (left), and carbon biomass (right) during Grid 1 (5m) in the Pomeranian Bay in June / July 1994. A: HNF, B: Ciliates.

The relative proportion of the respective protozoan groups to total carbon is depicted in Fig.83. Ciliates made up the bulk of protozoan carbon at stations west of the Swina mouth, and to the east off the polish coast. At stations in the central or northern part of the bay, HNF generally predominated.

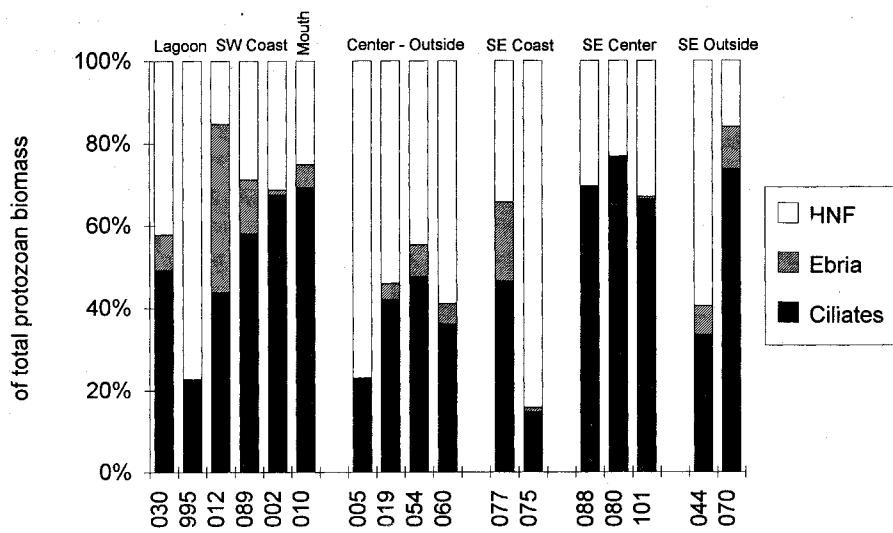


Fig.83 Protozoan distribution during Grid 1 (5m) in the Pomeranian Bay in June / July 1994.

4. Discussion

The following discussion consists of three parts. The methodological discussion includes a definition of some basic terms used frequently in aquatic ecology, and of some specific terms used in this study, followed by a critical discussion of the serial dilution method, and other methods used in this study to estimate grazing by microzooplankton. In the second part I will compare ultraphytoplankton and protozoan distributions and standing stocks and their interactions in the different investigation areas. Finally, I will try to evolve a general picture of the structure of the pelagic food web in environments of different trophic status.

4.1. Methodological considerations

4.1.1. Terminology

The term *protozoa* rather loosely paraphrases a group of protists that are considered to be strictly heterotrophic. Although modern systematic terminology does not use this term anymore in favour of the more general term *protists* (encompassing all single celled organisms, regardless of their feeding mode, SLEIGH 1991), I will use it nevertheless throughout this work in an ecological context to discriminate the strictly heterotrophic protists from mixotrophic and strictly autotrophic groups (SIEBURTH and ESTEP 1985).

SIEBURTH et al. (1978) classify the pelagic community operationally based on size, resulting in six main groups: the *picoplankton* (0.2 - 2 μ m), the *nanoplankton* (2 - 20 μ m), the *microplankton* (20 - 200 μ m), the *mesoplankton* (200 - 2,000 μ m), the *macroplankton* (2 - 20mm), and the *megaplankton* (>20mm). However, this coarse classification on the basis on size appears to be too restrictive, when applied to pico- and small nanoplankton. This is because the very small *nanoplankton* (i.e. 3 - 5 μ m), together with the *picoplankton*, predominantly contribute to autotrophic communities of most ecosystems. In this respect, some authors have used the term *ultraplankton* for the size group <5 μ m, whenever the term *picoplankton* appeared to be too restrictive. It will be also used here, as the approximate upper size limit for phytoplankton accessible by the flow cytometers used in this study used was 5 μ m.

Although the classification of plankton based on size ignores the rich taxonomic diversity within the respective size groups (SIEBURTH and ESTEP 1985), it has been widely accepted due to its simplicity and handiness. However, this terminology is inappropriate in a systematic context, given the fact that the *protozoa* belong to the kingdom of protists, and consequently are not animals, as implied by the prefix *zoa-*. As the term *microzooplankton* describes heterotrophic organisms in the size range <200 μ m, it not only includes the protozoa following the above definition, but also a variety of metazoan organisms, spanning from crustacean larval stages (i.e. nauplii) to small crustacean adults, rotifers, chaetognats, and fish larvae. On the other hand, some protozoa such as the radiolaria and the foraminifera may surpass the size range defined by the microzooplankton. The terms *protozoa* and *microzooplankton* will both be used within the scope of this work: standing stocks of *protozoa* were determined microscopically (ciliates, heterotrophic dino- and silicoflagellates, and heterotrophic nanoflagellates), but the grazer community in the dilution experiments, by definition, consisted of *microzooplankton*. The terms *grazing* (traditionally used for herbivorous activities, i.e. feeding on phytoplankton) and *predation* (for carnivory, i.e. feeding on animals, resp. heterotrophic organisms) will be used synonymously within this context, when applied to herbivory and bacterivory.

The two flow cytometers used in this study allowed the discrimination of different ultraphytoplankton groups, which are defined and described in the respective sections (section 3.2.4., Fig.28; section 3.3.2, Fig.40; section 3.5.2., Fig.70). However, it is noteworthy to mention here that the two machines really measured overlapping portions of the ultraphytoplankton

community: in the Arabian Sea, the COULTER was able to measure *Prochlorococcus* (mean cell diameter $\sim 0.6\mu\text{m}$), but cells larger than 2 - $3\mu\text{m}$ were off-scale, and thus could not be measured (Fig.28). In the case of the PARTEC, the situation was vice versa: signals of the small and dim *Synechococcus* (mean cell diameter $\sim 1\mu\text{m}$) partly overlapped with electronic background noise, and could not be properly quantified. This machine, however, allowed the measurement of the larger ultraphytoplankton (up to a mean cell diameter of $\sim 5\mu\text{m}$, Fig.40, 70). As a taxonomical classification of the eukaryotic ultraphytoplankton groups was not possible (with the exception of the cryptophytes in the Pomeranian Bay 1994, section 3.5.2.), they were denoted according to SIEBURTH et al. (1978) as pico- ($<2\mu\text{m}$), and small and large nano-eukaryotes (2 - $5\mu\text{m}$). All groups together will be referred to as ultraphytoplankton, as argued above.

However, where do these small algae belong taxonomically? As discussed above, the inability to account for taxonomic groups is a characteristic attribute of flow cytometry (except for those clusters sufficiently defined by their optical properties, such as *Prochlorococcus* due to its small size and the absence of orange fluorescence, and *Synechococcus* due to its small size and the presence of orange fluorescence, when excited with blue light). However, investigators using routine microscopical methods generally refer to this phytoplankton size group uniformly as "monads", " μ -Flagellates", or "ANF" (Autotrophic NanoFlagellates). Flow cytometry can differentiate and quantify ultraphytoplankton quicker and more precisely than microscopical methods, an exception being detailed taxonomical surveys using epifluorescence or electron microscopy (i.e. THRONDSSEN 1993). With the help of HPLC pigment analysis (Arabian Sea cruises: VELDHUIS et al. 1994; Baltic Sea cruises: MEYER-HARMS 1996), several taxonomic groups could be identified in the water column. In the Arabian Sea, divinyl-chlorophyll a and b confirmed the presence of *Prochlorococcus* (CHISHOLM et al. 1992), and different chlorophyll c derivatives together with 19-hexanoyl-oxy-fucoanthin pointed to the presence of prymnesiophyceae. Further pigment fingerprints demonstrated the presence of *Micromonas pusilla* - type flagellates (prasinophyceae), and also members of the newly classified pelagophyceae (ANDERSEN et al. 1993). In the Baltic Sea, lutein (representing chlorophyceae), 19-hexanoyl-oxy-fucoanthin and 19-butanoyl-oxy-fucoanthin (both for prymnesiophyceae), prasinoxanthin (for prasinophyceae), and alloxanthin (for cryptophyceae) also confirmed the presence of various small flagellates. All these taxonomical groups are well known representatives of the phytoplankton community $<5\mu\text{m}$, frequently found in neritic and oceanic environments (TOMAS 1993).

4.1.2. A critique of the serial dilution technique

This method to estimate the grazing impact on phytoplankton was introduced to aquatic ecology by LANDRY and HASSETT in 1982. Since that time it has been used extensively by various investigators in different regions, ranging from (sub-) polar (PARANJAPPE 1987, GIFFORD 1988, ANTIA 1991, LANDRY et al. 1993, REITMEIER 1994, BURKILL et al. 1995) and temperate (CAMPBELL and CARPENTER 1986, VERITY 1986, GALLEGOS 1989, BURKILL et al. 1993b), to subtropical and tropical environments (LANDRY et al. 1984, BURKILL et al. 1993c, LANDRY et al. 1995a, LANDRY et al. 1995b). Due to the simple approach and low requirements for the experimental equipment, it was agreed upon as the method of choice for microzooplankton herbivory in the JGOFS protocols (1994), acting as a guideline for the coordinated international use of methods. Major advantages of the method are the simultaneous estimation of both specific growth (μ) and grazing coefficients (g) of different components of the phytoplankton community (provided the phytoplankton is appropriately analyzed, see below), the comparably minor mechanical handling of the organisms, and the simple execution. There are, however, a number of critical points that may bias the interpretation of the results. Some of these restrictions were already considered in the original paper (LANDRY and HASSETT 1982), while others have been pointed out by various authors throughout the following years.

Critical assumptions of the method

The method is based upon a number of restrictive assumptions. (1) Growth and grazing coefficients are computed using the exponential growth model, which consequently must be applicable to the experimental conditions. Although this may not always be the case (TRENKEL 1992), it is nevertheless assumed by most investigators. (2) The specific phytoplankton growth rate (i.e. the division rate of an individual phytoplankton cell) must be density independent, i.e. the same in all dilution steps, and (3) the community grazing rate must be linearly dependent on the predator-prey encounter rate (proportional to the dilution factor), implying that (a) the individual ingestion rate of a grazer organism must be unaffected by phytoplankton density, and (b) grazer abundance must be constant over the incubation period in all dilutions. Assumptions (1) and (2) call for the sufficient and equal supply of light and nutrients and other dissolved growth factors in all dilution steps. To account for this problem, most investigators have added nutrients (LANDRY and HASSETT 1982, PARANJAPE 1987, BURKILL et al. 1987, GALLEGOS 1989, LANDRY et al. 1995a, LANDRY et al. 1995b) or nutrient-rich deep water (BURKILL et al. 1993b, this work), when they were assumed to be limiting. However, the addition of nutrients might harm fragile ciliates (LANDRY and HASSETT 1982, GIFFORD 1988), and it might also bias the interpretation of results due to artificially enhanced phytoplankton growth rates by surge uptake. Any nutrient limitation would have an effect first in the undiluted bottles because the phytoplankton density is highest there and nutrients will be used up most rapidly. This would result in an exaggerated slope of the regression line and an overestimation of both g and μ (ANTIA 1991). Treatments without nutrient additions should in any case be co-incubated to ensure the determination of the real, undisturbed *in situ* phytoplankton growth rate (PARANJAPE 1988, LANDRY et al. 1995a, LANDRY et al. 1995b, this work). Some experimentators have used dialysis bags (LANDRY and HASSETT 1982, VERITY 1986) or diffusion chambers (LANDRY et al. 1984) to overcome this problem by allowing ambient (recycled) nutrients to diffuse into the experimental containers. The absence of inorganic nitrogen compounds (nitrate, nitrite, ammonium), however, does not necessarily imply a nitrogen limitation. Amino acids and urea have been shown to support phytoplankton growth (EPPLEY et al. 1971, WHEELER et al. 1974, TURLEY 1986), but they are rarely measured. Moreover, nutrient recycling in the different dilutions may be quite complex (ANDERSEN et al. 1991). It can be expected to be most important in the undiluted treatments, with most prey and remineralising grazers present. With increasing dilution of grazers and their "substrate" (the prey), the importance of remineralisation decreases. On the other hand, this effect might be partly relieved, as in high dilutions fewer phytoplankton cells compete for the available nutrients, and the grazing activity in high dilutions may be reduced not only on phytoplankton, but also on small grazers (and potential remineralisers).

Although phytoplankton is generally assumed to grow exponentially (under the conditions described above), this might not always be the case. TRENKEL (1992) simulated cases in which the exponential growth model does not apply. In modelling experiments, she was able to show that with ceasing exponential growth and transition to the stationary phase, both grazing and growth rates are overestimated, when calculated according to the exponential model. Moreover, the linearity of the regression in the graphical dilution plots (fraction undiluted seawater vs. apparent phytoplankton growth rate, Fig.5) is not affected, meaning that a deviation from the exponential growth model cannot be detected in the plots.

The assumption that microzooplankton density and individual ingestion rate remain constant in all dilutions during the incubation period is difficult to verify on a routine basis, if not impossible (LANDRY 1993). Nevertheless, GIFFORD (1988) reports on differential losses of aloricate ciliates following the dilution procedure. Furthermore, it is known that most protozoan grazers may grow as fast as their prey, and they may also represent prey for larger predators; to what extent the two latter effects cancel one another, is not known.

The question whether the functional feeding response of the grazer (i.e. the ingestion rate as a function of food concentration) may always be assumed to be linear over the range of dilutions (as implied by the theory of the dilution method) was examined experimentally by GIFFORD (1988) and GALLEGOS (1989), and theoretically by GALLEGOS (1989) and EVANS and PARANJAPE (1992). The authors discuss the implications of nonlinear feeding kinetics on the interpretation of dilution results. If the functional response curve of the grazer is nonlinear over the food range encountered in the experiments, the estimation of both growth and grazing coefficients may be biased.

GIFFORD (1988) describes two scenarios: saturation feeding and threshold feeding. In both cases the individual ingestion rate is assumed to cease, either when the ambient food concentration is above a certain saturation level above which the feeding activity of the grazer is hampered (*saturation feeding*, e.g. by the biochemical constraint of digestion rates in food vacuoles, CAPRIULO and DEGNAN 1991), or when the ambient food concentration is less than a threshold level below which the feeding activity also ceases (*threshold feeding*). If saturation feeding occurs (at high ambient food concentrations), the apparent phytoplankton growth rate k will be unaffected by low dilution factors; it will increase only when food concentrations are sufficiently diluted to values below the saturating level. To obtain satisfying estimates for μ and g under these circumstances, GALLEGOS (1989) modified the Landry and Hassett - calculation to the effect that he computed μ from the two most dilute samples, where saturation effects could be excluded. g is then simply deduced from $k = \mu - g$ ("3-point-method"). He emphasises the need for very high dilutions (e.g. 15% and 5% of undiluted water), wherever saturation feeding can be expected. Conversely, if threshold feeding occurs, k will increase with increasing dilution up to the point where food becomes too scarce, and grazers stop their feeding activity. At higher dilutions, k will not increase any further. In this case, the y-intercept of the level part of the curve (i.e. where k does not increase with increasing dilution factor) represents μ (GIFFORD 1988).

While GIFFORD (1988) and GALLEGOS (1989) attempt to use two respective linear portions of the curve in order to account for best values for μ and g , EVANS and PARANJAPE (1992) make the point that, in most cases, natural feeding responses may not be appropriately described by linear functions, and that they are merely exceptions from the non-linear rule. They argue that Gallegos' "3-point-method", in attempting to cope with saturated feeding kinetics by using a linear model at very high dilutions, may not account for non-linear feeding kinetics at and even below these high dilutions. The authors computed two different non-linear models, and come to the conclusion that "...we must accept the possibility of curvature below the most dilute sample..., but we cannot resolve the issue how to estimate it..., we merely call for attention to its importance and the need for more work", and "...we have no magic answer and must face the fact that dilution experiments have not brought us as far as had been hoped" (EVANS and PARANJAPE 1992).

A new approach

Incited by these discouraging conclusions, LANDRY et al. (1995a) came up with a partial answer in form of a methodological supplement to the technique. By adding FLB (fluorescently labeled bacteria, SHERR et al. 1987) in trace amounts to every incubation bottle, and measuring their disappearance during the course of the incubation, the authors substituted the dilution factor (as proxy for the reduced grazing pressure with increasing dilution) with a measured indicator for grazing pressure in the different dilutions. The main advantage of this procedure is that the third assumption in all its aspects (i.e. changes in grazer activity and abundance) is resolved experimentally. By measuring the grazing impact directly in all dilutions, any deviation from linear feeding kinetics, or changing microzooplankton concentrations are automatically accounted for. The disappearance rate of FLB in the respective dilutions integrates all of these factors.

This method, however, adds some new uncertainties. (1) By using FLB as tracer food, the authors imply that FLB are fit as a surrogate for the prey organisms in question, namely the phytoplankton. This may hold true in oligotrophic regions, where picoplanktic food (in the same

size range as FLB) dominates the autotrophic community, and where FLB can be uniformly applied as surrogate for most prey types encountered: *Prochlorococcus*, *Synechococcus*-type cyanobacteria, pico-eukaryotes and heterotrophic bacteria. However, in more eutrophic regions, where larger phytoplankton predominate, various surrogate prey types would be required in order to cover the different algal sizes, e.g. different representative fluorescently labeled algae (FLA, RUBLEE and GALLEGOS 1989). (2) Under the circumstances where FLB can be used, flow cytometry is almost a necessary requirement for the quantification of the natural prey and the FLB. Epifluorescence microscopy may theoretically be used (not for *Prochlorococcus*, CAMPBELL et al. 1994), but it requires an unrealistically high amount of time to approach the precision achieved by flow cytometry. (3) Typical problems associated with surrogate food must be taken into consideration (optimal tracer concentration, discrimination between dead and living food particles, MCMANUS and OKUBO 1991). While LANDRY et al. (1995a) are aware of these potential problems, they state that "... if these potential technical problems can be overcome, however, the new hybrid approach will, at worst, allow us to understand the circumstances under which the standard dilution technique can be applied in a manner consistent with its assumptions. At best, the new technique will be able to provide unbiased estimates of growth and grazing rates even when conditions violate the assumptions of the standard dilution protocol" (LANDRY et al. 1995a). Nonetheless, under the test conditions for the new approach (nutrient replete north equatorial Pacific), the authors found no difference between the new and the "classical" approach.

The question how to analyze phytoplankton in dilution experiments

The dilution method involves the measurement of phytoplankton concentrations at the beginning and at the end of the incubation period. This can be done in several ways. Due to the easy and fast analysis, most investigators have used chlorophyll a as a quantitative measure of phytoplankton biomass. As a bulk parameter, the Chl.a signal integrates all different phytoplankton species, and cannot account for differential growth (and grazing) rates. Furthermore, the Chl.a - biomass ratio (assumed to be constant during the incubation period in all dilutions) is known to vary with environmental conditions (BANSE 1977, RIEMANN et al. 1989). Also, incomplete digestion of chloroplasts within grazers (BARLOW et al. 1988), and mixotrophic protists (STOECKER et al. 1987, LAVAL-PEUTO and RASSOULZADEGAN 1988, PORTER 1988) may bias the Chl.a signal. These problems can be tackled by using (epifluorescence-) microscopy (e.g. BURKILL et al. 1993c, REITMEIER 1994, this work), phytoplankton pigment analysis using HPLC techniques (BURKILL et al. 1987, STROM and WELSCHMEYER 1991, ANTIA 1991), and flow cytometry (LANDRY et al. 1995a, LANDRY et al. 1995b, this work). The HPLC technique provides information on different phytoplankton taxa (as defined by their respective pigment sets), but apart from that, it is subject to the other problems mentioned for Chl.a. Microscopical methods have the advantage to be species-specific (an experienced investigator provided), albeit at the cost of time and precision. Flow cytometric analysis combines the advantages of speed and precision with the ability of individual cell counts; however, these contain only limited taxonomical information, and are generally restricted to the ultraphytoplankton.

Problems arising from the production of particle free seawater and incubations

The production of filtered seawater is a crucial step in the dilution procedure. Filtration, however, may cause cell breakage and protoplasm leakage into the filtrate (e.g. NAGATA and KIRCHMAN 1990), causing either an enhanced or depressed phytoplankton growth rate in the diluted bottles, depending on the metabolic effects of the organic enrichments. Any pollution of the filtered seawater or the experimental gear (incubation vessels, tubings, fittings, filters) might likewise hamper growth and grazing activities. It is therefore absolutely necessary to choose non-toxic materials for any gear that might come into contact with the incubation water, and to thoroughly clean it prior to use (e.g. LANDRY 1993, LANDRY et al. 1995b).

The application of the dilution method in this study

Within the scope of this work, the dilution method was applied during three of the four cruises. During cruise B1 in the Arabian Sea (SW monsoon) and in the Pomeranian Bay in 1993, phytoplankton was measured as bulk Chl.a, whereas during cruise B2 (NE monsoon) and in the Gotland Sea, a flow cytometer was used to quantify the phytoplankton prey. Therefore, the former experiments give an estimation of the grazing impact by the entire microzooplankton community (<200µm) on the total phytoplankton community, while the latter allowed the discrimination of different phytoplankton groups.

Phytoplankton growth in the incubations was considered to be not limited by nutrient supply in the Arabian Sea and the Pomeranian Bay, as macronutrients were replete there (see sections 3.1.1., 3.2.1., and 3.4.1.). In the Gotland Sea, the euphotic zone was nutrient depleted (see section 3.3.1.), so the incubation bottles were enriched with nutrient rich deep water (see section 2.6.2.). This procedure is believed to be an appropriate way of coping with the problem of oligotrophy in dilution experiments (LANDRY 1993) and yielded reasonable results (section 3.3.4.).

Dilution experiments combined with size fractionation

The dilution approach involves the removal of mesozooplankton (>200µm) from the experimental containers prior to incubation. Likewise it is possible to successively remove also smaller grazer size classes by pre-incubation size fractionation. Within the scope of this study, this extension of the dilution method was carried out during two cruises (Arabian Sea B2, NE monsoon, and Gotland Sea, Baltic proper). Problems associated with pre-incubation size fractionation will be shortly discussed.

The size fractionation technique is a simple and straightforward approach to estimate grazing by simply removing large grazers from their small prey organisms (WRIGHT and COFFIN 1984). It has been used frequently and successfully in the past (RASSOUZADEGAN and SHELDON 1986, VERITY 1986, CARON et al. 1991, WEISSE and SCHEFFEL-MÖSER 1991, NAKAMURA et al. 1993), however, there may be some problems associated with size fractionation. First of all, it is hardly possible to quantitatively separate predators from their prey solely on the basis of size (e.g. SMETACEK 1981, FUHRMAN and MCMANUS 1984, CYNAR et al. 1985, SLEIGH 1991). Secondly, filtration may cause cell disruption and subsequent leakage of protoplasm into the filtrate (GOLDMAN and DENNETT 1985, NAGATA and KIRCHMAN 1990), leading to either a reduced or enhanced prey growth rate (phytoplankton or bacteria), depending on the biochemical properties of the cell sap constituents. In addition to that, the complicated interactions between the different components of the microbial food web involving feeding and nutrient regeneration (AZAM et al. 1983, SHERR et al. 1983, GOLDMAN and CARON 1985, STONE 1990, GLIBERT et al. 1992), make the extrapolation to the natural field situation difficult. However, within the scope of this study, different (size-) components of the microbial food web were intentionally decoupled to estimate their respective roles within the system, which would otherwise be masked. Similar experiments have uncovered interesting trophic interrelationships within the microbial food web (e.g. WIKNER and HAGSTRÖM 1988, WEISSE and SCHEFFEL-MÖSER 1991). A direct extrapolation to field conditions, however, can only be made using data from "unfractionated" treatments, encompassing the entire microplankton community (<200µm).

4.1.3. Alternative grazing methods used in this study

Metabolic inhibition

This method has been used successfully by a variety of authors in different environments (e.g. FUHRMAN and MCMANUS 1984, CAMPBELL and CARPENTER 1986, WEISSE 1989, CARON et al. 1991). It is possible to use specific metabolic inhibitors to stop proliferation of either prokaryotic or eukaryotic cells. The increased (when eukaryotic grazers are inhibited), or decreased (when the prokaryotic prey is inhibited) prey concentration in the inhibited treatments relative to the control

then allows the calculation of a grazing and specific growth rate (NEWELL et al. 1983). Metabolic inhibition is group specific for the different cell types; e.g. penicillin inhibits prokaryote cell wall synthesis, vanomycin inhibits the 70s subunit of prokaryote ribosomes; cycloheximide does so with the eukaryote specific 80s ribosome, and colchicine prevents microtubuli formation in eukaryote cells. In the experiment presented here (St. US0, Arabian Sea, SW monsoon, section 3.1.4.), a mixture of penicillin and vanomycin was used to inhibit prokaryote growth, and cycloheximide to inhibit grazer activity in the control treatment (*sensu* SHERR et al. 1986a, section 2.8.). Time series measurements (Fig.17) revealed that the inhibitory effect had ceased after 12h; consequently, growth and grazing rates were calculated from the first 12h. This demonstrates the importance of time series measurements (as frequent as possible) to account for these effects. At US0, *Prochlorococcus* was present, possibly counted as heterotrophic bacteria in the Acridine Orange stained samples under epifluorescence microscopy, thereby causing an overestimation of bacterial numbers. CAMPBELL et al. (1994) demonstrated this effect in a joint investigation in the central North Pacific.

Light-Dark incubations

A new approach was used in the Red Sea during the NE monsoon: the comparison of light and dark incubations (section 3.2.6). Its application, however, requires a highly synchronised cell division pattern of the population in question, and the knowledge of the timing of cell division. In this case, *Synechococcus* divided before sunset, thus allowing the assumption that cell disappearance in the dark was due solely to grazing. A comparison of cell numbers in the light (growth and grazing), and those after the dark period (only grazing) allowed the determination of μ and g (section 2.7.). The method is simple as it merely requires the measurement of cell concentrations over a diel cycle (or in artificially darkened incubations). Of course, the crucial point is to determine the time of synchronised cell divisions. Here, cell cycle analysis showed that cells did not divide in the dark. However, any other indications for a synchronised cell division could be used likewise, e.g. a sudden decrease of cell size (i.e. as indicated by scatter or fluorescence signals of a flow cytometer) accompanied with a sudden increase in cell numbers (VELDHUIS 1995). This approach is comparable to the chemical inhibition method, as both take advantage of a period of suppressed prey cell division, evoked artificially in the former and naturally in the latter case. In regions where a synchronised cell division pattern can be expected (i.e. open oceans), this method seems to be superior to many others, as it requires much less manipulation of the sample (a simulated *in situ* incubation on board, with frequent sub-sampling over a diel cycle). However, the method requires a flow cytometer (to allow small sub-sampling water volumes, and to account for differential growth of the different phytoplankton groups), and expertise in cell cycle analysis.

A variety of other methods exist which allow the estimation of herbivory and bacterivory, a discussion of which is beyond the scope of this work (e.g. fluorescently labeled prey, SHERR et al. 1987, RUBLEE and GALLEGOS 1989; radiolabeling methods, e.g. LESSARD and SWIFT 1985; frequency of dividing cells FDC, HAGSTRÖM et al. 1979). A survey of the most important approaches is given by LANDRY (1994). It is important to point out here that any experiment that is capable of measuring the specific growth rate μ of a prey organism (by whatever method) can deliver the grazing rate g (by resolving the equation $k = \mu - g$), provided the apparent growth rate k was measured, i.e. cell concentration changes were monitored in a confined water volume, and grazing is assumed the only loss factor. It seems that some new methods for the determination of specific growth rates in the sea (e.g. cell cycle analysis, CARPENTER and CHANG 1988) have not been fully exploited in this respect (e.g. VAULOT et al. 1995, but see VAN BLEJSWIJK and VELDHUIS 1995).

Finally it should be mentioned that there is not yet *the* ideal method for measuring microzooplankton grazing rates. Nevertheless, careful choice of the appropriate method from the existing spectrum for a specific goal, environment, or equipment, allows a reasonable estimation

of the *in situ* grazing impact of microzooplankton in different environments. However, some trophic links within the microbial food web remain obscure to date for methodological reasons. Relatively few investigations have attempted to quantitatively estimate trophic interactions within the microzooplankton compartment *in situ*, e.g. large HNF feeding on small HNF, ciliates feeding on HNF, large HNF feeding on small ciliates, heterotrophic dino- or silicoflagellates feeding on HNF or ciliates, and so on. Presently we must still consider the microzooplankton as a "black box" of which we can estimate in- and outputs, but barely any internal turnovers. To catch a glimpse of the interactions within this compartment, we can only resort to methods like size fractionation (VERITY 1986, WIKNER and HAGSTRÖM 1988, WEISSE 1989, WEISSE and SCHEFFEL-MÖSER 1991, this study), although the application of cell cycle analysis (with a variety of new DNA stains emerging) may in the future help resolve parts of this black box (e.g. WHITELEY et al. 1993). Recently, CLEVEN (1996) has successfully applied the FLP (fluorescently labeled prey) technique to fluorescently label heterotrophic nanoflagellates in order to estimate ciliate predation on HNF *in situ*.

4.2. Pelagic food web structure and trophic interactions in the Arabian Sea and the Baltic Sea

4.2.1. Standing stocks and distributions of ultraphytoplankton

The Arabian Sea and its adjacent areas

Phytoplankton distributions in the Arabian Sea have been described as fluoro- or photometrically measured Chl.a (KREY and BABENERD 1976), as basin-wide satellite pictures (BANSE and MCCLAIN 1986), or as microscopical analysis of microphytoplankton (i.e. diatoms and dinoflagellates, KREY 1973, KIMOR 1973). Phytoplankton biomass (as Chl.a) has been shown to be highly variable spatially and seasonally. In summer (June-September), the southwest (SW) monsoon creates intense upwelling along the Somali and Omani coasts. In these areas, high primary production and biomass values result in high sedimentation rates (RYTHER and MENZEL 1965). High vertical particle flux rates were also measured in the open Arabian Sea, due to wind-induced mixed layer deepening and associated nutrient entrainment into the euphotic zone (NAIR et al. 1989). The winter (NE) monsoon (December-March) cools the surface waters and results in a thermal convection, bringing new nutrients to the surface waters (BANSE 1994a). The two monsoon periods thus make the Arabian Sea one of the most productive areas of the world's ocean (BURKILL et al. 1993a). The inter-monsoon periods, on the other hand, are generally characterized by a pronounced stratification, a nutrient depleted mixed layer and the preponderance of picophytoplankton (JOCHM et al. 1993, JOCHM 1995). Vertical particle flux during this period of extreme oligotrophy seems to be primarily associated with the widespread deep chlorophyll maximum (DCM) which exhibits elevated primary production and phytoplankton biomass (POLLEHNE et al. 1993). However, phytoplankton blooms and associated enhanced vertical particle flux rates have also been observed in a non-upwelling off-shore site during the oligotrophic inter-monsoon period (PASSOW et al. 1993).

During the cruises in July-August 1992 (SW monsoon), the structure of the pelagic food web was very heterogeneous, as might be expected by the occurrence of local upwelling plumes off the Somali coast in an otherwise oligotrophic ocean. Especially the southern stations SB1 and US0 showed a distinct stratification and had a warm surface layer with low nutrient (nitrate $<0.3 \mu\text{M}$) and chlorophyll ($<0.3 \mu\text{g dm}^{-3}$) values in the euphotic zone. Here, no large phytoplankton was found, mainly the picoautotroph genera *Synechococcus* and *Prochlorococcus* were present. Although temperature and nutrient profiles showed clear signs of upwelling along the Somali coast and in the Somali Basin north of 5°N , the biological response to this cold nutrient enriched water was rather patchy. At station US2, an intensive bloom of large diatoms (a diverse composition of many large species, section 3.1.1.) was observed, with highest concentrations of phytoplankton

and protozoa (cast 230-23), while an earlier (230-9, 18 nautical miles from the bloom patch), and a later cast (257, 7 nautical miles from the patch) showed much lower phytoplankton and protozoan concentrations. Chlorophyll values above $0.5 \mu\text{g dm}^{-3}$ were recorded only in the bloom proper at US2 (highest value from the plankton pump: $13 \mu\text{g dm}^{-3}$), and downstream the upwelling plume southeast of Socotra ($0.9 \mu\text{g dm}^{-3}$ at SI). The high chlorophyll concentrations at SI, however, did not originate from large diatoms found in the bloom patch, but from smaller phytoplankton (*Synechococcus*, *Emiliania huxleyi* and other small nanoflagellates, VELDHUIS et al. 1994). The large diatoms from the bloom at US2 were not transported downstream but obviously sedimented out on the spot, while the Somali Current and the Great Whirl distributed nutrient enriched water east- and southwards from the upwelling areas off Somalia to the open Arabian Sea (Fig.1). Nonetheless, it remains unclear why the euphotic zone of most of the area was rich in nutrients, while phytoplankton biomass remained low except for US2 and SI. A striking observation, however, was the high number of large fecal pellets (ca. $280 \times 40 \mu\text{m}$) in the bloom water, probably originating from large copepods, pointing to a high grazing pressure on the blooming diatoms by mesozooplankton. In fact, high biomasses of mesozooplankton, including different stages of the upwelling copepod *Calanus carinatus*, were found in surface waters of the upwelling area (BAARS et al. 1994).

During the NE monsoon in Jan./Feb.1993, Chl.a concentrations were low ($<0.5 \mu\text{g dm}^{-3}$), and picoplankton (*Synechococcus*, *Prochlorococcus* and pico-eukaryotes) was for the most part the dominant phytoplankton. Large phytoplankton (i.e. dinoflagellates and diatoms) thrived only in the inner Gulf of Aden and in the inner Red Sea. During both monsoons, the distribution of *Prochlorococcus* was inversely related to the trophic state of the system: during the SW monsoon, they were only present at the oligotrophic southern station US0 and totally absent at the nutrient rich stations, while their concentrations during the mesotrophic NE monsoon were low (up to $66,000 \text{ cm}^{-3}$ in the Somali Basin) compared to oligotrophic periods (up to $276,000 \text{ cm}^{-3}$, VELDHUIS and KRAAY 1993), and even less in the inner Gulf of Aden and the southern Red Sea (from $13,000 \text{ cm}^{-3}$ to zero, respectively), where high nutrient values triggered the blooming of large phytoplankton.

A more detailed analysis of distribution patterns of autotrophic ultraplankton during the NE monsoon revealed that around 50% of the biomass was made up of pico-eukaryotes, while *Synechococcus* contributed to 20-60% of total ultraphytoplankton biomass. These two picoplankton classes clearly dominated the stocks of autotrophic ultraplankton. *Prochlorococcus* was only present in the Somali Current and the Gulf of Aden with rather low biomasses (less than 20%). A second type of eukaryotes, distinguished by their larger size, increased in importance towards the inner Gulf of Aden and the southern Red Sea (up to 40% of autotrophic ultraplankton biomass).

Tab.13 Spearman rank correlation coefficients between ultraphytoplankton carbon biomass and Chl.a in the Arabian Sea and adjacent areas during the NE monsoon. Numbers in parentheses represent the number of data points.

<i>Prochlorococcus</i>	<i>Synechococcus</i>	Small Eukaryotes	Large Eukaryotes	Σ Picophytoplankton
- 0.771 (6)	- 0.133 (9)	+ 0.286 (8)	+ 0.086 (6)	- 0.133 (9)

Autotrophic ultraplankton carbon was only weakly correlated to Chl.a, except for *Prochlorococcus*, which showed a strong negative correlation (Tab.13). This confirms earlier observations reporting highest *Prochlorococcus* abundances from subtropical and tropical oligotrophic waters low in chlorophyll (GOERICKE and WELSCHMEYER 1993, MAGAZZÙ and DECEMBRINI 1995, CHISHOLM et al. 1988), and its absence or low abundances in eutrophic neritic regions (Tab.16). The occurrence of *Prochlorococcus* in the Arabian Sea was shown indirectly by

pigment data (Pollehne et al. 1993); VELDHUIS and KRAAY (1993) found concentrations up to $276,000 \text{ cm}^{-3}$ during the oligotrophic phase in May in the Red Sea, the Gulf of Aden and the Somali Basin, which is about one order of magnitude above the numbers reported here from the NE monsoon. During the SW monsoon, *Prochlorococcus* was virtually absent except for the oligotrophic southernmost stations. OLSON et al. (1990), in a spatial and temporal survey of *Prochlorococcus* distributions in the North Atlantic, found highest concentrations in warm and stratified waters; moreover, *Prochlorococcus* concentrations were highest when *Synechococcus* concentrations were low and vice versa. The same was observed by CAMPBELL and VAULOT (1993) in the subtropical North Pacific. This distribution pattern (high concentrations in warm, stratified, oligotrophic waters - low concentrations in well mixed, enriched waters) is currently believed to apply to the autotrophic picoplankton in general (e.g. FOGG 1995); however, it seems to be a peculiar characteristic for *Prochlorococcus*. Some authors, however, have reported *Prochlorococcus* abundance peaks in the DCM (deep chlorophyll maximum), while others have found them to be evenly distributed over the euphotic zone. Partly, these conflicting results may originate from the inability of most flow cytometers (VELDHUIS and KRAAY 1990, JOCHEM 1995) and epifluorescence microscopes to detect the dim autofluorescence of *Prochlorococcus* in the light flooded surface waters at low latitudes. However, these tiny prokaryotic primary producers appear to be especially well adjusted to regenerating systems. In this context, it is interesting to note that culture media for *Prochlorococcus* exclusively use ammonium and urea as nitrogen sources (PC medium, J. Sexton, pers. comm., CCMP, Bigelow Laboratory), which are typical for regenerating systems. *Prochlorococcus* in culture does not grow on oxidized nitrogen compounds, which apparently reflects field conditions.

During the oligotrophic inter-monsoon period in May, VELDHUIS and KRAAY (1993) found *Synechococcus* concentrations up to $75,000 \text{ cm}^{-3}$. JOCHEM (1995), using epifluorescence microscopy, detected highest *Synechococcus* numbers close to the Omani coast (up to $230,000 \text{ cm}^{-3}$), decreasing to $23,000 \text{ cm}^{-3}$ - $61,000 \text{ cm}^{-3}$ towards the more oligotrophic open Arabian Sea; the pico-eukaryotes followed the same pattern (from $7,000 \text{ cm}^{-3}$ - $9,000 \text{ cm}^{-3}$ to $4,000 \text{ cm}^{-3}$ - $7,000 \text{ cm}^{-3}$). BURKILL et al. (1993c) report an opposite trend: *Synechococcus* cell numbers were highest in oligotrophic waters and decreased towards an upwelling center off the Omani coast. These contradicting results might reflect the different seasons during which the data were obtained: Jochem's data were produced during the onset of the spring inter-monsoon following the NE monsoon (at low but not depleted nutrient concentrations off the Omani coast), while Burkill's investigations took place just following the upwelling season of the SW monsoon, with coastal nitrate values above $5 \mu\text{M}$. Although own data from the NE monsoon off the Somali coast show a weak negative correlation of *Synechococcus* biomass to Chl.a (Tab.13), *Synechococcus* and pico-eukaryote numbers were highest in the Gulf of Aden, where nitrate concentrations were also highest (section 3.2., Fig.19, Tab.7). Thus, it seems that *Synechococcus* and the pico-eukaryotes profit from low amounts of new nutrients in the euphotic zone (e.g. $\text{NO}_3 < 0.5 \mu\text{M}$), such as the winter (i.e. NE) monsoon triggers by thermal convection. At high nutrient concentrations ($\text{NO}_3 > 5 \mu\text{M}$), which are found at the upwelling spots during the summer (SW monsoon), the ultraplankton is clearly outcompeted by larger phytoplankton.

At two stations during the NE monsoon, the flow cytometer was able to separate two distinct subpopulations of *Prochlorococcus*, characterized by different fluorescence intensities ("dim" and "bright", section 3.2.4., Tab.7, Fig.28). While a co-occurrence of different subpopulations of *Synechococcus* has been described by various authors for different regions (e.g. WOOD et al. 1985, OLSON et al. 1988, VELDHUIS et al. 1993, this study), this is a relatively new feature for *Prochlorococcus*. Two subpopulations of *Prochlorococcus* have also been detected by CAMPBELL and VAULOT (1993) in the subtropical North Pacific off Hawaii by flow cytometry, and by GOERICKE and REPETA (1993) in the subtropical North Atlantic, using HPLC pigment analysis.

The Gotland Sea (Baltic proper)

In the Gotland Sea during summer 1994, the abundance and biomass of *Synechococcus* was probably underestimated by the flow cytometer, as its fluorescence signals could not be completely separated from the background noise (Fig.40), and due to the too high sample flow speed (section 2.5.2). At St.747 (Experiment 1, section 3.3.4.), *Synechococcus* was counted by epifluorescence microscopy, as strong vibrations made flow cytometric counts impossible at this station. Here, at the start of the drift, *Synechococcus* concentrations were extremely high ($812,000 \text{ cm}^{-3}$). The other ultraplanktonic algae were probably counted accurately throughout the cruise, as they were well separated from the background in the red channel of the flow cytometer (Fig.40), and they were found at similar, or even higher abundances as reported in the literature. For the pico-eukaryotes, concentrations at the bottom of the euphotic zone amounted up to $30,000 \text{ cm}^{-3}$, which exceeds previous counts from the region by a factor of four (TRENKEL 1992). *Synechococcus* and the pico-eukaryotes generally showed highest concentrations at the bottom of the euphotic zone, while larger nano-eukaryotes preferred shallower depths (section 3.3.2., Fig.42, Fig.45). Total phytoplankton carbon biomasses in the euphotic zone (as accounted for by the flow cytometer) was estimated to about $40 - 100 \mu\text{g dm}^{-3}$; only at stations where the group "SC1" predominated, carbon values peaked to about $200 \mu\text{g dm}^{-3}$. Due to its specific optical characteristics (large light scatter, i.e. large size; low red fluorescence, i.e. low chlorophyll content), this cluster might represent small herbivorous flagellates, with ingested but still fluorescing *Synechococcus* or pico-eukaryotic cells. Phytoplankton cells of the same light scatter characteristics normally show much higher red fluorescence signals (i.e. large nano-eukaryotes, Fig.40). Peak concentrations for this group ranged between $2,000 - 4,600 \text{ cm}^{-3}$, which is in the same range as the microscopically counted HNF (section 3.3.3., Fig.47).

Phytoplankton biomass (as measured by flow cytometry) accounted only for a small portion of total POC in the water column (Fig.46). Highest percentages, however, were found at the stations with the "SC1" cluster predominating (up to 39%), possibly representing heterotrophic biomass. Where "SC1" played a minor role, only 4 - 14% of POC consisted of phytoplankton. When evaluating these figures, it should be kept in mind, that only phytoplankton $<5\mu\text{m}$ are presented here. Larger phytoplankton like dinoflagellates (*Dinophysis norvegica*, CARPENTER et al. 1995) or filamentous diazotrophic cyanobacteria (*Nodularia spumigena*, *Aphanizomenon flos aquae*) were not considered although present, as they were not accessible by flow cytometry due to their large sizes and low abundances. Their distribution and dynamics are described by MEYER-HARMS (1996).

Investigations on ultraphytoplankton in the Baltic Sea and their dynamics have been mainly carried out in the Tvärminne area at the entrance to the Gulf of Finland (KUOSA and MARCUSSEN 1988, KUOSA 1991, KUUPPO-LEINIKKI et al. 1994, see review by KUPARINEN and KUOSA 1993), in Kiel Bay, western Baltic Sea (JOCHEM 1988, JOCHEM 1989), and in the Skarerrak ("entrance" to the Baltic Sea) by KARLSON (1995). *Synechococcus* in the Baltic Sea may approach abundances of several 10^5 cm^{-3} in summer, but more than 10^6 cm^{-3} have been reported at an oligotrophic site at the entrance of the Gulf of Finland (KUOSA 1991). For the Gotland Sea, DETMER et al. (1993) have reported euphotic zone concentrations of *Synechococcus* of over $500,000 \text{ cm}^{-3}$, and of autotrophic eukaryotic ultraplankton of $6,000 - 8,000 \text{ cm}^{-3}$, similar high numbers were also given by TRENKEL (1992). KUOSA (1991) also reports high abundances of pico-eukaryotes (peak values over $30,000 \text{ cm}^{-3}$). These numbers represent summer peak values during a seasonal survey, and they were subject to considerable oscillations over periods of weeks (KUOSA 1991). These previous reports of ultraphytoplankton abundances are in the same order of magnitude, nonetheless somewhat lower than the concentrations found in this study ($812,000 \text{ cm}^{-3}$ for *Synechococcus*, $30,000 \text{ cm}^{-3}$ for pico-eukaryotes, $5,000-6,000 \text{ cm}^{-3}$ for small, $2,000-3,000 \text{ cm}^{-3}$ for large nano-eukaryotes, and $400-600 \text{ cm}^{-3}$ for an unidentified orange fluorescing $5\mu\text{m}$ sized alga ("PE1", presumably a small cryptophyte). These concentrations for ultraphytoplankton in the Baltic Sea exceed values from oligotrophic oceanic regions, but also from other inshore or

upwelling areas considerably (Tab.16). One possible explanation of this phenomenon may lie in the regular occurrence of large filamentous diazotrophic cyanobacteria in the Baltic proper in summer (RINNE et al. 1978, WALLSTRÖM 1988).

These large diazotrophic cyanobacteria are of fundamental importance to the trophic state of the euphotic zone in summer, as they provide the oligotrophic mixed layer with new (reduced) nitrogen in times of nitrate deficiency by N_2 -fixation (e.g. SÖRENSEN and SAHLSTEN 1987). At the time of the investigation, a bloom of *Aphanizomenon flos-aquae* and *Anabaena* sp. was declining, probably causing reduced nitrogen compounds (DON, dissolved organic nitrogen, or NH_4) to leach from the dying cells into the water column (HOPPE 1981, SAHLSTEN and SÖRENSEN 1989). LINDAHL et al. (1978) describe a significantly elevated primary production following a declining bloom of diazotrophic cyanobacteria. The autotrophic community seems to profit from the additional nitrogen from the dying cyanobacterial cells, resulting in higher production rates and biomasses. Heterotrophic bacteria profit from this phenomenon as well, with mean abundances well above those in oceanic regions ($2,700,000 - 7,200,000 \text{ cm}^{-3}$, HEINÄNEN 1992). This speculation fits well with the observations from the same area in 1993 (no own measurements), when the diazotrophic cyanobacteria began to bloom and thrived, and the biomass of other phytoplankton (estimated by microscopy and HPLC tracer pigment measurements) was significantly lower as in 1994 (MEYER-HARMS 1996). Thus, the new nitrogen diffusing into the system from the decaying N_2 -fixing cyanobacteria elevates the components of the regenerated system to a higher biomass level. The observation that even the high ultraphytoplankton biomasses (accessible by flow cytometry) observed in 1994 (in contrast to 1993) contribute only up to 14% of total POC implies that the bulk of the POC in the euphotic zone was present as large phytoplankton ($>5\mu\text{m}$), heterotrophs or detritus (e.g. the decaying filaments and flocs of *Aphanizomenon*). In a bloom situation, phytoplankton carbon can contribute up to 80 - 100% to POC, while in regenerating phases in summer, only 25 - 40% of total POC are phytoplankton. In winter, this portion is still lower: only 10% of POC are autotrophic at that time (approximated from a joint seasonal survey of particulate and dissolved water column constituents 1972 in Kiel Bay, VON BODUNGEN 1975, SMETACEK 1975).

The Pomeranian Bay (southern Baltic Sea)

In the Pomeranian Bay, flow cytometric measurements were made only in 1994. Most phytoplankton groups identified were smaller than $5\mu\text{m}$ in diameter (section 3.5., Tab.12, Fig.70). To my knowledge, this is the first report on ultraplankton in the Pomeranian Bay. During the first week of the cruise, a typical west-wind situation prevailed, followed by a wind shift to an easterly component a few days later. This allowed the study of distribution patterns of phytoplankton and protozoa during these opposite meteorological forcings (section 3.5.). During the first grid, a narrow belt of increased concentrations of phytoplankton and protozoa was observed along the Polish coast (Fig.71 - 81). However, there were some pronounced differences in phytoplankton distribution patterns during both grids. Some groups, especially the pico-eukaryotes, the large cryptophytes and "Cluster A" had much higher concentrations off the Usedom coast than downstream of the Swine mouth during the first grid; they most likely originated from the Greifswald lagoon rather than from the Szczecin lagoon. After the shift to easterly winds, concentrations of these groups decreased dramatically off Usedom. The other groups reacted differently to the shift in wind and current conditions. The small cryptophytes and especially the small nano-eukaryotes increased in cell numbers at the most easterly stations, while decreasing at the other stations (Fig.74, 76). This points to an active growth of these algae at these stations. The easterly wind had spread the narrow coastal band seawards, and deeper water replaced the seawards transported surface water. It can be expected that conditions for autotrophic growth had considerably increased under these circumstances (increased light conditions at ample nutrient supply). The same effect was shown during the drift experiment 1 in 1993 (section 3.4.). The large nano-eukaryotes, however, showed decreasing cell concentrations during the second grid throughout the bay, except in front of the Swina mouth, where an extremely high concentration

(11,600 cm⁻³) was measured (Fig.75). This coincides with the very high Chl.a value measured at the surface at this station (Fig.71), and is probably correlated with an outflow event from the lagoon at the surface.

The bay-scale distribution of *Synechococcus* dramatically differed from that of the other phytoplankton: concentrations were much more evenly distributed across the entire bay, with coastal numbers lower than those of the central and outer bay (Fig.72). There, abundances reached a spectacular 1,500,000 cm⁻³; these numbers are well within the range of bacterial abundances from the same location, which range between 500,000 and 2,000,000 cm⁻³ (Macziejowska, pers. comm.). Tab.14 shows Spearman rank correlation coefficients of the respective phytoplankton groups and Chl.a. With the exception of *Synechococcus*, all correlations are positive. *Synechococcus* was most abundant at stations where total phytoplankton biomass was low, i.e. in the central parts of the bay. There, nitrate concentrations were generally below 0.1µM, and phosphate concentrations were at or below the detection limit (phosphate also in the plume water). These conditions seemed to favour *Synechococcus* over the larger phytoplankton groups, whereas the opposite was observed in the plume water, where larger forms were most abundant.

Tab.14 Spearman rank correlation coefficients between ultraphytoplankton groups and Chl.a in the Pomeranian Bay in July 1994. Bold numbers are significant at $p < 0.01$, italic numbers are significant at $p < 0.1$. *Synechococcus* counted by epifluorescence microscopy, the other groups by flow cytometry.

	Depth	Synecho- coccus	n	Pico- Euks	Small Nano-Euks	Large Nano-Euks	Small Cryptos	Large Cryptos	"Cluster A"	n
1.Grid	Surface	-0.234	32	+0.712	+0.851	+0.775	+0.685	+0.678	+0.575	23
	Mid-Water	-0.631	31	+0.786	+0.889	+0.672	+0.583	+0.707	+0.655	18
	Bottom	-0.148	33	+0.483	+0.632	+0.719	+0.237	+0.411	+0.399	22
2.Grid	Surface	<i>-0.650</i>	9	+0.787	+0.808	+0.059	+0.378	+0.344	+0.543	18
	Mid-Water	-0.632	23	+0.727	+0.575	+0.143	+0.722	+0.428	+0.710	17
	Bottom	+0.188	10	+0.714	+0.344	+0.501	+0.501	+0.276	+0.442	17

The occurrence of ultraphytoplankton in the different areas - a comparison

When the Arabian Sea with its adjacent areas and the Baltic Sea are compared in terms of ultraphytoplankton distributions and standing stocks, an important paradigm of aquatic microbial ecology is largely confirmed by the data presented here: the more oligotrophic the region, the greater the importance of autotrophic picoplankton. A comparison of pico- (i.e. <2µm) and small nanoautotrophic biomasses (i.e. 2 - 5µm) as percentages of total phytoplankton biomasses (measured as Chl.a and converted to carbon biomass, see section 2.4.) in the different investigation areas reveals that picoplankton biomass had a much higher share in oligotrophic than in eutrophic water (Tab.15). In the Arabian Sea during the NE monsoon, 53% of total biomass was comprised of picoplankton, while in the Red Sea, which was eutrophic at the time, this share was only roughly 9%. In the Pomeranian Bay, the oligotrophic open bay water could be compared with the eutrophic plume water: picoplankton made up about 40% of autotrophic biomass in the oligotrophic open bay, but only 10% in the eutrophic plume water body. The most striking observation, however, is the extraordinarily high biomass of *Synechococcus* in Pomeranian Bay

water. The fraction of the picoplankton $<2\mu\text{m}$ of total ultraphytoplankton $<5\mu\text{m}$ decreased with increasing trophic state of the environment. The low value for the Gotland Sea may be due to the underestimation of *Synechococcus* there (section 4.1.1.). In the Arabian Sea and the Red Sea, the sensitivity of the cytometer was adjusted for *Prochlorococcus*, so that during these cruises, the larger ultraplankton was possibly underestimated.

Tab.15 Autotrophic ultraplankton carbon biomasses as percentages of total autotrophic biomass (measured by flow cytometry and as Chl.a, respectively, and converted to carbon) in the different research areas. Total Pico = phytoplankton carbon in the size class $<2\mu\text{m}$, Total Ultra = total phytoplankton carbon as accounted for by flow cytometry (i.e. including the Total Pico), S-Nano-Euks = small nano-eukaryotes, L-Nano-Euks = large nano-eukaryotes, Crypt. = cryptophytes. The Red Sea and Odra plume was eutrophic ($>1\mu\text{M}$ nitrate, numbers in italics), the other regions oligo-, resp. mesotroph ($<0.5\mu\text{M}$ nitrate).

	NE monsoon		Gotland Sea	Pomeranian Bay	
	Arabian Sea	Red Sea		Bay Water	Odra Plume
Prochloro	5.52% \pm 3.73	- -	- -	- -	- -
Syn	19.08% \pm 7.55	4.29% \pm 0.14	5.70% \pm 1.83	46.13% \pm 45.52	7.21% \pm 3.24
Pico-Euks	29.25% \pm 14.62	4.36% \pm 6.16	10.27% \pm 6.28	1.46% \pm 1.29	2.43% \pm 1.81
Total Pico	52.28% \pm 21.01	8.68% \pm 6.07	15.97% \pm 5.06	40.49% \pm 45.26	9.64% \pm 4.98
S-Nano-Euks	7.98% \pm 1.50	2.55% \pm 0.82	6.43% \pm 1.23	1.51% \pm 0.95	3.22% \pm 1.30
L-Nano-Euks	- -	- -	12.85% \pm 4.38	6.84% \pm 3.38	10.96% \pm 3.97
Small Crypt.	- -	- -	- -	1.44% \pm 1.93	2.44% \pm 1.40
Large Crypt.	- -	- -	- -	10.44% \pm 12.71	18.82% \pm 13.29
Total Ultra	56.84% \pm 23.59	11.23% \pm 5.25	35.34% \pm 8.59	60.73% \pm 49.28	45.08% \pm 18.99
% Pico of Ultra	92%	77%	45%	67%	21%

Table 16 compares worldwide distributions of three autotrophic picoplankton groups in different environments, as documented in the literature. A striking feature is the complete absence of *Prochlorococcus* in the Baltic Sea and other boreal, (sub-) arctic, or eutrophied regions. Here, we see the same picture at a world-wide scale, as was observed in the Arabian Sea during the two monsoons: *Prochlorococcus* abundance seems to be related inversely to the trophic state of the system. Moreover, despite the fact that the Baltic proper is completely oligotroph in summer (with respect to available oxidised nitrogen compounds), *Prochlorococcus* has not been detected (even using a highly sensitive flow cytometer, F. Jochem, pers.comm.).

Tab.16 Compilation of peak concentrations of autotrophic picoplankton from different regions. Concentrations are given as numbers per cm³.

Region	<i>Synech.</i>	Pico-Euks	<i>Prochl.</i>	Reference
<i>Arabian Sea</i>				
Gulf of Oman, post-SW-monsoon	19,000	-	-	Burkill et al. 1993c
Central, post-SW-monsoon	130,000	-	-	Burkill et al. 1993c
Gulf of Oman, inter-monsoon	230,000	9,000	-	Jochem 1995
Central, inter-monsoon	61,000	7,000	55,000	Jochem 1995
Red Sea, *Somali coast upwell. Pre-SW-monsoon	75,000	40,000*	276,000	Veldhuis and Kraay 1993
Somali basin, NE-monsoon	67,183	7,200	66,300	This study
Gulf of Aden, NE-monsoon	142,000	18,300	13,200	This study
<i>Baltic Sea</i>				
Baltic Proper, Gotland Sea	500,000	8,000	-	Detmer et al. 1993
Baltic Proper, Gotland Sea	230,000	7,900	-	Trenkel 1992
Baltic Proper, Gotland Sea	812,000	30,000	-	This study
Southern Baltic, Pomeranian Bay	1,500,000	11,000	-	This study
Northern Baltic, Tvärminne Area	1,700,000	32,000	-	Kuosa 1991
Northern Baltic, Tvärminne Area	814,000	7,900	-	Kuuppo-Leinikki et al. 1994
Western Baltic, Kiel Bight	260,000	-	-	Jochem 1988
Skagerrak	250,000	30,000	-	Karlson 1995
<i>Other regions: Oceanic</i>				
North Atlantic, off Newfoundland	16,500	8,000	-	Johnson and Sieburth 1982
North Atlantic, Sargasso Sea	14,000	-	-	Iturriaga and Marra 1988
North Atlantic, Sargasso Sea	6,000	2,600	100,000	Li et al. 1992
North Atlantic, Sargasso Sea	33,000	-	30,000	Olson et al. 1990
North Atlantic, Sargasso Sea	-	-	95,000	Vaulot et al. 1990
Eastern North Atlantic	58,000	41,000	-	Detmer 1995
Eastern North Atlantic	39,000	-	95,000	Veldhuis et al. 1993
East North Pacific, off California	15,000	-	100,000	Chisholm et al. 1988
Equatorial Pacific	-	-	150,000	Vaulot et al. 1995
West Pacific, off Japan	15,300	-	-	Kudoh et al. 1990
North Pacific Gyre	5,500	-	-	Iturriaga and Mitchell 1986
South Pacific, off Peru	88,000	-	-	Waterbury et al. 1979
South Pacific, off Peru	19,000	-	-	Waterbury et al. 1979
Subtrop. Pacific, ALOHA, Hawaii	2,450	2,200	272,000	Cambell and Vaulot 1993
Subtrop. Pacific, Oahu, Hawaii	-	-	227,000	Monger and Landry 1993
Eastern Mediterranean	10,000	500	400,000	Li et al. 1993
Mediterranean, div. locations	140,000	1,800	19,000	Magazzu and Decembrini 1995
Mediterranean, Levant. Sea	40,000	15,000	36,000	Detmer 1995
Mediterranean, Gulf of Lyon offsh.	-	-	52,000	Vaulot et al. 1990
North Atlantic, Greenland Sea	-	13,800	-	Gradinger 1990
South Polar Sea	-	8,400	-	Detmer 1995
Gulf of Alaska	10,000	-	-	Neuer 1992
<i>Neritic</i>				
Thau Lagoon, France	-	200,000	-	Courties et al. 1994
New Zealand, coastal upwelling	21,000	12,000	-	Hall and Vincent 1990
Seto Inland Sea, Japan	50,000	-	-	Nakamura et al. 1993
Vinyard Sound, Woods Hole	44,400	-	-	Caron et al. 1991
Mediterranean, Rhône estuary	-	-	9,000	Vaulot et al. 1990

Another interesting information from Table 16 are the considerably higher concentrations of *Synechococcus* in the Baltic Sea as compared to the rest of the world's oceans. They seem to be up to an order of magnitude higher as in other regions, and apparently reach peak values in neritic

rather than in oceanic waters (the Pomeranian Bay and the Tvärminne area in the Baltic Sea, the Gulf of Oman and Gulf of Aden in the Arabian Sea). Likewise, the eukaryotic ultraphytoplankton seems to follow this trophic gradient.

4.2.2. Standing stocks and distributions of protozoa

The Arabian Sea and its adjacent areas

To date, there are very few published reports on protozoan abundance and biomass distributions for the Arabian Sea and its adjacent areas. SOROKIN et al. (1985) give an extensive overview over abundance and dynamics of auto- and heterotrophic micro- and nanoplankton in the central Indian Ocean during the SW monsoon period of 1981, however, their stations are situated in the central tropical Indian Ocean (i.e. ~ 1600 nautical miles southeast of the investigation area of this study). WEISSE (1989) presents data of HNF abundances from the Gulf of Aden and the Red Sea during the spring intermonsoon 1987 (Tab.20).

HNF numbers and biomasses appear to be quite conservative across all provinces, while HDIN and especially ciliate concentrations are subject to large deviations; this is most evident at the eutrophic stations of both monsoons. This might reflect different trophic strategies of the respective protozoan groups: while HNF are primarily dependent on heterotrophic and autotrophic picoplankton, whose concentrations are relatively conservative, heterotrophic dinoflagellates and ciliates have a wider food spectrum to choose from, ranging from bacteria (SHERR et al. 1986b, SHERR and SHERR 1987) and HNF (CLEVEN 1996) to large diatoms (SMETACEK 1981, LESSARD 1991), and even other ciliates (DOLAN and COATS 1991). Thus, heterotrophic dinoflagellates and ciliates will react to changing food conditions (i.e. phytoplankton blooms) to a larger extent as the HNF as obligate feeders of the ubiquitous picoplankton. However, HNF concentrations and biovolumes also increased in the blooming upwelled water parcel, probably triggered by elevated concentrations and increased biovolumes of heterotrophic bacteria in the enriched water.

During both monsoons, HNF numbers were clearly dominated (60 - 90% of cells) by very small individuals ($<3\mu\text{m}$), but larger HNF ($<10\mu\text{m}$) dominated in terms of biomass (also 10 - 20 μm individuals in the upwelling area). This trend of smaller individuals at more oligotrophic stations, and larger ones at more eutrophic stations applied to both monsoons for all protozoan groups (Fig.14, Fig.26). Ciliates were dominated by oligotrich forms (over 90% of both numbers and biomass). Only in the upwelling water, a higher diversity (scuticociliates, didiniids, hypotrichs) was observed. This dominance of oligotrich forms was also found by SOROKIN et al. (1985) in the central Indian Ocean, and is typical for oceanic environments (e.g. STROM et al. 1993, SHERR et al. 1986b, BURKILL et al. 1993b). Almost all heterotrophic dinoflagellates were small (i.e. $<20\mu\text{m}$) members of the genus *Gymnodinium*, with larger individuals again occurring at the eutropic stations during both monsoons. Heterotrophic dinoflagellates have been shown to be vigorous grazers of diatoms and other large phytoplankton (SMETACEK 1981, LESSARD 1991), but may also to feed on heterotrophic and autotrophic picoplankton (LESSARD and SWIFT 1985, STROM 1991). In fact, using epifluorescence microscopy, I observed numerous *Synechococcus* cells within the food vacuoles of *Gymnodinium* individuals during both monsoon seasons. *Synechococcus* were found frequently also in HNF cells, but very rarely in food vacuoles of ciliates.

Table 17 shows spearman rank correlations between the respective protozoan biomasses and Chl.a, and between the three protozoan groups. However, these correlations are afflicted with the few data points available, making an interpretation difficult. The relatively strong positive correlations between Chl.a and HNF during both monsoons, and between Chl.a and ciliates during the NE monsoon, however, may point to a trophic relationship between these groups. As at most stations during both monsoons, Chl.a values were very low ($\sim 0.3\mu\text{g dm}^{-3}$), and phytoplankton was dominated by picoplankton, such a relationship might be expected. The HDIN, on the other hand,

were weakly negatively correlated to Chl.a, but showed strong positive correlations to the other protozoan groups.

However, correlations of grazer and potential prey biomasses are only of limited interpretative value, if not taken on a larger scale (Fig.84, Tab.21). A strong positive correlation between the grazer and the prey implies a close trophic relationship between the two. A strong negative correlation however, may imply the same thing, i.e. in a situation when prey biomass is reduced to the benefit of grazer biomass. Moreover, a strong positive relationship could also be caused by indirect effects, such as nutrient release or predation on the grazer by larger zooplankton, rather than direct trophic interactions. This will be discussed further below in the context of 'bottom-up' and 'top-down' effects (section 4.3.).

Tab.17 Spearman rank correlation coefficients between protozoan carbon biomasses and Chl.a (left), and between respective protozoan carbon biomasses (right) during both monsoon periods. Numbers in parentheses represent the number of data points. Bold numbers are significant at $p < 0.05$.

Period	Chl.a				Protozoa		
	HNF	HDIN	Ciliates	Σ Protozoa	HNF - HDIN	HNF - Cil.	HDIN - Cil.
SW (B1)	+ 0.443 (9)	- 0.167 (9)	+ 0.086 (6)	- 0.167 (9)	+0.657 (6)	+0.371 (5)	+0.886 (6)
NE (B2)	+ 0.429 (6)	- 0.143 (6)	+0.900 (5)	+ 0.143 (6)	+0.100 (5)	+0.300 (5)	+0.100 (5)

The Gotland Sea (Baltic proper)

Protozoan cell concentrations and carbon biomasses in the Gotland Sea were in the same range as those in the Arabian Sea (Tab.20). HNF biomass was comparable to ciliate biomass, while abundances differed by an order of magnitude. HNF numbers and biomasses were highest in the lower euphotic zone, while ciliates were concentrated at shallower depths (section 3.3.3., Fig.47). This pattern might reflect trophic preferences of the protozoa: HNF $< 5\mu\text{m}$ prefer picoautotrophs $< 2\mu\text{m}$ in deeper water, while ciliates may preferentially feed on the larger nanoautotrophs at shallower depths. Ciliate ($5,000 - 10,000 \text{ dm}^{-3}$) and HNF ($2,000 - 18,000 \text{ cm}^{-3}$) abundances were well within the range reported earlier by TRENKEL (1992) and DETMER et al. (1993) for the same region and period, and by KUOSA and MARCUSSEN (1988) for the Tvärminne area (Gulf of Finland).

The Pomeranian Bay (southern Baltic Sea)

During both cruises to the Pomeranian Bay (1993 and 1994, sections 3.4. and 3.5., resp.) protozoan cell concentrations and carbon biomasses were significantly higher than in the Arabian Sea, but also than in the Gotland Sea (Tab.20). Also, the range of concentrations was much higher in the Pomeranian Bay. In 1993, the two drifts differed somewhat in the water column composition of protozoa: during the first drift, with increasing mixing with bay water, protozoan concentrations decreased, with HNF and ciliates (mainly strombiids) each contributing about half of the measured protozoan biomass (Fig.64, 65). The heterotrophic silicoflagellate *Ebria tripartita* was present, but in low numbers. During the second drift, HNF made up the bulk of protozoan biomass, and didiniids contributed considerably to the ciliate community (about 50%, Fig.65).

Protozoan distributions during the first grid of the 1994 cruise showed the same pattern as the phytoplankton: high concentrations along the coast, lower concentrations in the central and outer bay. However, some protozoan groups were more closely correlated to phytoplankton than others. Especially the strombiid ciliates, *Lohmaniella*, and the heterotrophic silicoflagellate *Ebria tripartita* showed high positive correlations to all phytoplankton groups and Chl.a (Tab.18).

Almost all protozoan groups showed a strong negative correlation to *Synechococcus*, in a sharp contrast to the other phytoplankton groups, pointing to a close trophic relationship.

Tab.18 Spearman rank correlation coefficients between ultraphytoplankton numbers and Chl.a, and protozoan groups in the Pomeranian Bay in July 1994. Bold numbers are significant at $p < 0.1$.

	Synecho -coccus	Pico-Euks	Small Nano- Euks	Large Nano-Euks	Small Cryptos	Large Cryptos	"Cluster A"	Chl.a	<i>n</i>
Didiniids	-0.259	-0.111	+0.022	+0.348	-0.102	-0.119	-0.238	+0.141	18
Lohman.	-0.439	+0.126	+0.360	+0.664	+0.066	-0.137	+0.042	+0.400	17
Stromb.	-0.560	+0.456	+0.426	+0.556	+0.259	+0.424	+0.313	+0.494	18
Ciliates	-0.583	+0.318	+0.325	+0.513	+0.247	+0.290	+0.147	+0.364	18
Ebria	-0.180	+0.415	+0.319	+0.108	+0.262	+0.323	+0.297	+0.571	14
HNF	+0.004	-0.089	+0.109	+0.445	+0.116	+0.041	-0.080	+0.043	15
Protozoa	-0.362	+0.266	+0.424	+0.591	+0.040	+0.170	+0.143	+0.373	18

Tab.19 presents spearman rank correlations between the different protozoan groups in the Pomeranian Bay in June / July 1994. All ciliate groups are strongly positively correlated, and the didiniids and the strombiids also with HNF. *Ebria*, however, shows a weak negative correlation to the HNF. While the most ciliates are probably primarily bacterivorous (SHERR and SHERR 1987), especially didiniids are known to feed also on other protozoa (DOLAN and COATS 1991). On the other hand, *Ebria* and some strombiid species are herbivorous (CAPRIULO et al. 1991), and many species of the latter are reported to be mixotrophic (STOECKER et al. 1987, LAVAL-PEUTO and RASSOULZADEGAN 1988).

Tab.19 Spearman rank correlation coefficients between different protozoan groups in the Pomeranian Bay in July 1994. Numbers in parentheses represent the numbers of data points. Bold numbers are significant at $p < 0.05$, numbers in italics are significant at $p < 0.1$.

	Didiniids	Lohmaniella	Strombiids	Ciliates	Ebria
Lohmaniella	+0.636 (15)	-	-	-	-
Strombiids	+0.641 (16)	+0.632 (15)	-	-	-
Ebria	+0.239 (13)	-0.052 (12)	+0.387 (13)	+0.387 (13)	-
HNF	+0.538 (14)	+0.527 (13)	+0.156 (14)	+0.147 (14)	-0.223 (11)

Protozoan standing stocks and distributions in the different regions - a comparison

HNF and ciliate concentrations and biomasses differed considerably between the different regions. In the Arabian Sea and the Gotland Sea, they were substantially lower than in the Pomeranian Bay, where they also showed the largest range (Tab.20). There, highest concentrations were found in the plume water originating from the lagoon, with peak concentrations for HNF of $12,000 \text{ cm}^{-3}$ (carbon $60 \mu\text{g dm}^{-3}$), and for ciliates 176 cm^{-3} (carbon $81 \mu\text{g dm}^{-3}$). However, HNF, HDIN and ciliate concentrations and biomasses from the Arabian Sea and the Gotland Sea were well within the range reported for the equatorial Pacific (VØRS et al. 1995) and the North Atlantic (BURKILL et

al. 1993b). VERITY et al. 1993 present HDIN distributions and biomasses in the latter region, which also were very similar to those found in the Arabian Sea during both monsoon periods. In both regions (the north Atlantic, VERITY et al. 1993 and the Arabian Sea, this study), HDIN cell numbers and biomasses were dominated by individuals $<20\mu\text{m}$. Another striking concurrence between the two regions are the low correlations between HDIN and Chl.a, and the much higher ones between HDIN and ciliates (Tab.17).

Tab.20 Protozoan abundances and carbon biomasses in the Indian Ocean (with the Gulf of Aden and the Red Sea), the Baltic Sea, the tropical Pacific (VØRS et al. 1995) and the North Atlantic (BURKILL et al. 1993b, VERITY et al. 1993). Data from SOROKIN et al. from the central tropical Indian Ocean, data from WEISSE from the Gulf of Aden and the Red Sea. Numbers in parentheses are increment factors (max/min. value), representing the range of concentrations.

Area / Source	HNF		HDIN		Ciliates	
	# / cm^3	$\mu\text{g} / \text{dm}^3$	# / cm^3	$\mu\text{g} / \text{dm}^3$	# / dm^3	$\mu\text{g} / \text{dm}^3$
Arabian Sea Sorokin et al.1985	208 - 1,560 (7.5)	3.1 - 19.2 (6.2)	-	-	10 - 300 (30)	0.09 - 4.9 (54.4)
Weisse 1989	615 - 1,240 (2.0)	-	-	-	-	-
This study SW-monsoon	304 - 1,243 (4.1)	0.94 - 7.25 (7.7)	8 - 29 (3.6)	0.57 - 15.47 (27.1)	657 - 7,839 (11.9)	0.27 - 16.72 (61.9)
This study NE-monsoon	812 - 1,630 (2.0)	1.79 - 2.21 (1.2)	13 - 60 (4.6)	1.07 - 6.74 (6.3)	108 - 8,748 (81)	0.17 - 6.21 (36.5)
Equ. Pacific Vørs et al. 1995	559	1.42	41	3.03	4,000	1.01
N. Atlantic Verity et al. 1993	-	-	2 - 67 3 - 414	0.1 - 3.5 1 - 18	-	-
Burkill et al. 1993b	-	-	HDIN + Ciliate Carbon Biomass: 6.5 - 9.8 $\mu\text{g} / \text{dm}^3$			
Baltic Sea	HNF		<i>Ebria tripartita</i>		Ciliates	
This study	# / cm^3	$\mu\text{g} / \text{dm}^3$	# / dm^3	$\mu\text{g} / \text{dm}^3$	# / dm^3	$\mu\text{g} / \text{dm}^3$
Gotland Sea	1,700	12.61	-	-	1,318	2.38
Pomeranian Bay 1993	428 - 3,458 (8.1)	3.14 - 72.55 (23.1)	18 - 6,050 (336)	0.04 - 11.98 (299.5)	1,230 - 12,229 (9.9)	3.69 - 35.78 (9.7)
Pomeranian Bay 1994	447 - 11,909 (26.6)	2.95 - 58.52 (19.8)	236 - 10,872 (46.1)	0.06 - 17.49 (291.5)	5,909 - 175,841 (29.8)	2.77 - 80.82 (29.2)

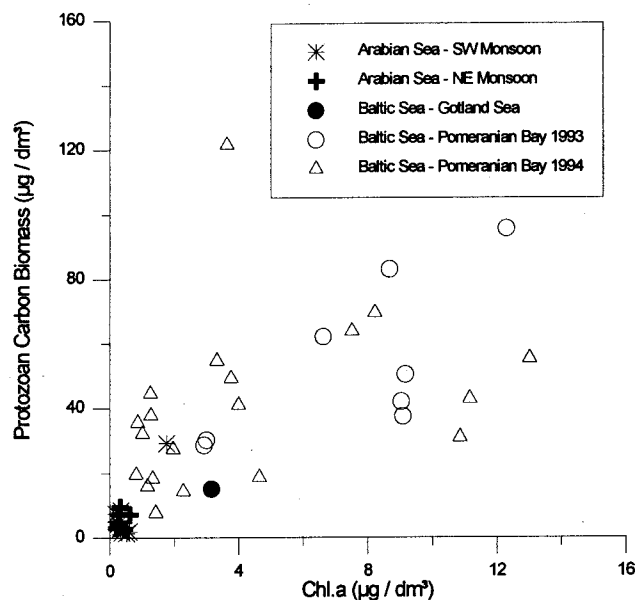


Fig.84 Protozoan biomass vs. Chl.a in all research areas.

Plotted across all regions, protozoan biomass was positively correlated with Chl.a (Fig.84, Tab.21). This was also found by BURKILL et al. (1993b) in the northeast North Atlantic, and by BURKILL et al. (1995) in the Bellinghousen Strait, Antarctica, pointing to a tight trophic relationship between protozoa and phytoplankton. The high positive correlation between HNF and Chl.a, however, will probably be an indirect effect: large blooming phytoplankton, which are largely responsible for the Chl.a signal, exude large quantities of DOC, on which bacteria can grow, the preferred food organism for HNF.

Tab.21 Spearman rank correlation coefficients between protozoa and Chl.a (left), and between different protozoan groups (right) for all cruises (data pooled). Numbers in parentheses represent the numbers of data points, bold numbers are significant at $p < 0.01$.

Chl.a				Protozoa		
HNF	Ciliates	HDIN/Ebria	Σ Protozoa	Cil. - HNF	Cil. - HDIN/Ebria	HNF - HDIN/Ebria
+0.807	+0.638	+0.236	+0.817	+0.568	+0.437	+0.104
(40)	(40)	(40)	(44)	(37)	(36)	(40)

4.2.3. Phytoplankton dynamics and grazing by microzooplankton

The Arabian Sea and its adjacent areas

Microzooplankton herbivory data from the northern Arabian Sea are available so far only for the inter-monsoon period for *Synechococcus* (BURKILL et al. 1993c). The authors found high growth and grazing rates, with up to 71% of the picocyanobacterial standing stock being consumed daily. They showed that growth and grazing was well balanced (with roughly 100% of production grazed daily), resulting in a steady state system exhibiting high turnover rates and minor changes in *Synechococcus* stock size. Steady state systems are typical for oligotrophic systems and prevail wherever phytoplankton biomasses remain constant over a long period of time (i.e. weeks or months, irrespective of short-term variability over a few days, BANSE 1994a). However, in situations where phytoplankton biomass accumulates (i.e. blooms develop), growth rates of phytoplankton must exceed the consumption rates of the zooplankton. On the other hand, when grazing rates exceed phytoplankton growth rates, the phytoplankton stock is reduced by grazers.

During the SW monsoon, the grazing impact on total phytoplankton (as Chl.a) was highest in the areas influenced by upwelling (US2 and OFZ); phytoplankton growth, however, still exceeded grazing by microzooplankton, resulting in a net increase in biomass. These experimental findings are well in agreement with the situation in the water column, where large phytoplankton was thriving in the upwelled water. Also for *Synechococcus* (as counted by epifluorescence microscopy), growth exceeded grazing, but both rates were much higher than for the total phytoplankton (Fig.15, Tab.4). For both Chl.a and *Synechococcus*, production and consumption increased in the upwelled water (OFZ) relative to the oligotrophic station SB1 (Tab.4). However, in absolute carbon units, *Synechococcus* made up only a few percent of the total phytoplankton carbon consumption (Fig.16), which at these stations was largely dominated by diatoms and other large phytoplankters. However, the high number of large fecal pellets (ca. $280 \times 40 \mu\text{m}$) found in the bloom water points to a high grazing pressure on the large phytoplankton by mesozooplankton.

During the NE monsoon, grazing experiments were analyzed not only using Chl.a as a proxy for total phytoplankton biomass, but also by flow cytometry to estimate dynamics of the autotrophic ultraplankton. The Chl.a signal integrates over all the different phytoplankton groups, each of which may experience different trophodynamics. Large phytoplankton will predominantly contribute to the integrated grazing signal, as it makes up the bulk of the chlorophyll signal.

In the case of Chl.a, growth exceeded grazing at most stations, except for the inner Gulf of Aden (GA2) and the southernmost station in the Red Sea (RS1). There, both were very high and roughly in balance (Tab.6, Fig.27). In terms of absolute phytoplankton carbon amounts consumed, the importance of the ultraphytoplankton decreased towards the eutrophied stations of the inner Gulf of Aden and the southern Red Sea. There, large phytoplankton not accounted for by the flow cytometer made up the bulk of the autotrophic carbon consumed. At the outer stations, however, phytoplankton was almost entirely consumed as ultraphytoplankton carbon (sum of all analyzed autotrophic ultraplankton groups); with the small eukaryotes being most important. Over 50% of ultraphytoplankton carbon was consumed in the form of small eukaryotes, up to 31% as *Synechococcus*, up to 16% as *Prochlorococcus* and only up to 8% as large eukaryotes (Fig.30).

This hierarchy may be typical for the mesotrophic conditions of the NE monsoon, with measurable amounts of new nutrients in the euphotic zone, favouring pico-eukaryotes and *Synechococcus* over *Prochlorococcus*. However, in more oligotrophic conditions, where *Prochlorococcus* has often been shown to be the dominant member of the autotrophic ultraplankton community (e.g. VELDHUIS and KRAAY 1993, MOREL et al. 1993, CAMPBELL and VAULOT 1993), they will probably play a more important role as diet for protozoan grazers. Nevertheless, in the conditions encountered during the NE monsoon, pico-eukaryotes appeared to dominate autotrophic ultraplankton carbon dynamics, due to their high biomass. Eukaryotic algae have also been shown

to dominate autotrophic ultraplankton biomass in other regions (e.g. in the Sargasso Sea, LI et al. 1992).

While consumption of total phytoplankton showed a wide range of variation across the different trophic systems with distinct peaks, consumption of *Synechococcus* (in the SW monsoon, Fig.16) and of total autotrophic ultraplankton (NE monsoon, Fig. 30A) was relatively constant, showing a much smaller range. In the NE monsoon, phytoplankton was almost quantitatively consumed as ultraplankton, only in the eutrophic Red Sea, large phytoplankton was most important (Fig.30A). This observation supports the idea of a basic evolutionary old, regenerating microbial community, which is superimposed by larger organisms and new production at times of high nutrient availability (SMETACEK et al. 1990).

No experiments on bacterivory were carried out during the NE monsoon, so that this information is still lacking for this monsoon period. Nevertheless, one experiment to estimate bacterivory was conducted during the SW monsoon at the oligotrophic station US0, which at the time was unaffected by upwelling. Daily bacterial carbon consumption rates amounted to about $25 \mu\text{g dm}^{-3} \text{d}^{-1}$ (section 3.1.4, Tab.5), which is roughly one order of magnitude higher than I estimated for *Synechococcus* in the same area ($3.4 \mu\text{g dm}^{-3} \text{d}^{-1}$, section 3.1.3., Tab.4), and slightly more than WEISSE (1989) presents for the Red Sea ($1.6 - 15.8 \mu\text{g dm}^{-3} \text{d}^{-1}$) and Gulf of Aden ($5.2 - 17.3 \mu\text{g dm}^{-3} \text{d}^{-1}$). In the experiment, bacteria were counted by epifluorescence microscopy after staining with Acridine Orange. As this technique possibly masks the dim red autofluorescence of *Prochlorococcus*, they were probably counted as heterotrophic bacteria, thereby significantly overestimating heterotrophic biomass, as was demonstrated by CAMPBELL et al. (1994). Irrespective of this possible overestimation, the experiment shows that heterotrophic bacterial carbon and picophytoplankton carbon (*Prochlorococcus*, *Synechococcus* and pico-eukaryotes) may be of equal importance for consumers of pico-sized prey, at least in oligotrophic situations. 77% of the bacterial standing stock was removed by grazing per day, demonstrating the extremely high grazing pressure heterotrophic bacteria are subject to. Primary bacterivores were protozoa $<15\mu\text{m}$; in the treatments incubated with this size fraction exclusively, grazing pressure was even higher (87% stock grazed per day) than that of total microzooplankton ($<200\mu\text{m}$).

At two stations (US2 and SI) during the NE monsoon, two subpopulations of *Prochlorococcus* could be discriminated by their different fluorescence intensities (Fig.28). While experiencing comparable grazing pressure, the "bright type", exhibiting stronger fluorescence signals, apparently did not grow under the experimental conditions, resulting in a dramatic decrease in cell numbers. Whether this is an artefact of the experimental conditions or reflects reality in the water column, I cannot say. Strikingly, however, LANDRY et al. 1995b found a similar effect in the equatorial Pacific: grazing on *Prochlorococcus* exceeded growth by a factor of 3, and *Prochlorococcus* exhibited very low specific growth rates. The authors explain this by suboptimal growth rates at surface irradiances for *Prochlorococcus*, for which VAULOT et al. (1995) reported highest division rates in subsurface waters (at 30m). As the incubation water for the experiments presented here was taken from the upper euphotic zone (20m), and experiments were conducted under simulated *in situ* conditions on board, this could have affected the experiments as well.

Two subpopulations were also detected for *Synechococcus* in the Gulf of Aden and the Red Sea. This diversification is a well known phenomenon and has been associated with different sets of phycobilin derivatives (e.g. OLSON et al. 1988). Grazing rates on the different pigment types, however, have not been reported so far. Growth and grazing was slightly higher for the "bright type" in the dilution experiments (Tab.8), but dramatically lower in the size fractionated light-dark experiment conducted at RS2 (Fig.35, Tab.9). Unfortunately it is not possible to resolve these contradicting results due to the low number of experiments.

The Gotland Sea (Baltic proper)

In the Gotland Sea 1994, grazing pressure on *Synechococcus* was higher than on the eukaryotic autotrophic ultraplankton in all experiments (generally over 100% of gross production grazed per day, Tab.10); in terms of carbon consumption, only the nano-eukaryotes were of comparable importance, due to their larger size. However, pico-and nano-eukaryotic production was not completely grazed (generally less than 100% grazed per day, Tab.10). If these experimental findings were extrapolated to the field, *Synechococcus* would have suffered a decrease in abundance, as grazing exceeded gross biomass production; the contrary would apply to the eukaryotic ultraphytoplankton. A high grazing pressure on *Synechococcus*, with growth and grazing well in balance (82 - 115% of production grazed per day), was reported by DETMER et al. (1993). Grazing estimates for ultraphytoplankton from the Tvärminne area during typical summer situations showed that HNF were feeding on autotrophic picoplankton vigorously (KUOSA and MARCUSSEN 1988, KUOSA 1991). These results confirm the general notion of a tightly coupled microbial food web in the oligotrophic euphotic zone, with high turnover rates, and growth and grazing roughly in balance.

Although the Gotland Sea was more oligotrophic in terms of available macronutrients in the euphotic zone than the western Arabian Sea during the NE monsoon, absolute biomasses and carbon turnover rates were about an order of magnitude higher in the Baltic proper. Total carbon consumption rates of all phytoplankton groups by microzooplankton as measured by flow cytometry ranged from $3.7 \mu\text{g dm}^{-3} \text{d}^{-1}$ (SB2) to $43.8 \mu\text{g dm}^{-3} \text{d}^{-1}$ (GA2) in the Arabian Sea, and from $58 \mu\text{g dm}^{-3} \text{d}^{-1}$ to $118 \mu\text{g dm}^{-3} \text{d}^{-1}$ in the Gotland Sea. When the latter values are compared to phytoplankton carbon consumption rates by mesozooplankton (max. $3.6 \mu\text{g dm}^{-3} \text{d}^{-1}$ for the Gotland Sea, MEYER-HARMS 1996), the dominance of microzooplankton grazing for the carbon turnover in the euphotic zone is clearly demonstrated: mesozooplankton only account for roughly 10% of the carbon turnover mediated by the microzooplankton.

The Pomeranian Bay (southern Baltic Sea)

In the Pomeranian Bay 1993, dilution grazing experiments indicated that phytoplankton growth in the fresh outflow plume was hampered by light limitation; this observation was confirmed by primary production measurements during the driftexperiments (POLLEHNE et al. 1995). Grazing exceeded growth considerably (up to 176% of daily phytoplankton production grazed) at the first station. However, with increasing mixing, phytoplankton production increased while microzooplankton grazing decreased (only 51% of daily production grazed). Absolute phytoplankton carbon consumption rates in the Pomeranian Bay ranged between 93 and $140 \mu\text{g dm}^{-3} \text{d}^{-1}$ (corresponding to 24 - 38% of phytoplankton standing stock grazed per day). These numbers are between one and two orders of magnitude higher than grazing estimates of adult copepods in the same water (max. $2.94 \mu\text{g dm}^{-3} \text{d}^{-1}$, MEYER-HARMS 1996). Hence, in the Pomeranian Bay, phytoplankton carbon consumption rates by mesozooplankton amounted to only 3 - 4 % of the consumption rates by microzooplankton.

Tab.22 Compilation of carbon consumption rates by microzooplankton (<200 μm) in the different research areas (numbers in $\mu\text{g dm}^{-3} \text{d}^{-1}$).

	Consumption of total phytoplankton	Consumption of Ultraphytoplankton	Consumption of heterotrophic bacteria
Arabian Sea			
SW monsoon			
Oligotrophic southern stations	19.81	3.38 (only Syn.)	24.92
Upwelling diatom bloom	118.21	-	-
Northern Somali Current and Basin	47.79 - 85.51	8.4 (only Syn.)	-
NE monsoon			
Somali Current and Somali Basin	2.31 - 26.67	3.73 - 28.1	-
Gulf of Aden and south. Red Sea	71.15 - 146.17	5.28 - 43.8	-
Baltic Sea			
Gotland Sea	-	57.72 - 118.2	-
Pomeranian Bay	93.25 - 139.65	-	-

A comparison of carbon consumption rates between the different regions (Tab.22) shows that absolute phytoplankton carbon consumption rates by microzooplankton in the Baltic Sea and the eutrophic stations in the Arabian Sea were of comparable magnitude. However, in more oligotrophic situations (southern stations during the SW monsoon, Somali Current and Somali Basin during the NE monsoon) showed considerably lower values. At the southernmost oligotrophic station during the SW monsoon, consumption of bacteria and phytoplankton were of comparable magnitude. There, *Synechococcus* contributed to a very small extent; probably other ultraphytoplankton (*Prochlorococcus* and eukaryotic algae) made up the bulk of phytoplankton prey for microzooplankton. Consumption rates of ultraphytoplankton in the Gotland Sea were considerably higher as in the Arabian Sea, however, this might partly be a consequence of the different sensitivities of the two flow cytometers used (see section 4.1.1.).

4.2.4. Multiple trophic interactions within the microbial food web

The number of trophic interactions within the microzooplankton community and the size of the principal grazers of autotrophic ultraplankton is an important variable when estimating carbon flux in ultraplankton dominated systems. However, few investigations have focussed on this question. Eukaryotic and prokaryotic bacterivores have been found in the bacterial size class (FUHRMAN and MCMANUS 1984, GUERRERO et al. 1986); WIKNER and HAGSTRÖM (1988) present experimental evidence for the existence of four trophic levels in the size class <12 μm levels, with the primary bacterivores being smaller than 3 μm and being controlled by the larger protozoa. Such a "trophic cascade" between the predators of the first-order consumers and the prey is a well known feature in terrestrial ecology and limnology (CARPENTER et al. 1985, STRONG 1992), and has recently also been described for marine pelagic food webs of different trophic status (RASSOULZADEGAN and SHELDON 1986, WIKNER and HAGSTRÖM 1988, WEISSE and SCHEFFEL-MÖSER 1991, HANSEN et al. 1993).

In the Arabian Sea during the NE monsoon and in the Gotland Sea, the serial dilution technique was combined with pre-incubation size fractionation to gain information of trophic interactions within the microbial food web. The removal of specific size classes of the microbial food web may dramatically alter the interactions of the different microbial compartments, meaning that these experiments do not reflect the *in situ* conditions in the water column and should not be interpreted as such. They may, however, give information about the number of trophic steps within the microbial food web, which otherwise would remain hidden in the "microzooplankton" black box.

The Arabian Sea during the NE monsoon

For the Red Sea, WEISSE (1989) reports on a two-step protozoan food chain: heterotrophic bacteria profit from larger protozoa feeding on the major bacterivores, the heterotrophic nanoflagellates (HNF). The presented data imply that this holds also true for the autotrophic ultraplankton of the Arabian Sea and its adjacent areas. The increased grazing pressure on the ultraphytoplankton in the absence of grazers $>10\mu\text{m}$ and $>3\mu\text{m}$ at all stations implies that primary consumers of ultraplankton were grazed by nanozooplankton and microzooplankton, which may act as mediators in carbon transfer from ultraphytoplankton to higher trophic levels. The extent of this transfer largely depends on the metabolic rates of the primary consumers of the autotrophic ultraplankton. However, if predators around $3\mu\text{m}$ in size with high metabolic rates (and representing the most abundant protozoan size class) contribute predominantly to the consumption of ultraphytoplankton in the area, then a major fraction of carbon fixed by picophytoplankton will be remineralized through respiration. The current observations suggest the existence of potent grazers in that size range, significantly contributing to the removal of prokaryotic and eukaryotic ultraphytoplankton. Small HNF are known to be mainly responsible for the removal of heterotrophic bacteria (AZAM et al. 1983, FENCHEL 1986), but also to consume coccoid cyanobacteria *in situ* (CARON et al. 1991), while larger HNF and dinoflagellates have been reported to be primarily herbivorous (SANDERS 1991). PARLOW et al. (1986) report that the small heterotrophic nanoflagellate *Pseudobodo* ($2 \times 4 \mu\text{m}$) is capable of rapidly reproducing on the pico-eukaryotic alga *Micromonas pusilla* ($1\text{-}2\mu\text{m}$) as sole food source. It is shown here that small HNF in the Arabian Sea consume *Prochlorococcus*, *Synechococcus* and pico-eukaryotes at high rates, and that they are able to quantitatively remove their daily biomass production.

Calculations assuming HNF being the only consumers of autotrophic ultraplankton carbon imply that they could well be able to satisfy their daily carbon demand exclusively from this source (Tab.23). If a gross growth efficiency of 50% (FENCHEL 1986, BERNINGER et al. 1991) is assumed (i.e. 50% of the ingested prey carbon can be used for reproduction by the grazer), a flagellate would have to ingest four times its own biomass per day in order to be able to double its biomass. The daily rations (i.e. ingested prey carbon as percentage of grazer body carbon) of ultraphytoplankton biomass in the unfractionated treatments estimated in this study ($<200\mu\text{m}$, with the entire microzooplankton community present) approach or exceed this value (Tab.23), indicating that autotrophic carbon may well play an important role for the nutrition of small HNF. However, this calculation likely overestimates the contribution of ultraphytoplankton to HNF nutrition, as dinoflagellates and ciliates will also feed on ultraphytoplankton, and heterotrophic bacteria will also be a major diet for HNF. Despite these caveats, it nevertheless shows that HNF in fact can apply a viruous grazing pressure on ultraphytoplankton. WEISSE (1989) reports on daily ingestion rates of heterotrophic bacteria by HNF in the Red Sea of 696 cells per HNF and day, corresponding to a carbon ingestion rate of 10.4 pg per individual and day. The per cell ingestion rates presented in Tab.23 are in the same order of magnitude, indicating that HNF may well live on a mixed diet of auto- and heterotrophic prey. There is also direct microscopical evidence for the ingestion of autotrophic ultraplankton by HNF: epifluorescence observations of DAPI-stained HNF revealed a large number of HNF $<3\mu\text{m}$ containing one or two whole or partly digested cells of *Synechococcus*, which can be identified reliably by their bright yellow

autofluorescence under blue excitation. Although some dinoflagellates also contained *Synechococcus* cells, their frequency was much lower than the *Synechococcus* - containing HNF.

From Tab.23, it is possible to estimate the grazing pressure by larger predators on the primary consumers. Tab.23 shows per cell ingestion rates (i.e. prey ingested per individual and day) for different size classes. It can be seen that these are highest in the $<10\mu\text{m}$ (US2, upper panel) and $<3\mu\text{m}$ fractions. If we assume that the "true" individual ingestion rate of a grazer was not affected by the size fractionation (i.e. a HNF cell in the $<200\mu\text{m}$ fraction does not ingest significantly more or less prey cells per unit time as in the $<10\mu\text{m}$ fraction), then the higher ("apparent") per cell ingestion rates in the smaller fractions (as depicted in Table 23) represents in reality an elevated HNF biomass in these fractions.

Tab.23 "Apparent" per cell ingestion rates of ultraphytoplankton by HNF at two stations during the NE monsoon (US2 and SI). Values are given in cells and carbon units ingested per individual and day, as well as daily carbon rations of the grazer (prey carbon ingested per day as % of grazer cell carbon).

	"Apparent" Ingestion per HNF and Day	$<200\mu\text{m}$	$<20\mu\text{m}$	$<10\mu\text{m}$	$<3\mu\text{m}$	$<2\mu\text{m}$
US2						
<i>Prochlorococcus</i>	Cells	16	22	32	3	-
	pg Carbon	1.51	2.01	2.98	0.27	-
	Daily Ration	69%	93%	137%	33%	-
<i>Synechococcus</i>	Cells	17	20	29	4	-
	pg Carbon	2.90	3.42	5.02	0.67	-
	Daily Ration	133%	157%	231%	83%	-
<i>Eukaryotes</i>	Cells	2	3	4	0.1	-
	pg Carbon	4.80	6.28	8.84	0.24	-
	Daily Ration	221%	289%	406%	30%	-
Σ Pico	pg Carbon	9.21	11.72	16.84	1.17	-
	Daily Ration	423%	538%	774%	145%	-
SI						
<i>Prochlorococcus</i>	Cells	-	-	30	39	18
	pg Carbon	-	-	2.80	3.56	1.66
	Daily Ration	-	-	216%	570%	265%
<i>Synechococcus</i>	Cells	-	-	25	28	17
	pg Carbon	-	-	4.34	4.94	2.90
	Daily Ration	-	-	334%	790%	464%
<i>Eukaryotes</i>	Cells	-	-	4	4	1
	pg Carbon	-	-	8.77	9.49	2.26
	Daily Ration	-	-	674%	1519%	361%
Σ Pico	pg Carbon	-	-	17.21	19.95	8.18
	Daily Ration	-	-	1323%	3192%	1309%

Furthermore, it can be assumed that the relative increase in HNF biomass in the smaller fractions was caused by reduced predation on the HNF in these fractions. Hence, the relative increments in the apparent per cell ingestion rates should be proportional to the reduction in feeding pressure

that larger protozoan predators applied on the smaller grazers in the larger size fractions and allow a direct estimation of predation.

If we take all these assumptions to be reasonable, then the respective biomass ingestion increment factors in the small relative to the large fractions ($\text{Ing.}_{\text{Small}} / \text{Ing.}_{\text{Large}}$) gives the percentage of HNF biomass that was removed per day by predators in the larger size fraction. For instance, in the size class 20 - 200 μm at US2 (Tab.23), the increment factor is $11.72 / 9.21 = 1.27$; hence 27% of HNF biomass was removed by predators in the size class 20-200 μm per day. Likewise, protozoa 10 - 20 μm removed 44% of grazers <10 μm ($16.84 / 11.72 = 1.44$), and total protozoa >10 μm removed 83% of grazers <10 μm ($16.84 / 9.21 = 1.83$). At SI, data are available only for the size class 3-10 μm : 16% of HNF <3 μm were removed by predator of this size class ($19.95 / 17.21 = 1.16$). Combining these findings with microscopical evidence (the majority of HNF being <3 μm), it can be generally stated that small HNF, which applied the main grazing pressure on picautotrophs, are likely to experience considerable predation by larger protozoa.

The Gotland Sea (Baltic proper)

Evidence for the presence of multiple trophic steps within the microzooplankton community in the Gotland Sea is much weaker as in the Arabian Sea. Only in the first experiment, grazing on *Synechococcus* increased when grazers >20 μm and >5 μm were removed (Tab.10). The first experiment also revealed some interesting aspects of size fractionation. This experiment was sub-sampled at $t=18\text{h}$ to account for diel changes in growth and grazing activity. As could be expected, grazing exceeded growth during the dark period in the unscreened (<200 μm) sample. In the smaller fractions, another effect evolved: over the first 18h, grazing was much lower in the fractions <20 μm and <5 μm than in the fraction <200 μm ; in the fraction <5 μm , it almost decreased to zero. During the second period however (18 - 42h), grazing pressure in the small fractions increased dramatically (Fig.48). These observations may reflect two effects: (1) a filtration trauma for flagellates in the first few hours, and (2) the sudden increase in grazer biomass due to the absence of large predators. Filtration through the 5 μm filter removed larger grazers on both *Synechococcus* and HNF; the fact that grazing on *Synechococcus* almost ceased in this fraction could point to a major importance of larger *Synechococcus* - grazers in this area; on the other hand, grazing on *Synechococcus* in the <5 μm fraction increased sharply in the 24h following the first 18h. Relieved from the pressure by their predators, the HNF obviously were able to increase their biomass in a short period of time. During the 24h period following the initial 18h, grazing pressure on *Synechococcus* increased by a factor of 3.4 relative to the first 18h, which would correspond to a specific grazer growth rate μ of 1.22 d^{-1} . If we assume the increase in grazing pressure to reflect the increase in grazer biomass, then $\mu = 1.22$ can be deduced from $N_t = N_{t_0} * e^{\mu t}$; with $e^{\mu} = 3.4$. This is not an unreasonably high growth rate for HNF; in fact, much higher growth rates have been reported in laboratory cultures at temperatures similar to those encountered during this study (e.g. SHERR et al. 1983, PARSLow et al. 1986). In <1 μm filtrates, KUOSA (1991) found HNF growth rates of up to 1.98 d^{-1} . After an apparent lag phase during the first 18h, HNF in the <5 μm filtrate were obviously able to increase their biomass within a day.

In the other experiments, grazing pressure on any of the phytoplankton groups was affected by size fractionation only to a small extent, with grazing in the small fractions similar or even smaller than that of the total microzooplankton (Tab.10, Fig.50). Hence, in the Baltic proper, there was apparently not one confined size class responsible for the bulk of the grazing on the ultraphytoplankton, as it was the case in the Arabian Sea. Larger grazers (i.e. >5 μm and >20 μm) were apparently able to exert a considerable grazing pressure on the ultraphytoplankton. Although there was undoubtedly predation on small grazers by larger protozoa and metazoa, this did not have a recognizable effect on the autotrophic ultraplankton, as in the Arabian Sea at the time of the NE monsoon.

The size fractionated grazing data presented here imply a two-step transfer of carbon to larger predators, at least for the Arabian Sea, as had been demonstrated earlier for the Red Sea and Gulf of Aden (WEISSE 1989). On the one hand, this means that a certain amount of carbon is passed from the autotrophic ultraplankton via small flagellates and larger protozoa to the mesozooplankton; on the other hand, the high turnover rates and the small size of these primary consumers imply that the amount of ultraplanktonic new and regenerated production reaching higher trophic levels will be smaller than in systems with larger protozoan herbivores, and recycling within the euphotic zone will be rather large. In the Baltic proper, however, the different trophic levels within the microbial food web appeared to "overlap" to a higher extent than in the Arabian Sea since size fractionation had a clear impact on the ultraplankton dynamics in the latter region, whereas this effect was not so evident in the Baltic proper.

4.3. The concept of the microbial food web in pelagic ecosystems of different trophic status

Probably the most comprehensive concept to characterize and explain the specific features of eutrophic (in-shore areas, estuaries, upwelling areas) and oligotrophic systems (generally oceanic environments) is the concept of new and regenerated production (DUGDALE and GOERING 1967). *New* production regimes are based on the allochthonous supply of biomass-limiting nutrients, i.e. nutrients from without the euphotic zone, whereas *regenerating* regimes fully depend on autochthonous nutrients, i.e. on nutrients recycled within the system. New and regenerating systems are extremes along a continuum of various intermediate forms, which can be specified by the *f*-ratio: the ratio of primary production based on new nutrients (basically nitrate in marine environments) to that based on regenerated nutrients (generally ammonium and urea). New production systems are generally characterized by large (i.e. $>5\mu\text{m}$) algae, often forming blooms of one or few species, followed by intensive particle sedimentation events (e.g. SMETACEK 1985). In fact, EPPLEY and PETERSON (1979) have defined the amount of production leaving the euphotic zone by sedimentation as the share of new production.

The classical food chain paradigm (phytoplankton \rightarrow zooplankton \rightarrow fish) was largely a reflection of new production systems, as their protagonists could be studied easily due to their large size. With better microscopes and new experimental techniques available, this simple view of a marine food chain was challenged by POMEROY (1974) and STEELE (1974), who introduced the concept of a *microbial food web*, which was further elaborated by WILLIAMS (1981), and AZAM et al. (1983).

The role of protozoa

Protozoa play three important roles in the microbial food web. Firstly, they are the principal grazers of heterotrophic bacteria and small autotrophs and in that respect control their standing stocks; secondly, they are preferred prey organisms for larger zooplankton (SHELDON et al. 1986, STOECKER and MCDOWELL CAPUZZO 1990, GIFFORD and DAGG 1991, DOLAN 1991, HANSEN et al. 1993), thus representing the "missing link" of SHERR et al. (1986c) between the bacteria-sized prey and the crustacean grazers (e.g. copepods), whose grazing apparatus is too coarse to retain particles of bacterial size (NIVAL and NIVAL 1976, O'CONNORS et al. 1980). This especially applies to oligotrophic ocean environments, where the vast majority of the phytoplankton is smaller than $2\mu\text{m}$ (FOGG 1995). The third role for protozoa is also most important in oligotrophic environments: due to their high metabolic rates, they are potent remineralisers of inorganic nutrients (BERMAN et al. 1987, BERMAN 1991, CARON 1991). Possibly, they also play an important role in making colloid-bound iron available to phytoplankton, as demonstrated in laboratory experiments by BARBEAU et al. (1996).

Unlike the larger mesozooplankton, whose reproduction rates last several weeks (KLEIN BRETELER et al. 1982), protozoa have growth rates equal to, or even exceeding those of their prey (e.g. GOLDMAN and CARON 1985). This places them into a central position within the *microbial*

loop (AZAM et al. 1983), were they enable phytoplankton growth by providing regenerated nutrients (WILLIAMS 1981). The phytoplankton, on the other hand, nourishes the heterotrophic bacteria by exudation, which in turn form the diet for protozoa. These links make the microbial loop a prerequisite for regenerated production *sensu* DUGDALE and GOERING (1967). In regenerating systems, protozoan grazing on small phytoplankton and their growth rates are just two sides of the same medal. High protozoan grazing rates reduce the ultraplankton standing stock, but by making recycled nutrients available to the rest of the phytoplankton, they allow for sufficiently high growth rates to sustain a constant biomass level. When this interaction is running smoothly over a longer period of time, a true steady state system (where growth completely compensates for grazing losses), typical for oligotrophic conditions, may develop under the assumption that sedimentation losses are negligible or are compensated by diffusive nutrient fluxes into the euphotic zone.

While in oligotrophic environments the remineralising activity and "link"-function of protozoa is a crucial part of regenerating systems, their role is less well defined in eutrophic environments. Blooms of large phytoplankton (i.e. cells unavailable to protozoan grazers) are triggered by a combination of environmental preconditions, such as the availability of new nutrients (nitrate in the marine environment, DUGDALE and GOERING 1967), a deepening of the euphotic zone beneath the mixed layer depth or vice versa (SVERDRUP 1953), and the absence of large crustacean grazers at the onset of the bloom (BANSE 1994b). Protozoa play only a minor role in this scenario. They will, however, profit from the bloom, as the microbial food web with all its components will also be spiked by the new nutrients and the dissolved organic carbon exuded by the large phytoplankton (e.g. FOGG 1983). This was demonstrated clearly in the diatom bloom at the upwelling station US2 during the SW monsoon (section 3.1.2, Fig.12), where protozoan biomass was roughly an order of magnitude higher than at the non-blooming stations nearby; however, most of this biomass increase was due to increased cell sizes rather than to increased concentrations (Fig.9 - 11, Fig.14). In a seasonal survey in Kiel Bay, SMETACEK (1981) found protozoan biomass to be five-fold higher in phytoplankton blooms than in regenerating phases. In a freshwater environment, WEISSE et al. (1990) showed that the microbial loop responded quickly to the spring bloom and dominated carbon turnover. However, with large omnivorous zooplankton exploiting the bloom, protozoa will be preyed upon at a similar rate as the large phytoplankton, due to their similar sizes.

Thus it seems that the importance of the protozoan community (defined as catalyst for the functioning of the system) is relatively lower in eutrophic as compared to oligotrophic systems. Absolute biomasses and turnover rates of the protozoa (both in the role of grazers/predators, and as prey) are naturally much higher in eutrophic systems as in oligotrophic ones, as discussed above. Hence, the microbial loop as nutrient recycling machine is by no means less active in eutrophic as in pure regenerating systems, but it becomes less obvious in the presence of thriving large phytoplankton.

The role of autotrophic ultraplankton

It is now generally agreed that autotrophic communities in oligotrophic environments are dominated by very small phytoplankton (i.e. $<5\mu\text{m}$, mostly $<2\mu\text{m}$, LI et al. 1983, STOCKNER 1988, LENZ 1992, MAGAZZÙ and DECEMBRINI 1995, FOGG 1995). Why is this so? The main reason is probably the high nutrient uptake efficiency due to the higher surface to volume ratio of picoplankton, helping them to exploit even smallest amounts of regenerated nutrients (KRUPATKINA 1990), thus maintaining very high specific growth rates. Furthermore, LENZ (1992) makes the point that this advantage over larger algae still increases with rising temperatures. Also, gravitational sinking rates of picoplankton cells are very low, allowing them to remain within the light flooded mixed layer. The larger phytoplankton, on the other hand, suffer from higher sinking rates at slower specific growth rates. Under oligotrophic conditions, this prevents the

establishment of high biomasses of large phytoplankton in the euphotic zone, despite a very low grazing pressure (RIEGMAN et al. 1993).

The relative ecological importance of ultraphytoplankton as compared to the larger nano- and microphytoplankton decreases with increasing trophic status. The occurrence of both *Prochlorococcus* (in the Arabian Sea, Tab.13) and *Synechococcus* (in the Pomeranian Bay, Tab.14) was negatively correlated to Chl.a. However, there seem to be some profound differences between the major components of the picoautotrophic community: while picocyanobacteria and pico-eukaryotic algae are ubiquitous in marine, brackish and freshwater environments (JOHNSON and SIEBURTH 1982, ITURRIAGA and MITCHELL 1986, STOCKNER 1988, KUPARINEN and KUOSA 1993), and thrive also under eutrophic conditions (where it is largely concealed by blooming of larger algae), *Prochlorococcus* seems to be restricted to true oligotrophic, subtropical and tropical oceanic waters (OLSON et al. 1990, VELDHUIS and KRAAY 1990, CAMPBELL and VAULOT 1993, GOERICKE and WELSCHMEYER 1993, CAMPBELL et al. 1994, see also Tab.16).

As discussed above, these tiny prokaryotic autotrophs seem to thrive only on reduced nitrogen compounds, which are available in regenerating systems exclusively. From an evolutionary point of view, it is interesting to speculate that the oceanic *Prochlorococcus* might have evolved their distinct features in an ocean poor in oxidised nitrogen compounds, and in that respect the oligotrophic open oceans would be evolutionary resorts for *Prochlorococcus*. Recent rRNA fingerprint analysis indicated that the oceanic prochlorophyte *Prochlorococcus* is much closer related to oceanic *Synechococcus* than to the freshwater prochlorophyte species *Prochlorothrix* and *Prochloron*, despite similar photosynthetic pigment sets (URBACH et al. 1992). The authors conclude that the order prochlorocales should be abandoned and reclassified in the cyanobacteria. Furthermore, they conclude that the oceanic *Prochlorococcus* separated from *Synechococcus* relatively recently. Warm periods in recent geological history (possibly associated with Milankovic cycles) could have caused an extensive nitrate deficiency in the upper ocean due to an increased stratification and associated reduced vertical NO_3^- flux into the euphotic zone. A reduced nitrate availability in the surface layers of the ocean is believed to have contributed to reduced vertical particle flux in the recent earth's history (CODISPOTI 1989). The evolution of a very small autotroph, specialized on reduced nitrogen compounds exclusively, could have been favoured in these warm, NO_3^- deficient periods (also taking into consideration the allometric growth advantage of small algae relative to large algae at higher temperatures, LENZ 1992).

The question of why there are no *Prochlorococcus* in the oligotrophic Baltic proper leads to the question of how oligotrophic conditions are defined. Generally, the availability of "new" nutrients is taken as a definition, e.g. the high ambient nutrient levels at the onset of the spring bloom. Compared to the conditions in spring, the summer period in the Gotland Sea may be regarded "oligotrophic", as the euphotic zone is practically free of nitrate; however, compared to the mesotrophic Arabian Sea during the NE monsoon with low amounts of nitrate available, the Gotland Sea in summer sustains much higher biomasses of protozoa and phytoplankton. This may be due to the spatially confined geographic situation of the Baltic Sea, with high nutrient inputs through the rivers throughout the year. Although most of this is turned over and buried in the sediments of coastal regions, it nevertheless propagates the pelagic biomass levels during the oligotrophic period to a level that is much higher than in oligotrophic oceans. Also, the regularly occurring extensive blooms of filamentous N_2 -fixing cyanobacteria in the Baltic proper spike the system with new, albeit reduced nitrogen. Another considerable input of "new" nitrogen is the atmospheric fallout in this area.

Cascading trophic interactions within the microbial food web

The presence of multiple trophic steps within the nanoplankton size class has been described for different marine environments (RASSOULZADEGAN and SHELDON 1986, WIKNER and HAGSTRÖM 1988, WEISSE 1989, WEISSE and SCHEFFEL-MÖSER 1991, this study). The removal of higher

trophic levels had measurable repercussions on lower trophic levels. However, this might not always be the case (WEISSE and SCHEFFEL-MÖSER 1991, this study).

These observations lead to the question of what controls the flux of energy in the microbial food web. Is it the availability of substrate at the lowest trophic level ('bottom-up'), or is it predation at the respective highest trophic level ('top-down')? A top-down effect, or *trophic cascade* (POWER 1992, STRONG 1993) applies if a removal of secondary consumers has an effect on the basic trophic level: low secondary consumer biomass (-) → high primary consumer biomass (+) → low picoplankton biomass (-). This concept of a trophic cascade is contrary to the view that biomass at higher trophic levels is entirely controlled by substrate availability at the lowest trophic level (bottom-up-control): high nutrient concentrations (+) → high picoplankton biomass (+) → high primary consumer biomass (+) → high secondary consumer biomass (+). In the bottom-up concept, the concentrations of all components are positively correlated, while the top-down concept predicts concentrations of successive trophic levels to be negatively correlated (LAMPERT and SOMMER 1993).

The lowest trophic levels in the microbial food web (i.e. bacteria and autotrophic picoplankton) are always under top-down control, as grazing pressure on picoplankton by small protozoa is ubiquitous. The large phytoplankton (>5µm), on the other hand, can be generally be regarded to be bottom-up controlled: when nutrients and light are available at sufficient amounts, a bloom may develop. However, when large grazers are present at the onset of the bloom (e.g. in the North Pacific, PARSONS and LALLI 1988) a bloom cannot develop despite the availability of bottom-up resources. On the other hand, the microbial food web may also experience bottom-up effects, when new nutrients enter the euphotic zone. Then, biomasses of all components of the microbial food web will increase, however not to the same extent as the large (>5µm) phytoplankton. Their response will be a surge uptake of the new nutrients, followed by a rapid biomass accumulation. Their possible grazers (large microzooplankton and mesozooplankton) will then take advantage of the situation and also increase their biomass. In oligotrophic (regenerating) systems, grazing and nutrient regeneration by protozoa cannot be separated; the population will be controlled *and* stimulated by protozoan grazing. In this situation, the 'top-down' - 'bottom-up' dichotomy becomes irrelevant. Both effects cannot be separated.

What effects do blooms of large phytoplankton have on the autotrophic ultraplankton community? When crustacean zooplankton are able to exploit the bloom, this may also result in an increased grazing pressure on the protozoa, from which their ultraplankton prey might benefit. However, the diversification of the protozoan community (probably encompassing 2 -3 trophic levels) might also lead to an increased grazing pressure on the ultraplankton. Thus, the co-occurrence of large zooplankton with large phytoplankton in eutrophic environments may influence the ultraplankton through a trophic cascade; however, due to the diversification and ramifications of the microbial food web, it is not possible to predict the effect on the ultraplankton.

The following scheme (Fig.85) illustrates standing stocks of the principal components of the microbial food web and their trophic interactions in two different ecosystems. The first (panel A) is an oligotrophic system with low standing stocks of large phytoplankton and zooplankton; the protozoa and the ultraphytoplankton dominate production and consumption within the system, there are no new nutrients available. The bulk of carbon is turned over between the ultraphytoplankton, the bacteria and the small (nano-) protozoa, and the system is entirely dependent on an efficient recycling of nutrients.

In the second situation (panel B), the system is boosted with new nutrients (be it nitrate or reduced nitrogen compounds), and the large phytoplankton thrives. The mesozooplankton and larger microzooplankton take advantage of the situation, also increasing their biomasses; the carbon flow between these compartments of large sized organisms (symbolized by the arrows) increases

dramatically. The small ($<5\mu\text{m}$) phytoplankton will also profit from the new nutrients (exception: *Prochlorococcus*) and increase their biomass, and the heterotrophic bacteria will profit from high DOC-exudation rates from the large blooming phytoplankton. The small (nano-) protozoa will exert a high grazing pressure on both of these compartments, itself suffering from intense predation by the microzooplankton. This is why the stocks of bacteria, ultraphytoplankton and small protozoa will change less dramatically as those of the larger components: although their 'bottom-up' supply (DOC, new nutrients) increases under eutrophic conditions, grazing by the small protozoa and larger microzooplankton (i.e. 'top-down' control) will largely keep pace with this increased 'bottom-up' supply.

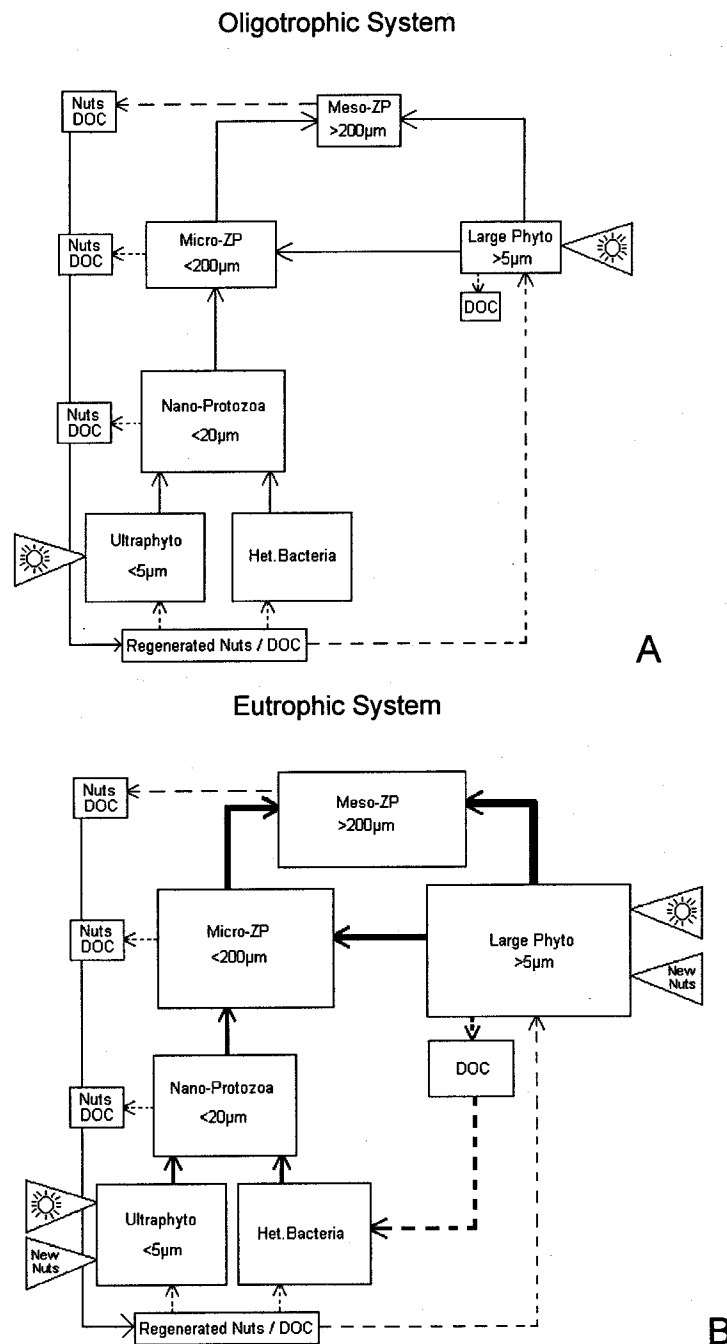


Fig.85 Schematic model of the different compartments of an aquatic pelagic ecosystem under oligotrophic (A) and eutrophic conditions (B); arrows symbolize energy fluxes. The lower half of the respective panels represents the microbial food web, the upper half stands for the classical food chain.

Both the Arabian Sea during the NE monsoon and the Gotland Sea in summer represent an intermediate stage between the two extremes: in the Arabian Sea, vertical convection triggered by cool temperatures and strong winds brings low amounts of nitrate into the euphotic zone, not enough to promote a real bloom, but elevating biomasses of the microbial food web members to levels well above true oligotrophic situations. In the Gotland Sea, the nitrogen inputs from N_2 fixation and other sources also lead to high microbial biomasses. An example for a true eutrophic environment, represented by the panel B in Fig.85, is the upwelling station US2 during the SW monsoon, the inner Gulf of Aden and southern Red Sea stations during the NE monsoon, with large diatoms and dinoflagellates blooming, and the Odra plume water entering the Pomeranian Bay. There, the components of the microbial food web did not increase their biomass to the same extent as the large phytoplankton, although a tendency towards larger cells was observed at all levels.

5. Summary

Ultraplankton (<5µm) and protozoan standing stocks, as well as their trophic interactions were investigated during five cruises to environments of different trophic status. The Arabian Sea, the Gulf of Aden and the southern Red Sea were sampled during two monsoon periods (SW monsoon in summer 1992, NE monsoon during winter 1993). The Pomeranian Bay (a coastal area in the southern Baltic Sea, receiving the runoff of the Odra river) was investigated during two cruises in summer 1993 and 1994, respectively. The Gotland Sea (Baltic proper) was sampled in 1994.

Ultraplankton standing stocks and distributions

Ultraplankton comprised approximately 60% of phytoplankton biomass during the oligo- to mesotrophic NE monsoon in the Arabian Sea, but only 11% in the southern Red Sea. As discriminated by flow cytometry, the ultraplankton community was composed of the prokaryote genera *Prochlorococcus* and *Synechococcus* as well as at least two eukaryotic ultraplankton groups. The latter two and *Synechococcus* dominated in terms of biomass. The eukaryotes became more prominent at increasing trophic status.

In the oligotrophic Gotland Sea (Baltic proper), ultraplankton contributed to about 35% of phytoplankton biomass. *Synechococcus* and four eukaryotic ultraplankton types were distinguished by flow cytometry. Within the ultraplankton community, biomass was dominated by the eukaryotic algae.

In the meso- to oligotrophic open Pomeranian Bay, ultraplankton <5µm contributed to approximately 60% of phytoplankton biomass, whereas this share was reduced to 45% in the eutrophic river plume. In the Pomeranian Bay, up to 7 ultraplankton groups were discriminated by flow cytometry and epifluorescence microscopy. Next to *Synechococcus*, three unidentified eukaryotic algae and two cryptophyte species comprised the ultraplankton. Biomass in the open Bay water was dominated by *Synechococcus*, and by larger eukaryotes and cryptophytes in the Odra plume water.

Epifluorescence microscopy revealed extraordinarily high abundances of *Synechococcus* in the Baltic Sea in 1994 (Gotland Sea: up to 812,000 cm⁻³, Pomeranian Bay: up to 1,500,000 cm⁻³). In the Arabian Sea, the picoautotrophic prokaryote *Prochlorococcus* reached high abundances only at oligotrophic stations, and decreased to very low numbers at eutrophic stations. From these observations, together with additional references from the literature, it is speculated that *Prochlorococcus* is a true obligate open ocean organism, highly adjusted to regenerating systems.

Protozoan standing stocks and distributions

In the Arabian Sea, heterotrophic nanoflagellates (HNF: cell concentrations 304 - 1630 cm⁻³, carbon biomass 1 - 7 µg dm⁻³) and heterotrophic dinoflagellates (HDIN: 8 - 60 cm⁻³ and 0.6 - 15 µg dm⁻³) dominated protozoan biomass, except for the upwelling station US2 during the SW monsoon, and at the eutrophic stations in the Gulf of Aden and the southern Red Sea during the NE monsoon, where ciliates predominated (up to 7,800 dm⁻³ and 17 µg dm⁻³). At these eutrophic stations, biomasses of all protozoan groups were considerably higher than at the more oligotrophic stations, due to increased cell concentrations, but to a large extent also to larger biovolumes of individual cells. Small HNF <3µm dominated flagellate abundances throughout.

In the Baltic Sea, protozoan biomasses were generally higher than in the Arabian Sea. In the Gotland Sea, HNF (1,700 cm⁻³ and 12.6 µg dm⁻³) were far more important than ciliates (1,300

cm^{-3} and $2.4 \mu\text{g m}^{-3}$). Protozoan biomasses in the Pomeranian Bay reached peak values in the Odra plume water, with ciliate abundances reaching up to 176 cm^{-3} (carbon biomass: $81 \mu\text{g dm}^{-3}$), and HNF up to $12,000 \text{ cm}^{-3}$ (58 mg m^{-3}). The heterotrophic silicoflagellate *Ebria tripartita* was present but was of minor importance in terms of biomass.

Grazing on ultraphytoplankton by microzooplankton

Serial dilution experiments, combined with flow cytometric analysis, allowed the estimation of grazing pressure on different ultraphytoplankton groups. In the Arabian Sea during the NE monsoon, all groups were subject to vigorous grazing by small protozoa ($<10\mu\text{m}$). Generally, around 100% (36 - 139%) of the cells produced were consumed per day, more or less sustaining a steady state system. Grazing on ultraphytoplankton ($<3\mu\text{m}$) contributed to about 100% of total phytoplankton carbon biomass consumption by microzooplankton (absolute values: $4 - 28 \mu\text{g dm}^{-3} \text{ d}^{-1}$), except for the Gulf of Aden and the southern Red Sea, where a much higher proportion of larger phytoplankton was consumed ($71 - 146 \mu\text{g dm}^{-3} \text{ d}^{-1}$).

During the SW monsoon, phytoplankton carbon consumption rates were substantially higher at the eutrophic upwelling station ($118 \mu\text{g dm}^{-3} \text{ d}^{-1}$) than at the mesotrophic northern stations ($48 - 86 \mu\text{g dm}^{-3} \text{ d}^{-1}$) and at an oligotrophic southern station ($20 \mu\text{g dm}^{-3} \text{ d}^{-1}$). At the oligotrophic southern station, an experiment to estimate bacterivory showed bacterial consumption rates by microzooplankton to be very similar to phytoplankton consumption ($25 \mu\text{g dm}^{-3} \text{ d}^{-1}$).

Carbon consumption rates of phytoplankton in the Pomeranian Bay were in the same order of magnitude than in the eutrophic Arabian Sea stations ($93 - 140 \mu\text{g dm}^{-3} \text{ d}^{-1}$). Ultraphytoplankton carbon consumption in the Gotland Sea, analysed by flow cytometry, ranged from $58 - 119 \mu\text{g dm}^{-3} \text{ d}^{-1}$.

A trophic cascade within the microbial food web

Size fractionation combined with serial dilution experiments allowed the identification of at least two trophic steps within the nanoplankton ($<20\mu\text{m}$) size range in the Arabian Sea during the NE monsoon. A removal of secondary predators ($>10\mu\text{m}$) enhanced grazing on autotrophic ultraplankton in the $<10\mu\text{m}$ size range considerably. It is estimated that up to 83% of grazers $<10\mu\text{m}$ are removed by nano- and microzooplankton predators ($10 - 200\mu\text{m}$) per day. In the Gotland Sea, this effect was not evident.

Conclusions

Ultraphytoplankton is an ubiquitous and mostly dominating part of the autotrophic community in pelagic ecosystems of different trophic state. However, the biomass and diversity of eukaryotic ultraplankton seems to increase with increasing trophic state, i.e. with increased supply of nutrients. For the prokaryotic picoautotrophic *Prochlorococcus*, the contrary seems to hold true: its concentrations and biomasses are inversely related to the trophic state of the system. *Prochlorococcus* seems to be especially well adjusted to evolutionary old regenerating systems. So far, it has not been found in the Baltic Sea.

Synechococcus, on the other hand, seems to be about one order of magnitude more abundant in the Baltic Sea than in open ocean environments. In sharp contrast to *Prochlorococcus* it attains high biomasses in eutrophic and coastal environments although it is then concealed by bloom forming large phytoplankton (diatoms, dinoflagellates, filamentous cyanobacteria). Possibly the *Synechococcus* from the Baltic Sea (and other neritic environments) and those from the open ocean belong to different species. The overall higher biomass of the microbial food web components in the Baltic Sea can be explained by the high nutrient and energy inputs from land

into the spatially confined basins of the Baltic Sea. Moreover, the regularly blooming N_2 fixing cyanobacteria as well as atmospheric inputs add new nitrogen to the system. These conditions lead to high plankton biomasses in the euphotic zone despite a nutrient depleted mixed layer. In simple terms, the recycling machine of the *microbial loop* runs at a higher level in the nutrient depleted euphotic zone of the Baltic proper in summer than in oligotrophic ocean environments.

Small heterotrophic nanoflagellates are mostly the dominant members of protozoan communities, especially in oligotrophic environments. They seem to fulfil the requirements of regenerating systems exceptionally well, i.e. high growth, feeding and nutrient regeneration rates. Ciliates, on the other hand, seem to gain importance in more eutrophic environments.

Grazing on ultraphytoplankton seems to be vigorous in all environments, with roughly 100% of the produced biomass removed per day, thus sustaining a steady state. However, with large phytoplankton ($>5\mu\text{m}$) thriving, the relative constant carbon flow within the microbial food web is concealed by large microzooplankton and mesozooplankton grazing on the large algae, and substantially increasing the overall carbon turnover in the system.

It was shown in the Arabian Sea during the NE monsoon that autotrophic ultraplankton biomass and production was controlled largely by predators of the primary herbivores ('top down' control).

Flow cytometry has proven to be the perfect tool for microbial food web research, as it is able to characterize and quantify practically all autotrophic protagonists of the microbial food web quickly and precisely. With a specified instrument, heterotrophic bacteria can be counted as well. Specific metabolic stains and probes offer a wide range of applications in the future.

6. References

- ANDERSEN T., SCHARTAU A.K.L., PAASCHE E., 1991. Quantifying external and internal nitrogen and phosphorus pools, as well as nitrogen and phosphorus supplied through remineralisation, in coastal marine plankton by means of a dilution technique. *Mar. Ecol. Prog. Ser.*, **69**, 67-80.
- ANDERSEN R.A. SAUNDERS G.W., PASKIND M.P., SEXTON J.P., 1993. Ultrastructure and 18rRNA sequence for *Pelagomonas calceolata* gen. et sp. nov., and the description of a new algal class, the Pelagophyceae classis nov. *J. Phycol.* **29**, 701-715.
- ANTIA, A.N., 1991. Microzooplankton in the pelagic food web of the East Greenland Sea and its role in sedimentation processes. Dissertation thesis, Inst. f. Meeresk. Kiel.
- AZAM F., FENCHEL T., FIELD J.G., GRAY J.S., MEYER-REIL L.A., THINGSTAD F., 1983. The ecological role of water-column microbes in the sea. *Mar. Ecol. Prog. Ser.*, **10**, 257-263.
- BAARS M.A., 1994 (ed.). Monsoons and pelagic systems. Cruise reports Netherland's Indian Ocean Programme, Vol.1. National Museum of Natural History, Leiden 1994.
- BAARS M.A., BAKKER K.M.J., DE BRUIN T.F., VAN COUWELAAR M., HIEHLE M., KRAAY G.W., OOSTERHUIS S.S., SCHALK P.H., SPRONG I., VELDHUIS M.J.W., WIEBINGA C.J., WITTE J.I.J., 1994. Seasonal fluctuations in plankton biomass and productivity in the ecosystems of the Somali Current, Gulf of Aden and southern Red Sea. In: BAARS M.A. (Ed.): Monsoons and pelagic systems. Cruise reports Netherland's Indian Ocean Programme, Vol.1. National Museum of Natural History, Leiden 1994.
- BANSE K., 1977. Determining the Carbon-to-Chlorophyll ratio of natural phytoplankton. *Mar. Biol.*, **41**, 199-212.
- BANSE K. and MCCLAIN C., 1986. Winter blooms of phytoplankton in the Arabian Sea as observed by the Coastal Zone Color Scanner. *Mar. Ecol. Prog. Ser.*, **34**, 201-211.
- BANSE K., 1994A. On the coupling of hydrography, phytoplankton, zooplankton, and settling organic particles offshore in the Arabian Sea. In: LAL D. (Ed.): Biogeochemistry of the Arabian Sea. Indian Academy of Sciences, Bangalore 560 044, pp 27-63.
- BANSE K., 1994B. Grazing and zooplankton production as key controls of phytoplankton production in the oceans. *Oceanography*, **7** (1), 13-20.
- BANSE K., 1995. Zooplankton: Pivotal role in the control of oceanic production. *ICES J.Mar. Sci.*, **52**, 265-277.
- BARBEAU K., MOFFETT J.W., CARON D.A., CROOT P.L., ERDNER D.L., 1996. Role of protozoan grazers in relieving iron limitation of phytoplankton. *Nature* **380**, 61-64.
- BARLOW R.G., BURKILL P.H., MANTOURA R.F.C., 1988. Grazing and degradation of algal pigments by the marine protozoan *Oxyrrhis marina*. *J. exp. Mar. Biol. Ecol.* **119**, 119-129.
- BERMAN T., NAWROCKI M., TAYLOR G.T., KARL D.M., 1987. Nutrient flux between bacteria, bacterivorous nanoplankton protists and algae. *Mar. Microbiol. Food Webs*, **2** (2), 69-82.

- BERMAN T., 1991. Protozoa as agents in planktonic nutrient cycling. In: PATTERSON D.J. AND LARSEN J. (EDS.): The biology of free-living heterotrophic flagellates. The Systematics Association Special Vol. 45, Clarendon Press Oxford 1991. pp 21-38.
- BERNINGER U.-G., CARON D.A., SANDERS R.W., FINLAY B.J., 1991. Heterotrophic flagellates of planktonic communities: their characteristics and methods of study. In: PATTERSON D.J. AND LARSEN J. (EDS.): The biology of free-living heterotrophic flagellates. The Systematics Association Special Vol. 45, Clarendon Press Oxford 1991. pp. 39-56.
- BLEIJSWIJK J.D.L. VAN and VELDHUIS M.J.W., 1995. *In situ* growth rates of *Emiliana huxleyi* in enclosures with different phosphate loadings revealed by diel changes in DNA content. *Mar. Ecol. Prog. Ser.* **121**, 271-277.
- BODUNGEN B. VON, 1975. Der Jahresgang der Nährsalze und der Primärproduktion des Planktons in der Kieler Bucht unter Berücksichtigung der Hydrographie. Dissertation thesis, Inst. f. Meereskunde, Universität Kiel.
- BODUNGEN B. VON, GRAEVE M., KUBE J., LASS U., MEYER-HARMS B., MUMM N., NAGEL K., POLLEHNE F., POWILLEIT M., RECKERMANN M., SATTLER C., SIEGEL H., WODARG D., 1995. Stoff-Flüsse am Grenzfluss: Transport und Umsatzprozesse im Übergangsbereich zwischen Oderästuar und Pommerscher Bucht (TRUMP). *Geowissenschaften* **13** (12), 479-485.
- BURKILL, P.H., MANTOURA, R.F.C., LLEWELLYN, C.A., OWENS, N.J.P., 1987. Microzooplankton grazing and selectivity of phytoplankton in coastal waters. *Mar. Biol.*, **93**, 581-590.
- BURKILL P.H., MANTOURA R.F.C., OWENS N.J.P., 1993A. Biogeochemical cycling in the NW Indian Ocean: a brief overview. *Deep Sea Res. II*, **40**, 643-649.
- BURKILL P.H., EDWARDS E.S., JOHN A.W.G., SLEIGH M.A., 1993B. Microzooplankton and their herbivorous activity in the north eastern Atlantic Ocean. *Deep Sea Res. II*, **40**, (1/2), 479-493.
- BURKILL P.H., LEAKEY R.J.G., OWENS N.J.P., MANTOURA R.F.C., 1993C. *Synechococcus* and its importance to the microbial food web of the northwest Indian Ocean. *Deep Sea Res. II*, **40**, 773-782.
- BURKILL P.H., EDWARDS E.S., SLEIGH M.A., 1995. Microzooplankton and their role in controlling phytoplankton growth in the marginal ice zone of the Bellinghausen Sea. *Deep Sea Res. II*, **42**, (4/5), 1277-1290.
- BURSA A.S., 1963. Epibioses on *Nodularia spumigena* (Mertens) in the Baltic Sea. *Arch. Hydrobiol.* **10**, 267-297.
- CAMPBELL L. and CARPENTER E.J., 1986. Estimating the grazing pressure of heterotrophic nanoplankton on *Synechococcus* ssp. using the sea water dilution and selective inhibitor techniques. *Mar. Ecol. Prog. Ser.* **33**, 121-129.
- CAMPBELL L. and D. VAULOT, 1993. Photosynthetic picoplankton community structure in the subtropical North Pacific Ocean near Hawaii (station ALOHA). *Deep Sea Res. I*, **40** (10), 2043-2060.

- CAMPBELL L., NOLLA H.A., VAULOT D., 1994. The importance of *Prochlorococcus* to community structure in the central North Pacific Ocean. *Limnol. Oceanogr.*, **39** (4), 954-961.
- CAPRIULO G.M. and DEGNAN C., 1991. Effect of food concentration on digestion and vacuole passage time in the heterotrichous marine ciliate *Fibrea salina*. *Mar. Biol.* **110**, 199-202.
- CAPRIULO G.M., SHERR E.B., SHERR, B.F., 1991. Trophic behavior and related community feeding activities of heterotrophic marine protists. In: PATTERSON D.J. AND LARSEN J. (EDS.): The biology of free-living heterotrophic flagellates. The Systematics Association Special Vol. 45, Clarendon Press Oxford 1991. pp 21-38.
- CARON D.A., LIM E.L., MICELI G., WATERBURY J.B., VALOIS F.W., 1991. Grazing and utilization of crococoid cyanobacteria and heterotrophic bacteria by protozoa in laboratory cultures and a coastal community. *Mar. Ecol. Prog. Ser.*, **76**, 205-217.
- CARPENTER S.R., KITCHELL J.F., HODGSON J.R., 1985. Cascading trophic interactions and lake productivity. *BioScience*, **35** (10), 634-639.
- CARPENTER E.J. and CHANG J., 1988. Species-specific phytoplankton growth rates via diel DNA synthesis cycles. I. Concept of the method. *Mar. Ecol. Prog. Ser.*, **43**, 105-111.
- CARPENTER E.J., JANSON S., BOJE R., POLLEHNE F., CHANG J., 1995. The dinoflagellate *Dinophysis norvegica*: biological and ecological observations in the Baltic Sea. *Eur. J. Phycol.* **30**, 1-9.
- CHISHOLM S.W., OLSON R.L., ZETTLER E.R., GOERICKE R., WATERBURY J.B., WELSCHMEYER N.A., 1988. A novel free-living prochlorophyte abundant in the euphotic zone. *Nature*, **334**, 340-343.
- CHISHOLM S.W., FRANKELS L., GOERICKE R., OLSON R.L., PALENIK B., WATERBURY J.B., WEST-JOHNSTAD L., ZETTLER E.R., 1992. *Prochlorococcus marinus* nov. gen. nov. spec.: an oxyphototrophic marine prokaryote containing divinyl chlorophyll *a* and *b*. *Arch. Microbiol.*, **157**, 297-300.
- CLAPARÈDE E. and LACHMANN J., 1858. Études sur les Infusoires et des rhizopodes. *Mémoires de l'Institut National Genevois* **6**, 261-482.
- CLEVEN E.-J., 1996. Indirectly fluorescently labelled flagellates (IFLF): a tool to estimate the predation on free-living heterotrophic flagellates. *J. Plankt. Res.* **18** (3), 429- 442.
- CODISPOTI L.A., 1989. Phosphorus vs. Nitrogen limitation of new and export production. In: Berger W.H., Smetacek V.S., Wefer G. (Eds.): Productivity of the ocean: present and past. John Wiley and Sons Chichester 1989. pp 377-394.
- COURTIES C., VAQUER A., TROUSSELLIER M., LAUTIER J., CHRETIENNOT-DINET M.J., NEVEUX J., MACHADO C., CLAUSTRE H., 1994. Smallest eukaryotic organism. *Nature* **370**, 255.
- CYNAR F.J., ESTEP K.W., SIEBURTH J. MCN., 1985. The detection and characterization of bacteria-sized protists in "protist-free" filtrates and their potential impact on experimental marine ecology. *Microb. Ecol.* **11**, 281-288.

- DARZYNKIEWICZ Z. and MELAMED M.R., 1993. Flow cytometry and sorting - An historical perspective. *Cytometry Res.* **3** (1), 1-9.
- DETMER A.E., 1995. Verbreitung, Abundanz und Bedeutung von autotrophen Pico- und Nanoplankton in polaren, temperierten und subtropischen Regionen. *Ber. Inst. f. Meeresk. Kiel* Nr. **263**.
- DETMER A.E., GIESENHAGEN H.C., TRENKEL V.M., AUF DEM VENNE H., JOCHEM F.J., 1993. Phototrophic and heterotrophic pico- and nanoplankton in anoxic depths of the central Baltic Sea. *Mar. Ecol. Prog. Ser.* **99**, 197-203.
- DUBELAAR G.B.J., GROENEWEGEN A.C., STODDIK W., VAN DEN ENGH G.J., VISSER J.W.M., 1989. Optical Plankton Analyser: A flow cytometer for plankton analysis, II: Specifications. *Cytometry* **10**, 529-539.
- DUGDALE R.C. and GOERING J.J., 1967. Uptake of new and regenerated forms of nitrogen in primary productivity. *Limnol. Oceanogr.*, **12**, 196-206.
- DOLAN J.R., 1991. Microphagous ciliates in mesohaline Chesapeake Bay waters: estimates of growth rates and consumption by copepods. *Mar. Biol.*, **111**, 303-309.
- DOLAN J.R. and COATS D.W., 1991. A study of feeding in predacious ciliates using prey ciliates labeled with fluorescent microspheres. *J. Plankt. Res.*, **13** (3), 609-627.
- EPPLEY R.W., CARLUCCI A.F., HOLM-HANSEN O., KIEFER D., MCCARTHY J.J., VENRICK E., WILLIAMS P.M., 1971. Phytoplankton growth and composition in shipboard cultures supplied with nitrate, ammonium, or urea as the nitrogen source. *Limnol. Oceanogr.*, **16** (5), 741-751.
- EPPLEY R.W. and PETERSON B.J., 1979. Particulate organic matter flux and planktonic new production in the deep ocean. *Nature*, **282**, 677-680.
- EDLER, L., 1979. Recommendations for marine biological studies in the Baltic sea: Phytoplankton and Chlorophyll. *Baltic Marine Biologists*.
- EVANS G.T. and PARANJAPPE M.A., 1992. Precision of estimates of phytoplankton growth and microzooplankton grazing when the functional response of grazers may be nonlinear. *Mar. Ecol. Prog. Ser.* **80**, 285-290.
- FAURÉ-FREMIET E., 1924. Contribution à la connaissance des Infusoires planktoniques. *Supplements au Bulletin Biologique de France et de Belgique, Supplement VI*. 171 pp.
- FENCHEL T., 1986. The ecology of heterotrophic microflagellates. *Advances in Microbial Ecology*, **9**, 57-97.
- FOGG G.E., 1983. The ecological significance of extracellular products of phytoplankton photosynthesis. *Bot. Mar.*, **26**, 3-14.
- FOGG G.E., 1995. Some comments on picoplankton and its importance in the pelagic ecosystem. *Aquat. Microbial. Ecol.* **8**, 33-39.
- FRANKEL S.L., BINDER B.J., CHISHOLM S.W., SHAPIRO H.M., 1990. A high sensitivity flow cytometer for studying picoplankton. *Limnol. Oceanogr.* **35** (5), 1164-1169.

- FRANSISCO D.E., MAH R.A., RABIN A.C., 1973. Acridine-Orange epifluorescence technique for counting bacteria in natural waters. *Trans. Am. Microsc. Soc.* **92**, 416-421.
- FUHRMAN J.A. and G.B. MCMANUS, 1984. Do bacteria-sized marine eukaryotes consume significant bacterial production? *Science*, **224**, 1257-1260.
- GALLEGOS C.L., 1989. Microzooplankton grazing on phytoplankton in the Rhode River, Maryland: nonlinear feeding kinetics. *Mar. Ecol. Prog. Ser.* **57**, 23-33.
- GIESKES W.W. and KRAAY G.W., 1983. Unknown chlorophyll a derivatives in the North sea and the tropical Atlantic Ocean revealed by HPLC analysis. *Limnol. Oceanogr.* **28**, 757-766.
- GIFFORD D.J., 1988. Impact of grazing by microzooplankton in the Northwest arm of Halifax Harbour, Nova Scotia. *Mar. Ecol. Prog. Ser.* **47**, 249-257.
- GIFFORD D.J. and DAGG M.J., 1991. The microzooplankton-mesozooplankton link: consumption of planktonic protozoa by the calanoid copepods *Acartia tonsa* Dana and *Neocalanus plumchrus* Murukawa. *Mar. Microb. Food Webs*, **5** (1), 161-177.
- GLIBERT P.M., MILLER C.A., GARSIDE C., ROMAN M.R., MCMANUS G.B., 1992. NH_4^+ regeneration and grazing: interdependent processes in size-fractionated $^{15}\text{NH}_4^+$ experiments. *Mar. Ecol. Prog. Ser.* **82**, 65-74.
- GOERICKE R. and REPETA D.J., 1993. Chlorophylls *a* and *b* and divinyl chlorophylls *a* and *b* in the open subtropical North Atlantic Ocean. *Mar. Ecol. Prog. Ser.* **101**, 307-313.
- GOERICKE R. and WELSCHMEYER N.A., 1993. The marine prochlorophyte *Prochlorococcus* contributes significantly to phytoplankton biomass and primary production in the Sargasso Sea. *Deep-Sea Res. I*, **40** (11/12), 2283-2294.
- GOCKE K., 1996. Mikrobielle Stoffumsetzungen. In: RHEINHEIMER G. (Ed.): *Meereskunde der Ostsee*. Springer Verlag Berlin Heidelberg 1996, pp 123-130.
- GOLDMAN J.C. and CARON D.R., 1985. Experimental studies on an omnivorous microflagellate: implications for grazing and nutrient regeneration in the marine microbial food chain. *Deep Sea Res.* **32** (8), 899-915.
- GOLDMAN J.C. and DENNETT M.R., 1985. Susceptibility of some marine phytoplankton species to cell breakage during filtration and post-filtration rinsing. *J. Exp. Mar. Biol. Ecol.*, **86**, 47-58.
- GRADINGER R., 1990. Zur Bedeutung des Pico- und Nanoplanktons in polaren Regionen am Beispiel der Grönländischen See. *Ber. Inst. f. Meeresk. Kiel*, Nr. 196.
- GRASSHOFF K., 1976. *Methods of seawater analysis*. Verlag Chemie Weinheim, 317 pp.
- GRIEBMANN K., 1913. Über marine Flagellaten. *Arch. für Protistenkunde* **132**, 1-78.
- GUERRERO R., PEDROS-ALIO C., ESTEVE I., MAS J., CHASE D. MARGULIS L., 1986. Predatory prokaryotes: predation and primary consumption evolved in bacteria. *Proc. Natl. Acad. Sci. USA*, **83**, 2138-2142.

- HAAS L.W., 1982. Improved epifluorescence microscopy for observing planktonic microorganisms. *Ann. Inst. Oceanogr., Paris* **58** (S), 261-266.
- HAGSTRÖM A., LARSSON U., HÖRSTEDT P., NORMARK S., 1979. Frequency of dividing cells, a new approach to the determination of bacterial growth rates in aquatic ecosystems. *Appl. Environ. Microbiol.* **37** (5), 805-812.
- HALL J.A. and VINCENT W.F., 1990. Vertical and horizontal structure in the picoplankton communities of a coastal upwelling system. *Mar. Biol.* **106**, 465-471.
- HANSEN, F.C., RECKERMANN M., KLEIN BRETELER W.C.M., RIEGMAN R., 1993. *Phaeocystis* blooming enhanced by copepod predation on protozoa: evidence from incubation experiments. *Mar. Ecol. Prog. Ser.*, **102**, 51-57.
- HEINÄNEN A., 1992. Bacterioplankton in the open Baltic Sea. Dissertation thesis, University of Helsinki. Finnish Marine Research No. 260.
- HOBBIE J.E., DALEY R., JASPER S., 1977. Use of Nucleopore filters for counting bacteria by epifluorescence microscopy. *Appl. Environ. Microbiol.*, **33**, 1225-1228.
- HOFSTRAAT J.W., VAN ZEIJL W.J.M., DE VREEZE M.E.J., PEETERS J.C.H., PEPPERZAK L., COLIJN F., RADEMAKER T.W.M., 1994. Phytoplankton monitoring by flow cytometry. *J. Plankt. Res.* **16** (9), 1197-1224.
- HOPPE H.-G., 1981. Blue-green algae agglomeration in surface water: a microbiotope of high bacterial activity. *Kieler Meeresforsch. Sonderh.*, **5**, 291-303.
- HÜLLER R., GLOSSNER E., SCHAUB S., WEINGÄRTNER J., KACHEL V., 1994. The Macro Flow Planktometer: A new device for volume and fluorescence analysis of macroplankton including triggered video imaging in flow. *Cytometry* **17**, 109-118.
- ITURRIAGA R. and MITCHELL B.G., 1986. Chroococcoid cyanobacteria: a significant component in the food web dynamics of the open ocean. *Mar. Biol. Prog. Ser.*, **28**, 291-297.
- ITURRIAGA R. and MARRA J., 1988. Temporal and spatial variability of chroococcoid cyanobacteria *Synechococcus* ssp. specific growth rates and their contribution to primary production in the Sargasso Sea. *Mar. Biol. Prog. Ser.*, **44**, 175-181.
- JGOFS, 1994. JGOFS core measurement protocols - June 1994.
- JOCHEM F., 1988. On the distribution and importance of picocyanobacteria in a boreal inshore area (Kiel Bight, Western Baltic). *J. Plankt. Res.*, **19** (5), 1009-1022.
- JOCHEM F., 1989. Distribution and importance of autotrophic ultraplankton in a boreal inshore area (Kiel Bight, Western Baltic). *Mar. Ecol. Prog. Ser.*, **53**, 153-168.
- JOCHEM F.J., POLLEHNE F., ZEITZSCHEL B., 1993. Productivity regime and phytoplankton size structure in the Arabian Sea. *Deep Sea Res. II*, **40**, 711-735.
- JOCHEM F., 1995. Phototrophic picoplankton community structure in three different pelagic regimes in the Arabian Sea. *Mar. Ecol. Prog. Ser.*, **117**, 307-314.

- JOHNSON P.W. and SIEBURTH J.M., 1982. In-situ morphology and occurrence of eukaryotic phototrophs of bacterian size in the picoplankton of estuarine and oceanic waters. *J. Phycol.*, **18**, 318-327.
- KARLSON B., 1995. On the role of pico- and nanoplankton in the Skagerrak. Dissertation thesis, University of Göteborg.
- KIMOR B., 1973. Plankton Relations of the Red Sea, Persian Gulf and Arabian Sea. In: ZEITZSCHEL B. (ED.): *The Biology of the Indian Ocean*. Springer Verlag Berlin 1973. 549 pp.
- KLEIN BRETELER W.C.M, FRANSZ H.G., GONZALES S.R., 1982. Growth and development of four calanoid copepod species under experimental and natural conditions. *Neth. J. Sea Res.* **16**, 195-207.
- KREY J., 1973. Primary production in the Indian Ocean I. In: ZEITZSCHEL B. (ED.): *The Biology of the Indian Ocean*. Springer Verlag Berlin 1973. 549 pp.
- KREY J. and BABENERD B. 1976. Phytoplankton production. Atlas of the Indian Ocean expedition. Institut für Meereskunde Kiel. 70 pp.
- KRUPATKINA D.K., 1990. Estimates of primary production in oligotrophic waters and metabolism of picoplankton: a review. *Mar. Microb. Food Webs*, **4** (1), 87-101.
- KUDOH S., KANDA J., TAKAHASHI M., 1990. Specific growth rates and grazing mortality of crococoid cyanobacteria *Synechococcus* spp. in pelagic surface waters in the sea. *J. Exp. Mar. Biol. Ecol.*, **142**, 201-212.
- KUOSA H., 1991. Picoplanktic algae in the northern Baltic Sea: Seasonal dynamics and flagellate grazing. *Mar. Ecol. Prog. Ser.* **73**, 269-276.
- KUOSA H. and MARCUSSEN B., 1988. Grazing of bacteria and phytoplankton by heterotrophic nanoflagellates in a Baltic Sea sample. *Hydrobiologica* **161**, 211-216.
- KUPARINEN J. and KUOSA H., 1993. Autotrophic and heterotrophic picoplankton in the Baltic Sea. *Adv. Mar. Biol.*, **29**, 73-128.
- KUUPPO-LEINIEMI P., AUTIO R., HÄLLFORS S., KUOSA H., KUPARINEN J., PAJUNIEMI R., 1994. Trophic interactions and carbon flow between picoplankton and protozoa in pelagic enclosures manipulated with nutrients and a top predator. *Mar. Ecol. Prog. Ser.* **107**, 89-102.
- LAL D., 1994. Biogeochemistry of the Arabian Sea: Present information and gaps. In: LAL D. (Ed.): *Biogeochemistry of the Arabian Sea*. Indian Academy of Sciences, Bangalore 560 044, pp 1-7.
- LAMPERT W. and SOMMER U., 1993. *Limnoökologie*. Georg Thieme Verlag Stuttgart 1993, 440 p.
- LANDRY M.R. and HASSETT R.P., 1982. Estimating the grazing impact of marine microzooplankton. *Mar. Biol.*, **67**, 283-288.

- LANDRY M.R., HAAS L.W., FAGERNESS V.L., 1984. Dynamics of microbial plankton communities: experiments in Kaneohe Bay, Hawaii. *Mar. Ecol. Prog. Ser.* **16**, 127-133.
- LANDRY M.R., 1993. Estimating rates of growth and grazing mortality of phytoplankton by the dilution method. In: *Handbook of methods in aquatic microbial ecology*, Kemp P.F., B.F. Sherr and J.J. Cole (Eds), pp 715-722, Lewis, Boca Raton.
- LANDRY M.R., 1994. Methods and controls for measuring the grazing impact of planktonic protists. *Mar. Microb. Food Webs*, **8** (1-2), 37-57.
- LANDRY M.R., KIRSHEIN J., CONSTANTINOU J., 1995A. A refined dilution technique for measuring the community grazing impact of microzooplankton, with experimental tests in the central equatorial Pacific. *Mar. Ecol. Prog. Ser.* **120**, 53-63.
- LANDRY M.R., KIRSHEIN J., CONSTANTINOU J., 1995B. Microzooplankton grazing in the central equatorial Pacific during February and August 1992. *Deep-Sea Res. II*, **42** (2-3), 657-671.
- LAVAL-PEUTO M. and RASSOULZADEGAN F., 1988. Autofluorescence of marine planktonic Oligotrichina and other ciliates. *Hydrobiologica* **159**, 99-110.
- LAW C.S. and OWENS N.J.P., 1990. Significant flux of atmospheric nitrous oxide from the northwest Indian Ocean. *Nature*, **346**, 826-828.
- LEAKEY R.J.G. 1989. The ecology of planktonic ciliates in Southampton water. Doctoral thesis, University of Southampton.
- LENZ J., 1992. Microbial loop, microbial food web and classical food chain: Their significance in pelagic marine ecosystems. *Arch. Hydrobiol. Beihh. Ergebn. Limnol.* **37**, 265-278.
- LESSARD E.J., 1991. The trophic role of heterotrophic dinoflagellates in diverse marine environments. *Mar. Microb. Food Webs*, **5** (1), 49-58.
- LESSARD E.J. and SWIFT E., 1985. Species-specific grazing rates of heterotrophic dinoflagellates in oceanic waters, measured with a dual-label radioisotope technique. *Mar. Biol.* **87**, 289-296.
- LESSARD E.J. and SWIFT E., 1986. Dinoflagellates from the North Atlantic classified as phototrophic or heterotrophic by epifluorescence microscopy. *J. Plankt. Res.* **8** (6), 1209-1215.
- LI W.K.W., SUBBA RAO D.V., HARRISON W.G., SMITH J.C., CULLEN J.J., IRWIN B., PLATT T., 1983. Autotrophic picoplankton in the tropical ocean. *Science* **219**, 292-295.
- LI W.K.W., DICKIE P.M., IRWIN B.D., WOOD A.M., 1992. Biomass of bacteria, cyanobacteria, prochlorophytes and photosynthetic eukaryotes in the Sargasso Sea. *Deep Sea Res.* **39** (3/4), 501-519.
- LI W.K.W., ZOHARY T., YACOBI B.Z., WOOD A.M., 1993. Ultraphytoplankton in the eastern Mediterranean Sea: towards deriving phytoplankton biomass from flow cytometric measurements of abundance, fluorescence and light scatter. *Mar. Ecol. Prog. Ser.* **102**, 79-87.

- LINDAHL G., WALLSTRÖM K., BRATTBERG G., 1978. On nitrogen fixation in a coastal area of the northern Baltic. *Kieler Meeresforsch. Sonderh.* **4**, 171-177.
- LOHMANN, 1908. Untersuchungen zur Feststellung des vollständigen Gehaltes des Meeres an Plankton. *Wiss. Meeresunters.* N.F. **10**, 129-370.
- LORENZEN C.J. and JEFFREY S.W., 1978. Determination of chlorophyll in sea water. Unesco technical papers in marine science, **35**.
- MAGAZZU G. and DECEMBRINI F., 1995. Primary production, biomass and abundance of phototrophic picoplankton in the Mediterranean Sea: a review. *Aquat. Microb. Ecol.* **9**, 97-104.
- MANTOURA R.F.C. and LLEWELLYN C.A., 1983. The rapid determination of chlorophyll and carotenoid pigments and their breakdown products in natural waters by reverse phase HPLC. *Analyt. Chim. Acta.* **151**, 297-314.
- MANTOURA R.F.C., LAW C.S., OWENS N.J.P., BURKILL P.H., WOODWARD E.M.S., HOWLAND R.J.M., LLEWELLYN C.A., 1993. Nitrogen biogeochemical cycling in the northwestern Indian Ocean. *Deep Sea Res. II*, **40**, 651-671.
- MATTHAEUS W., LASS U., TIESEL R., 1993. The major Baltic inflow in January 1993. ICES Statutory Meeting Dublin, Paper ICES C M 1993/C:51.
- MCMANUS G.B. and OKUBO A., 1991. On the use of surrogate food particles to measure protistan ingestion. *Limn. Oceanogr.* **36** (3), 613-617.
- MEYER-HARMS B., 1996. Ernährungsstrategie calanoider Copepoden in zwei unterschiedlich trophierten Seegebieten der Ostsee (Pommernbucht, Gotlandsee). Dissertation thesis, Universität Rostock.
- MONGER B.C. and M.R. LANDRY, 1993. Flow cytometric analysis of marine bacteria with Hoechst 33342. *Appl. Environ. Microbiol.*, **59**, 905-911.
- MOREL A., AHN Y.-H., PARTENSKY F., VAULOT D., CLAUSTRE H., 1993. *Prochlorococcus* and *Synechococcus*: A comparative study of their optical properties in relation to their size and pigmentation. *J. Mar. Res.*, **51**, 617-649.
- NAGATA T. and KIRCHMAN D.L., 1990. Filtration-induced release of dissolved free amino acids: application to cultures of marine protozoa. *Mar. Ecol. Prog. Ser.*, **68**, 1-5.
- NAIR R.R., ITTEKKOT V., MANGANINI S.J., RAMASWAMY V., HAAKE B., DEGENS E.T., DESAI B.N., HONJO S., 1989. Increased particle flux to the deep ocean related to monsoons. *Nature*, **338**, 749-751.
- NAQVI S.W.A. and SHAILAJA M.S., 1993. Activity of the respiratory electron transport system and respiration rates within the oxygen minimum layer of the Arabian Sea. *Deep-Sea Res. II*, **40** (3), 687-695.
- NAQVI S.W.A., 1994. Denitrification processes in the Arabian Sea. In: LAL D. (Ed.): Biogeochemistry of the Arabian Sea. Indian Academy of Sciences, Bangalore 560 044, pp 181-202.

- NAKAMURA Y., SAKASI S., HIROMI J., FUKAMI K., 1993. Dynamics of picocyanobacteria in the Seto Inland Sea (Japan) during summer. *Mar. Ecol. Prog. Ser.* **96**, 117-124.
- NEUER S., 1992. Growth dynamics of marine *Synechococcus* ssp. in the Gulf of Alaska. *Mar. Ecol. Prog. Ser.* **83**, 251-262.
- NEWELL S.Y., SHERR B.F., SHERR E.B., FALLON R.D., 1983. Bacterial response to the presence of eukaryotic inhibitors in water from a coastal environment. *Mar. Environ. Res.* **10**, 147-157.
- NIVAL P. and NIVAL S., 1976. Particle retention efficiencies of a herbivorous copepod, *Acartia clausi* (adult and copepodite stages): effects on grazing. *Limnol. Oceanogr.* **21**, 24-38.
- O'CONNORS H.B., BIGGS D.S., NINIVAGGI, D.V., 1980. Particle size dependent maximum grazing rates for *Temora longicornis* fed natural particle assemblages. *Mar. Biol.* **56**, 65-70.
- OHMAN M.D. and SNYDER R.A., 1991. Growth kinetics of the omnivorous oligotrich ciliate *Strombidium* sp. *Limnol. Oceanogr.* **36** (5), 922-935.
- OLSON R.J., VAULOT D., CHISHOLM S.W., 1985. Marine phytoplankton distributions measured using shipboard flow cytometry. *Deep Sea Res.*, **32**, 1273-1280.
- OLSON R.J., CHISHOLM S.W., ZETTLER E.R., ARMBRUST E.V., 1988. Analysis of *Synechococcus* pigment types in the sea using single and dual beam flow cytometry. *Deep Sea Res.*, **35** (3), 425-440.
- OLSON R.J., CHISHOLM S.W., ZETTLER E.R., ALTABET M.A., DUSENBERRY J.A., 1990. Spatial and temporal distributions of prochlorophyte picoplankton in the North Atlantic Ocean. *Limnol. Oceanogr.*, **37** (6), 1033-1051.
- ORMEROD M.G., 1990. Flow Cytometry: A practical approach. IRL press at Oxford University press, Oxford 1990. 279 pp.
- OWENS N.J.P., LAW C.S., MANTOURA R.F.C., BURKILL P.H., LLEWELLYN C.A., 1991. Methane flux to the atmosphere from the Arabic Sea. *Nature*, **354**, 293- 296.
- PARANJAPPE M.A., 1987. Grazing by microzooplankton in the eastern Canadian arctic in summer 1983. *Mar. Ecol. Prog. Ser.* **40**, 239-246.
- PARSLOW J.S., DOUCHETTE G.J., TAYLOR F.J.R., HARRISON P.J., 1986. Feeding by the zooflagellate *Pseudobodo* sp. on the picoplanktic prasinomonad *Micromonas pusilla*. *Mar. Ecol. Prog. Ser.* **29**, 237-246.
- PARSONS T.R. and LALLI C.M., 1988. Comparative oceanic ecology of the plankton communities of the subarctic Atlantic and Pacific Oceans. *Oceanogr. Mar. Biol. Annu. Rev.* **26**, 317-359.
- PARTENSKY F., HOEPPFNER N., LI W.K.W., ULLOA O., VAULOT D., 1993. Photoacclimation of *Prochlorococcus* sp. (Prochlorophyta) strains isolated from the North Atlantic and the Mediterranean Sea. *Plant Physiol.* **101**, 285-296.

- PASSOW U., PEINERT R., ZEITZSCHEL B., 1993. Distributions and sedimentation of organic matter during the inter-monsoon period off Oman (West Arabian Sea). *Deep-Sea Res. II*, **40** (3), 833-849.
- PEETERS J.C.H., DUBELLAR G.B.J., RINGELBERG J., VISSER J.W.M., 1989. Optical Plankton Analyser: A flow cytometer for plankton analysis, I: Design considerations. *Cytometry* **10**, 522-528.
- PHINNEY D.A. and CUCCI T.L., 1989. Flow cytometry and phytoplankton. *Cytometry* **10**, 511-521.
- POLLEHNE F., KLEIN B., ZEITZSCHEL B., (1993) Low light adaptation and export production in the deep chlorophyll maximum layer in the northern Indian Ocean. *Deep Sea Res. II*, **40**, 737-752.
- POLLEHNE F., BUSCH S., JOST G., MEYER-HARMS B., NAUSCH M., RECKERMANN M., SCHAENING P., SETZKORN D., WASMUND N., WITEK Z., 1995. Primary production patterns and heterotrophic use of organic material in the Pomeranian Bay (southern Baltic). *Bulletin of the Fisheries Institute MIR*, **3** (136), 43-60.
- POMEROY L.R., 1974. The ocean's food web, a changing paradigm. *Bioscience* **24**, 499-504.
- PORTER K.G. and FEIGG Y.S., 1980. The use of DAPI for identifying and counting aquatic microflora. *Limnol. Oceanogr.*, **25** (5), 943-948.
- PORTER K.G. 1988. Phagotrophic phytoflagellates in microbial food webs. *Hydrobiologica* **159**, 89-97.
- POWER M.E., 1992. Top-Down and Bottom-Up forces in food webs: do plants have primacy? *Ecology* **73** (3), 733-746.
- PUTT M. and STOECKER D.K., 1989. An experimentally determined carbon : volume ratio for marine "oligotrichous" ciliates from estuarine and coastal waters. *Limnol. Oceanogr.*, **34** (6), 1097-1103.
- RASSOULZADEGAN F. and SHELDON R.W., 1986. Predator-prey interactions of nanozooplankton and bacteria in an oligotrophic marine environment. *Limnol. Oceanogr.*, **31** (5), 1010-1021.
- REDFIELD A.C., KETCHUM B.H., RICHARDS F.A., 1963. The influence of organisms on the composition of sea-water. In: Hill, M.N. (ed.): *The Sea*, Vol.2. Ideas and observations on progress in the study of the seas. Interscience Publishers, Wiley and sons, New York, London: pp 26-77.
- REITMEIER S., 1994. Untersuchungen zur Verbreitung, zur Biomasse, und zum Grazing des Mikrozooplanktons in polaren Gewässern. Ber. SFB 313 Nr. 48., Universität Kiel.
- RIEGMAN R., KUIPERS B.R., NOORDELOOS A.A., WITTE H.J., 1993. Size-differential control of phytoplankton and the structure of plankton communities. *Neth. J. Plankt. Res.* **31** (3), 255-265.
- RIEMANN B., SIMONSEN P., STENSGAARD L., 1989. The carbon and chlorophyll content of phytoplankton from various nutrient regimes. *J. Plank. Res.*, **11** (5), 1037-1045.

- RINNE I., MELVASO V., NIEMI A., NIEMIESTO L., 1978. Nitrogen fixation by blue-green algae in the Baltic Sea. *Kieler Meeresforsch. Sonderh.* **4**, 178-187.
- RUBLEE P.A. and GALLEGOS C.L., 1989. Use of fluorescently labelled algae (FLA) to estimate microzooplankton grazing. *Mar. Ecol. Prog. Ser.* **51**, 221-227.
- RYTHER J.H. and MENZEL D.W., 1965. On the production, composition and distribution of organic matter in the western Arabian Sea. *Deep-Sea Res.*, **12**, 199-209
- SAHLSTEN E. and SÖRENSEN F., 1989. Planktonic nitrogen transformations during a declining cyanobacteria bloom in the Baltic Sea. *J. Plank. Res.*, **11** (6), 1117-1128.
- SANDERS R.W., 1991. Trophic strategies among heterotrophic flagellates. In: PATTERSON D.J. AND LARSEN J. (EDS.): The biology of free-living heterotrophic flagellates. The Systematics Association Special Vol. 45, Clarendon Press Oxford 1991. pp 21-38.
- SCHOTT F., SWALLOW J.C., FIEUX M., 1990. The Somali Current at the equator: annual cycle of currents and transports in the upper 1000m and connection to neighboring latitudes. *Deep-Sea Res.* **37**, 1825-1848.
- SHELDON R.W., NIVAL P., RASSOULZADEGAN F., 1986. An experimental investigation of a flagellate-ciliate-copepod food chain with some observations relevant to the linear biomass hypothesis. *Limnol. Oceanogr.*, **31** (1), 184-188.
- SHERR B.F., SHERR E.B., BERMAN, T., 1983. Grazing, growth and ammonium excretion rates of a heterotrophic microflagellate fed with four species of bacteria. *Appl. Environ. Microbiol.*, **45** (4), 1196-1201.
- SHERR B.F., SHERR E.B., ANDREW T.L., FALLON R.D., NEWELL S.Y., 1986A. Trophic interactions between heterotrophic protozoa and bacterioplankton in estuarine water analysed with selective metabolic inhibitors. *Mar. Ecol. Prog. Ser.*, **32**, 169-179.
- SHERR B.F., SHERR E.B., FALLON R.D., NEWELL S.Y., 1986B. Small, aloricate ciliates as a major component of the marine heterotrophic nanoplankton. *Limnol. Oceanogr.*, **31** (1), 177-183.
- SHERR E.B., SHERR B.F., PAFFENHÖFER G.-A., 1986C. Phagotrophic protozoa as food for metazoans: a 'missing' trophic link in marine pelagic food webs? *Mar. Microb. Food Webs*, **1** (2), 61-80.
- SHERR E.B. and SHERR B.F., 1987. High rates of consumption of bacteria by pelagic ciliates. *Nature*, **325**, 710-711.
- SHEYTHE S.R., GOUVEIA A.D., SHENOI S.S.C., 1994. Circulation and water masses of the Arabian Sea. In: LAL D. (Ed.): Biogeochemistry of the Arabian Sea. Indian Academy of Sciences, Bangalore 560 044, pp 9-25.
- SIEBURTH J. MCN., SMETACEK V., LENZ J., 1978. Pelagic ecosystem structure: Heterotrophic compartments of the plankton and their relationship to plankton size fractions. *Limnol. Oceanogr.* **23** (6), 1256-1263.
- SIEBURTH J. MCN. and ESTEP K.W., 1985. Precise and meaningful terminology in marine microbial ecology. *Mar. Microb. Food Webs*, **1**, 1-16.

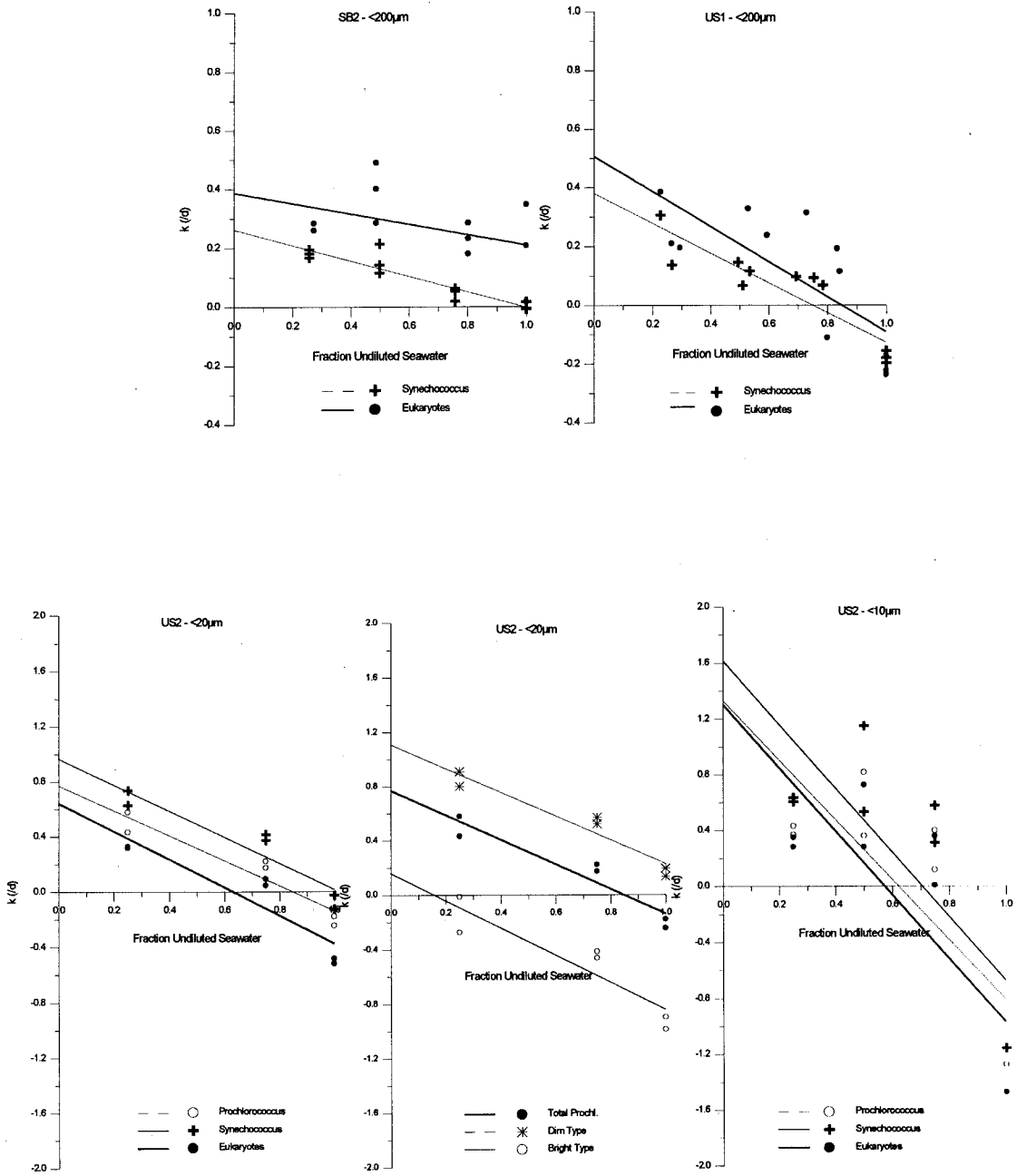
- SIEGEL H., GERTH M., SCHMIDT T., 1996. Water exchange in the Pomeranian Bight investigated by satellite data and shipbourne measurements. *Cont. Shelf Res.*, in press.
- SLEIGH M.A., 1991. A taxonomic review of heterotrophic protists important in marine ecology. In: REID P.C., TURLEY C.M., BURKILL P.H. (EDS.): Protozoa and their role in marine processes. NATO ASI Series, Series G: Vol.25. Springer Verlag Berlin 1991. pp 9-38.
- SMETACEK V., 1975. Die Sukzession des Phytoplanktons in der Kieler Bucht. Dissertation thesis. Inst. f. Meereskunde, Universität Kiel.
- SMETACEK V., 1981. The annual cycle of protozooplankton in the Kiel Bight. *Mar. Biol.*, **63** 1-11.
- SMETACEK V., 1985. Role of sinking in diatom life-history cycles: ecological, evolutionary and geological significance. *Mar. Biol.*, **84**, 293-251.
- SMETACEK V., SCHAREK R., NÖTHIG E.-M., 1990. Seasonal and regional variation in the pelagial and its relationship to the life history cycle of the Krill. In: KERRY, K.R. and G. HEMPEL (EDS.) Antarctic Systems. Ecological change and conservation. Springer-Verlag Berlin Heidelberg 1990, pp 103-114.
- SÖRENSSEN F. and SAHLSTEN E., 1987. Nitrogen dynamics of a cyanobacteria bloom in the Baltic Sea: New vs. regenerated production. *Mar. Ecol. Prog. Ser.* **37**, 277-284.
- SOMASUNDAR K., RAJENDRAN A., DILEEP KUMAR M., SEN GUPTA R., 1990. Carbon and nitrogen budgets of the Arabian Sea. *Mar. Chem.*, **30**, 363-377.
- SOROKIN Y.I., KOPYLEV A.I., MAMAIEVA N.V., 1985. Abundance and dynamics of microplankton in the central tropical Indian Ocean. *Mar. Ecol. Prog. Ser.*, **24**, 27-41.
- STEELE J.H., 1974. The structure of marine ecosystems. Harvard University press, Cambridge, Mass. 128 pp.
- STEEN H.B., 1983. A microscope based flow cytometer. *Histchem. J.* **15**, 147-170.
- STOCKNER J.G., 1988. Phototrophic picoplankton: an overview from marine and freshwater ecosystems. *Limnol. Oceanogr.*, **33**, 765-775.
- STOECKER D.K., MICHAELS A.E., DAVIS L.H., 1987. Large proportion of marine planktonic ciliates found to contain functional chloroplasts. *Nature*, **326**, 790-792.
- STOECKER D.K. and MCDOWELL CAPUZZO J., 1990. Predation on protozoa: its importance to microzooplankton. *J. Plankt. Res.* **12** (5), 891-908.
- STONE L., 1990. Phytoplankton-bacteria-protozoa interactions: a qualitative model portraying indirect effects. *Mar. Ecol. Prog. Ser.*, **64**, 137-145.
- STROM S.L., 1991. Growth and grazing rates of the herbivorous dinoflagellate *Gymnodinium* sp. from the open subarctic Pacific Ocean. *Mar. Ecol. Prog. Ser.*, **78**, 103-113.
- STROM S.L. and WELSCHMEYER N.A., 1991. Pigment-specific rates of phytoplankton growth and microzooplankton grazing in the open subarctic Pacific Ocean. *Limnol. Oceanogr.*, **36** (1), 50-63.

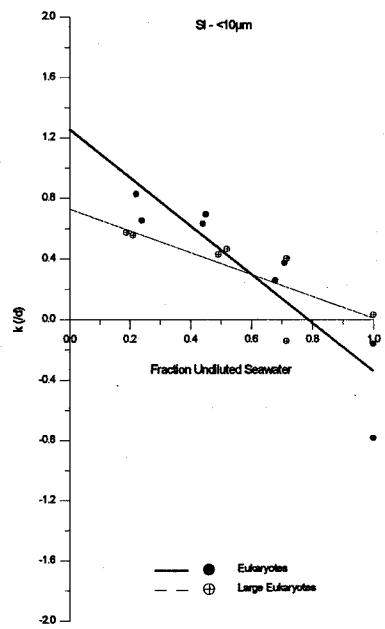
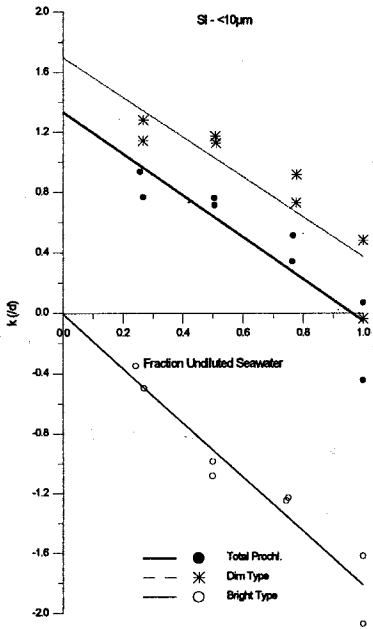
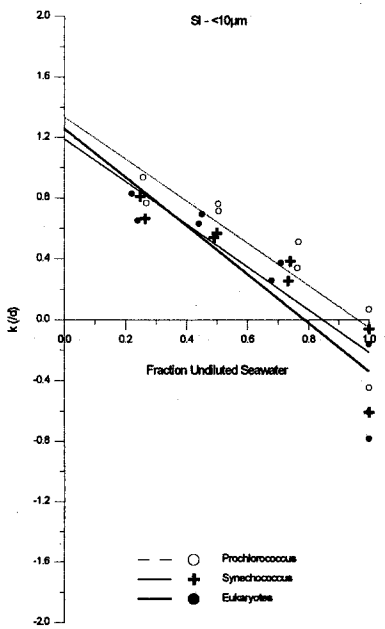
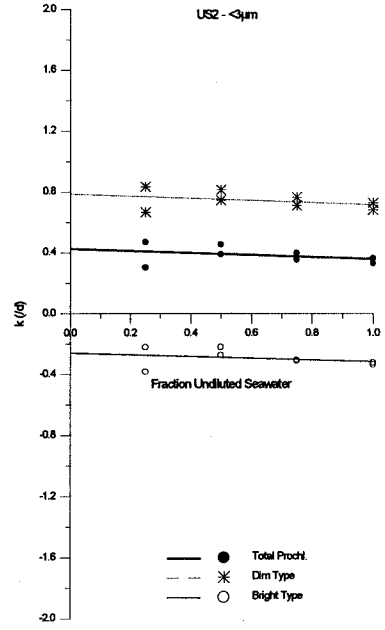
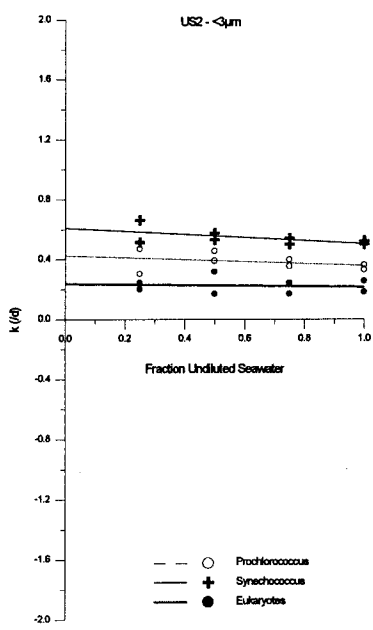
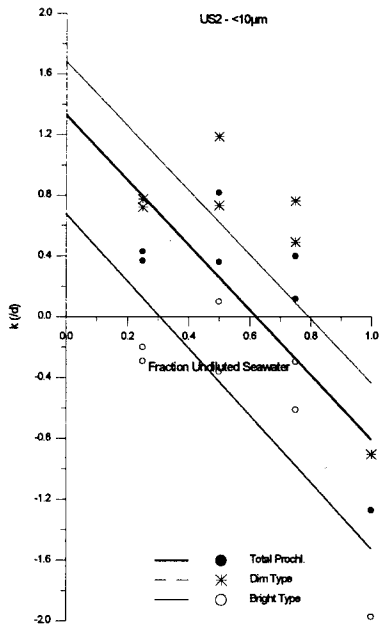
- STROM S.L., POSTEL J.R., BOOTH B.C., 1993. Abundance, variability and potential grazing impact of planktonic ciliates in the open subarctic Pacific Ocean. *Prog. Oceanog.*, **32**, 185-203.
- STRONG D.R., 1992. Are trophic cascades all wet? Differentiation and donor-control in speciose ecosystems. *Ecology*, **73** (3), 747-754.
- SVERDRUP H.U., 1953. On conditions for the vernal blooming of phytoplankton. *J. Cons. Explor. Mer.* **18**, 287-295.
- THRONSEN J., 1993. The planktonic marine flagellates. In: TOMAS C.R. (Ed.) *Marine Phytoplankton. A guide to naked flagellates and Coccolithophorids*. Academic Press Inc. San Diego 1993. pp. 7-146.
- TOMAS C.R., 1993. *Marine Phytoplankton. A guide to naked flagellates and Coccolithophorids*. Academic Press Inc. San Diego 1993, 251p.
- TRENKEL V., 1992. Untersuchungen zu trophischen Beziehungen der Organismen im "Microbial Loop". Diploma thesis, Inst. f. Meeresk. Kiel.
- TURLEY C.M., 1986. Urea uptake by phytoplankton at different fronts and associated stratified and mixed waters on the European shelf. *Br. Phycol. J.*, **21**, 225-238.
- URBACH E., ROBERTSON D.L., CHISHOLM S.W., 1992. Multiple evolutionary origins of prochlorophytes within the cyanobacterial radiation. *Nature* **355**, 267-270.
- UTERMÖHL H., 1958. Zur Vervollkommnung der quantitativen Phytoplankton-Methodik. *Mitt. Int. Theor. Angew. Limnol.* **9**, 1-38.
- VAULOT D., MARIE D., OLSON R.J., CHISHOLM S.W., 1995. Growth of *Prochlorococcus*, a photosynthetic prokaryote, in the equatorial Pacific Ocean. *Science* **268**, 1480-1482.
- VAULOT D., PARTENSKY F., NEVEUX J., MANTOURA R.F.C., LLEWELLYN C.A., 1990. Winter presence of prochlorophytes in surface waters of the northwestern Mediterranean Sea. *Limnol. Oceanogr.* **35** (5), 1156-1164.
- VELDHUIS M.J.W. and KRAAY G.W., 1990. Vertical distribution and pigment composition of a picoplanktonic prochlorophyte in the subtropical North Atlantic: a combined study of HPLC-analysis of pigments and flow cytometry. *Mar. Ecol. Prog. Ser.*, **68**, 121-127.
- VELDHUIS M.J.W. and KRAAY G.W., 1993. Cell abundance and fluorescence of picoplankton in relation to growth irradiance and nitrogen availability in the Red Sea. *Neth. J. Sea Res.*, **31**, 135-145.
- VELDHUIS M.J.W., KRAAY G.W., GIESKES W.W.C., 1993. Growth and fluorescence characteristics of ultraplankton on a north-south transect in the eastern North Atlantic. *Deep-Sea Res. II*, **40** (1/2), 606-626.
- VELDHUIS M.J.W., KRAAY G.W., BLEIJSWIJK J.D.L. VAN, 1994. Phytoplankton biomass and productivity. In: Baars M.A. (Ed.): *Monsoons and pelagic systems. Cruise reports Netherland's Indian Ocean Programme, Vol.1*. National Museum of Natural History, Leiden 1994.

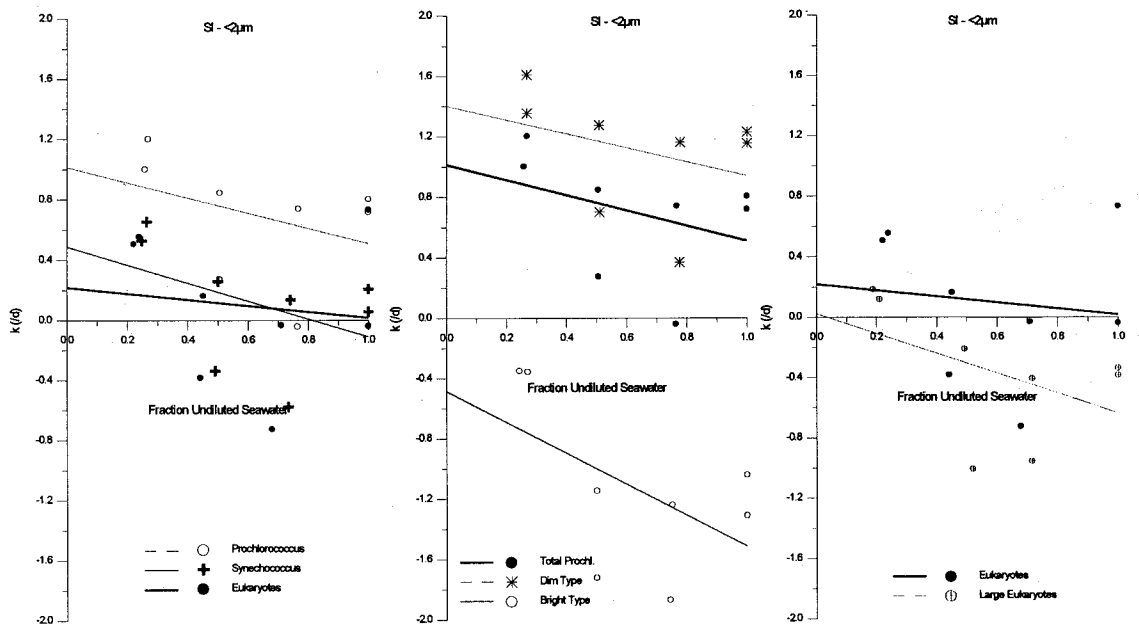
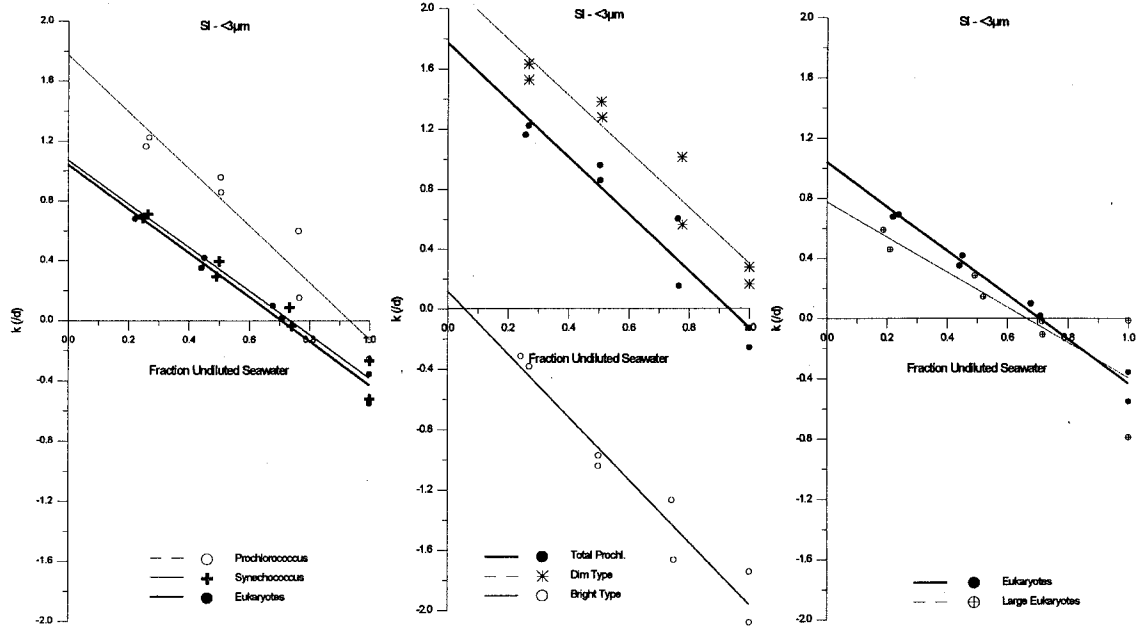
- VERITY P.G., 1986. Grazing of phototrophic nanoplankton by microzooplankton in Narragansett Bay. *Mar. Ecol. Prog. Ser.* **29**, 105-115.
- VERITY P.G., ROBERTSON C.Y., TRONZO C.R., ANDREWS M.G., NELSON J.R., SIERACKI M.E., 1992. Relationships between cell volume and the carbon and nitrogen content of marine photosynthetic nanoplankton. *Limnol. Oceanogr.* **37** (7), 1434-1446.
- VERITY P.G., STOECKER D.K., SIERACKI M.E., BURKILL P.H., EDWARDS, E.S., TRONZO, C.R., 1993. Abundance, biomass and distribution of heterotrophic dinoflagellates during the North Atlantic spring bloom. *Deep Sea Res. II*, **40** (1/2), 227-244.
- VØRS N., BUCK K.R., CHAVETZ F.P., EIKREM W., HANSEN L.E., ØSTERGAARD J.B., THOMSEN H.A., 1995. Nanoplankton of the equatorial Pacific with emphasis on the heterotrophic protists. *Deep Sea Res. II*, **42** 3-4, 585-602.
- WALLSTRÖM K., 1988. The occurrence of *Aphanizomenon flos-aquae* (Cyanophyceae) in a nutrient gradient in the Baltic. *Kieler Meeresforsch. Sonderh.* **6** 210-220.
- WATERBURY J.B., WATSON S.B., GUILLARD R.R.L., BRAND L.E., 1979. Widespread occurrence of a unicellular, marine, planktonic cyanobacterium. *Nature*, **277**, 293-294.
- WEISSE T., 1989. The microbial loop in the Red Sea: dynamics of pelagic bacteria and heterotrophic nanoflagellates. *Mar. Ecol. Prog. Ser.*, **55**, 241-250.
- WEISSE T., MÜLLER H., PINTO-COELHO R.M., SCHWEITZER A., SPRINGMANN D., BALDRINGER G., 1990. Responses of the microbial loop to the phytoplankton spring bloom in a large prealpine lake. *Limnol. Oceanogr.*, **35** (4), 781-794.
- WEISSE, T. and SCHEFFEL-MÖSER U., 1991. Uncoupling the microbial loop: growth and grazing loss rates of bacteria and heterotrophic nanoflagellates in the North Atlantic. *Mar. Ecol. Prog. Ser.* **71**, 195-205.
- WHEELER P.A., NORTH B.B., STEPHENS G.C., 1974. Amino acid uptake by marine phytoplankters. *Limnol. Oceanogr.*, **19** (2), 249-259.
- WHITELEY A.S., BURKILL P.H., SLEIGH M.A., 1993. Rapid method for cell cycle analysis of a predatory marine dinoflagellate. *Cytometry* **14**, 903-909.
- WIKNER J. and HAGSTRÖM A., 1988. Evidence for a tightly coupled nanoplanktonic predator-prey link regulating the bacterivores in the marine environment. *Mar. Ecol. Prog. Ser.*, **50**, 137-145.
- WILLIAMS P.J. LE B., 1981. Incorporation of microheterotrophic processes into the classical paradigm of the planktonic food web. *Kieler Meeresforsch., Sonderh.*, **5**, 1-28.
- WOOD A.M., HORAN P.K., MUIRHEAD K., PHINNEY D.A., YENTSCH C.M., WATERBERRY J.B., 1985. Discrimination between types of pigments in marine *Synechococcus* ssp. by scanning spectroscopy, epifluorescence microscopy, and flow cytometry. *Limnol. Oceanogr.*, **30** (6), 1303-1315.
- WRIGHT R.T. and COFFIN R.B., 1984. Measuring microzooplankton grazing on planktonic marine bacteria by its impact on bacterial production. *Microb. Ecol.* **10**, 137-149.

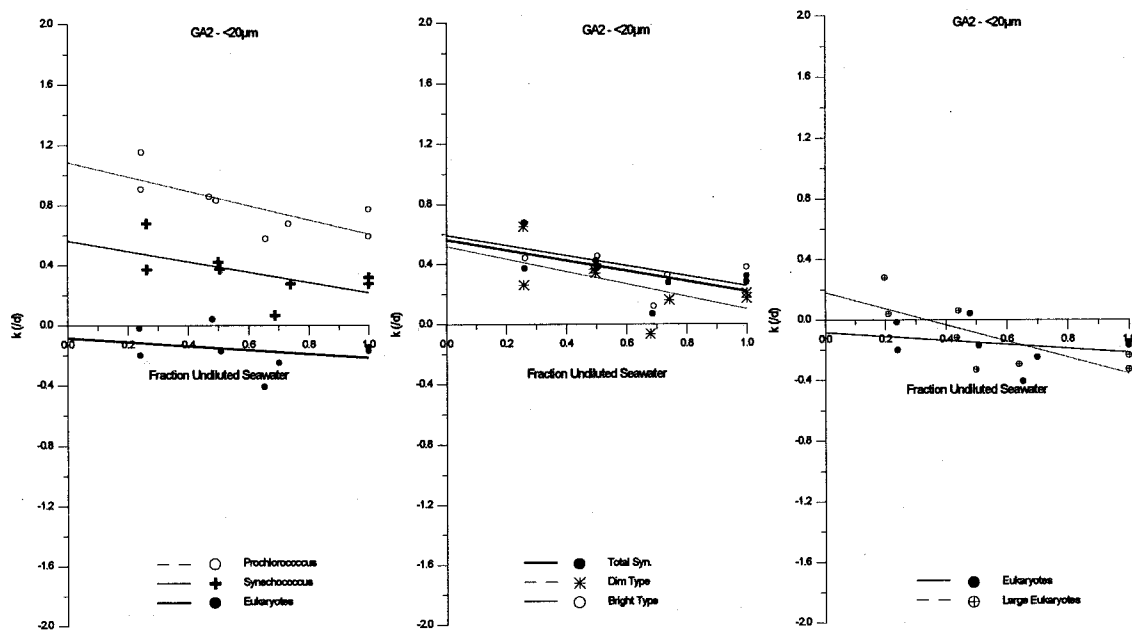
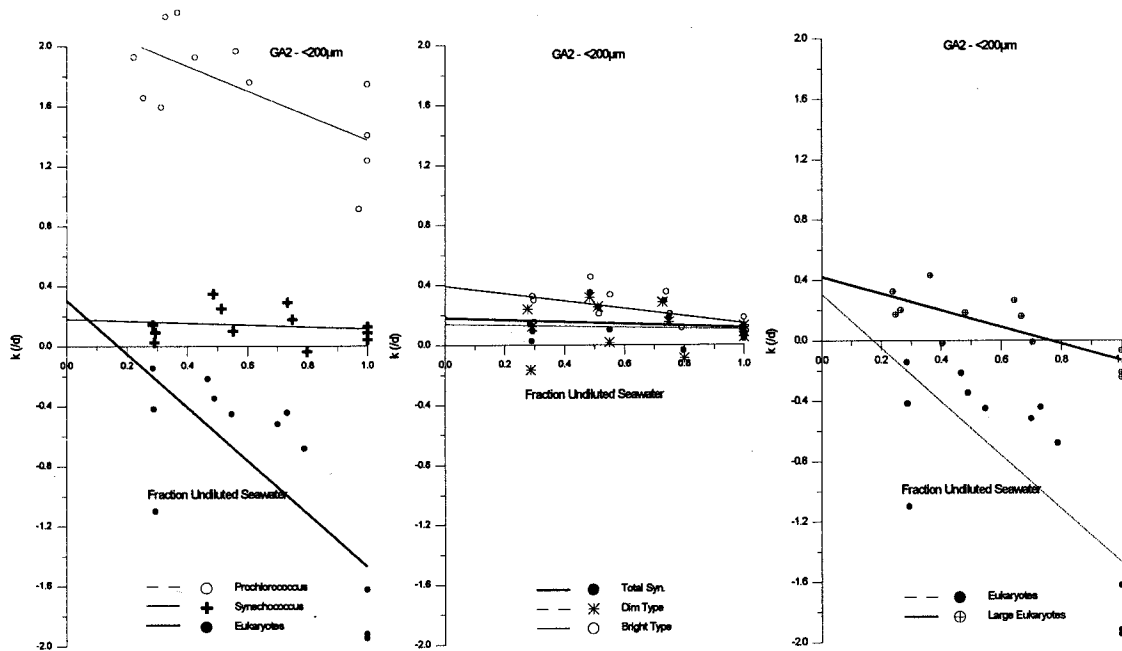
Appendix

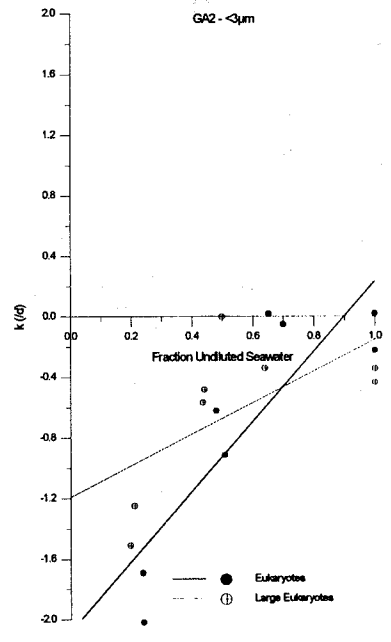
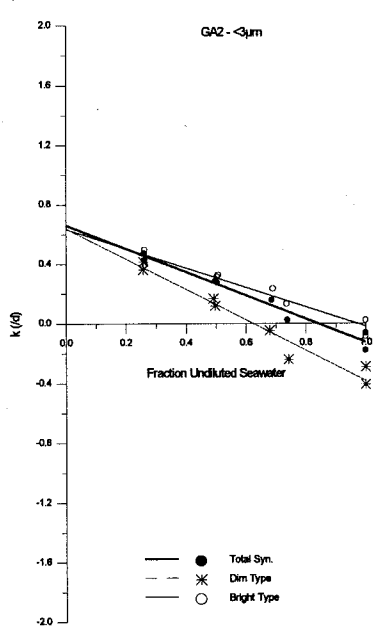
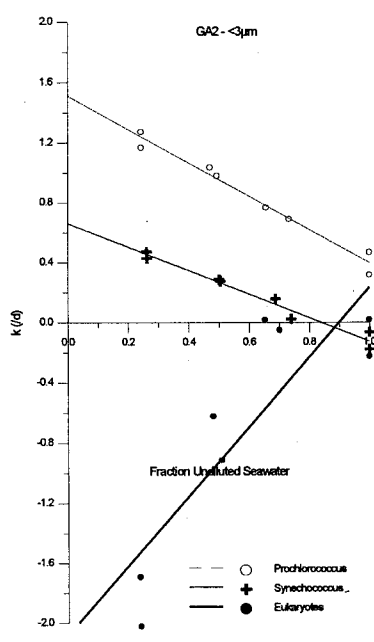
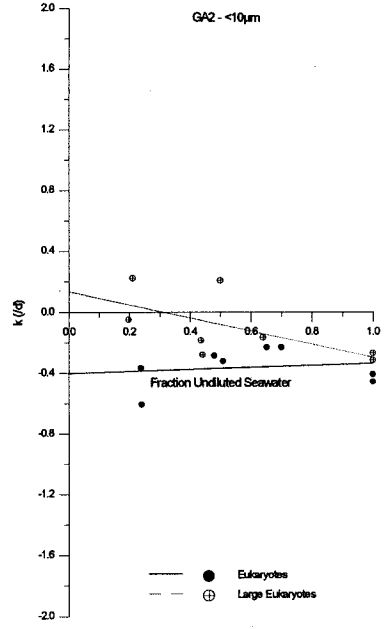
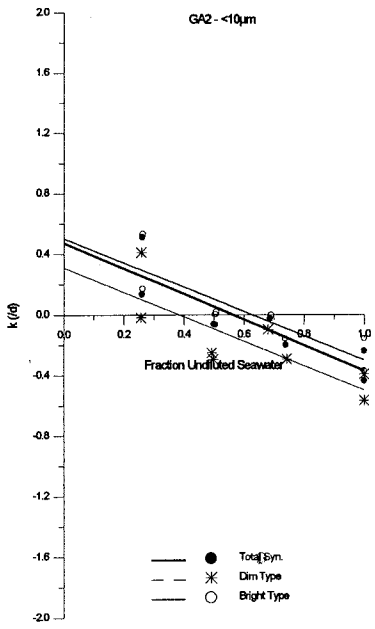
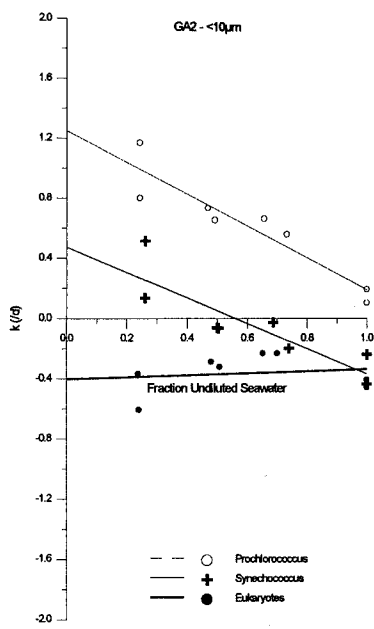
Dilution plots of size fractionated serial dilution grazing experiments during cruise B2 (NE monsoon, section 3.2.).

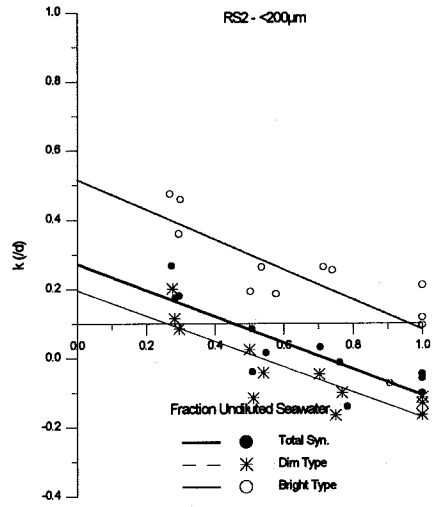
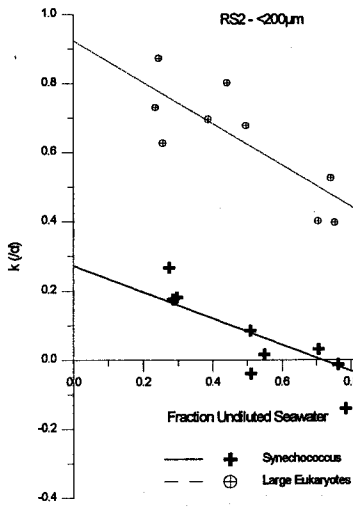












Danksagung - Acknowledgements

Einen herzlichen Dank zunächst an meinen Doktorvater Prof. Bodo von Bodungen, der mir diese Arbeit ermöglicht hat und der mir besonders in der Endphase mit Kompetenz und Humor zur Seite stand.

Dr. Falk Pollehne möchte ich für seine ständige Diskussionsbereitschaft danken, die auch in Streßsituationen nicht nachließ. Prof. Karin Lochte, Dr. Maren Voß und Dr. Christoph Humborg gaben mir wertvolle Hinweise zur Verbesserung dieser Arbeit, wodurch diese profitiert hat. Dr. Günter Jost verdanke ich einige unveröffentlichte Zahlen.

Dann sind da all die anderen Leute am IOW, die wissentlich oder nicht, zur Vervollständigung dieser Arbeit beigetragen haben: allen voran Annemarie Schröder und Brigitte Sievert aus der Bibliothek, die mit Geduld und Hingabe meine seitenlangen Wunschlisten abarbeiteten. Bernd Schlichting und Herr Gust lösten die aufgetretenen Computerprobleme schnell und kompetent, vielen Dank dafür. Dank Ute Fensky's schneller Reaktionszeit hatten logistische Probleme keine Chance. Allen Technikern der Abteilung, die mir ebenfalls geholfen haben, vielen Dank. Vielen Dank auch meinen beiden Zimmergenossinnen Bettina Meyer-Harms und Katrin Schmidt für die gute Arbeitsstimmung.

Besonderen Dank verdienen die Crews der beiden Institutsschiffe Penck und Humboldt: sie trugen dazu bei, daß die Fahrten in die Ostsee nicht nur erfolgreich waren, sondern auch Spaß machten.

A large part of this work for this thesis was conducted during my stay in the Netherlands, respectively on the TYRO in the Arabian Sea. I am very grateful to Dr. Martien Baars who enabled me to participate in the two cruises to the Arabian Sea. I am especially thankful to Dr. Marcel Veldhuis, who not only let me use his flow cytometer during the NE monsoon - cruise, but infected me with his enthusiasm concerning the opportunities of flow cytometry in our science. My gratitude also to the many people who helped me at the NIOZ and on the TYRO: Gijsbert Kraay, Annette van Koutrik and Karel Bakker, just to mention a few. The crew and technical staff of the TYRO solved all problems in a professional manner. All this made both cruises a very pleasant scientific and non-scientific experience for me. Hartelijk bedankt!

Meereswissenschaftliche Berichte

MARINE SCIENCE REPORTS

- 1 (1990) Postel, Lutz:
Die Reaktion des Mesozooplanktons, speziell der Biomasse, auf küstennahen Auftrieb vor Westafrika (The mesozooplankton response to coastal upwelling off West Africa with particular regard to biomass)
- 2 (1990) Nehring, Dietwart:
Die hydrographisch-chemischen Bedingungen in der westlichen und zentralen Ostsee von 1979 bis 1988 – ein Vergleich (Hydrographic and chemical conditions in the western and central Baltic Sea from 1979 to 1988 – a comparison)
Nehring, Dietwart; Matthäus, Wolfgang:
Aktuelle Trends hydrographischer und chemischer Parameter in der Ostsee, 1958 – 1989 (Topical trends of hydrographic and chemical parameters in the Baltic Sea, 1958 – 1989)
- 3 (1990) Zahn, Wolfgang:
Zur numerischen Vorticityanalyse mesoskaliger Strom- und Massfelder im Ozean (On numerical vorticity analysis of mesoscale current and mass fields in the ocean)
- 4 (1992) Lemke, Wolfram; Lange, Dieter; Ender, Rudolf (Eds.):
Proceedings of the Second Marine Geological Conference – The Baltic, held in Rostock from October 21 to October 26, 1991
- 5 (1993) Ender, Rudolf; Lackschewitz, Klas (Eds.):
Cruise Report RV "Sonne" Cruise SO82, 1992
- 6 (1993) Kulik, Dmitri A.; Harff, Jan:
Physicochemical modeling of the Baltic Sea water-sediment column: I. Reference ion association models of normative seawater and of Baltic brackish waters at salinities 1–40 ‰, 1 bar total pressure and 0 to 30 °C temperature
(system Na–Mg–Ca–K–Sr–Li–Rb–Cl–S–C–Br–F–B–N–Si–P–H–O)
- 7 (1994) Nehring, Dietwart; Matthäus, Wolfgang; Lass, Hans-Ulrich; Nausch, Günther:
Hydrographisch-chemische Zustandseinschätzung der Ostsee 1993
- 8 (1995) Hagen, Eberhard; John, Hans-Christian:
Hydrographische Schnitte im Ostrandstromsystem vor Portugal und Marokko 1991 - 1992
- 9 (1995) Nehring, Dietwart; Matthäus, Wolfgang; Lass, Hans Ulrich; Nausch, Günther; Nagel, Klaus:
Hydrographisch-chemische Zustandseinschätzung der Ostsee 1994
Seifert, Torsten; Kayser, Bernd:
A high resolution spherical grid topography of the Baltic Sea
- 10 (1995) Schmidt, Martin:
Analytical theory and numerical experiments to the forcing of flow at isolated topographic features
- 11 (1995) Kaiser, Wolfgang; Nehring, Dietwart; Breuel, Günter; Wasmund, Norbert; Siegel, Herbert; Witt, Gesine; Kerstan, Eberhard; Sadkowiak, Birgit:
Zeitreihen hydrographischer, chemischer und biologischer Variablen an der Küstenstation Warnemünde (westliche Ostsee)
Schneider, Bernd; Pohl, Christa:
Spurenmittelkonzentrationen vor der Küste Mecklenburg-Vorpommerns

- 12 (1996)** Schinke, Holger:
Zu den Ursachen von Salzwassereinbrüchen in die Ostsee
- 13 (1996)** Meyer-Harms, Bettina:
Ernährungsstrategie calanoider Copepoden in zwei unterschiedlich trophierten Seegebieten der Ostsee (Pommernbucht, Gotlandsee)
- 14 (1996)** Reckermann, Marcus:
Ultraplankton and protozoan communities and their interactions in different marine pelagic ecosystems (Arabian Sea and Baltic Sea)